MODERN MISSILE GUIDANCE

Rafael Yanushevsky



MODERN MISSILE GUIDANCE

MODERN MISSILE GUIDANCE

Rafael Yanushevsky


CRC Press
Taylor & Francis Group
Boca Raton London New York

CRC Press is an imprint of the
Taylor & Francis Group, an **informa** business

CRC Press
Taylor & Francis Group
6000 Broken Sound Parkway NW, Suite 300
Boca Raton, FL 33487-2742

Printed in the United States of America on acid-free paper
10 9 8 7 6 5 4 3 2 1

International Standard Book Number-13: 978-1-4200-6226-7 (Hardcover)

Library of Congress Cataloging-in-Publication Data

Yanushevsky, Rafael.
Modern missile guidance / Rafael Yanushevsky.
p. cm.
Includes bibliographical references and index.
ISBN-13: 978-1-4200-6226-7 (alk. paper)
ISBN-10: 1-4200-6226-3 (alk. paper)
1. Guided missiles--Guidance systems. 2. Flight control. 3. Guidance systems (Flight) I. Title.

UG630.Y35 2007
623.4’519--dc22 2007015487

Visit the Taylor & Francis Web site at
http://www.taylorandfrancis.com

and the CRC Press Web site at
http://www.crcpress.com

Dedication

To
Daniel and Camilla

Contents

Preface

At the dawn of control theory development the aerospace industry was the most important supplier of problems and ideas. The most important results in the theory of nonlinear systems and stability analysis were stimulated by the aerospace industry needs.

Control experts were closely involved in the solution of many aerospace problems and aerospace system design. Optimal control theory was also raised mostly by aerospace problems. This was in the last century.

Nowadays aerospace specialists have more solid mathematical backgrounds. They are familiar with the newest results in control theory and are able not only to formulate control problems but also solve them without attracting the attention of control experts. Moreover, they try to apply new results in control theory to specific aerospace problems. As a result, control theory is losing its biggest supplier and, to a certain degree, this slows down its progress. However, the aerospace disciplines also suffer from this separation.

The application of new control methods can easily be found in aerospace journals. But what about the old ones? It seems strange that the proportional navigation (PN) method, the analog of a proportional controller, still remains the most widespread guidance law for homing guidance.

The author of this book has worked in the control area for more than 30 years. Starting working in the aerospace area he was surprised to find the gap between the high level of sophisticated control systems used in the aerospace industry and the rather simple guidance laws used in modern interceptors.

The author hopes that the material of this book will help to fill this gap in the future.

Guidance law design is considered from the point of view of control theory (i.e., as the design of controls guiding missiles to hit targets).

Two books dedicated to missile guidance deserve to be mentioned. Different in style and content, they are written by high-level experts who have in-depth understanding of guidance problems. The book by N. Shneydor, *Missile Guidance and Pursuit*, contains a concise description of various types of guidance laws with a short characterization of the main known results. The book by P. Zarchan, *Tactical and Strategic Missile Guidance*, summarizes the extensive experience of its author in guidance systems analysis and design and contains a detailed description of the PN guidance law.

This book is different from the above-mentioned ones. Guidance law design is considered as the design of controls. The design procedure is presented in the time domain and in the frequency domain. The different approaches, in the time and frequency domains, generate different guidance laws that supplement each other. Basic facts about missile guidance are given in Chapter 1. Parallel navigation and a description of PN guidance law are presented in Chapter 2. Proportional navigation is also considered as a control problem. The analysis of the PN guided systems in the time domain based on the method of adjoints is given in Chapter 3. Chapter 4 contains analysis of the PN guided systems in the frequency domain. The obtained analytical expressions for the miss distance can be used for missile system design. They enable the analysis of the influence of the guidance system parameters on its performance. The generalized missile guidance system model that also includes the target model is considered. The relationship between the frequency response and the miss step response is discussed. The procedure of determination of the optimal frequency for which the amplitude of the miss distance has a maximum is presented. Chapter 5 contains a detailed description of a class of guidance laws obtained based on the Lyapunov approach. It is shown that this class of guidance laws improves the effectiveness of the PN law for maneuvering and nonmaneuvering

targets. Moreover, the approach offered can also be considered as another justification of the widely used PN law. The analytical expressions of the guidance law are given for the generalized planar and three-dimensional engagement models for missiles with and without axial controlled acceleration. The modification of the PN guidance law using the results of classic control theory is considered in Chapter 6. The approach is based on using feedforward/feedback control signals to make the real missile acceleration close to the commanded acceleration generated by the PN guidance law. The effectiveness of these guidance laws against highly maneuvering targets is demonstrated. The analysis of the missile guidance systems performance under various types of noises is considered in Chapter 7. Analytical expressions for analysis of the PN guided systems are obtained. The computational algorithms are presented. Chapter 8 deals with the simulation models that can be used effectively for analysis of the guidance laws performance and the comparative analysis of various guidance laws. In Chapter 9 an attempt is made to discuss the problem of the integrated design of guidance and control laws. This problem is considered because of an increasing interest in integrated design of the flight vehicle systems. Finally, in Chapter 10 some computational programs that can be used to test missile guidance laws are considered.

The attractiveness of the guidance laws considered in this book is in their simplicity. They are as simple as the PN guidance law, which is widely used in practice mostly because of its simplicity. The material in this book can serve as a basis for several graduate courses in aerospace departments. It can be used by researchers and engineers in their everyday practice. The author hopes that this book will supply aerospace scientists and engineers with new ideas that, being crystallized, will bring significant improvement to missile systems performance.

About the Author



Rafael Yanushevsky was born in Kiev, Ukraine. He received a B.S. in mathematics and M.S. degree (with honors) in electromechanical engineering from Kiev University and Kiev Polytechnic Institute, respectively, and a PhD degree in the optimization of multivariable systems in 1968 from the Institute of Control Sciences of the USSR Academy of Sciences, Moscow, Russia.

From 1968 he worked at the Institute of Control Sciences. His research interests were in optimal control theory and its applications (especially in aerospace), optimal control of differential-difference systems, signal processing, game theory, and operations research. He published over 40 papers in these areas and two books, *Theory of Linear Optimal Multivariable Control Systems* and *Control Systems with Time-lag*. He was an editor of 14 books published by Nauka. In 1971, the Presidium of the USSR Academy of Sciences gave him the rank of senior scientist in automatic control.

After immigration to the United States in December 1987, he taught at the University of Maryland, first in the department of electrical engineering, then in the department of mechanical engineering, and at the University of the District of Columbia, in the department of mathematics. Since 1999 he has been involved in projects related to the aerospace industry. He participated in the development of an engagement model as part of the Battlespace Engineering Assessment Tool, weapon control system software, new guidance laws, and wrote sections of the *Modeling and Simulation Handbook* related to the weapon control system and fire control system of SM-3 missiles. In 2002 he received a letter of appreciation from the Department of the Navy, Navy Area Theater Ballistic Missile Program.

Dr. Yanushevsky's research interests include guidance and control, signal processing and control, tracking of maneuvering targets, and integrated missile guidance and control systems design. His company, Research and Technology Consulting (www.randtc.com), provides consulting services in these areas. He has published over 80 papers, was the chair of the Lyapunov Session of the Second and Fourth World Congresses on Nonlinear Analysis, and was a member of the Organizing Committee of the Fourth Congress. He is included in *Who's Who in America*, *Who's Who in Science and Engineering*, and *Who's Who in American Education.*

1 Basics of Missile Guidance

1.1 INTRODUCTION

The natural process of improvement of all aspects of our lives includes advances in the development of sophisticated weapon systems, the means to defend ourselves from enemies and those who consider wars as a way to improve their living conditions. In lieu of the thrown stone, the cast spear, the fired bullet, the dropped bomb, and the launched rocket, defensive or destructive functions are better performed by missiles. The fundamental goal of destruction or defense, to destroy the target, has not changed. However, targets have become more sophisticated. Technological progress did not bypass them.

A missile is defined as a space-traversing unmanned vehicle that contains the means for controlling its flight path. A guided missile is considered to operate only above the surface of the Earth, so guided torpedoes do not meet the above definition. Missiles are classified by the physical areas of launching and the physical areas containing the target. The four general categories of guided missiles are: surface-to-surface; surface-to-air; air-to-surface; and air-to-air.

The first attempts to use a pilotless plane guided to a target and crashed into it in a power dive, as an airborne counterpart of the naval torpedo, took place in the United States during World War I. In 1916–1917, a prototype called the Hewitt-Sperry Automatic Airplane made a number of short test flights proving that the idea was sound. Twenty pilotless aircraft, called Bugs, were produced and a successful test flight was made in October 1918. After World War I ended, all projects were discontinued except for some experiments with Bugs. This project was dropped in 1925. During the next decade, there was little missile research, but progress in aviation and developments in electronics produced results that were later applied to missiles. In 1936, the Navy began another pilotless aircraft program intended to provide realistic targets for antiaircraft gunnery practice, but which directly influenced missile development. In January 1941, work began on the conversion of a TG-2 (torpedo plane) and a BG-1 (dive bomber) into missiles.

Many missile research and development programs were initiated during World War II. The most advanced were the German surface-to-surface missiles, the V-1 (German FZG-76) and the V-2 (German A-4). V stood for *Vergeltungswaffe* (vengeance weapon). The advent and rapid development of jet aircraft following the World War II changed forever the character of air-to-air combat. It was believed that the high speed and maneuverability of jet aircraft signaled the end of the dogfight and a requirement to engage targets at beyond visual ranges. The solution to this problem was air-to-air or surface-to-air missiles. Post-war research in the upper atmosphere gained a new tool with the advent of high-altitude rockets. The improvement of missile guidance and its accuracy became the most important problem of research and development.

A *guided missile system* is defined as a combination of a guided missile and its launching, guidance, test, and handling equipment.

A *missile guidance system* is defined as a group of components that measures the position of the guided missile with respect to its target and changes the missile flight path in accordance with a guidance law. Usually, the missile guidance system includes sensing, computing, and control components.

A *guidance law* is defined as an algorithm that determines the required commanded missile acceleration.

Guided missile systems have tactical duties similar to those of conventional weapons (guns, rockets, and bombs). However, in conventional weapon systems, information concerning the target

is gathered by observation. After it is evaluated, the weapon is aimed, and the projectile is fired. From the time the bullet or rocket is aimed or the bomb is dropped, the trajectory is strictly dependent upon gravity, wind, and the ballistics of the projectile. The time from launch of the projectile until the hit at the target is called the *time of flight*. In contrast to the bullet, rocket, or bomb, the missile in flight is constantly reaimed based on the target information obtained by sensors. The target is tracked to gain intelligence as to its current position, as well as its future behavior. Advanced guidance systems operate with data also estimating the target acceleration and the predicted intercept point.

In order to guide and control a missile several functions must be achieved:

1. The launch function monitors the launch events sequence and establishes the initial missile position and velocity after launch.
2. The targeting function establishes the basic geometry between the missile and target and operates in the coordinate system relative to which the missile targeting and guidance must be performed.
3. The missile guidance function generates guidance commands directing a missile toward the target.
4. The flight control function converts guidance commands into vehicle response; this function is performed by autopilots. The control actuator of a missile generally consists of thrusters that control the direction of the propulsion subsystem's thrust vector or mechanical devices that move external surfaces of the missile in order to alter the aerodynamic forces acting on it.

Discussion of the principles of missile guidance involves many fields and subfields of science, which are impossible to cover in one book. Our main focus will be on the missile guidance function—the guidance laws that serve as control actions guiding a missile toward the target. All other functions mentioned can be considered as auxiliary ones because, on the one hand, they create conditions for the guidance function operation and, on the other hand, make a missile motion possible in accordance with the guidance function commands.

Guidance is the dynamic process of directing an object toward a given point that may be stationary or moving. Usually, in the case of the stationary point, the guidance process is called *navigation*. Until the twentieth century, this term referred mainly to guiding ships across the seas. The word "navigate" comes from the Latin *navis*, meaning "ship," and *agere*, meaning "to move or direct." Today, however, the word also encompasses the guidance of travel on land, in the air, and in inner or outer space. It means finding the way from one place to another (i.e., guiding toward a stationary point. In this book, we will not distinguish between stationary and moving points and consider the general case of a moving point, which will be called a target).

1.2 GUIDANCE PROCESS

The goal of guidance is to reach a target. When getting to a target, an object's position coincides with a target position. Additional requirements to an object's velocity specify various types of guidance. *Rendezvous* is guidance when an object's velocity equals a target's velocity. Applied to missiles, as guided objects, the goal of guidance is to *intercept* a target. It means that at a certain moment in time a missile's position should coincide with a target's position and target velocity should be sufficient to destroy the target.

The goal of guidance, expressed either with mathematical precision or by using "humanitarian language," should be supported by an adequate rule that is able to realize this goal.

One of the ancient guidance rules, successfully used by mariners wishing to rendezvous each other at sea or sea pirates trying to catch a boat, is called *parallel navigation* ("constant bearing" and "collision course navigation" are also used to characterize this type of guidance). This antique rule required an approach with a constant bearing angle (angle measured horizontally from whatever

direction is pointed) and assumed constant speeds of target and pursuer boats. From a purely geometrical consideration, it is easy to establish what velocity the pursuer should have to reach the target. Parallel navigation is widely used by animals, which, in general, depend on the environment and the task they have to solve. For example, predators and organisms pursuing mates commonly adjust their position to maintain a constant angle with respect to the target.

The rule, obtained many years ago under the assumption of constant velocities, is also applied now to accelerating moving target and objects.

The parallel navigation principle was first used in the Lark missiles in 1950 [2,3]. So-called proportional navigation (PN) was used to implement parallel navigation. Since that time PN has been used in almost all of the world's tactical guided missiles.

In general, missile flight consists of three phases: the boost, midcourse, and homing stages. Guidance at each stage has its own specifics. The boost stage is the part of missile flight between the initial firing and the time when the missile reaches a velocity at which it can be controlled. During the midcourse stage the missile is guided by an external weapon control system. The homing stage corresponds to terminal guidance when the missile-contained system controls the missile flight. Currently, parallel navigation is used mostly at the homing stage. However, it can be applied also at the midcourse stage.

In this book, we will consider the guidance problem as a control problem and characterize guidance laws from the position of control theory. Taking into account that a guidance law controls the flight of an object, that is, it presents a controlled input to the moving object, we should characterize the object from the position of control theory. We will formulate the goal of control and introduce the parameters that describe the object's behavior and the parameters that describe the environment that includes external forces that influence the object's behavior.

Despite the rigorousness and attractiveness of such an approach, it is difficult to present a universal dynamic model of various moving objects pursuing targets. That is why we will first ignore an object's inertia and consider a model of objects ignoring their dynamics. This makes the model, to some degree, "universal." However, the guidance law obtained for this model cannot be considered as the best for various moving objects because it does not consider their dynamics. It will allow us to establish the kind of universal guidance laws that can be later improved based on information concerning the dynamic properties of a concrete moving object.

1.3 MISSILE GUIDANCE

The following consideration is focused on missile guidance. Missile guidance system dynamics will be considered and missile guidance laws will be examined.

Among external factors influencing object behavior, target information is the most important. It has been pointed out that the two basic categories of targets are moving and stationary targets. Missile targets are classified into two broad classes: air targets, usually aircraft or other missiles; and surface targets, which include ships and various objects on the ground. To be destroyed the targets must be detected, identified, and tracked by the missile or associated equipment. All guided missiles, launched to engage moving targets, use units that observe or sense the target. The point of observation may vary. It can be observed from the missile or a station outside the missile. Based on a target observation, its behavioral characteristics can be determined. Stationary targets are usually situated at long range, and the information about them is gathered and presented by intelligence so that the missile trajectory is determined in advance and can be corrected only during its flight. When a stationary target is at short range and guided missiles are used to deliver sufficient destructive power, the information about the target can be obtained by the units that observe and sense the target and by intelligence.

As mentioned above, the goal of missile guidance is to hit a target (i.e., to nullify the distance between a missile and the target). However, this obvious goal is usually accompanied by additional conditions such as minimization of the time of flight or maximization of missile terminal velocity. Such criteria dictate the path (optimal trajectory) on which the guidance system must direct the

missile. In the case of a stationary target, the guidance law, obtained as the solution of an optimal problem, enables us to generate and analyze the optimal trajectory that will require only insignificant corrections during the missile flight. The solution of an optimal problem for a moving target requires information about its future behavior. In the general case, such information is not available, so that optimal guidance problems for moving targets have limited application.

Early missile systems used a variety of guidance laws including beam riders and pursuit guidance. However, proportional navigation proved to be the most versatile and, with suitable modification or augmentation, still remains in use in most contemporary guided missile systems. Many current missile guidance laws are generally based on one of several forms of proportional navigation.

The effectiveness of guidance laws depends on the parameters of a missile's flight control system that realizes the flight control function and characterizes the missile's dynamics. Aerodynamics is part of the missile's airframe subsystem, the other major parts being propulsion and structure. The autopilot receives guidance commands and processes them to controls such as deflections or rates of deflection of control surfaces or jet controls. The control subsystem transfers the autopilot commands to aerodynamic or jet control forces and moments to change the position of the airframe, to attain the commanded maneuver by rotating the body of a missile to a desired angle of attack. The autopilot response should be accomplished quickly with minimum overshoot. Minimum overshoot enables a missile to avoid exceeding structural limitations.

Three types of aerodynamic controls are used: canard (small surface forward on the body), wing (main lifting surface near the body), and tail (small surface far aft on the body) controls. In contrast to the canard and wing controls, the tail steering controls initially give acceleration in a direction opposite to the intended one. The airframe reacts to the control commands with speed depending on the airframe inertia and system damping. The influence of the flight control system on guidance accuracy will be examined in detail.

1.4 REPRESENTATION OF MOTION

We will consider the so-called two-point systems involving a missile M and a target T. In the inertial reference frame of coordinates the positions of M and T are given by the vectors $\boldsymbol{r}_{\mathrm{M}} = (R_{M1}, R_{M2}, R_{M3})$ and $\boldsymbol{r}_{\mathrm{T}} = (R_{T1}, R_{T2}, R_{T3})$, respectively, and the vector $\boldsymbol{r} = (R_1, R_2, R_3)$

$$\boldsymbol{r} = \boldsymbol{r}_{\mathrm{T}} - \boldsymbol{r}_{\mathrm{M}} \tag{1.1}$$

is called the *range*-vector. Its negative derivative, which equals the difference between missile $\boldsymbol{v_M} = (V_{M1}, V_{M2}, V_{M3})$ and target $\boldsymbol{v_T} = (V_{T1}, V_{T2}, V_{T3})$ velocities

$$\dot{\boldsymbol{r}} = -(\dot{\boldsymbol{r}}_{\mathrm{T}} - \dot{\boldsymbol{r}}_{\mathrm{M}}) = \boldsymbol{v}_{\mathrm{M}} - \boldsymbol{v}_{\mathrm{T}} = \boldsymbol{v}_{cl} \tag{1.2}$$

is called the *closing velocity* vector $\boldsymbol{v}_{cl} = (v_{cl1}, v_{cl2}, v_{cl3})$. In future we will use also the *range* r and *closing velocity* v_{cl} (scalars) terms when dealing with absolute values of $\boldsymbol{r}$ and $v_{cl} = -\dot{r}$.

It follows from equations (1.1) and (1.2) that

$$v_{cls} = V_{Ms} - V_{Ts} = \dot{R}_{Ms} - \dot{R}_{Ts} \quad (s = 1,2,3) \tag{1.3}$$

A two-point guidance is said to be *planar* if $\boldsymbol{r}_M$, $\boldsymbol{v}_M$ and $\boldsymbol{r}_T$, $\boldsymbol{v}_T$ remain in the same fixed plane. In general, the guidance process takes place in three-dimensional (3-DOF) space. In some cases, it can be presented as a combination of two orthogonal planar guidance processes.

The solution of the intercept problem requires the utilization of several frames of reference (coordinate axes) to specify relative positions and velocities, forces, accelerations, and so forth.

An inertial fixed reference plane is a necessary part of every dynamic problem. The inertial coordinate system ignores both the gravitational attraction of the sun, moon, and other bodies and the orbital motion of the Earth that exists because of this attraction. In many problems of aerospace dynamics, the orbital motion of the Earth can be neglected, and any reference plane fixed to the Earth can be used as an inertial frame. However, for hypervelocity and space flights the angular velocity of the Earth usually must be taken into account. Two Earth-fixed frames are used: (i) the Earth-centered fixed inertial (ECI) coordinate system with origin at the center of the Earth and axis directions fixed by a reference point on the equator and the Earth's axes; and (ii) the Earth-surface fixed (ESF) coordinate system with origin at the arbitrary Earth surface (usually close to vehicle) with axes directed north, east, and vertically (mostly downward, but sometimes it is convenient to choose the upward direction).

It is more convenient to consider the missile and target motions relative to these inertial coordinate systems. However, missile dynamics are usually analyzed in the missile body-fixed frame, and the tracking process requires a different reference frame.

It is known that a moving object has six degrees of freedom: three translations and three rotations. The principal missile motions of interest to the guidance problem are

1. Translation along the longitudinal axis (velocity)
2. Rotation about the longitudinal axis (roll)
3. Rotation about the lateral horizontal axis (pitch)
4. Rotation about the vertical axis (yaw)

The origin of the body-fixed coordinate system is situated at the missile center of gravity. The orientation of the axes is usually taken to be coincident with principle axes of inertia. These motions are controlled by autopilot in accordance with the guidance law. The so-called vehicle-carried vertical frame, called also the north-east-down (NED) frame, has the origin situated usually at the missile center of gravity and axes directed north, east and vertically downward. It is commonly used for tactical missiles. The NED system is not precisely an inertial coordinate system because the missile axes are slowly changing their orientation in space as the missile moves over the Earth's surface. However, except at the North Pole, the rotational effects are negligible.

During the midcourse and terminal stages guidance commands are based on measurements obtained in various coordinate systems (in addition to the frames mentioned above there exist other frames, for example, atmosphere-fixed and air-trajectory reference frames that are used for specific analysis [1]). There exist transformations from one coordinate system to another.

As indicated above, for analytical investigation the choice of the reference frame is usually a matter of convenience. In atmospheric flights Earth-fixed and vehicle-fixed coordinate systems are commonly used.

The following consideration will be mostly based on analysis of the Earth-surface fixed coordinate system or the NED coordinate system. However, theoretical results should be compared with the simulation results obtained also by using the six-dimensional model of the intercept process that includes and operates with the various coordinate systems.

The position of moving objects is usually determined in polar (spherical) coordinate systems. The position of a target determined by a missile's sensors is typically specified by direction cosines (cosines of the angles that the position vector makes with the coordinate axes, respectively) relative to the missile body axes, which can be transformed to direction cosines (Λ_N, Λ_E, Λ_D), with respect to the NED axes. Target angular position with respect to the NED coordinate system can also be specified by azimuth α and elevation β angles

$$\alpha = -\sin^{-1} \Lambda_D, \quad \beta = \tan^{-1} (\Lambda_E/\Lambda_N) \tag{1.4}$$

The target coordinates (R_N, R_E, R_D) in the NED Cartesian coordinate system can be obtained based on range r and direction cosines (Λ_N, Λ_E, Λ_D):

$$R_N = r\Lambda_N = r \cos \alpha \cos \beta, \quad R_E = r\Lambda_E = r \sin \alpha \cos \beta, \quad R_D = r\Lambda_D = r \sin \beta \tag{1.5}$$

(here the sign of the elevation angle is defined to be positive in the downward direction).

Polar coordinates (r, α, β) are related to the Cartesian coordinates (R_N, R_E, R_D) by

$$r = \sqrt{R_N^2 + R_E^2 + R_D^2}\,, \quad \alpha = \tan^{-1}(R_E / R_N), \quad \beta = -\sin^{-1}(r / R_D) \tag{1.6}$$

In future, the north, east, and vertical coordinates will be denoted by the low indices 1, 2, and 3, respectively. For ground-based defense systems, the missile and target positions are determined relative to the ESF Cartesian coordinate system. The vertical coordinate is target (missile) altitude. In the case of space-based strategic systems, the ECI coordinate system is most convenient. In general, tracking is performed in Cartesian position coordinates. However, for single sensor systems, such as airborne radar, the option to track in spherical coordinates may be considered.

1.5 LINE-OF-SIGHT

In order to view an object, one must sight along a line to that object. The line-of-sight (LOS) that passes through the objective of the guidance is an important concept of guidance. Its orientation with respect to the reference coordinate system enables one to formulate guidance rules precisely.

For the three-dimensional case and the Earth-based coordinate system, the LOS can be represented as

$$\boldsymbol{\lambda}(t) = \lambda_1(t)\boldsymbol{i} + \lambda_2(t)\boldsymbol{j} + \lambda_3(t)\boldsymbol{k} \tag{1.7}$$

where ***i, j,*** and ***k*** are unit vectors along the north, east, and vertical coordinate axes, respectively,

$$\lambda_s(t) = \frac{R_s}{r} \quad (s = 1,2,3) \tag{1.8}$$

R_s (s = 1,2,3) are the range-vector coordinates [see equations (1.1) and also equations (1.3)–(1.7)]. Here, for convenience, we assume that ***k*** is directed upward.

The LOS vector can also be presented as the sum of two vectors in the horizontal **x-y** (north-east) plane and the vertical **x-y** resultant-**z** plane (see Figure 1.1). The LOS's position in the vertical

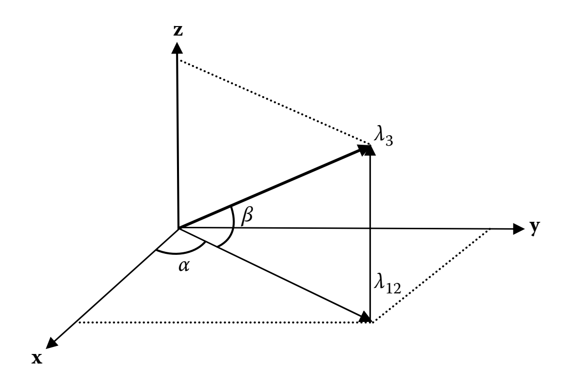


FIGURE 1.1 Three-dimensional presentation of LOS.

plane λ_3 is determined by the elevation angle β. Its position in the horizontal plane is presented by $\lambda_{12} = \cos\beta$ that is determined by the azimuth angle α, so that λ_s coordinates ($s = 1,2,3$) are determined by the expressions that can also be obtained directly from equations (1.6) and (1.9), i.e.,

$$\lambda_1 = \cos\alpha\cos\beta, \quad \lambda_2 = \sin\alpha\cos\beta, \quad \lambda_3 = \sin\beta \tag{1.9}$$

The expressions for the LOS rate in the three-dimensional Cartesian coordinate system

$$\dot{\boldsymbol{\lambda}}(t) = \dot{\lambda}_1(t)\boldsymbol{i} + \dot{\lambda}_2(t)\boldsymbol{j} + \dot{\lambda}_3(t)\boldsymbol{k} \tag{1.10}$$

can be obtained from equations (1.3), (1.7), and (1.8)

$$\dot{\lambda}_s(t) = \frac{\dot{R}_s r - R_s \dot{r}}{r^2} = \frac{V_{Ts} - V_{Ms}}{r} + \frac{R_s v_{cl}}{r^2} \quad (s = 1,2,3) \tag{1.11}$$

where, based on equations (1.3) and (1.8),

$$v_{cl} = -\dot{r} = -\frac{\sum_{s=1}^{3} R_s (V_{Ts} - V_{Ms})}{r} = \frac{\sum_{s=1}^{3} R_s v_{cls}}{r} = \sum_{s=1}^{3} \lambda_s v_{cls} \tag{1.12}$$

When operating with the vertical and horizontal planes, it is convenient to use the vertical R_v and horizontal (ground) R_h ranges and velocities V_v and V_h:

$$R_v = R_3 = r\sin\beta, \quad R_h = \sqrt{R_1^2 + R_2^2} = r\cos\beta, \quad R_1 = R_h\cos\alpha, \quad R_2 = R_h\sin\alpha \tag{1.13}$$

$$V_v = -v_{cl3} = \dot{R}_v, \quad V_h = -v_{clh} = \dot{R}_h = -\frac{\sum_{s=1}^{2} R_s v_{cls}}{R_h} \tag{1.14}$$

$$v_{cl} = -\dot{r} = \frac{R_h v_{clh} + R_v v_{clv}}{r} \tag{1.15}$$

The LOS rate components $\dot{\lambda}_s$ of equation (1.10) can be presented by the polar coordinates α and β by using equation (1.9)

$$\dot{\lambda}_1(t) = \dot{\alpha}\sin\alpha\cos\beta - \dot{\beta}\cos\alpha\sin\beta, \quad \dot{\lambda}_2 = \dot{\alpha}\cos\alpha\cos\dot{\beta} - \beta\sin\alpha\sin\beta, \quad \dot{\lambda}_3(t) = \dot{\beta}\cos\beta \tag{1.16}$$

Using the relationship between the vectors $\boldsymbol{r}(t)$ and $\boldsymbol{\lambda}(t)$

$$\boldsymbol{r}(t) = r(t)\,\boldsymbol{\lambda}(t) \tag{1.17}$$

$$\dot{\boldsymbol{r}}(t) = (\dot{\lambda}_1(t)r + \dot{r}(t)\lambda_1(t))\boldsymbol{i} + (\dot{\lambda}_2(t)r + \dot{r}(t)\lambda_2(t))\boldsymbol{j} + (\dot{\lambda}_3(t)r + \dot{r}(t)\lambda_3(t))\boldsymbol{k} \tag{1.18}$$

$$\ddot{\boldsymbol{r}}(t) = (\ddot{\lambda}_1(t)r(t) + 2\dot{r}(t)\dot{\lambda}_1(t) + \ddot{r}(t)\lambda_1(t))\boldsymbol{i} + (\ddot{\lambda}_2(t)r(t) + 2\dot{r}(t)\dot{\lambda}_2(t) + \ddot{r}(t)\lambda_2(t))\boldsymbol{j}$$
$$+ (\ddot{\lambda}_3(t)r(t) + 2\dot{r}(t)\dot{\lambda}_3(t) + \ddot{r}(t)\lambda_3(t))\boldsymbol{k} \quad (1.19)$$

we can present the equation of motion

$$\ddot{\boldsymbol{r}}(t) = \boldsymbol{a_T}(t) - \boldsymbol{a_M}(t) \quad (1.20)$$

where $\boldsymbol{a_M}(t) = (a_{M1}, a_{M2}, a_{M3})$ and $\boldsymbol{a_T}(t) = (a_{T1}, a_{T2}, a_{T3})$ are the vectors of the missile and target accelerations created by forces acting on the missile and target, respectively.

Missile acceleration is the result of the propulsion forces (thrust), the aerodynamic forces (lift, drag), and gravity forces. In the following chapters this equation will be examined in detail.

REFERENCES

1. Hemsch, M., Tactical missile aerodynamics, *Progress in Astronautics and Aeronautics*, 141, American Institute of Astronautics and Aeronautics, Inc., Washington, DC, 1992.
2. Shneydor, N.A., *Missile Guidance and Pursuit*, Horwood Publishing, Chichester, 1998.
3. Zarchan, P., Tactical and strategic missile guidance, *Progress in Astronautics and Aeronautics*, 176**,** American Institute of Astronautics and Aeronautics, Inc., Washington, DC, 1997.

2 Parallel Navigation

2.1 INTRODUCTION

According to parallel navigation (the "constant bearing") rule the line-of-sight (LOS) direction relative to the inertial coordinate system is kept constant, i.e., during guidance the LOS remains parallel to the initial LOS. Using equations (1.10) and (1.11), this rule can be presented in the form

$$\dot{\boldsymbol{\lambda}}(t) = \dot{\lambda}_1(t)\boldsymbol{i} + \dot{\lambda}_2(t)\boldsymbol{j} + \dot{\lambda}_3(t)\boldsymbol{k} = 0 \tag{2.1}$$

or

$$\dot{R}_s r - R_s \dot{r} = 0 \quad (s = 1, 2, 3) \tag{2.2}$$

The last equation shows that for each moment of time guidance realizing parallel navigation keeps the ratio of $\dot{R}_s$ and R_s ($s = 1, 2, 3$) constant, i.e.,

$$\frac{\dot{R}_1}{R_1} = \frac{\dot{R}_2}{R_2} = \frac{\dot{R}_3}{R_3} = \frac{\dot{r}}{r} \tag{2.3}$$

This means that the vectors $\dot{\boldsymbol{r}}$ and $\boldsymbol{r}$ are collinear and the vectors $\boldsymbol{r}(t)$, $\boldsymbol{v}_M(t)$, and $\boldsymbol{v}_T(t)$ are instantaneously coplanar (the engagement need not be coplanar). The last statement follows immediately from the zero value of the determinant of the 3×3 matrix formed by the above-indicated vectors.

The product of $\dot{r}r = 0.5(r^2)'$ must be negative, otherwise the distance between the missile and target will increase rather than decrease. This is equivalent to $\dot{r} < 0$ or $v_{cl} > 0$.

The character of motion in accordance with the parallel navigation rule can be observed clearly on a fixed plane (see Figure 2.1) by assuming that the target is nonmaneuvering (i.e., $\boldsymbol{a}_T(t) = 0$, and the ratio of speeds v_M and v_T is a constant).

Considering the scalar product of $\dot{\boldsymbol{r}}(t)$ and $\boldsymbol{\lambda}(t)$ in equation (1.2) and taking into account equations (1.10) and (1.18) we obtain

$$\dot{r} = v_T \cos\theta - v_M \cos\delta \tag{2.4}$$

and the condition $\dot{r} < 0$ is equivalent to

$$v_M \cos\delta > v_T \cos\theta \tag{2.5}$$

The collinearity condition (2.3) is equivalent to

$$v_T \sin\theta - v_M \sin\delta = 0 \tag{2.6}$$

If the target is moving with a constant speed and conditions (2.5) and (2.6) are satisfied, a missile with a constant speed will intercept the target by moving in a straight line.

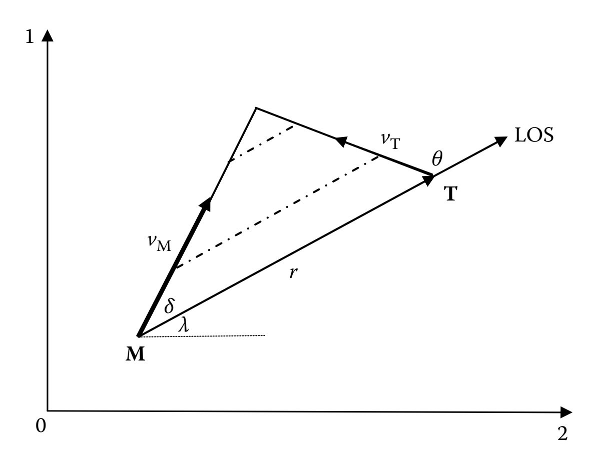


FIGURE 2.1 Geometry of planar engagement.

Figure 2.1 shows an engagement triangle consisting of the missile and target positions, the vectors of their velocities, the LOS, and range vectors. The LOS angle λ is measured with respect to the horizontal reference line 02. The angle δ is called *the lead angle*. The angle $180° - \theta$ is called the *aspect angle*. If conditions (2.5) and (2.6) are satisfied, a missile with an appropriate constant velocity can intercept the nonaccelerating target. The dash-dotted lines show the position of the missile M and target T (the position of the LOS line) according to the parallel navigation rule. The triangle in Figure 2.1 is called the *collision triangle*.

2.2 PROPORTIONAL NAVIGATION. PLANAR ENGAGEMENT

Proportional navigation (PN) guidance is the most widely used law in practice. The basic philosophy behind PN is that missile acceleration should nullify the line-of-sight (LOS) rate between the target and interceptor. Proportional navigation, the guidance law that implements parallel navigation, is based on physical intuition. According to parallel navigation, the LOS rate must be equal to zero. In reality, it differs from zero, so that the guidance command that is proportional to the rate of the LOS change may decrease the absolute value of the LOS rate and it will tend closer to zero. The PN law states that commanded acceleration is proportional to the LOS rate; the proportionality constant can be broken down into the product of the effective navigation ratio N times the relative missile-to-target closing velocity, i.e.,

$$a_c(t) = N v_{cl} \dot{\lambda}(t) \tag{2.7}$$

where $a_c(t)$ is a commanded acceleration acting perpendicular to the instantaneous LOS.

In many tactical endoatmospheric missiles, PN guidance determines the lift that should be created by moving a missile's control surfaces. Exoatmospheric missiles create the acceleration required by the PN law by using thrust vector control, lateral divert engines, or squibs. In tactical radar homing missiles, the LOS rate is measured by the radar seeker. In tactical infrared (IR) missiles equipped with the imaging IR seekers the LOS rate information is obtained by using pattern image scanning techniques. The measurement of the target IR intensity enables the IR seekers to even provide estimates of range and range rate based on the intensity of image data. The future generation of IR seekers will be able to provide these estimates with high accuracy. However, now only radar missiles provide estimates of range and range rate (closing velocity).

The PN guidance problem should be formulated as a three-dimensional control problem. However, by assuming that the lateral and longitudinal maneuver planes are decoupled by means

of roll control, it is possible to reduce the three-dimensional guidance problem to the equivalent two-dimensional planar problems. That is why we discuss the planar problem first.

Denoting the vertical projection of the range-vector ***r*** by y, we can present the LOS angle λ as

$$\sin \lambda = y/r \tag{2.8}$$

For small λ equation (2.8) can be presented approximately as

$$\lambda = y/r \tag{2.9}$$

where $y(t)$ characterizes the displacement between the missile and target at a moment t and is called the miss distance, or simply, *miss*. This expression is widely used in the so-called linearized engagement models.

Analogous to equation (1.11), the approximate value of the LOS rate equals

$$\dot{\lambda} = \frac{\dot{y}r + yv_{cl}}{r^2} \tag{2.10}$$

Assuming the closing velocity to be constant (the missile and target do not maneuver in the future), equations (2.9) and (2.10) can be written as

$$\lambda(t) = \frac{y(t)}{v_{cl}t_{go}} \tag{2.11}$$

$$\dot{\lambda}(t) = \frac{\dot{y}(t)r + y(t)v_{cl}}{r^2} = \frac{\dot{y}(t)t_{go} + y(t)}{v_{cl}t_{go}^2} = \frac{ZEM}{v_{cl}t_{go}^2} \tag{2.12}$$

where $t_{go} = t_F - t$ is the time-to-go until the end of the flight assuming that it will correspond to intercept (t_F is the time at the end of the flight) and

$$ZEM = \dot{y}(t)t_{go} + y(t) \tag{2.13}$$

is called the *zero-effort miss* (i.e., the miss, the future relative separation between missile and target, that would result if the missile does not accelerate and the target does not maneuver after the moment t).

Assuming that by using the acceleration $a_c(t)$ the intercept will take place, ZEM can be considered as the predicted intercept coordinate, and the PN guidance law (2.7) can be rewritten in the following form:

$$a_c(t) = N\frac{\dot{y}(t)t_{go} + y(t)}{t_{go}^2} = N\frac{ZEM}{t_{go}^2} \tag{2.14}$$

By interpreting ZEM as a predicted intercept point, which can be calculated based on some knowledge (or assumptions) of the future motion of the target, the PN guidance law (2.14) can be considered as predictive guidance.

The analytical analysis (see Reference [6] and Chapter 3) shows that for the case of ideal dynamics (i.e., no lags between the LOS rate and the commanded acceleration, the LOS rate is a decreasing function of time converging to zero at the pursuit end). When actual dynamics are considered, PN guidance tends to diverge at the vicinity of interception (i.e., the LOS rate diverges). Despite the assertion of some scientists that this divergence may severely affect the miss distance, we will ignore this fact.

2.3 PROPORTIONAL NAVIGATION. THREE-DIMENSIONAL ENGAGEMENT

As indicated earlier, the three-dimensional motion can be presented as a combination of the orthogonal planar motions (see Figure 1.1).

Using the azimuth α and elevation β angles instead of λ in equation(2.7) we obtain the following accelerations $a_{ch}(t)$ and $a_{cv}(t)$ in the horizontal and vertical planes, respectively.

$$a_{ch}(t) = Nv_{cl}\dot{\alpha}(t), \quad a_{cv}(t) = Nv_{cl}\dot{\beta}(t) \tag{2.15}$$

The total commanded acceleration $a_c(t) = (a_{c1}(t), a_{c2}(t), a_{c3}(t))$ [see equations (1.13) and (2.15)] equals

$$a_{c1}(t) = -a_{ch}(t)\sin\alpha - a_{cv}(t)\cos\alpha\sin\beta, \tag{2.16}$$

$$a_{c2}(t) = a_{ch}(t)\cos\alpha - a_{cv}(t)\sin\alpha\sin\beta, \tag{2.17}$$

$$a_{c3}(t) = a_{cv}(t)\cos\beta \tag{2.18}$$

The components of equations (2.16)–(2.18) are written taking into account that $a_{ch}(t)$ and $a_{cv}(t)$ are perpendicular to the LOS projections in the horizontal and vertical planes, respectively (see also Figure 1.1 and Figure 2.1).

The PN acceleration command that follows directly from equation (1.10) has the following form:

$$\boldsymbol{a}_c(t) = Nv_{cl}\dot{\boldsymbol{\lambda}}(t) \tag{2.19}$$

Taking into account equations (1.16) and (2.15), they can be rewritten as

$$a_{c1}(t) = -a_{ch}(t)\sin\alpha\cos\beta - a_{cv}(t)\cos\alpha\sin\beta, \tag{2.20}$$

$$a_{c2}(t) = a_{ch}(t)\cos\alpha\cos\beta - a_{cv}(t)\sin\alpha\sin\beta, \tag{2.21}$$

$$a_{c3}(t) = a_{cv}(t)\cos\beta \tag{2.22}$$

A slight difference between equations (2.16)–(2.18) and equations (2.20)–(2.22) is stipulated by the restriction on the PN guidance components (2.16)–(2.18). In the case of PN guidance (2.15), we operate with two guidance components $a_{ch}(t)$ and $a_{cv}(t)$ acting in two orthogonal planes. The $a_{cs}(t)$ (s = 1,2,3) components follow from $a_{ch}(t)$ and $a_{cv}(t)$. The PN guidance (2.19) and the expressions (2.20)–(2.22) are free from these restrictions. For small elevation angles the above expressions give very close results.

The horizontal and vertical acceleration commands are linked with the north-east-down (NED) coordinate system and realized in practice by the roll and pitch autopilots, respectively. The α and

β angles are determined by on-board sensors, and the acceleration commands are generated by the missile. This process corresponds to the terminal guidance phase. During the midcourse phase the missile relies on off-board sensors. The guidance components are determined by ground (space)-based defense systems in the Earth-fixed coordinate systems.

The PN guidance law in the Earth-fixed coordinate systems is

$$a_{cs}(t) = N v_{cl} \dot{\lambda}_s(t) \quad (s = 1,2,3) \tag{2.23}$$

where $\dot{\lambda}_s(t)$ and $\boldsymbol{v}_{cl}$ are determined by equations (1.11) and (1.12), respectively.

Analogous to equation (2.14) we can write

$$a_{cs}(t) = N \frac{\dot{R}_s(t)t_{go} + R_s(t)}{t_{go}^2} = N \frac{ZEM_s}{t_{go}^2} \quad (s = 1,2,3) \tag{2.24}$$

where the *zero-effort miss* vector $ZEM = (ZEM_1, ZEM_2, ZEM_3)$

$$ZEM_s = \dot{R}_s(t)t_{go} + R_s(t) \quad (s = 1,2,3) \tag{2.25}$$

is perpendicular to the LOS. This property can be established directly from equations (1.8), (1.11), (2.12), (2.14), (2.25), and the equality

$$\sum_{s=1}^{3} \dot{\lambda}_s \lambda_s = 0.$$

2.4 AUGMENTED PROPORTIONAL NAVIGATION

The basic guidance parameter of the PN law is the LOS rate. Knowledge of range and time-to-go are not required, so PN can be implemented using only angle sensors on board the missile, which is its great advantage. Although the PN guidance law was not derived rigorously with target acceleration as a major consideration, it is applied against maneuvering targets. It is intuitively clear that additional information concerning target acceleration can be a source of improving the efficiency of PN guidance.

The zero-effort miss in equation (2.13) was introduced under the assumption that the missile would not accelerate during t_{go}. In the case of a constant target maneuver with acceleration a_T, the zero-effort miss must be augmented by adding a quadratic term $0.5 a_T t_{go}^2$, i.e.,

$$ZEM = \dot{y}(t)t_{go} + y(t) + 0.5 a_T t_{go}^2 \tag{2.26}$$

By substituting equation (2.26) in equation (2.14) and returning to the basic variables $\dot{\lambda}(t)$ and $\boldsymbol{v}_{cl}$ of the PN law [see equations (2.10)–(2.12)], for planar engagements the augmented proportional navigation (APN) law $a_{aug}(t)$ can be presented as

$$a_{aug}(t) = a_c(t) + 0.5 N a_T = N v_{cl} \dot{\lambda}(t) + 0.5 N a_T \tag{2.27}$$

For the three-dimensional case, the coordinates of the missile-commanded acceleration $\boldsymbol{a}_{aug}(t) = (a_{aug1}, a_{aug2}, a_{aug3})$ and the target acceleration $\boldsymbol{a}_T(t) = (a_{T1}, a_{T2}, a_{T3})$ are related by the following equation:

$$\boldsymbol{a}_{augs}(t) = a_{cs}(t) + 0.5Na_{Ts} \quad (s = 1,2,3) \tag{2.28}$$

Although the APN law was derived assuming step-target maneuvers, it was recommended without rigorous justification, and is used in practice for all types of maneuvering targets.

2.5 PROPORTIONAL NAVIGATION AS A CONTROL PROBLEM

The basic philosophy behind PN guidance, which implements parallel navigation, is that missile acceleration should nullify the LOS rate. However, the realization of this philosophy was based on physical intuition: when the LOS rate differs from zero, an acceleration command proportional to the deviation from zero is created to eliminate this deviation.

Below we will consider the PN as a control problem that realizes the parallel navigation rule $\dot{\lambda}(t) = 0$. First, the linearized planar model of engagement is considered [see Figure 2.1 and the equations (2.10) and (2.11)]. By differentiating equation (2.11) can be rewritten in the form

$$\dot{\lambda}(t) = \frac{\dot{y}(t)r(t) - y(t)\dot{r}(t)}{r^2(t)} = \frac{\dot{y}(t)}{r(t)} - \frac{\lambda(t)\dot{r}(t)}{r(t)} \tag{2.29}$$

$$\ddot{\lambda}(t) = \frac{\ddot{y}(t)r(t) - \dot{y}(t)\dot{r}(t)}{r^2(t)} - \frac{(\dot{\lambda}(t)\dot{r}(t) + \lambda(t)\ddot{r}(t))r(t) - \lambda(t)\dot{r}^2(t)}{r^2(t)}$$

$$= \frac{\ddot{y}(t) - \dot{\lambda}(t)\dot{r}(t) - \lambda(t)\ddot{r}(t)}{r(t)} - \frac{\dot{r}(t)}{r(t)}\frac{(\dot{y}(t) - \lambda(t)\dot{r}(t))}{r(t)}$$

$$= \frac{\ddot{y}(t) - \dot{\lambda}(t)\dot{r}(t) - \lambda(t)\ddot{r}(t) - \dot{\lambda}(t)\dot{r}(t)}{r(t)} = \frac{\ddot{y}(t) - 2\dot{\lambda}(t)\dot{r}(t) - \lambda(t)\ddot{r}(t)}{r(t)} \tag{2.30}$$

and introducing the time-varying coefficients

$$a_1(t) = \frac{\ddot{r}(t)}{r(t)} \tag{2.31}$$

$$a_2(t) = \frac{2\dot{r}(t)}{r(t)} \tag{2.32}$$

$$b(t) = \frac{1}{r(t)} \tag{2.33}$$

expression (2.30) can be presented in the form

$$\ddot{\lambda}(t) = -a_1(t)\lambda(t) - a_2(t)\dot{\lambda}(t) + b(t)\ddot{y}(t) \tag{2.34}$$

Taking into account that

$$\ddot{y}(t) = -a_M(t) + a_T(t) \tag{2.35}$$

equation (2.34) can be transformed in

$$\ddot{\lambda}(t) = -a_1(t)\lambda(t) - a_2(t)\dot{\lambda}(t) - b(t)a_M(t) + b(t)a_T(t) \tag{2.36}$$

Let $x_1 = \lambda(t)$ and $x_2 = \dot{\lambda}(t)$. The missile-target engagement is described by the following system of first-order differential equations:

$$\dot{x}_1 = x_2$$

$$\dot{x}_2 = -a_1(t)x_1 - a_2(t)x_2 - b(t)u + b(t)f \tag{2.37}$$

where control $u = a_M(t)$ and disturbance $f = a_T(t)$.

First, let us consider the case of a nonaccelerating target (i.e., $f = 0$, the assumption that accompanies the main relations used in PN guidance).

The asymptotic stability with respect to x_2 (i.e., lim $x_2 \to 0$, corresponds to the parallel navigation rule, so that the control law that satisfies this condition is the guidance law that implements parallel navigation).

The guidance problem can be formulated as the problem of choosing control u to guarantee the asymptotic stability of system (2.37) with respect to x_2. (Because in reality we deal with a finite problem, for simplicity and a more rigorous utilization of the term "asymptotic stability" we assume disturbance to be a vanishing function, that is, it contains a factor $e^{-\varepsilon t}$, where ε is an infinitely small positive number.)

It is important to mention that the guidance law is determined based on the partial stability of the system dynamics under consideration, only with respect to the LOS derivative [1–3]. The approach for examining asymptotic stability is based on the Lyapunov method (see Appendix A). For equation (2.37), it is natural to choose the Lyapunov function Q as a square of the LOS derivative, i.e.,

$$Q = \frac{1}{2}cx_2^2 \tag{2.38}$$

where c is a positive coefficient.

Its derivative along any trajectory of equation (2.37) equals

$$\dot{Q} = cx_2(-a_1(t)x_1 - a_2(t)x_2 - b(t)u) \tag{2.39}$$

The negative definiteness of equation (2.39), that is, the asymptotic stability of equation (2.35) with respect to x_2, can be presented in the form

$$\dot{Q} = cx_2(-a_1(t)x_1 - a_2(t)x_2 - b(t)u) \le -c_1x_2^2 \tag{2.40}$$

where c_1 is a positive coefficient.

Under the near-collision course assumption (collision course assumes nonaccelerating motion), $\ddot{r}(t) = 0$, that is, $a_1(t) = 0$, and the inequality (2.40) can be written as

$$(-a_2(t) + c_1 / c)x_2^2 - a_1(t)x_1x_2 - b(t)x_2u \le 0 \tag{2.41}$$

It follows from equations (2.40) and (2.41) that for $a_1(t) = 0$ and $c_1 << c$ the control

$$u = kx_2 = k\dot{\lambda}(t) \tag{2.42}$$

stabilizes system (2.37) if k satisfies

$$kb(t) + a_2(t) > 0$$

or

$$k > -\frac{a_2(t)}{b(t)} \tag{2.43}$$

Introducing the closing velocity $v_{cl} = -\dot{r}(t)$ and the effective navigation ratio N, expression (2.43) can be written as $k > 2v_{cl}$ and the control law can be presented as

$$u = Nv_{cl}\dot{\lambda}(t), \quad N > 2 \tag{2.44}$$

which is the well-known property established for the PN guidance law (2.7).

For the three-dimensional case and the Earth-based coordinate system, the LOS and its derivative are presented by equations (1.10) and (1.11), so that analogous to equation (2.36)

$$\ddot{\lambda}_s(t) = -a_1(t)\lambda_s(t) - a_2(t)\dot{\lambda}_s(t) + b(t)(a_{Ts}(t) - u_s) \quad (s = 1,2,3) \tag{2.45}$$

where $\ddot{\lambda}_s$ $(s = 1,2,3)$ are the LOS second derivative coordinates, $a_{Ts}(t)$ $(s = 1,2,3)$ are the coordinates of the target acceleration vector, and $u_s(t)$ are the coordinates of the missile acceleration vector, which are considered as controls.

The Lyapunov function is chosen as the sum of squares of the LOS derivative components that corresponds to the nature of proportional navigation.

$$Q = \frac{1}{2}\sum_{s=1}^{3} d_s\dot{\lambda}_s^2 \tag{2.46}$$

where d_s are positive coefficients.

Its derivative can be presented in the following form:

$$2\dot{Q} = \sum_{s=1}^{3} d_s\ddot{\lambda}_s\dot{\lambda}_s \tag{2.47}$$

or

$$2\dot{Q} = \sum_{s=1}^{3} d_s(-a_1(t)\lambda_s\dot{\lambda}_s - a_2(t)\dot{\lambda}_s^2 + b_1(t)\dot{\lambda}_s(a_{Ts}(t) - u_s)) \tag{2.48}$$

Analogous to the planar engagement, under the near-collision course assumption, the controls $u_s(t)$ that guarantee $\lim\left\|\dot{\lambda}\right\| \to 0$, $t \to \infty$, can be presented as

$$u_s = Nv_{cl}\dot{\lambda}_s, \quad N > 2 \quad (s = 1,2,3) \tag{2.49}$$

which coincides with equation (2.23).

2.6 AUGMENTED PROPORTIONAL NAVIGATION AS A CONTROL PROBLEM

For maneuvering targets and the planar engagement the derivative of the Lyapunov function (2.38) along any trajectory of equation (2.37) equals

$$Q = cx_2(-a_1(t)x_1 - a_2(t)x_2 - b(t)u + b(t)f) \tag{2.50}$$

The negative definiteness of equation (2.39) (i.e., the asymptotic stability of equation (2.37) with respect to x_2) can be presented in the form

$$Q = cx_2(-a_1(t)x_1 - a_2(t)x_2 - b(t)u + b(t)f) \le -c_1x_2^2 \tag{2.51}$$

From the condition of negative definiteness of the derivative of the Lyapunov function (2.51) we can derive the guidance law

$$u = Nv_{cl}\dot{\lambda} + a_T(t), \quad N > 2 \tag{2.52}$$

where the acceleration term is 0.5 N times less than in the augmented PN law obtained for step maneuvers [see equation (2.27)].

Analogously, from equation (2.48) we can obtain the guidance law for the three-dimensional case

$$u_s = Nv_{cl}\dot{\lambda}_s + a_{Ts}(t), \quad N > 2 \quad (s = 1,2,3) \tag{2.53}$$

where the acceleration term is 0.5 N times less than in the augmented PN law obtained for step maneuvers [see equation (2.28)].

The comparison of equations (2.52) and (2.53) with equations (2.27) and (2.28) shows that the APN gain $N/2$ in the target acceleration terms is larger than obtained above based on the Lyapunov approach.

Law (2.53) is given as a possible law to compare with the existing augmented law. Later more general expressions will be given.

2.7 WHEN IS THE PN LAW OPTIMAL?

The PN law (2.7) is a result of a simple logical inference. If the LOS rate differs from zero (i.e., a nonzero error exists), an action proportional to this error should be taken to eliminate it. The more rigorous formulation of the problem of nullifying the LOS rate was given earlier in this chapter, where PN was presented as a control problem. Commanded acceleration was considered as a control and the LOS and its derivative were chosen as the state variables.

In a different way the PN guidance law was considered as a control action in Reference [1]. The 1960s were marked by significant results in optimal control theory. It was shown that linear controls are optimal in the case of systems characterized by linear differential equations and a

quadratic functional as their performance index [3]. For the equation of motion (1.20) [equation (2.35)] (for simplicity we consider here the planar case) such a performance index should be found for which the PN guidance law (2.7) is the optimal control. Problems of this kind are called inverse optimal problems.

Using the near-collision course assumptions, that is, assuming that the missile approaches the target at a constant closing velocity v_{cl}, near a collision course, and ignoring missile dynamics, we can write

$$\ddot{y} = -a_M, \quad y = r\lambda << r, \quad r(\tau) = v_{cl}\tau \tag{2.54}$$

The performance index, or cost functional, is defined as

$$I = \frac{1}{2}(Cy^2(t_F) + \int_0^{t_F} a_M^2(t)dt) \tag{2.55}$$

where C is a constant coefficient, often called weighting factor, and the initial time of flight is zero.

The first term of equation (2.55) presents the miss distance and the second one characterizes the energy spent during the flight. A high C emphasizes the importance of achieving a small miss distance, whereas a small C implies the importance of having sufficient energy at the end of the flight.

The optimal problem consists of finding $a_M(t)$, which minimizes the functional (2.55). The solution of the formulated optimal problem was obtained in [1] (see also Appendix A) as

$$a_M(t) = \frac{3\tau}{3/C + \tau^3}(y(t) + \dot{y}(t)\tau) \tag{2.56}$$

Zero miss corresponds to $C \to \infty$, so that the optimal guidance law becomes

$$a_M(t) = \frac{3}{\tau^2}(y(t) + \dot{y}(t)\tau) \tag{2.57}$$

Taking into account equation (2.12) that can be rewritten as

$$\dot{\lambda}(t) = \frac{y(t) + \dot{y}(t)\tau}{v_{cl}\tau^2}$$

instead of equation (2.57) we have

$$a_M(t) = 3v_{cl}\dot{\lambda}(t) \tag{2.58}$$

This means that under the above assumptions the PN law minimizes the functional (2.55), and the optimal value of the navigation ratio $N = 3$ guarantees zero miss distance. By ignoring missile dynamics and considering a nonmaneuvering target we excessively simplified the guidance problem, so that the above result has a "pure" theoretical rather than practical importance. Difficulties connected with the solution of more realistic guidance problems were mentioned before.

REFERENCES

1. Bryson, A.E., Linear feedback solution for minimal effort intercept rendezvous, and soft landing, *AIAA Journal*, 3, 8, 1542–1548, 1965.
2. Rumyantsev, V.V., On asymptotic stability and instability of motion with respect to a part of the variables, *Journal of Applied Mathematics and Mechanics,* 35, 1, 19–30, 1971.
3. Yanushevsky, R., *Theory of Optimal Linear Multivariable Control Systems*, Nauka, Moscow, 1973.
4. Yanushevsky, R. and Boord, W., New approach to guidance law design, *Journal of Guidance, Control, and Dynamics*, 28, 1, 162–166, 2005.
5. Zadeh, L. and Desoer, C., *Linear System Theory,* McGraw Hill, New York, 1963.
6. Zarchan, P., Tactical and strategic missile guidance, *Progress in Astronautics and Aeronautics*, 176**,** American Institute of Astronautics and Aeronautics, Inc., Washington, DC, 1997.

3 Analysis of Proportional Navigation Guided Missile Systems in the Time Domain

3.1 INTRODUCTION

It is well known that investigation of processes and phenomena is linked, first of all, with the construction of mathematical models describing these processes and phenomena using mathematical language. The model is characterized by some parameters, including input variables or control actions, as they are called, or simply controls, output variables or output coordinates, or controlled variables, and also intermediate variables, the so-called state variables. In most cases processes are not considered in isolation but in direct connection with other processes and phenomena. The influence of external conditions—environment—is characterized by the so-called disturbing influences or, simply, disturbances.

As a matter of fact, the mathematical model is nothing but the analytical expression of an interconnection of the specified parameters. The parameters chosen are determined by the problem under consideration.

In the previous chapter the control theory approach was used to obtain the proportional navigation (PN) guidance law. The line-of-sight (LOS) rate was considered as the system output; the PN law, the commanded missile acceleration, was considered as control, or input; and the target acceleration was considered as disturbance.

Below we will build and analyze the models of PN guided missile systems. The miss distance, the parameter that characterizes the missile guidance system performance, is the system output. The missile and target accelerations are control and disturbance, respectively.

In control theory analytical tools were developed for describing the characteristics of control systems based on the concept of the system error. The goal of control is to reduce the error to the smallest feasible amount. The ability to adjust the transient and steady-state response of a control system to meet certain performance requirements is the main goal of its design. To analyze systems their performance criterion should be defined. Then, based on the desired performance, the parameters of the system and its structure should be adjusted to provide the desired response. Because the actual input signals are usually unknown, a standard test input signal is normally chosen. The time-domain analysis is usually based on the so-called step input.

The miss distance in guidance system analysis and design is, to a certain degree, analogous to the error in conventional control systems. The goal of guidance is to reduce the miss distance to the smallest feasible amount. Target maneuvering plays a major role in determining missile system performance. The miss distance due to a step target maneuver is the miss step response, similar to the well-known time-domain characteristic in control theory. Below we obtain analytical expressions of miss distance for simple models of PN guidance systems. Unfortunately, in the time domain the closed-form solutions cannot be obtained for high-order models realistically reflecting autopilot and airframe dynamics. Nevertheless, the models under consideration enable us to establish some properties of linear models of PN guided missile systems.

3.2 INERTIALESS PN GUIDANCE SYSTEM

Although PN guidance presents a nonlinear control problem, to apply known technique of analysis and design, the system equations are linearized, yielding a linear time-varying system. The linearization is valid when it is assumed that the missile and target approach the so-called collision course. The results of simulation of linear and nonlinear models show that the linearized model faithfully represents the guidance system dynamics, that is, the linearization is valid close to the interception where the closing velocity can be considered constant, so that the range can be approximated by a linear function of time [5].

In the previous chapter we considered equation (2.35) to obtain the expression for the PN guidance law. We will use this equation to analyze the performance of the idealized linearized inertialess model of the PN missile guidance system (2.35). Substituting expression (2.7) into equation (2.35) we have

$$\ddot{y}(t) = -Nv_{cl}\dot{\lambda}(t) + a_T(t) \tag{3.1}$$

After integration of both parts of equation (3.1) and taking into account equations (2.9) and (2.11), it becomes

$$\dot{y}(t) = -Nv_{cl}\lambda(t) + \int a_T(t)dt = -\frac{N}{t_F - t}y(t) + V_T(t) \tag{3.2}$$

The solution of equation (3.2) is presented in the following form

$$y(t) = \frac{1}{M(t)}\left(\int V_T(t)M(t)dt + C\right) \tag{3.3}$$

where C is a constant of integration and

$$M(t) = \exp\left(\int \frac{N}{t_F - t}dt\right) = (t_F - t)^{-N} \tag{3.4}$$

It can be simplified as

$$y(t) = C(t_F - t)^N + \frac{t_F - t}{N-1}a_T(t) - \frac{(t_F - t)^N}{N-1}\int (t_F - t)^{-N+1}a(t)dt \tag{3.5}$$

In the case of a step target maneuver (i.e., $a_T(t) = a_T$) the last expression has the form

$$y(t) = C(t_F - t)^N + \left(\frac{t_F - t}{N-1} - \frac{(t_F - t)^2}{(N-1)(N-2)}\right)a_T \tag{3.6}$$

where the constant C is determined based on the initial conditions for $y(t)$.

The analysis of equation (3.6) enables us to conclude that the miss distance $y(t_F)$ is zero (i.e., PN with the effective navigation ratio $N > 2$ is an effective way to hit a target). To be more rigorous, we should mention that expression (3.6) indicates that only values $N = 1$ and $N = 2$ are dangerous. But by choosing $N > 2$ we guarantee zero miss.

The model of the missile guidance system considered above is too simple to immediately make too optimistic estimates of the PN law performance. Even a slightly more complicated linear model of the missile guidance system (e.g., by presenting autopilot inertia by the first-order dynamic unit) makes the problem of the miss distance analysis very complicated.

The miss distance model for a missile with a first-order acceleration lag τ_1, against a target undergoing a step acceleration maneuver, is described by the following equations:

$$\begin{aligned}
\dot{y}_1 &= y_2 \\
\dot{y}_2 &= a_T - a_M \\
\dot{a}_M &= (a_c - a_M) / \tau_1 \\
\dot{a}_T &= \delta(t) \\
y(t) &= y_1 \\
a_c(t) &= N\left(\frac{y_1}{(t_F - t)^2} + \frac{y_2}{t_F - t}\right)
\end{aligned} \tag{3.7}$$

In this case the commanded acceleration $a_c(t)$ does not coincide with the real missile acceleration $a_M(t)$ and is presented in the form (2.14). A step maneuver $a_T(t)$ at $t = 0$ is described by a differential equation with the delta-function $\delta(t)$ in its right part.

It is impossible to obtain a visible analytical solution $y(t)$ of the above linear equation with time-varying coefficients and singularity at $t = t_F$). The general approach to analysis of this type of equations is the use of simulation tools. Since our main interest lies in analyzing the miss distance $y(t_F)$, it means that we should simulate system (3.7) for various t_F. To avoid multiple simulation trials and obtain $\boldsymbol{y}(t_F)$ in one computer run the method of adjoints is used [4,5]. Moreover, the specific structure of equation (3.7) enables us, based on the method of adjoints, to obtain the analytical solution of equation (3.7) with respect to $\boldsymbol{y}(t_F)$.

3.3 METHOD OF ADJOINTS

The method of adjoints, which is a useful tool for simulating the impulse response $P(\sigma,t)$ of time-varying linear systems for the fixed observation time $\sigma = t_F$ with respect to the impulse application time t, has been widely used in missile guidance system design and analysis, especially for linearized engagement models. An approach to obtaining the adjoint system is based on a structural representation of the guidance system model.

The method of adjoints will be explained on the example of a linear time-varying system described by the system of a differential equation presented in the vector-matrix form

$$\dot{\boldsymbol{y}} = \boldsymbol{A}(t_F - t)\boldsymbol{y} + \boldsymbol{f}, \quad 0 \le t \le t_F \tag{3.8}$$

where $\boldsymbol{y}$ and $\boldsymbol{f}$ are n-dimensional vectors, and $\boldsymbol{A}$ is a matrix with coefficients depending on $t_F - t$.

By introducing the system adjoint to equation (3.8) as

$$\dot{\boldsymbol{x}} = -\boldsymbol{A}^T(t_F - t)\boldsymbol{x} \tag{3.9}$$

it is easy to check that the adjoint vector $\boldsymbol{x}$ satisfies the condition

$$\frac{d(\boldsymbol{x}^T\boldsymbol{y})}{dt} = \boldsymbol{x}^T\boldsymbol{f} \tag{3.10}$$

or

$$\boldsymbol{x}^T(t_F)\boldsymbol{y}(t_F) - \boldsymbol{x}^T(0)\boldsymbol{y}(0) = \int_0^{t_F} \boldsymbol{x}^T(\sigma)\boldsymbol{f}(\sigma)d\sigma \tag{3.11}$$

where the superscript T denotes transposition.

To present the miss distance $\boldsymbol{y}(t_F)$ due to a constant target maneuver, we should put $\boldsymbol{x}^T(t_F) = (1, 0,\ldots,0)$ and $\boldsymbol{f}(t) = \delta(t)$, so that

$$\boldsymbol{y}(t_F) = \boldsymbol{x}^T(0)\boldsymbol{y}(0) \tag{3.12}$$

It is easy to verify that the transition matrix of the adjoint system (3.9) $\boldsymbol{\Phi}_a(t,t_0) = \boldsymbol{\Phi}^T(t_0,t)$, where $\boldsymbol{\Phi}(t,t_0)$ is the transition matrix of equation (3.8).

For the class of guidance problems under investigation we should present disturbances (target acceleration and other external factors) as the result of the solution of a system of differential equations. As seen from equation (3.7), for the case of a step acceleration maneuver (see the condition $\dot{\boldsymbol{f}}(t) = \delta(t)$), it reduces to a simple operation of differentiation.

The initial conditions $\boldsymbol{x}(0)$ of the adjoint system (3.9) can be obtained by integrating equation (3.9) backward in time or by considering the modified adjoint system with respect to time $\tau = t_F - t$, i.e., the miss distance $y(t_F)$ can be obtained in one run by simulating the system

$$\dot{\boldsymbol{z}} = \boldsymbol{A}^T(\tau)\boldsymbol{z}, \quad y(t_F) = \boldsymbol{z}^T(t_F)\boldsymbol{y}(0) \tag{3.13}$$

where $z^T(0) = (1, 0,\ldots,0)$.

For equation (3.7) the modified adjoint system has the following form:

$$\begin{aligned}
\dot{z}_1 &= \frac{N}{\tau_1\tau^2} z_3 \\
\dot{z}_2 &= z_1 + \frac{N}{\tau_1\tau} z_3 \\
\dot{z}_3 &= -z_2 - \frac{1}{\tau_1} z_3 \\
\dot{z}_4 &= z_2
\end{aligned} \tag{3.14}$$

with the initial condition $z^T(0) = (1, 0,\ldots,0)$.

The matrix of coefficients of equation (3.13) is transposed with respect to the matrix $\boldsymbol{A}(t_F - t)$ of the initial system (3.8). Hence, the adjoint modified system can be modeled by changing inputs by outputs and vice versa in all elements of the initial system (3.8) and by changing time t in the arguments of all time-varying coefficients by $t_F - t$. Changing inputs by outputs is equivalent to the following structural changes: nodes of the original system become summation units of the modified adjoint system; summation units of the original system become nodes of the modified adjoint system;

the direction of all signal flow is reversed. In addition, as mentioned above, the structural changes of the original system may be needed to convert its actual input to the equivalent impulsive input.

By differentiating the second equation of system (3.14), it can be transformed to

$$\ddot{z}_2 = \frac{N}{\tau_1 \tau} \dot{z}_3 \tag{3.15}$$

Using the Laplace transform and substituting z_3 from the third equation of (3.14), equation (3.15) can be presented as

$$\frac{d}{ds}(s^2 Z_2(s)) = \frac{Ns^2}{s(\tau_1 s + 1)} Z_2(s)$$

or

$$\frac{d}{ds} X(s) = NH(s)X(s) \;, \tag{3.16}$$

where s is the symbol of the Laplace transform,

$$X(s) = s^2 Z_2(s) \tag{3.17}$$

$$H(s) = \frac{1}{s(\tau_1 s + 1)} = \frac{W(s)}{s} \tag{3.18}$$

The solution of equation (3.16) can be presented as

$$X(s) = s^2 Z_2(s) = C \exp(\int NH(s)ds) = C(\frac{s}{s + 1/\tau_1})^N \tag{3.19}$$

where C is a constant determined by the initial conditions.

From the last equation of system (3.14) we obtain

$$Z_4(s) = s^{-3} C(\frac{s}{s + 1/\tau_1})^N = s^{-1} X(s) \tag{3.20}$$

The constant $C = 1$ is determined from the condition $z_1(0) = \dot{z}_2(0) = 1$, which follows from the first two equations of (3.14), so that $\lim_{s\to\infty} s^2 Z_2(s) = \lim_{s\to\infty} X(s) = 1$ and equation (3.20) becomes

$$Z_4(s) = s^{-3} (\frac{s}{s + 1/\tau_1})^N \tag{3.21}$$

Taking into account equations (3.13) and (3.21), for the effective navigation ratio $N = 4$ the miss distance due to the unit step target acceleration can be shown to be

$$y(t_F) = t_F^2 \exp(-t_F / \tau_1)(0.5 - t_F / 6\tau_1) \tag{3.22}$$

The block-diagram of the original missile guidance system (3.7) is given in Figure 3.1 (D denotes the operator of differentiation).

The adjoint system (3.14) structure is presented in Figure 3.2.

The above block diagrams of the original (3.7) and adjoint (3.14) systems for the unit step target acceleration $a_T = 1$ can be simplified. Their simplified form, based on equations (2.10)–(2.14), is presented in Figure 3.3 and Figure 3.4, respectively.

The modified systems are more convenient for analysis. The modified original system operates directly with the LOS $\lambda = y/(v_{cl}\tau)$ and its derivative. The modified adjoint system corresponds to the transformation (3.16)–(3.18); the closing velocity v_{cl} is shown in Figure 3.4 to correspond fully to Figure 3.3.

The result of simulation of the adjoint system shown in Figure 3.5 for $\tau_1 = 0.5\ s$ and $a_T = 1g$ (the acceleration of gravity $g = 9.81\ m/s^2$) presents the miss step response of the missile guidance system.

As seen in Figure 3.5, in contrast to the idealized linearized inertialess model (3.1) the miss distance of the inertial missile guidance system (3.7) is not zero. The acceleration time lag τ_1 influences significantly the miss step characteristic. It is obvious [see, e.g., equation (3.22)] that the miss distance is smaller for smaller τ_1.

The analysis of the analytical expressions (3.6) and (3.22) for the miss distance due to a step target maneuver allows us to conclude that despite the commanded acceleration of the linearized PN guidance system model [see equation (3.7)] tends to infinity when t tends to t_F, it does not influence significantly the miss distance $y(t_F)$; it does not influence the idealized inertialess model at all.

The miss step response is one of the most used estimates of missile system performance. It is an important time-domain characteristic of missile guidance systems that allows designers to choose appropriate parameters of the missile guidance system to minimize the miss step. The method of adjoints was developed to simplify the simulation procedure. However, the necessity to simulate the system response for each impulse application time by using the model of the original system or using the adjoint system to simplify this procedure was stipulated by the inability

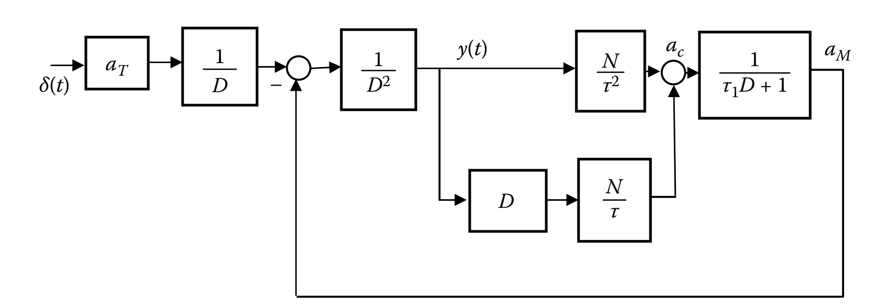


FIGURE 3.1 Block diagram of original guidance system.

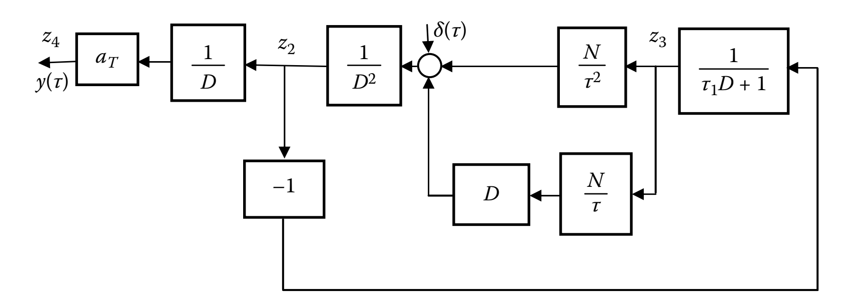


FIGURE 3.2 Block diagram of adjoint system.

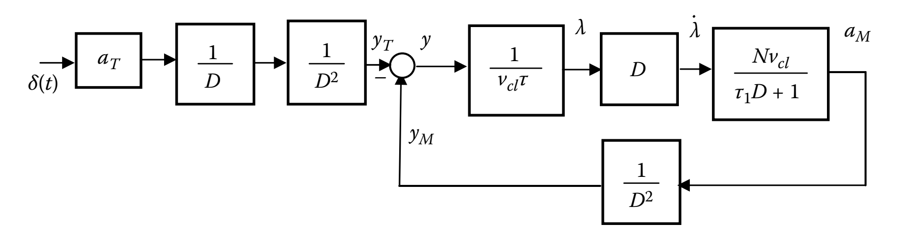


FIGURE 3.3 Modified block diagram of original guidance system.

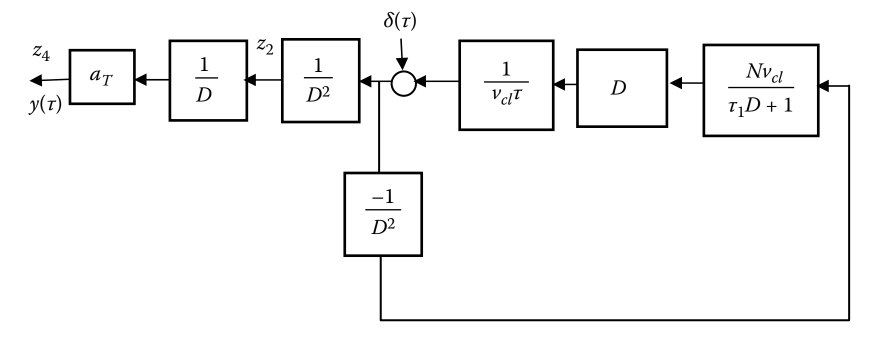


FIGURE 3.4 Modified block diagram of adjoint system.

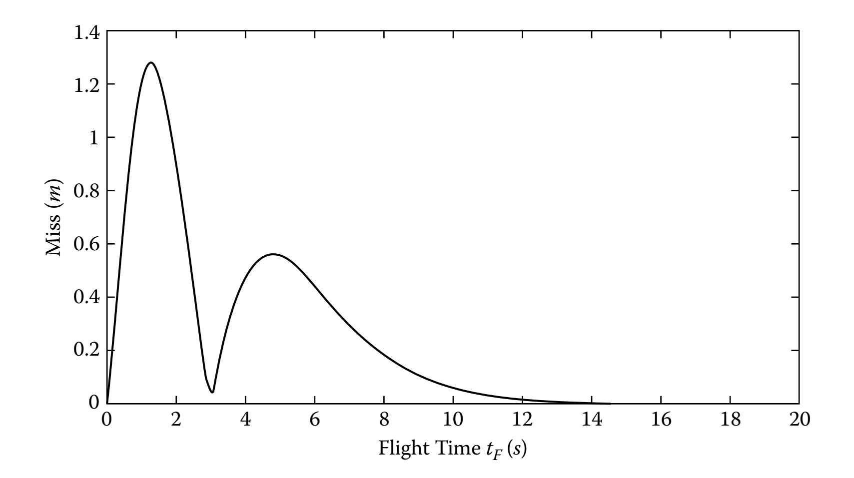


FIGURE 3.5 Miss distance for step target maneuver.

to obtain an analytical expression for the miss step that can be used for analysis and design of missile guidance systems.

The zero and single lag guidance systems are convenient analytical models, but they do not quite match reality. The binomial representation $1/(1 + sT/n)^n$, where T is the effective guidance system time constant and n the system order, used for more accurate high-order guidance system models in [5], still does not accurately reflect flight control system dynamics. The binomial units are usually used to approximate delay units [3] and, therefore, they cannot be considered a reliable tool for guidance system design.

Because of the inability to obtain analytical expressions for the miss step for the high-order planar models, the simulation process using the method of adjoints still remains a very useful tool

for time-domain analysis. The analytical difficulties do not allow researchers to build and analyze more complicated models that also include the dynamics of a maneuvering target. The frequency approach to analysis and design of missile guidance systems, described in the next chapter, enables us to overcome the difficulties mentioned above.

REFERENCES

1. Yanushevsky, R. and Boord, W., New approach to guidance law design, *Journal of Guidance, Control, and Dynamics*, 28, 1, 162–166, 2005.
2. Yanushevsky, R., Concerning Lyapunov-based guidance, *Journal of Guidance, Control, and Dynamics*, 29, 2, 509–511, 2006.
3. Yanushevsky, R., Optimal control of differential-difference systems of neutral type, *International Journal of Control*, 1, 1835–1850, 1989.
4. Zadeh, L. and Desoer, C., *Linear System Theory,* McGraw Hill, New York, 1963.
5. Zarchan, P., Tactical and strategic missile guidance, *Progress in Astronautics and Aeronautics*, 176, American Institute of Astronautics and Aeronautics, Inc., Washington, DC, 1997.

4 Analysis of Proportional Navigation Guided Missile Systems in the Frequency Domain

4.1 INTRODUCTION

The difficulty of the analysis of differential equations with time-varying coefficients describing linearized models of guidance systems is that it does not allow researchers to obtain analytical expressions for miss distance that can be effectively utilized in practice. As mentioned in Reference [10], "the disadvantage of the single time constant representation of a missile guidance system is that the miss distance can be seriously underestimated." The same remark can also be applied to the binomial representation.

The method of adjoints used in the previous chapter can be presented in integral form as the impulse response of the adjoint system (i.e., its reaction to a unit impulse function). In the case of a single time-constant guidance system, the transfer function between the target acceleration and the guidance system miss distance can be obtained from equation (3.21). In control theory, the method of transfer functions, as input–output characteristics of linear systems, is the foundation of frequency methods (i.e., analysis of systems in the frequency domain). Analogous to the unit step signal in the time domain, the unit sinusoidal input signal is the standard test signal in the frequency domain. The response of the system to a changing frequency is considered. The frequency response is defined as the steady-state response of the system to a sinusoidal input signal. The frequency approach is very popular among engineers because the design of a system in the frequency domain provides the designer with control of the bandwidth of a system. It is very physical and enables researchers and designers to build realistic models and make justifiable simplifications.

The following analysis of the linearized proportional navigation (PN) guidance system model is based on the frequency response of the linearized guidance system, which corresponds to the miss distance due to a weaving target (i.e., due to sinusoidal acceleration). As shown later, miss due to a step target maneuver (i.e., the miss step response) can also be obtained from the frequency characteristics of the system under consideration.

The block diagram of an interceptor's main subsystems is given in Figure 4.1.

The seeker provides a guidance system with target information, which together with information from onboard sensors, is necessary to generate a guidance law. The guidance system generates acceleration commands for the autopilot channels to control the motion of the missile. The warhead subsystem receives a burst-hit command from the guidance system. Performance of the guided missile systems is assessed by their terminal effect. The generation and intelligent control of this "terminal effect" is one of the key requirements of missile systems.

The above-mentioned subsystems are interconnected. The performance of a separate subsystem dictates requirements to the interconnected ones. For example, the missile airframe parameters determine the airframe poles ω_z that significantly influence missile dynamics and, as a result, influence autopilot system τ_1 characteristic requirements. Higher accuracy guidance and autopilot

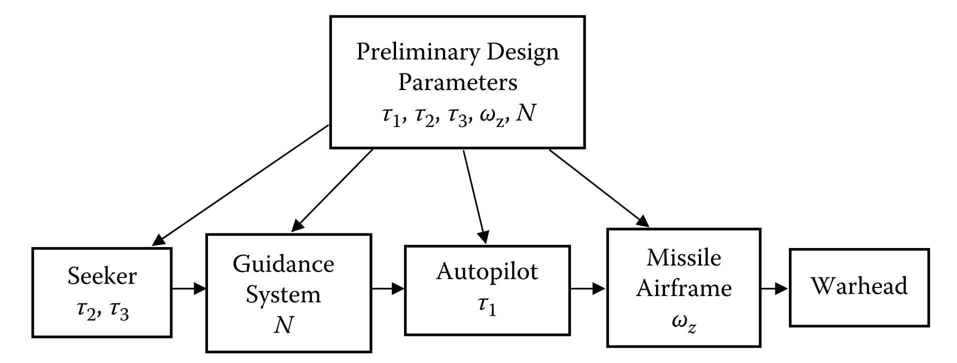


FIGURE 4.1 Block diagram of an interceptor's main subsystem.

systems can employ smaller warheads. The seeker dynamic parameters τ_2 and τ_3 influence the guidance system accuracy. The traditional approach to designing missile guidance and autopilot systems usually neglects the interaction between these systems and treats individual missile subsystems separately. The subsystems are designed separately and then integrated before verifying their performance. The quantification of the impact of missile parameters on the miss distance is the first important step toward integrated design of missile guidance and autopilot systems. The main factors that influence the miss distance in homing missiles are the seeker errors, aeroframe characteristics, autopilot lag τ_1, and target maneuvers. An appropriate choice of the estimation system parameters (in Figure 4.1 it is combined with a seeker and presented by τ_2 and τ_3) can reduce requirements to a seeker's accuracy and a guidance law effective navigation ratio N. The above shows the importance of establishing an analytical relationship between the miss distance and main parameters of the missile guidance system.

The analytical expressions for the miss distance (frequency response) and related expressions for missile system performance are obtained below for the PN law and the guidance control system that reflects the most important characteristics of the flight control system that combines airframe and autopilot dynamics (damping, natural frequency, time constant, and airframe zero frequency). The obtained analytical expressions need to employ significantly simpler computational programs than by using the method of adjoints to analyze the influence of the basic guidance system parameters on the miss distance for step and weave maneuvers.

4.2 ADJOINT METHOD. GENERALIZED MODEL

As shown earlier, the method of adjoints is a useful tool for simulating the impulse response of the system (i.e., its response to an impulse function). The analysis in the time domain was bounded by the consideration of a step target acceleration signal. Because the frequency-domain analysis uses a different test signal, it is convenient to consider a more general model of the adjoint system commonly used in modern control theory.

In contrast to equations (3.8), (3.9), and (3.13), here we present the equations of the system in a more general form than in equation (3.8). We will consider the so-called canonical form used in modern control theory

$$\dot{\boldsymbol{x}}(t) = \boldsymbol{A}(t)\boldsymbol{x}(t) + \boldsymbol{B}(t)\boldsymbol{u}(t) \qquad y(t) = \boldsymbol{C}(t)\boldsymbol{x}(t) \tag{4.1}$$

where the state equation similar to equation (3.8) is accompanied by the output equation; $\boldsymbol{x}(t)$ is the state vector, $\boldsymbol{u}(t)$ and $\boldsymbol{y}(t)$ are the input (control) and output, respectively; and $\boldsymbol{A}(t)$, $\boldsymbol{B}(t)$, and $\boldsymbol{C}(t)$ are matrices of appropriate dimensions.

The adjoint system of equations has the form

$$\dot{z}(t) = -\boldsymbol{A}^T(t)z(t) + \boldsymbol{C}^T(t)\boldsymbol{v}(t) \quad w(t) = \boldsymbol{B}^T(t)z(t) \tag{4.2}$$

where $\boldsymbol{z}(t)$, $\boldsymbol{v}(t)$, and $\boldsymbol{w}(t)$ are the state vector, input, and output, respectively.

Similar to the relationship between the transition matrices of the original and adjoint systems, the impulse response matrices $\boldsymbol{P}(t,\sigma)$ of equation (4.1) and $\boldsymbol{P}_a(t,\sigma)$ of equation (4.2) are connected by

$$\boldsymbol{P}_a(t,\sigma) = \boldsymbol{P}^T(\sigma,t) \tag{4.3}$$

The structure of the original and the adjoint system is shown in Figure 4.2 (note the reversal of flow direction of signals). For the single input–output systems and for $\sigma = t_F$ we have $\boldsymbol{P}(t_F,t) = \boldsymbol{P}_a(t,t_F)$, i.e., $\boldsymbol{P}(t_F,t)$ corresponds to the reaction of the adjoint system to the delta function $\delta(t - t_F)$, that is, to the δ function applied at time t_F. In contrast to the physically realizable initial system in equation (4.1) with $\boldsymbol{P}(t_F,t) = 0$ for $t_F < t$ (it is also called *causal* or *nonanticipative*, as the system output does not anticipate future values of the input) the adjoint system in equation (4.2) with $\boldsymbol{P}_a(t,t_F) = 0$ for $t > t_F$ is physically unrealizable (it is also called *pure anticipative* [9]). To operate with the physically realizable adjoint system we will consider the dynamics of equation (4.2) with respect to time $\tau = t_F - t$. The modified adjoint system has the impulse response $\boldsymbol{P}_{ma}(t_F - \tau,0)$, $0 \le \tau \le t_F$, and is described by the following equations

$$\dot{z}(\tau) = \boldsymbol{A}^T(t_F - \tau)z(\tau) + \boldsymbol{C}^T(t_F - \tau)\boldsymbol{v}(\tau) \quad w(\tau) = \boldsymbol{B}^T(t_F - \tau)z(\tau) \tag{4.4}$$

The structure of the modified adjoint system is shown in Figure 4.3. It follows from the comparison of Figure 4.1 and Figure 4.3, that to build the modified adjoint system we should

(i) replace t by $t_F - \tau$ in all arguments of all time-varying coefficients;
(ii) reverse all signal flow, redefining nodes as summing junctions and vice versa.

Instead of equation (4.3) we can write

$$\boldsymbol{P}_{ma}^T(t_F - \tau,0) = \boldsymbol{P}(t_F,\tau) \tag{4.5}$$

that is, the impulse response $\boldsymbol{P}(t_F,\tau)$ can be obtained by applying the delta function $\delta(\tau)$ in the modified adjoint system.

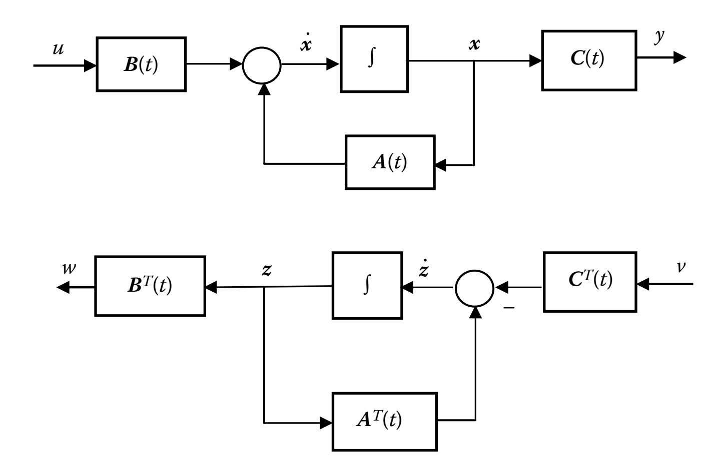


FIGURE 4.2 Original and adjoint systems.

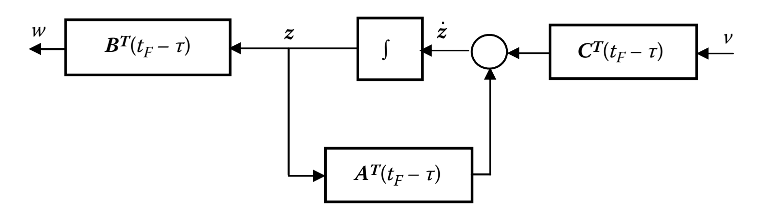


FIGURE 4.3 Modified adjoint system.

The state, input, and output matrices of equation (3.7) presented in the form of equation (4.1) are

$$A = \begin{vmatrix} 0 & 1 & 0 \\ 0 & 0 & -1 \\ \dfrac{N}{\tau_1 \tau^2} & \dfrac{N}{\tau_1 \tau} & \dfrac{-1}{\tau_1} \end{vmatrix} \quad B = \begin{bmatrix} 0 \\ 1 \\ 0 \end{bmatrix} \quad C = \begin{bmatrix} 1\,0\,0 \end{bmatrix} \tag{4.6}$$

It follows from equation (4.3) that the output of the adjoint system is $w(\tau) = z_2 = \boldsymbol{P}(t_F,\tau)$, where $\boldsymbol{P}(t_F,\tau)$ is the impulse response to $a_T(t)$ at time t_F. Specifics of the linearized models of missile guidance systems that contain a time-varying coefficient depending on $t_F - t$ [see, e.g., equation (3.8)] enable us to use the method of adjoints not only as a simulation tool but also to obtain analytical expressions for the impulse response. As seen from equations (4.1) and (4.3), for a class of linear time-varying systems with the state matrix $\boldsymbol{A}(t) = \boldsymbol{A}(t_F - t)$, the state matrix of the modified adjoint system $\boldsymbol{A}(t_F - \tau) = \boldsymbol{A}(\tau)$ depends on adjoint time τ, rather than directly on t_F. In this case, the impulse response of the modified adjoint system does not depend directly on t_F, and the adjoint time $0 \le \tau \le t_F$ can be interpreted as time of flight t_F. For this class of system we will denote the impulse response as $P(t_F,t)$.

The block diagram of the system with the state, input, and output matrices in equation (4.6) and $W(s) = (\tau_1 s + 1)^{-1}$ shown in Figure 4.4 is similar to Figure 3.3. The input-output relationships in the frequency domain are characterized by the transfer functions of the corresponding units, which will be analyzed in detail later. Based on the above, the relationship between the target trajectory $y_T(t)$, the target acceleration $a_T(t)$, and the miss distance $y(t_F)$ can be obtained from the analysis of the block diagram of the modified adjoint system in Figure 4.5, which for $W(s) = (\tau_1 s + 1)^{-1}$ is similar to Figure 3.4.

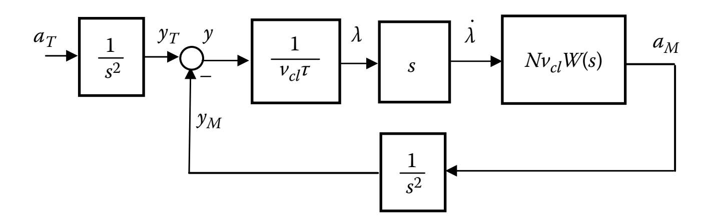


FIGURE 4.4 Modified block diagram of original system.

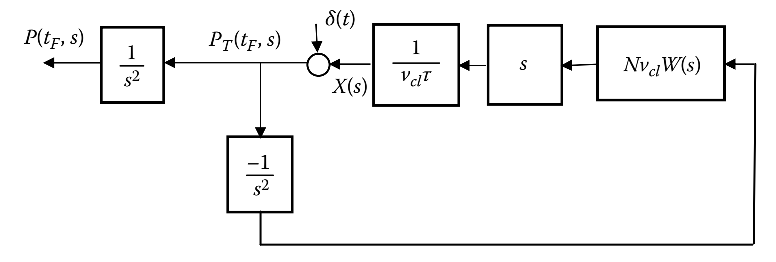


FIGURE 4.5 Modified block diagram of adjoint system.

As mentioned earlier, a simple first-order transfer function representation with time constant τ_1 does not accurately describe the relationship between the line of sight (LOS) rate and the missile acceleration. The transfer function $W(s)$ should reflect the dynamic responses of the airframe, autopilot, guidance filters, and seeker. However, the more complicated $W(s)$ does not change the structure of Figure 4.5. Analyzing this structure we will obtain the analytical expression for the transfer function $P(t_F,s)$, corresponding to the impulse response $P(t_F,t)$, and the transfer function $P_T(t_F,s)$, corresponding to the impulse response $P_T(t_F,t)$ to $y_T(t)$.

Let $X(\tau)$ be the impulse response of the closed loop of the structure in Figure 4.5. Then taking into account equation (3.18), the closed-loop dynamics can be presented as

$$\frac{1}{\tau}\int_0^{\tau} NH(\tau-\sigma)(\delta(\sigma)-X(\sigma))d\sigma = X(\tau) \tag{4.7}$$

or using the Laplace transform

$$\int_s^{\infty} NH(q)(1-X(q))dq = X(s) \tag{4.8}$$

Differentiating equation (4.8) we obtain

$$-\frac{d(1-X(s))}{ds} = NH(s)(1-X(s)) \tag{4.9}$$

which is similar to equation (3.16). Taking into account that $P_T(t_F,s) = 1 - X(s)$ we can write similar to equation (3.19)

$$P_T(t_F,s) = \exp(\int_{\infty}^{s} NH(\sigma)d\sigma) \tag{4.10}$$

and, correspondingly,

$$P(t_F,s) = \frac{1}{s^2}\exp(\int_{\infty}^{s} NH(\sigma)d\sigma) = \frac{1}{s^2}P_T(t_F,s) \tag{4.11}$$

where the lower infinite limit in equations (4.10) and (4.11) follows from the condition $\lim_{s\to\infty} P_T(t_F,s) = 0$.

The step miss equals the integral of the impulse response (i.e., in the frequency domain it corresponds to $s^{-1}P(t_F,s)$). It is easy to check that for the first-order system it coincides with the expression for $Z_4(s)$ obtained in the previous chapter [see equation (3.20)]. However, the above approach is not limited to determining only the miss step, the miss distance due to a step target maneuver. It will be used to determine the miss distance for a wide class of target maneuvers.

4.3 FREQUENCY DOMAIN ANALYSIS

First we consider the fourth-order flight control system, which is widely used in the initial stage of analysis and design. Then the obtained expressions will be generalized for the n-th order system.

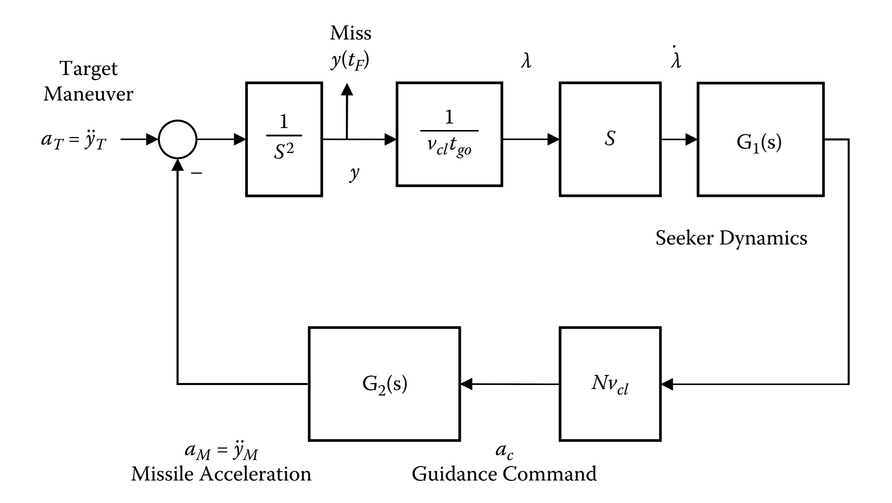


FIGURE 4.6 Missile guidance model.

A block diagram of the guidance system under consideration is given in Figure 4.6. Here, missile acceleration a_M is subtracted from target acceleration a_T, and the result is integrated to obtain the relative separation between a missile and target y, which at the end of flight t_F is the miss distance $y(t_F)$. Division by range (closing velocity v_{cl} multiplied by time-to-go t_{go} until intercept) yields the geometric LOS angle λ, where the time-to-go is defined as $t_{go} = t_F - t$. The missile seeker is presented formally as a perfect differentiator that effectively provides a measurement of the rotation rate of LOS from the interceptor to the target. The filter and seeker dynamics are represented by a transfer function

$$G_1(s) = \frac{\tau_z s + 1}{\tau_2 s + 1},$$

where τ_z and τ_2 are constant coefficients. An estimation of the LOS rate generates a guidance command a_c based on the proportional navigation law with the effective navigation ratio $N > 2$.

The flight control system guides the missile to follow this acceleration command.

The flight control system dynamics, which combine its airframe and autopilot dynamics, are represented by the following transfer function:

$$G_2(s) = \frac{a(s)}{(1+\tau_1 s)(\frac{s^2}{\omega_M^2} + \frac{2\zeta}{\omega_M} s + 1)} \quad (4.12)$$

where

$$a(s) = 1 - \frac{s^2}{\omega_z^2}$$

for tail-controlled missiles and $a(s)$ is a first-order polynomial for nontail-controlled missiles; the flight control system damping ζ, natural frequency ω_M, time constant τ_1, and airframe zero ω_z are the flight control system parameters.

According to equation (4.10), in the complex domain, the miss distance at time t_F can be presented as

$$Y(t_F, s) = \exp(N \int_{\infty}^{s} H(\sigma)d\sigma) Y_T(s) \tag{4.13}$$

where $Y_T(s)$ is the Laplace transform of a target vertical position $y_T(t)$, $Y(t_F,s)$ is the Laplace transform of $y(t_F)$, and similar to equation (3.18)

$$H(s) = \frac{W(s)}{s} \tag{4.14}$$

$$W(s) = G_1(s) * G_2(s) = \frac{1 + r_1 s + r_2 s^2 + r_3 s^3}{(1+\tau_1 s)(1+\tau_2 s)(1 + \frac{2\zeta}{\omega_M}s + \frac{s^2}{\omega_M^2})} \tag{4.15}$$

where r_k ($k = 1,\ldots,3$) are constant coefficients.

The integral $\int_{\infty}^{i\omega} H(\sigma)d\sigma$ can be calculated by writing $H(s)$ in the form

$$H(s) = \frac{A}{s} + \frac{B_1/\tau_1}{s + 1/\tau_1} + \frac{B_2/\tau_2}{s+1/\tau_2} + \frac{Cs + D}{\frac{s^2}{\omega_M^2} + \frac{2\zeta}{\omega_M}s + 1} \tag{4.16}$$

where the coefficients A, B_1, B_2, C, and D can be calculated as

$$\begin{aligned}
&A = 1 \\
&B_1 = \frac{\tau_1^2 - r_1\tau_1 + r_2 - \frac{r_3}{\tau_1}}{(1 - \frac{\tau_2}{\tau_1})(\frac{2\zeta}{\omega_M} - \tau_1 - \frac{1}{\tau_1\omega_M^2})} \\
&B_2 = \frac{\tau_2^2 - r_1\tau_2 + r_2 - \frac{r_3}{\tau_2}}{(1 - \frac{\tau_1}{\tau_2})(\frac{2\zeta}{\omega_M} - \tau_2 - \frac{1}{\tau_2\omega_M^2})} \\
&C = -\frac{1}{\omega_M^2} - \frac{B_1}{\tau_1\omega_M^2} - \frac{B_2}{\tau_2\omega_M^2} \\
&D = r_1 - B_1 - B_2 - (\tau_1 + \tau_2) - \frac{2\zeta}{\omega_M}
\end{aligned} \tag{4.17}$$

For $\tau_2 = 0$

$$B_2 = 0 \quad \text{and} \quad \lim_{\tau_2 \to 0} \frac{B_2}{\tau_2\omega_M^2} = -\frac{r_3}{\tau_1} \tag{4.18}$$

If also $\tau_1 = 0$ and $r_3 = 0$, then

$$B_1 = 0 \quad \text{and} \quad \lim_{\tau_1 \to 0} \frac{B_1}{\tau_1\omega_M^2} = -r_2 \tag{4.19}$$

To obtain the transfer function $P(t_f,s)$ of the guidance system with respect to a target acceleration the components of equation (4.16) of the integral $\int_{\infty}^{i\omega} H(\sigma)d\sigma$ should be calculated.

The upper limit of integration of the first three terms of equation (4.16) gives, respectively,

$$\ln s, \quad \frac{B_1}{\tau_1}\ln(s+1/\tau_1) \quad \text{and} \quad \frac{B_2}{\tau_2}\ln(s+1/\tau_2).$$

The integral of the last term of equation (4.16) can be presented as

$$\int_{\infty}^{s} \frac{Cs+D}{\frac{s^2}{\omega_M^2}+\frac{2\zeta}{\omega_M}s+1}ds = \int_{\infty}^{s} \frac{C\omega_M^2 s + D\omega_M^2}{s^2+2\omega_M\zeta s+\omega_M^2}ds =$$

$$\frac{C\omega_M^2}{2}\ln(s^2+2\omega_M\zeta s+\omega_M^2) - \int_{\infty}^{s} \frac{\omega_M^2(\zeta\omega_M C - D)}{s^2+2\omega_M\zeta s+\omega_M^2}ds =$$

$$\frac{C\omega_M^2}{2}\ln(s^2+2\omega_M\zeta s+\omega_M^2) + \omega_M^2(D-\zeta\omega_M C)\frac{1}{\omega_M\sqrt{1-\zeta^2}}\,Arc\tan\frac{s+\zeta\omega_M}{\omega_M\sqrt{1-\zeta^2}} = \tag{4.20}$$

$$\frac{C\omega_M^2}{2}\ln(s^2+2\omega_M\zeta s+\omega_M^2) + \omega_M^2(D-\zeta\omega_M C)\frac{1}{\omega_M\sqrt{1-\zeta^2}}\frac{1}{2i}\ln\frac{i\omega_M\sqrt{1-\zeta^2}-(s+\zeta\omega_M)}{i\omega_M\sqrt{1-\zeta^2}+(s+\zeta\omega_M)}$$

Based on equations (4.13), (4.15), and (4.20), the upper limit of equation (4.13) for

$$Y_T(s) = \frac{1}{s^2}a_T(s)$$

and $a_T(s) = g$ can be presented as

$$P(t_F,s)$$

$$= gs^{N-2}\prod_{k=1}^{2}(s+\frac{1}{\tau_k})^{B_kN/\tau_k}(s^2+2\omega_M\zeta s+\omega_M^2)^{CN\omega_M^2/2}\left(\frac{-s-\zeta\omega_M+i\omega_M\sqrt{1-\zeta^2}}{s+\zeta\omega_M+i\omega_M\sqrt{1-\zeta^2}}\right)^{\frac{N\omega_M(D-\zeta\omega_M C)}{2i\sqrt{1-\zeta^2}}} \tag{4.21}$$

The lower infinite limit of integration of equation (4.13) for the transfer function of equation (4.15) with the degree of its numerator less than the degree of its denominator equals zero, as will be explained later in detail (see also Reference [5]), and the above equation represents the transfer function characterizing the relationship between the miss distance and target acceleration.

The frequency response of the guidance system follows from equation (4.21) when $s = i\omega$. For $s = i\omega$ the last term of equation (4.20) can be written as

$$-i\frac{\omega_M(D-\zeta\omega_M C)}{2\sqrt{1-\zeta^2}}\ln\frac{i(-\omega+\omega_M\sqrt{1-\zeta^2})-\zeta\omega_M}{i(\omega+\omega_M\sqrt{1-\zeta^2})+\zeta\omega_M} = \text{Re}(.)+i\text{Im}(.) \tag{4.22}$$

where

$$\mathrm{Re}(.) = \frac{\omega_M(D-\zeta\omega_M C)}{2\sqrt{1-\zeta^2}}(\tan^{-1}\frac{\omega-\omega_M\sqrt{1-\zeta^2}}{\zeta\omega_M} - \tan^{-1}\frac{\omega+\omega_M\sqrt{1-\zeta^2}}{\zeta\omega_M}) \quad (4.23)$$

and

$$\mathrm{Im}(.) = -\frac{\omega_M(D-\zeta\omega_M C)}{4\sqrt{1-\zeta^2}}\ln(\frac{\omega_M^2+\omega^2-2\omega\omega_M\sqrt{1-\zeta^2}}{\omega_M^2+\omega^2+2\omega\omega_M\sqrt{1-\zeta^2}}) \quad (4.24)$$

Here the symbol "Acrtan" is used to denote the inverse tangent function of the complex variable and the symbol "$\tan^{-1}$" denotes the inverse tangent function of the real variable, which characterizes the argument of the complex variable of the logarithmic function.

By substituting equations (4.22)–(4.24) in equation (4.13) we can present the last factor of equation (4.21) for $s = i\omega$ in the following form (it follows directly from equation (4.21) based on the definition of complex exponents [2])

$$(\frac{-i\omega-\zeta\omega_M+i\omega_M\sqrt{1-\zeta^2}}{i\omega+\zeta\omega_M+i\omega_M\sqrt{1-\zeta^2}})^{\frac{N\omega_M(D-\zeta\omega_M C)}{2i\sqrt{1-\zeta^2}}} = \exp(N\,\mathrm{Re}(.))\exp(iN\,\mathrm{Im}(.)) \quad (4.25)$$

The amplitude and frequency characteristics of the guidance system follow immediately from equations (4.21)–(4.25).

The amplitude characteristic $|P(t_F, i\omega|$ has the following form:

$$|P(t_F,i\omega)| = g\omega^{N-2}\prod_{k=1}^{2}(\omega^2+1/\tau_k^2)^{B_k N/2\tau_k}((\omega_M^2-\omega^2)^2+4\omega_M^2\omega^2\zeta^2)^{CN\omega_M^2/4}\exp(.) \quad (4.26)$$

where

$$\exp(.) = \exp(N\frac{\omega_M(D-\zeta\omega_M C)}{2\sqrt{1-\zeta^2}}(\tan^{-1}\frac{\omega-\omega_M\sqrt{1-\zeta^2}}{\zeta\omega_M} - \tan^{-1}\frac{\omega+\omega_M\sqrt{1-\zeta^2}}{\zeta\omega_M})) \quad (4.27)$$

The phase characteristic $\varphi(t_F, i\omega)$ has the following form:

$$\varphi(t_F,i\omega) = -\pi + N\frac{\pi}{2} + N\frac{B_1}{\tau_1}\tan^{-1}(\omega\tau_1) + N\frac{B_2}{\tau_2}\tan^{-1}(\omega\tau_2)$$
$$+N\frac{C}{2}\omega_M^2\tan^{-1}(\frac{2\omega\omega_M\zeta}{\omega_M^2-\omega^2}) - \frac{\omega_M(D-\zeta\omega_M C)}{4\sqrt{1-\zeta^2}}\ln(\frac{\omega_M^2+\omega^2-2\omega\omega_M\sqrt{1-\zeta^2}}{\omega_M^2+\omega^2+2\omega\omega_M\sqrt{1-\zeta^2}}) \quad (4.28)$$

The first factor of equation (4.25) corresponds to exp(.) in equation (4.27), and the second factor corresponds to the last term of the phase characteristic.

The above expressions were obtained for the fourth-order model. Below we generalize them assuming that the flight control system has an arbitrary n-th order. Instead of equation (4.15) we have

$$W(s) = G_1(s) * G_2(s) = \frac{1 + \sum_{k=1}^{n-1} r_k s^k}{\prod_{q=1}^{l} (1 + \tau_q s) \prod_{j=1}^{m} (1 + \frac{2\zeta_j s}{\omega_j} + \frac{s^2}{\omega_j^2})} \tag{4.29}$$

where $l + 2m = n$; $l = 2$ and $m = 1$ correspond to the denominator of equation (4.15); r_k ($k = 1,\ldots, n-1$) are constant coefficients.

The partial-fraction expansion of $H(s)$ has the form

$$H(s) = \frac{A}{s} + \sum_{q=1}^{l} \frac{B_q / \tau_q}{s + 1/\tau_q} + \sum_{j=1}^{m} \frac{C_j s + D_j}{\frac{s^2}{\omega_j^2} + \frac{2\zeta_j s}{\omega_j} + 1} = \frac{A}{s} + \sum_{p=1}^{n} \frac{K_p}{s - \alpha_p} \tag{4.30}$$

where α_p ($p = 1,..,n$) are the poles of $W(s)$ (for simplicity they are assumed to be distinct) and the coefficients A, B_q, C_j, D_j, and K_p can be calculated as

$$K_p = \lim_{s \to \alpha_p} (s - \alpha_p) H(s), \quad A = \lim_{s \to 0} sH(s) = W(0) = 1; \tag{4.31}$$

for the real poles $\alpha_p = -1/\tau_p$

$$B_q = K_q \tau_q; \tag{4.32}$$

for the pair of complex-conjugated poles $\alpha_{p,p+1} = -\zeta_p \omega_p \pm i\omega_p \sqrt{1 - \zeta_p^2}$ the coefficients K_p and K_{p+1} are also complex-conjugated, so that from equation (4.30) and

$$\frac{\operatorname{Re} K_p + i \operatorname{Im} K_p}{s + \zeta_p \omega_p + i\omega_p \sqrt{1 - \zeta_p^2}} + \frac{\operatorname{Re} K_p - i \operatorname{Im} K_p}{s + \zeta_p \omega_p - i\omega_p \sqrt{1 - \zeta_p^2}} =$$

$$2 \frac{\operatorname{Re} K_p s + \zeta_p \omega_p \operatorname{Re} K_p + \omega_p \sqrt{1 - \zeta_p^2} \operatorname{Im} K_p}{s^2 + 2\zeta_p \omega_p s + \omega_p^2}$$

we have

$$C_j = \frac{2 \operatorname{Re} K_p}{\omega_p^2}, \quad D_j = \frac{2(\zeta_p \operatorname{Re} K_p + \sqrt{1 - \zeta_p^2} \operatorname{Im} K_p)}{\omega_p}, \quad p = 2j - 1 \tag{4.33}$$

The transfer function $P(t_F,s)$ for the n-dimensional flight control system is

$$P(t_F, s) =$$

$$g s^{N-2} \prod_{k=1}^{l} (s + \frac{1}{\tau_k})^{\frac{B_k N}{\tau_k}} \prod_{j=1}^{m} (s^2 + 2\omega_j \zeta_j s + \omega_j^2)^{\frac{C_j N \omega_j^2}{2}} \left(\frac{-s - \zeta_j \omega_j + i\omega_j \sqrt{1 - \zeta_j^2}}{s + \zeta_j \omega_j + i\omega_j \sqrt{1 - \zeta_j^2}}\right)^{\frac{N\omega_j (D_j - \zeta_j \omega_j C_j)}{2i\sqrt{1 - \zeta_j^2}}} \tag{4.34}$$

The frequency response of the guidance system follows from equation (4.34) when $s = i\omega$. The amplitude characteristic $|P(t_F,i\omega)|$ has the following form:

$$|P(t_F,i\omega)| = g\omega^{N-2}\prod_{k=1}^{l}(\omega^2+1/\tau_k^2)^{\frac{B_kN}{2\tau_k}}\prod_{j=1}^{m}((\omega_j^2-\omega^2)^2+4\omega_j^2\omega^2\zeta_j^2)^{C_jN\omega_j^2/4}\exp(.) \quad (4.35)$$

where

$$\exp(.) = \exp(N\sum_{j=1}^{m}\frac{\omega_j(D_j-\zeta_j\omega_jC_j)}{2\sqrt{1-\zeta_j^2}}(\tan^{-1}\frac{\omega-\omega_j\sqrt{1-\zeta_j^2}}{\zeta_j\omega_j}-\tan^{-1}\frac{\omega+\omega_j\sqrt{1-\zeta_j^2}}{\zeta_j\omega_j})) \quad (4.36)$$

The phase characteristic $\varphi(t_F,i\omega)$ has the following form:

$$\varphi(t_F,i\omega) = -\pi+N\frac{\pi}{2}+N\sum_{k=1}^{l}\frac{B_k}{\tau_k}\tan^{-1}(\omega\tau_k)+$$

$$N\sum_{j=1}^{m}\frac{C_j}{2}\omega_j^2\tan^{-1}(\frac{2\omega\omega_j\zeta_j}{\omega_j^2-\omega^2})-\frac{\omega_j(D_j-\zeta_j\omega_jC_j)}{4\sqrt{1-\zeta_j^2}}\ln(\frac{\omega_j^2+\omega^2-2\omega\omega_j\sqrt{1-\zeta_j^2}}{\omega_j^2+\omega^2+2\omega\omega_j\sqrt{1-\zeta_j^2}}) \quad (4.37)$$

Equations (4.35)–(4.37) follow immediately from the expressions below, which present the generalization of equations (4.22)–(4.27)

$$\sum_{j=1}^{m}-i\frac{\omega_j(D_j-\zeta_j\omega_jC_j)}{2\sqrt{1-\zeta_j}}\ln\frac{i(-\omega+\omega_j\sqrt{1-\zeta_j^2})-\zeta_j\omega_j}{i(\omega+\omega_j\sqrt{1-\zeta_j^2})+\zeta_j\omega_j} = \mathrm{Re}(.)+i\,\mathrm{Im}(.) \quad (4.38)$$

where

$$\mathrm{Re}(.) = \sum_{j=1}^{m}\frac{\omega_j(D_j-\zeta_j\omega_jC_j)}{2\sqrt{1-\zeta_j^2}}(\tan^{-1}\frac{\omega-\omega_j\sqrt{1-\zeta_j^2}}{\zeta_j\omega_j}-\tan^{-1}\frac{\omega+\omega_j\sqrt{1-\zeta_j^2}}{\zeta_j\omega_j}) \quad (4.39)$$

$$\mathrm{Im}(.) = \sum_{j=1}^{m}-\frac{\omega_j(D_j-\zeta_j\omega_jC_j)}{4\sqrt{1-\zeta_j^2}}\ln(\frac{\omega_j^2+\omega^2-2\omega\omega_j\sqrt{1-\zeta_j^2}}{\omega_j^2+\omega^2+2\omega\omega_j\sqrt{1-\zeta_j^2}}) \quad (4.40)$$

and

$$\prod_{j=1}^{m}(\frac{-i\omega-\zeta_j\omega_j+i\omega_j\sqrt{1-\zeta_j^2}}{i\omega+\zeta_j\omega_j+i\omega_j\sqrt{1-\zeta_j^2}})^{\frac{N\omega_M(D-\zeta\omega_MC)}{2i\sqrt{1-\zeta^2}}} = \exp(N\,\mathrm{Re}(.))\exp(iN\,\mathrm{Im}(.)) \quad (4.41)$$

Based on equation (4.21), analogous to equations (4.35) and (4.37), for the amplitude $|P_T(t_F,i\omega)|$ and phase $\varphi_T(t_F,i\omega)$ characteristics of $P_T(t_F,i\omega$ we have

$$|P_T(t_F,i\omega)| = \omega^N\prod_{k=1}^{l}(\omega^2+1/\tau_k^2)^{\frac{B_kN}{2\tau_k}}\prod_{j=1}^{m}((\omega_j^2-\omega^2)^2+4\omega_j^2\omega^2\zeta_j^2)^{C_jN\omega_j^2/4}\exp(.) \quad (4.42)$$

and

$$\varphi_T(t_F,i\omega) = N\frac{\pi}{2} + N\sum_{k=1}^{l}\frac{B_k}{\tau_k}\tan^{-1}(\omega\tau_k) +$$

$$N\sum_{j=1}^{m}\frac{C_j}{2}\omega_j^2\tan^{-1}\left(\frac{2\omega\omega_j\zeta_j}{\omega_j^2-\omega^2}\right) - \frac{\omega_j(D_j-\zeta_j\omega_jC_j)}{4\sqrt{1-\zeta_j^2}}\ln\left(\frac{\omega_j^2+\omega^2-2\omega\omega_j\sqrt{1-\zeta_j^2}}{\omega_j^2+\omega^2+2\omega\omega_j\sqrt{1-\zeta_j^2}}\right) \quad (4.43)$$

The real and imaginary parts of $P(t_F,i\omega)$ and $P_T(t_F,i\omega)$ are

$$\mathrm{Re}\left[P(t_F,i\omega)\right] = \left|P(t_F,i\omega)\right|\cos(\varphi(t_F,i\omega)),$$
$$\mathrm{Re}\left[P_T(t_F,i\omega)\right] = \left|P_T(t_F,i\omega)\right|\cos(\varphi_T(t_F,i\omega)) \quad (4.44)$$

$$\mathrm{Im}\left[P(t_F,i\omega)\right] = \left|P(t_F,i\omega)\right|\sin(\varphi(t_F,i\omega)),$$
$$\mathrm{Im}\left[P_T(t_F,i\omega)\right] = \left|P_T(t_F,i\omega)\right|\sin(\varphi_T(t_F,i\omega)) \quad (4.45)$$

The obtained analytical expressions for the missile guidance system transfer function and its frequency characteristics enable us to analyze the missile system performance without resorting to simulation using adjoint models in the time domain.

4.4 STEADY-STATE MISS ANALYSIS

Frequency approach also enables us to analyze the steady-state miss for various types of maneuvers analogous to the analysis of the steady-state mode in control theory [3]. As is known, the steady-state solution may be a good approximation for sufficiently large values of time.

For the step maneuver the steady-state miss $Miss_s$ is determined as

$$Miss_s = P(t_F,s)\big|_{s=0} \quad (4.46)$$

It follows from equations (4.21) and (4.34) that $Miss_s = 0$ if $N \geq 2$.

For the ramp maneuver

$$Miss_s = \frac{d}{ds}(P(t_F,s))\big|_{s=0} \quad (4.47)$$

It follows from equations (4.21) and (4.34) that $Miss_s = 0$ if $N \geq 3$.

For the parabolic maneuver

$$Miss_s = \frac{d^2}{ds^2}(P(t_F,s))\big|_{s=0} \quad (4.48)$$

It follows from equations (4.21) and (4.34) that $Miss_s = 0$ if $N \geq 4$.

For weave maneuvers the miss steady-state response is determined directly from the frequency response in equations (4.26)–(4.28), (4.35)–(4.37), (4.44), and (4.45).

4.5 WEAVE MANEUVER ANALYSIS

Maneuvers present the best strategy for missiles to achieve their goals. Evasive maneuvers are one of the most effective defense penetration features used on offensive missiles. The evasive maneuver causes the interceptor to expend additional energy, so that it becomes unable to reach the necessary point of engagement. As a result, interceptor miss distances are inevitable and subsequently intolerable, especially for hit-to-kill missiles. If designed properly, the maneuver can render the entire defense system useless. As indicated in References [7,8], sinusoidal or weave maneuvers of a target can make it particularly difficult for a pursuing missile to engage the threat. Targets with very low weaving frequency appear as targets with "near-constant" maneuvers and in many cases will cause no problems for a PN guidance system. Targets with very high weaving frequencies also cause minimal problems for a missile guidance system because there is very little resultant target displacement as a result of maneuver. The miss distance increases between these target-weaving frequency extremes. The existence of the optimal maneuvering frequency, that is, the frequency that maximizes the steady-state miss distance amplitude, was established in Reference [5].

The above closed-form solution for the miss distance as a function of the effective navigation ratio, guidance system time constant, natural frequency, and damping ratio makes it possible to use frequency analysis in practice. The established existence of the optimal evasive weave frequency and the procedure for determining it lead to the optimization approach for the design of attacking maneuvering missiles, as well as to the evaluation of the worst-case scenario when developing defensive missiles to defeat maneuvering targets.

First, we consider the simplest dynamic model of the missile guidance system with $W(s) = (\tau_1 s + 1)^{-1}$. As it follows from equations (4.26) and (4.28), the amplitude and phase characteristics $|P(t_F, i\omega)|$ are

$$|P(t_F, i\omega)| = g\omega^{N-2}(\omega^2 + 1/\tau_1^2)^{B_1 N/2\tau_1} \tag{4.49}$$

$$\varphi(t_F, i\omega) = -\pi + N\frac{\pi}{2} + N\frac{B_1}{\tau_1}\tan^{-1}(\omega\tau_1) \tag{4.50}$$

where $B_1 = -\tau_1$.

The steady-state miss distance due to a weaving target with a frequency ω can be presented in the time domain as

$$y(t_F) = |P(t_F, i\omega)|\sin(\omega t_F + \varphi(t_F, i\omega)) \tag{4.51}$$

For example, for $N = 3$ we have

$$y(t_F) = \frac{g\omega}{(\omega^2 + 1/\tau_1^2)^{1.5}}\sin(\omega t_F + \pi/2 - 3\tan^{-1}(\omega\tau_1)) \tag{4.52}$$

For $\tau_1 = 0.5$ s the peak miss as a function of a target frequency is shown in Figure 4.7.

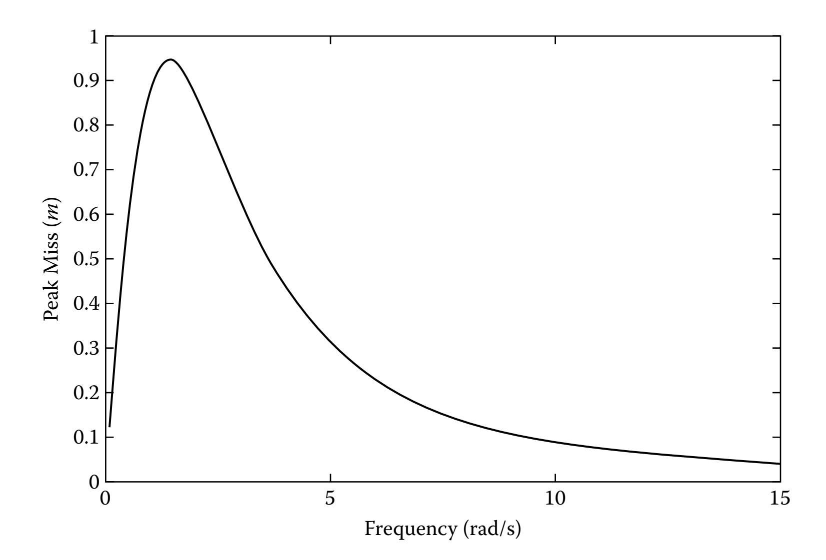


FIGURE 4.7 Peak miss distance for 1-g target maneuver amplitude.

The maximum magnitude of the steady-state miss distance 0.93 *m* corresponds to a target frequency 1.5 *rad/s* (i.e., the weaving period is 4.2 *s*).

4.6 EXAMPLE

To illustrate the effectiveness of the approach described above we consider a realistic example of a tail-controlled aerodynamic missile operating at high altitude [5,12].

The flight control dynamics are assumed to be presented by a third-order transfer function with damping $\zeta = 0.7$ and natural frequency $\omega_M = 20$ *rad/s*, the flight control system time constant $\tau_1 = \tau = 0.5$ *s*; and the right-half plane zero $\omega_z = 5$ *rad/s* corresponds to high altitudes of missile flight. The filter and seeker dynamics are neglected ($G_1(s) = 1$) and perfect estimation of the LOS rate is assumed to generate a guidance command a_c based on the PN law, so that in equation (3.34) $\tau_2 = 0$, $r_1 = 0$, $r_3 = 0$ and $r_2 = -1/\omega_z^2$.

The flight control system of a tail-controlled endoatmospheric missile with the indicated parameters was considered in Reference [12]. It was shown that at high altitude the performance of a tail-controlled aerodynamic missile can deteriorate because of the existence of low-frequency right half-plane zeroes ω_z.

Table 4.1 shows the influence of the flight control system parameters on the miss amplitude and the optimal weaving frequency ω_{opt}; deviations were considered with respect to the values used in Figure 4.7. As seen from Table 4.1, the peak miss decreases drastically when $\omega_z \geq 10$ *rad/s*, but right half-plane zeroes do not significantly influence the optimal weaving frequency. The increase of the amplitude miss for smaller values of time constant and larger values of damping and natural frequency is stipulated by the unsatisfactory dynamic properties of the flight control system (peak overshoot, settling time, and so forth).

The frequency analysis enables us to evaluate the miss without simulation of the guidance system. Moreover, the miss for weave maneuvers, which are more realistic than step maneuvers, can be analyzed directly from the analytical expressions for the frequency response given above. They allow us to examine the influence of the guidance system parameters on the missile system performance.

TABLE 4.1
Influence of Flight Control System Parameters on Optimal Weaving Frequency and Peak Miss Distance

Case Number	ω_z rad/s	τ s	ζ	ω_M rad/s	Peak miss m	ω_{opt} rad/s
1	5	0.5	0.7	20	234	1.4
2	10	0.5	0.7	20	7.9	1.3
3	20	0.5	0.7	20	3.4	1.3
4	100	0.5	0.7	20	2.8	1.3
5	5	0.2	0.7	20	22100	4.5
6	5	0.6	0.7	20	151	1.2
7	5	0.7	0.7	20	115	1.0
8	5	0.5	0.6	20	265	1.4
9	5	0.5	0.8	20	208	1.4
10	5	0.5	0.7	10	33.8	1.3
11	5	0.5	0.7	30	2325	1.5

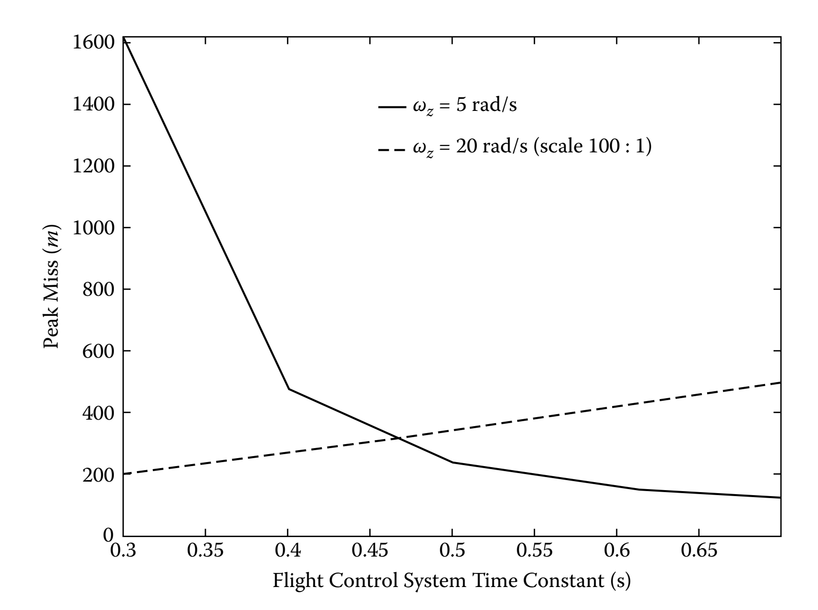


FIGURE 4.8 Relationship between the maximum miss and the flight control system time constant.

The model of the flight control system in equation (3.1) is more precise than the binomial model considered in References [6,10,11]. The results obtained based on this model are more reliable.

For example, the larger effective guidance time constant in binomial models gives the larger miss [10,11]. However, for the given example, because of the significant influence of the right-half plane zero $\omega_z = 5$ *rad/s*, the decrease of the flight control system time constant τ increases the miss. The solid line in Figure 4.8 presents the relationship between the maximum miss and τ obtained from equation (4.26) for $\omega_z = 5$ *rad/s* and demonstrates tail-controlled missile performance problems at very high altitudes. For lower altitudes (i.e., for higher values of ω_z), the maximum miss decreases with the decrease of τ (see dashed line in Figure 4.8 for $\omega_z = 20$ *rad/s*; for this case the maximum miss scale is 100:1).

4.7 FREQUENCY ANALYSIS AND MISS STEP RESPONSE

There exists a relationship between the frequency response and the step response [3] that enables us to use frequency analysis to build the miss step response based on the frequency response of the missile guidance system.

The relationship between the transfer function and the impulse response of the missile guidance system is described by

$$P(t_F,s) = \int_0^\infty P(t_F,t)e^{-st}dt \tag{4.53}$$

Assuming $s = i\omega$, we obtain the expressions that relate the frequency and impulse response

$$P(t_F,i\omega) = \int_0^\infty P(t_F,t)e^{-i\omega t}dt \tag{4.54}$$

$$P(t_F,t) = \frac{1}{2\pi}\int_{-\infty}^\infty P(t_F,i\omega)e^{\omega t}d\omega \tag{4.55}$$

which are valid only for a stable $P(t_F,s)$; otherwise the integral of the right part of equation (4.54) would diverge.

By presenting

$$P(t_F,i\omega) = \mathrm{Re}\left[P(t_F,i\omega)\right] + i\,\mathrm{Im}\left[P(t_F,i\omega)\right] \tag{4.56}$$

and taking into account that

$$e^{i\omega t} = \cos\omega t + i\sin\omega t$$

the expression for the impulse response can be written as

$$\begin{aligned} P(t_F,t) = {} & \frac{1}{2\pi}\int_{-\infty}^\infty (\mathrm{Re}[P(t_F,i\omega)]\cos\omega t - \mathrm{Im}[P(t_F,i\omega)]\sin\omega t)d\omega \\ & + \frac{1}{2\pi}\int_{-\infty}^\infty (\mathrm{Re}[P(t_F,i\omega)]\sin\omega t + \mathrm{Im}[P(t_F,i\omega)]\cos\omega t)d\omega \end{aligned} \tag{4.57}$$

The integrand of the second integral is an odd function of frequency ω, so that this integral equals zero. The integrand of the first integral is an even function of frequency ω, so that this integral can be changed by the double value of the integral with limits 0 and ∞, i.e.,

$$P(t_F,t) = \frac{1}{\pi}\int_0^\infty (\mathrm{Re}[P(t_F,i\omega)]\cos\omega t - \mathrm{Im}[P(t_F,i\omega)]\sin\omega t)d\omega \tag{4.58}$$

Taking into account the condition of physical realization

$$P(t_F,t) \equiv 0 \quad \text{for } t \le 0$$

i.e.,

$$P(-t_F,t) = \frac{1}{\pi}\int_0^\infty (\mathrm{Re}[P(t_F,i\omega)]\cos(-\omega t) - \mathrm{Im}[P(t_F,i\omega)]\sin(-\omega t))d\omega = 0$$

or

$$P(-t_F,t) = \frac{1}{\pi}\int_0^\infty (\mathrm{Re}[P(t_F,i\omega)]\cos\omega t + \mathrm{Im}[P(t_F,i\omega)]\sin\omega t)d\omega = 0 \tag{4.59}$$

and adding equations (4.58) and (4.59) we obtain

$$P(t_F,t) = \frac{2}{\pi}\int_0^\infty \mathrm{Re}[P(t_F,i\omega)]\cos\omega t d\omega \tag{4.60}$$

The miss step response equals the integral of the impulse response $P(t_F,t)$, i.e.,

$$\mathrm{Miss} = \int_0^{t_F} P(t_F,\sigma)d\sigma \tag{4.61}$$

Substituting equation (4.60) in equation (4.61) and changing the order of integration we have

$$\mathrm{Miss} = \frac{2}{\pi}\int_0^\infty \mathrm{Re}[P(t_F,i\omega)]\int_0^{t_F} \cos\omega\sigma d\sigma d\omega$$

or

$$\mathrm{Miss} = \frac{2}{\pi}\int_0^\infty \frac{\mathrm{Re}[P(t_F,i\omega)]}{\omega}\sin\omega t_F d\omega \tag{4.62}$$

As established in control theory (see, e.g., References [3,4]), if ω_s is the frequency that characterizes a system bandwidth, then the time of the transient response satisfies the inequality

$$\frac{\pi}{\omega_s} \le t \le \frac{4\pi}{\omega_s},$$

which for guidance systems can be reformulated in the following way: if determined from the real part of the frequency response ω_s characterizes the guidance system bandwidth, then the step miss is small for the flight time

$$t_F \geq \frac{4\pi}{\omega_s} \tag{4.63}$$

The procedure for obtaining the miss step response based on equation (4.62) is demonstrated in the example of the guidance system analyzed above.

The frequency response of the guidance system [see equations (4.44) and (4.45)] for $N = 3$ is given in Figure 4.9. Figure 4.10 presents the real part of the frequency response [see equation (4.44)]. As indicated above, based on this characteristic it is possible to evaluate the time of flight t_F, when the miss becomes small enough. Substituting in equation (4.63) $\omega_s \approx 3$ *rad/s* (see Figure 4.10), we obtain the estimate $t_F \geq 4.2$ *s*.

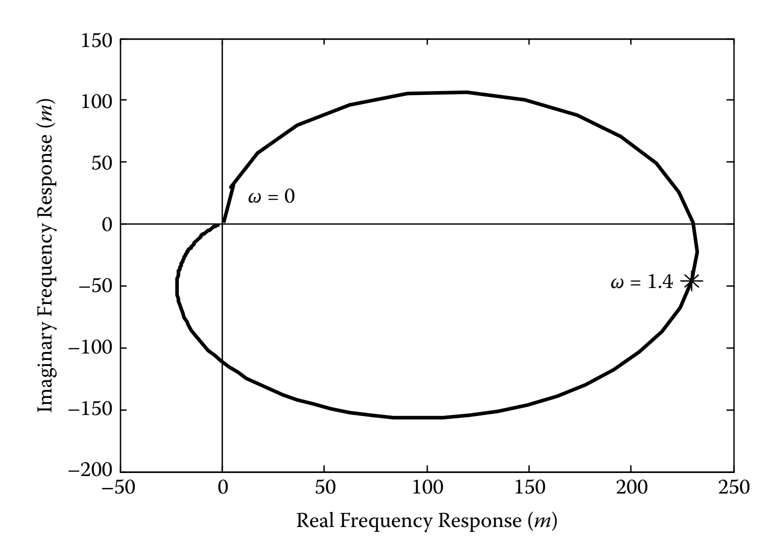


FIGURE 4.9 Frequency response of guidance system.

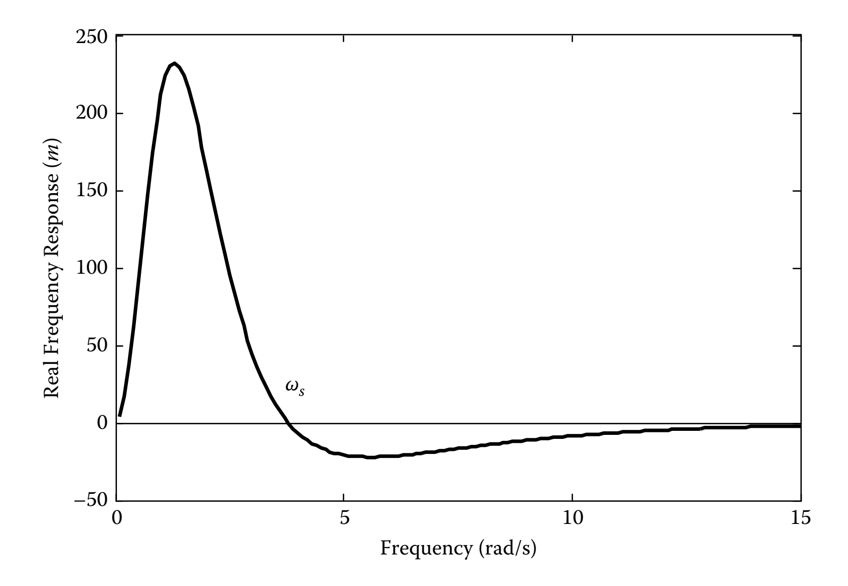


FIGURE 4.10 Real frequency response of guidance system.

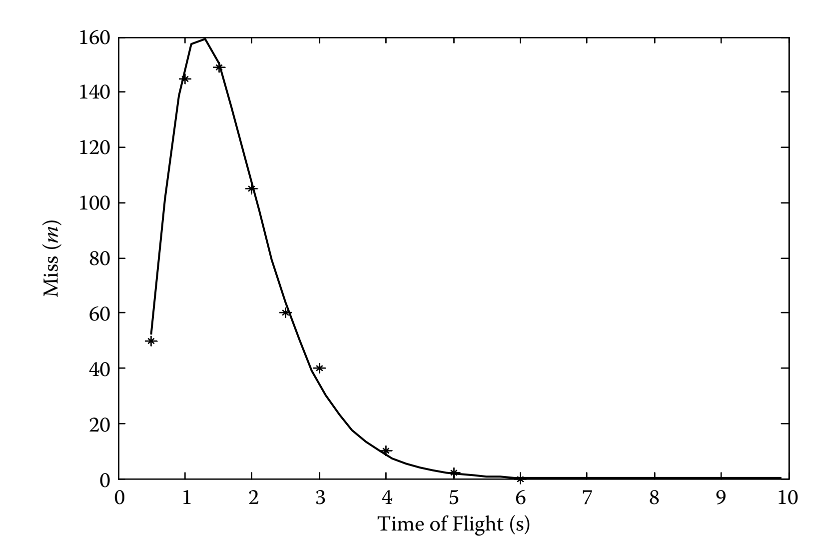


FIGURE 4.11 Miss due to step maneuver.

The miss due to the step maneuver is calculated based on equation (4.62). The miss values are shown in Figure 4.11 by the "*" symbol. The miss due to the unit step maneuver, obtained by simulation of the guidance system in Figure 4.6, is shown in Figure 4.11 by the solid line.

As seen from Figure 4.11, the frequency analysis enables us to evaluate the miss step without simulation of the missile guidance system.

4.8 BOUNDED INPUT–BOUNDED OUTPUT STABILITY

The expression for the frequency response of the missile guidance system is obtained assuming that the Fourier transform in equations (4.54) and (4.55) exists or, in other words, the system is stable with respect to $y(t_F)$, $t_F \in [0, \infty)$ However, the stability conditions present the most difficult part of analysis and synthesis of guidance systems. Since guidance systems operate on a finite time interval, their stability is determined as finite-time stability and is called in Reference [1] Lyapunov stability. The known conditions are sufficient and are based on results related to the stability of nonlinear systems.

In contrast to finite-time stability that analyzes $y(t)$, $t \in [0, t_F)$ the input-output relation between the miss distance $y(t_F)$ and target acceleration [see equations (4.13), (4.14), and (4.34)] enables us to analyze $y(t_F)$, $t_F \in [0, \infty)$ and formulate the stability of the PN guidance systems as bounded input-bounded output (BIBO) stability.

Definition: The PN guidance system is BIBO stable if for any bounded target acceleration its miss $y(t_F)$ is bounded for all times of flight $t_F \in [0, \infty)$.

It is obvious that $y(t_F)$ is bounded on a finite interval. We can expect that $y(t_F)$ is bounded, when $t_F \rightarrow \infty$ because $1/t_{go} \rightarrow 0$.

Using the expression for the transfer function in equation (4.34), the stability condition can be written similar to the BIBO stability condition of linear systems, that is, $L^{-1}(P(t_F,s))$ should be absolutely integrable on $[0,\infty)$ (L is the symbol of the Laplace transform). This condition is equivalent to the requirement for the transfer function $P(t_F,s)$ to be analytical in the right half-plane of a complex variable (including the imaginary axis) and $\lim_{s\rightarrow\infty} P(t_F,s) = 0$.

Theorem: The proportional navigation guidance system with the transfer function $W(s)$ [see equation (4.29)] is BIBO stable if and only if the following condition is satisfied:

$$N - 2 + N\sum_{k=1}^{l} B_k / \tau_k + N\sum_{j=1}^{m} C_j\omega_j^2 < 0 \tag{4.64}$$

where τ_k and ω_j are parameters of the missile guidance system, N is the effective navigation ratio; B_k, and C_j are coefficients of the partial fraction expansion (equation 4.30) of $W(s)/s$.

Proof. Necessity: If equation (4.64) does not hold, then $\lim_{s\to\infty} P(t_F,s) \neq 0$. This contradicts the condition of the existence of an inverse Laplace transform.

Sufficiency: Let condition (4.64) hold. The function $P(t_F,s)$ defined by equation (4.34) is analytic in the region $C_v = \{s\text{: Re}s > -\sigma\}$, where $\sigma = \min(1/\tau_k, \zeta_j\omega_j)$, $k = 1,..,l$, $j = 1,\ldots,m$, that is, it is analytic in the right-half plane (Re$s \geq 0$), so that $L^{-1}(P(t_F,s))$ is absolutely integrable on $[0,\infty)$. The last statement needs additional clarification taking into account that $P(t_F,s)$ is a multiple-valued function of the complex variable s. Appendix B contains the rigorous proof of this statement.

Corollary. Proportional navigation missile guidance systems with the transfer function (4.29) are BIBO stable for all r_i ($i = 1,\ldots,n-1$).

Since $H(s)$ is a proper rational function and the degree of its numerator equals $n-1$, presenting equation (4.30) in the form of equation (4.29) and equating to zero the term of the numerator of power n, we have

$$1 + N\sum_{k=1}^{l} B_k / \tau_k + N\sum_{j=1}^{m} C_j\omega_j^2 = 0\ ,$$

so that the inequality of equation (4.64) is always satisfied.

The established property of the structures in Figure 4.6 serves as justification of the described procedure that can be used for analysis and synthesis of proportional navigation guidance systems in the frequency domain.

4.9 FREQUENCY RESPONSE OF THE GENERALIZED MISSILE GUIDANCE MODEL

The missile guidance models widely used in the literature do not take into account target dynamics. Target acceleration, considered in most publications, is, in essence, a commanded target acceleration rather than a real target acceleration. Nevertheless, this acceleration is compared with a missile acceleration that is presented as a result of the transformation of a missile-commanded acceleration by a certain dynamic unit (first-order or higher) that reflects dynamic features of a missile flight control system.

Ignoring target missile dynamics can bring inaccuracies when evaluating engagement performance. The generalized missile guidance model presented in Figure 4.12 can be used to obtain more accurate results.

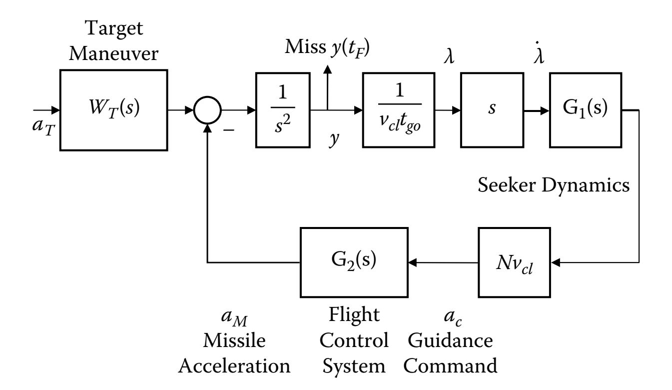


FIGURE 4.12 Generalized missile guidance model.

Analogous to equation (4.12), the flight control dynamics of a target are presented by a third-order transfer function (below we consider a tail-controlled missile)

$$W_T(s) = \frac{1 - \frac{s^2}{\omega_{Tz}^2}}{(1+\tau_T s)(1 + \frac{2\zeta_T}{\omega_T} s + \frac{s^2}{\omega_T^2})} \tag{4.65}$$

with damping ζ_T, natural frequency ω_T, the flight control system time constant τ_T and the right-half plane zero ω_{Tz}.

The transfer function $P_G(t_F,s)$ of the generalized model of the guidance system with respect to a commanded target acceleration can be presented as the product of $P(t_F,s)$ and $W_T(s)$. Taking into account that the frequency response of the target flight control system $W_T(i\omega)$ is

$$W_T(i\omega) = |P_T(i\omega)| \exp(i\varphi_T(i\omega)) \tag{4.66}$$

where

$$|P_T(i\omega)| = \omega_T^2(1+\omega^2/\omega_{Tz}^2)(\tau_T^2\omega^2+1)^{-2}((\omega_T^2-\omega^2)^2+4\zeta_T^2\omega_T^2\omega^2)^{-2} \tag{4.67}$$

$$\varphi_T(i\omega) = -\tan^{-1}(\omega\tau_T) - \tan^{-1}(\frac{2\omega\omega_T\zeta_T}{\omega_T^2-\omega^2}) \tag{4.68}$$

The amplitude $|P_G(t_F,i\omega)|$ and phase $\varphi_G(t_F,i\omega)$ characteristics of the generalized model of the missile guidance system have the following form:

$$|P_G(t_F,i\omega)| = |P(t_F,i\omega)| * |P_T(i\omega)| \tag{4.69}$$

$$\varphi_G(t_F,i\omega) = \varphi(t_F,i\omega) + \varphi_T(i\omega) \tag{4.70}$$

The other frequency characteristics of the generalized model and the estimates of the miss distance can be obtained from equations (4.44)–(4.48) and (4.62) by changing $|P(t_F,i\omega)|$ and $\varphi(t_F,i\omega)$ to $|P_G(t_F,i\omega)|$ and $\varphi_G(t_F,i\omega)$, respectively.

As mentioned, the generalized missile guidance model gives more accurate results than the model that does not take into account target dynamics. Figure 4.13 presents the amplitude characteristics of the missile guidance system considered above (dashed line) and the generalized missile guidance model (solid line) for a target with $\zeta_T = 0.8$, $\omega_T = 3.5$ *rad/s*, $\tau_T = 0.15$ *s*, and $\omega_{T_z} = 15$ *rad/s*. The miss for the generalized model is less than for the model that ignores target dynamics.

The above discussion and examples were focused mainly on tail-controlled missiles. As shown in Figure 4.8, the airframe zeroes can significantly decrease missile performance. The tail configuration is also known as the nonminimum phase, due to the location of a zero in the right half s-plane in the corresponding transfer function of the linear model representation. The long moment arm between the tail controls and the forward position of the center of gravity after burnout requires smaller control forces for constructing the angle of attack, resulting in a lower drag configuration. These control forces are exerted in a direction opposite to the required maneuver, thus, generating a delay in the missile response in the correct direction.

The delayed response of the tail controls can be compensated for by employing an additional forward control device, using either divert thrusters or aerodynamic canard fins. Missiles with forward control fins, or canards, have been used for many years. However, this type of missile can suffer from adverse induced rolling moments. The use of grid fins, or "lattice controls," for the tail control surfaces instead of conventional planar fins was recently proposed as a possible remedy for the roll control problems. Studies have shown that when compared to conventional planar fins, grid fins have certain advantages, such as effective aerodynamic control at high angles of attack and high Mach number, attenuated body-vortex interference, and improved roll control. The primary disadvantage of the grid fin concept is a higher drag than conventional planar fins. The canard fins, located in the front part of the fuselage, generate an aerodynamic force that is in the same direction as the required maneuvering force, thus generating an immediate response in the correct direction. Canard missiles have forward and aft control systems. In contrast to equation (4.12) and Figure 4.6, the flight control system dynamics of this type of missile can be represented by two transfer

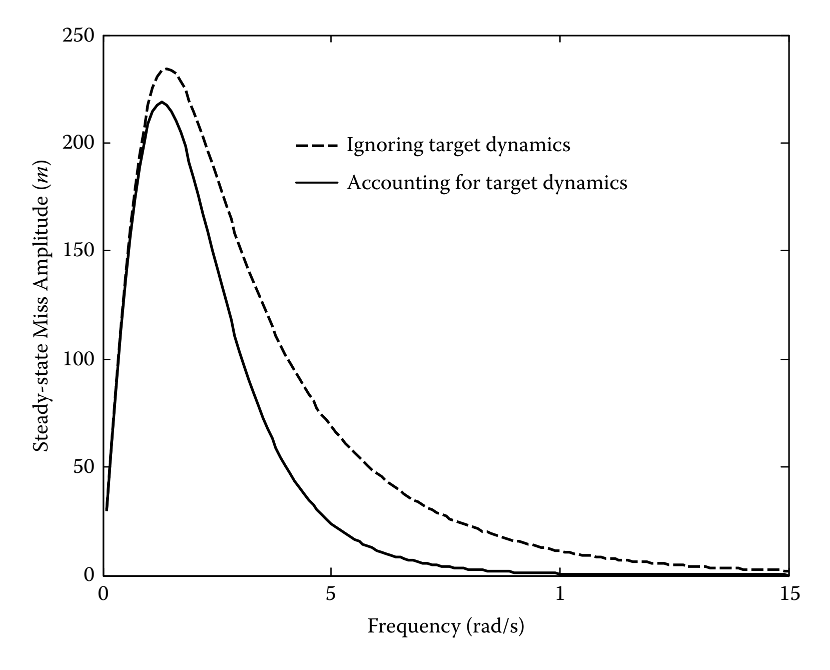


FIGURE 4.13 Amplitude characteristics of frequency response.

functions: a minimum phase transfer function for the forward control and a nonminimum phase transfer function for the aft control. The use of two control systems offers new capabilities, for example, the ability to generate a very high angle of attack for fast and large turns. The additional degree of freedom offered by the dual control system requires special consideration in the guidance and control design. The appropriate blending of the two controls can significantly improve performance of canard missiles. The material of this chapter allows readers to obtain the analogous equations for this type of missile.

REFERENCES

1. Bhat, S. and Bernstein, D., Finite-time stability of continuous autonomous systems. *SIAM Journal of Control and Optimization*, 38, 3, 751–766, 2000.
2. Churchill, R.V., *Complex Variables and Applications*, McGraw-Hill, New York, 1960.
3. Dorf, R.C., *Modern Control Systems*, Addison-Wesley, Inc., Reading, MA, 1989
4. Solodovnikov, V.V., *Introduction to the Dynamics of Automatic Control Systems*, Dover, New York, 1960.
5. Yanushevsky, R., Analysis of optimal weaving frequency of maneuvering targets, *Journal of Spacecraft and Rockets*, 41, 3, 477–479, 2004.
6. Yanushevsky, R., Optimal control of differential-difference systems of neutral type, *International Journal of Control*, 1, 1835–1850, 1989.
7. Yanushevsky, R., Analysis and design of missile guidance systems in frequency domain, 44th AIAA Space Sciences Meeting, paper AIAA 2006-825, Reno, Nevada, 2006.
8. Yanushevsky, R., Frequency domain approach to guidance system design, *IEEE Transactions on Aerospace and Electronic Systems*, 43, 2007.
9. Zadeh, L. and Desoer, C., *Linear System Theory,* McGraw-Hill, New York, 1963.
10. Zarchan, P., Tactical and strategic missile guidance, *Progress in Astronautics and Aeronautics*, 176, American Institute of Astronautics and Aeronautics, Inc., Washington, DC, 1997.
11. Zarchan, P., Proportional navigation and weaving targets, *Journal of Guidance, Control, and Dynamics*, 18, 5, 969–974, 1995.
12. Zarchan, P., Greenberg, E., and Alpert, J., Improving the high altitude performance of tail-controlled endoatmospheric missiles, AIAA Guidance, Navigation and Control Conference, AIAA Paper 2002-4770, Aug. 2002.

5 Design of Guidance Laws Implementing Parallel Navigation. Time-Domain Approach

5.1 INTRODUCTION

Proportional navigation (PN) has attracted a considerable amount of interest in the literature related to missile guidance and continues to be a benchmark for new missile guidance laws. The detailed analytical study of this empirical guidance law for nonmaneuvering and maneuvering targets was undertaken in References [5,9,17]. Capture regions and conditions for the existence of capture regions were also examined in References [3,4].

As mentioned earlier, the basic philosophy behind PN guidance is that missile acceleration should nullify the line-of-sight (LOS) rate. Analysis of PN guidance for the homing stage was usually undertaken for nonmaneuvering targets assuming a constant closing velocity. The so-called augmented PN law and other modifications of the proportional navigation law were obtained based mostly on the relationships established for nonmaneuvering targets. It was discussed in Chapter 2 (see also References [9,17]).

Results from the theory of linear multivariable control systems applied to homing guidance (where linear approximation can be justified) enable one to evaluate the performance of the guidance system as well as to generate modified proportional navigation laws [9,17]. Guidance laws using the idea of PN and based on the results of control theory related to sliding modes and systems with variable structure (see, e.g., Reference [7]) cannot be considered as practical for missile guidance applications. The practical realization of systems with sliding mode is limited because of chatter, and related simplified control laws need rigorous justification and testing. A systematic framework for an almost sliding mode control that eliminates chatter was given in Reference [13]. However, this approach was not used in Reference [7] and other applications of sliding mode controls in guidance systems. Also, in the presence of a maneuvering target the sliding mode area depends on target acceleration, and for small LOS derivatives the sliding mode can disappear. A variable structure (different from the ones considered, e.g., in Reference [7]) that requires measurement of target acceleration is needed.

The empirical PN law was also obtained as a solution to an optimization problem (see, e.g., References [1,6,17]) that justifies this law as an optimal one corresponding to a certain quadratic performance index. The game approach to guidance laws based on the theory of differential games with a quadratic performance index was considered in Reference [2]. The guidance laws developed counteract target maneuvers better than the ordinary PN law.

However, any optimal guidance law assumes that the trajectory of a maneuvering target, as well as time-to-go and the intercept point, is known. In practice, such information is unknown and can only be evaluated approximately. The accuracy of prediction significantly influences the accuracy of the intercept.

Taking into account that the PN law is a widely accepted guidance law and has been tested in practice, it is of interest to consider the possibility of its improvement.

The Lyapunov approach, offered in Chapter 2, can also be considered as another justification of the PN law. Moreover, this approach enables us to offer other laws that will improve the effectiveness of the PN law for maneuvering and nonmaneuvering targets. A new class of the PN guidance laws is obtained as the solution of a stability problem using the Lyapunov method. Analogous to the section of Chapter 2 where the PN guidance was formulated as a control problem, here the Lyapunov function is chosen as a square of the LOS derivative for the planar model and as the sum of the LOS derivative components for the three-dimensional case. The applicability of the laws is determined by the negative definiteness of the derivative of the Lyapunov function. The module of the Lyapunov function derivative is used as the performance index for comparing the PN guidance laws and creating the new ones.

It is important to mention that the guidance laws are determined based on the partial stability of the system dynamics under consideration, only with respect to the LOS derivative [8].

5.2 GUIDANCE CORRECTION CONTROLS

As discussed in Chapter 2, PN is the guidance law that implements parallel navigation, which is defined by the rule $\dot{\lambda}(t) = 0$ with an additional requirement $\dot{r}(t) < 0$, where $\lambda(t)$ is the LOS angle with respect to a reference axis and $r(t)$ represents the target-to-missile range.

To describe the missile–target engagement dynamics, first we consider planar engagements and use a Cartesian frame of coordinates (FOC) (see Figure 2.1) with the origin O of an inertial reference coordinate system: $y(t)$ is the relative separation between the missile and target perpendicular to the horizontal reference axis; a_M and a_T are the missile and target acceleration, respectively. Using a small-angle approximation, the expressions for the second derivative of the LOS angle can be presented in the following form [see equations (2.9), (2.29)–(2.37)]:

$$\ddot{\lambda}(t) = -a_1(t)\lambda(t) - a_2(t)\dot{\lambda}(t) - b(t)a_M(t) + b(t)a_T(t) \tag{5.1}$$

Let $x_1 = \lambda(t)$ and $x_2 = \dot{\lambda}(t)$. The missile–target engagement is described by the following system of the first-order differential equations

$$\dot{x}_1 = x_2$$

$$\dot{x}_2 = -a_1(t)x_1 - a_2(t)x_2 - b(t)u + b(t)f \tag{5.2}$$

where the control $u = a_M(t)$ and disturbance $f = a_T(t)$,

$$a_1(t) = \frac{\ddot{r}(t)}{r(t)} \tag{5.3}$$

$$a_2(t) = \frac{2\dot{r}(t)}{r(t)} \tag{5.4}$$

$$b(t) = \frac{1}{r(t)} \tag{5.5}$$

[see equations (2.31)–(2.33)].

Analogous to the approach in Chapter 2, the guidance problem can be formulated as the problem of choosing control u to guarantee the asymptotic stability of system (5.2) with respect to x_2.

For the Lyapunov function

$$Q = \frac{1}{2} c x_2^2 \tag{5.6}$$

where c is a positive coefficient, its derivative along any trajectory of equation (5.2) equals

$$\dot{Q} = c x_2(-a_1(t)x_1 - a_2(t)x_2 - b(t)u + b(t)f) \tag{5.7}$$

The PN guidance law (2.44) is called admissible if it guarantees intercept for a finite time t_F.

We consider the PN class of guidance laws that have the form (2.44) or contain (2.44) as a component. Despite the fact that even the PN laws of the form (2.44) with various N were compared by experiments, we will introduce a criterion of comparison that has a certain physical justification. Because PN is the guidance law that implements parallel navigation ($\dot{\lambda}(t) = 0$), we will compare the laws belonging to the PN class by their closeness to parallel navigation.

Of course, the most reliable performance index should evaluate the guidance law during the entire engagement time. However, this time is unknown and, in turn, depends on the guidance law implemented. To avoid this "catch 22" situation, we assume that the guidance law with $\dot{\lambda}(t)$ tending to zero faster (closer to parallel navigation) at each t is preferable.

The module of the Lyapunov function derivative $|\dot{Q}(t)|$ [see equation (5.7)] will be the performance index for comparing the PN laws and creating the new ones. Proceeding in this way, we change the finite interval engagement problem to a specific infinite interval partial stability problem. The Lyapunov approach will be used to compare and design controls–guidance laws.

5.3 LYAPUNOV APPROACH TO CONTROL LAW DESIGN

The Lyapunov approach to control law design can be explained in the following way (more rigorous formulations and theorems can be found, e.g., in References [8,14]): if there exist positive definite functions $Q(\boldsymbol{x},t)$ and $R(\boldsymbol{x},t)$ so that the derivative $\dot{Q}$ with respect to t along any trajectory of the system of equations that describes the control system under consideration ($\boldsymbol{x}$ and $\boldsymbol{u}$ are its state vector and control, respectively) satisfy the inequality

$$\dot{Q} = \dot{Q}(\boldsymbol{x}, \boldsymbol{u}, t) \le -R(\boldsymbol{x}, t) \tag{5.8}$$

then the system is stabilized by control $\boldsymbol{u}$, which can be determined from this inequality.

To apply this sufficient condition in practice, the above indicated positive definite forms must be found. Unfortunately, there are no universal recommendations how to find these forms. The relation between $Q(\boldsymbol{x},t)$ and $R(\boldsymbol{x},t)$ was established for the so-called linear quadratic optimal control problems (Riccati-type equations) [6,13]. Based on this, the design procedure was expanded on a certain class of nonlinear system [13].

However, for special types of equations it is not difficult to find $Q(\boldsymbol{x},t)$ and $R(\boldsymbol{x},t)$ satisfying the inequality (5.8). Below the control law design procedure based on Lyapunov approach is demonstrated for the guidance problem [see equations (5.2)–(5.7); for simplicity, we consider in equation (5.2) $f = 0$)].

By choosing $Q(\boldsymbol{x},t)$ in the form (5.6) and $R(\boldsymbol{x},t) = c_1 x_2^2$, where c_1 is a positive coefficient, the inequality (5.8) can be written as [see also equation (5.7)]

$$\dot{Q} = cx_2(-a_1(t)x_1 - a_2(t)x_2 - b(t)u) \le -c_1x_2^2 \tag{5.9}$$

or

$$(-a_2(t) + c_1 / c)x_2^2 - a_1(t)x_1x_2 - b(t)x_2u \le 0 \tag{5.10}$$

It follows from equation (5.10) that for $a_1(t) = 0$ and $c_1 << c$ the control $u = kx_2$ [see equations (2.42) and (2.44)] stabilizes the system (5.2) if k satisfies equation (2.43).

For $R(\boldsymbol{x},t) = c_1x_2^2 + c_2x_2^4$, where c_2 is a positive coefficient, instead of equation (5.9) we have

$$\dot{Q} = cx_2(-a_1(t)x_1 - a_2(t)x_2 - b(t)u) \le -c_1x_2^2 - c_2x_2^4 \tag{5.11}$$

or

$$(-a_2(t) + c_1 / c)x_2^2 - a_1(t)x_1x_2 + \frac{c_2}{c}x_2^4 - b(t)x_2u \le 0 \tag{5.12}$$

It is easy to conclude that for $a_1(t) = 0$, $c_1 << c$ and the control $u = kx_2 + N_1x_2^3$, where k satisfies equation (2.43) and $N_1 > 0$, the left part of equation (5.12) is negative definite, so that this control stabilizes system (5.2) with respect to x_2.

By including the additional term in $R(\boldsymbol{x},t)$ we imposed "harder" requirements on the rate of decreasing Q. Although $|\dot{Q}|$ is used as a system estimate in some applications of the Lyaponov method (see, e.g., Reference [13]), it cannot be applied as a reliable criterion of quality of control systems. It serves only as an instantaneous criterion. The quality estimate of control system includes (directly or indirectly) time of control. For example, an oscillatory long transient even with a small amplitude in many cases is unacceptable. However, when choosing the guidance laws implementing parallel navigation, the only requirement is to be closer, as soon as possible, to zero LOS rate. The $|\dot{Q}|$ criterion reflects this requirement.

Let us assume that there exists a capture range domain over which the control (guidance law) $u(t)$ guarantees engagement ($x_2(t) \to 0$). Then based on the above mentioned, it is easy to conclude that the guidance law

$$u = Nv_{cl}\dot{\lambda}(t) + N_1\dot{\lambda}^3(t), \quad N > 2, N_1 > 0 \tag{5.13}$$

is better than the PN law (2.44).

The PN law reacts almost identically to various changes of LOS rate (assuming that the closing velocity does not vary drastically) (i.e., small and fast changes of LOS result in proportional changes of acceleration). According to equations (5.11) and (5.13), by increasing N in the PN law, we can more quickly decrease the LOS rate. But this will increase the level of noise when the LOS rate becomes small and, hence, the accuracy of guidance is decreased. Moreover, big gains can make the whole guidance system unrobust. From a purely physical consideration, we can assume that the system with a variable gain that is bigger when the LOS rate is big and smaller when the LOS rate is small will act better than the traditional PN system. The second component of equation (5.13) (the "cubic" term) with a properly chosen N_1 serves this purpose.

It was shown that the PN law (2.44) can be improved by using a complex exponential type function of time $N(t)$ instead of a constant N [2,18]. This function is obtained as the result of the solution of an optimal guidance problem and depends on the predicted time-to-go. Its calculation presents certain difficulties for utilization of such laws in practice.

The guidance law (5.13) can be written in the form (2.44)

$$u(t) = (N + \frac{N_1}{v_{cl}}\dot{\lambda}^2(t))v_{cl}\dot{\lambda}(t) = N(t)v_{cl}\dot{\lambda}(t) \tag{5.14}$$

with a time-varying coefficient $N(t)$, which formally is an exponential-type function (asymptotic with respect to x_2 solution of equation (5.2), under the assumption mentioned above, is an exponential-type function). The form (5.14) looks similar to the guidance laws considered in Reference [2]. In contrast to the law with variable $N(t)$, obtained as optimal guidance in Reference [2], the guidance law (5.13) does not require special complex computations.

If in equation (5.7) $f \neq 0$, instead of equation (5.11) we have

$$\dot{Q} = cx_2(-a_1(t)x_1 - a_2(t)x_2 - b(t)u + b(t)f) \leq -c_1x_2^2 - c_2x_2^4 \tag{5.15}$$

An additional component $a_T(t) = f$ in control "compensates" in equation (5.15) the $b(t)f$ term, so that the control $u = kx_2 + N_1x_2^3 + a_T(t)$ stabilizes the system (5.2) with respect to x_2 [see also equation (2.52)].

The Lyapunov approach is demonstrated here in details for the system (5.2), when $a_1(t) = 0$. In an analogous way, it is easy to establish the negative definiteness of equation (5.7) for $a_1(t) \neq 0$ and $a_2(t) \leq 0$ if the control u is [10]

$$u(t) = Nv_{cl}\dot{\lambda}(t) + N_1\dot{\lambda}^3(t) - N_2\ddot{r}(t)\lambda(t) + N_3a_T(t) \quad N > 2,\ N_1 > 0, \tag{5.16}$$

$$N_2 \begin{matrix} \geq 1 \\ \leq 1 \end{matrix} \quad \text{if } sign(\ddot{r}(t)\dot{\lambda}(t)\lambda(t)) \begin{matrix} \leq 0 \\ \geq 0 \end{matrix}$$

$$N_3 \begin{matrix} \leq 1 \\ \geq 1 \end{matrix} \quad \text{if } sign(a_T(t)\dot{\lambda}(t)) \begin{matrix} \leq 0 \\ \geq 0 \end{matrix}$$

The term $N_3a_T(t)$ differs from the corresponding term in the augmented proportional navigation (APN) law because the parameter N_3 is time-varying. The term $N_2\ddot{r}(t)\lambda(t)$ (the shaping term) acts along the LOS, changes the shape of the missile trajectory, and also influences the terminal velocity of a missile.

5.4 MODIFIED LINEAR PLANAR MODEL OF ENGAGEMENT

The majority of guidance laws have one objective: to reduce to zero the miss distance between the missile and target. However, this is not always sufficient. The direction from which the missile approaches the target is also important. In certain scenarios, the mission requirements call for the payload to impact the target from a specific direction. Final impact angle requirements are very important for hitting ground targets. There exist specific angles to hit a target most effectively.

When we guide a missile with a seeker, the impact point (the point of the missile warhead detonation and/or hitting a target) is heavily dependent upon the target information provided by the seeker. In the case of infrared (IR) seekers, the most probable impact point lies near the heat source of the target, if the conventional guidance law is used. However, the heat source of many targets is located near the tail of the fuselage, and therefore the kill probability could be significantly low if the missile simply follows the heat source. The concern about low kill probability due to the impact point can be partially resolved by properly choosing the impact angle.

The above-considered linear planar model of engagement can be enhanced by specifying a missile–target impact achieved at a fixed LOS angle λ_0.

By introducing the state variables

$$z_1 = \lambda - \lambda_0 = x_1 - \lambda_0, \quad x_2 = \dot{z}_1 \tag{5.17}$$

and acting analogously to the situation described above, instead of equation (5.2) we obtain

$$\dot{z}_1 = x_2$$

$$\dot{x}_2 = -a_1(t)(z_1 + \lambda_0) - a_2(t)x_2 - b(t)u + b(t)a_T \tag{5.18}$$

In contrast to equation (5.6), the Lyapunov function Q is chosen as

$$2Q = cx_2^2 + c_0 z_1^2 \tag{5.19}$$

and the guidance law is obtained from the stability conditions of the whole system (5.18) rather than the partial stability with respect to x_2 coordinate.

From the condition of negative definiteness of the derivative of the Lyapunov function (5.19)

$$\dot{Q} = cx_2(-a_1(t)(z_1 + \lambda_0) - a_2(t)x_2 - (b(t)u - b(t)a_T)) + c_0 z_1 x_2) \tag{5.20}$$

we can derive the following guidance law:

$$u(t) = Nv_{cl}\dot{\lambda}(t) + N_1\dot{\lambda}^3(t) - N_2(\ddot{r}(t) - \frac{c_0}{c}r(t))(\lambda(t) - \lambda_0) - \ddot{r}(t)\lambda_0 + N_3 a_T(t) \tag{5.21}$$

$$N_2 \begin{matrix} \geq 1 \\ \leq 1 \end{matrix} \quad \text{if } sign((\ddot{r}(t) - \frac{c_0}{c}r(t))\dot{\lambda}(t)(\lambda(t) - \lambda_0)) \begin{matrix} \leq 0 \\ \geq 0 \end{matrix}$$

Comparing the guidance laws and equations (5.16) and (5.21), we can see that the specified missile–target impact LOS angle λ_0 influences only the shaping term

$$N_2(\ddot{r}(t) - \frac{c_0}{c}r(t))(\lambda(t) - \lambda_0) - \ddot{r}(t)\lambda_0.$$

5.5 GENERAL PLANAR CASE

Instead of using a small linear approximation (2.9), we will consider a general nonlinear case. The expressions for the LOS angle [see equation (2.8)] and its derivatives can be presented in the following form:

$$\sin(\lambda(t)) = \frac{y(t)}{r(t)} \tag{5.22}$$

$$\ddot{\lambda}(t)\cos(\lambda(t)) - \dot{\lambda}^2(t)\sin(\lambda(t)) = -a_1(t)\sin(\lambda(t)) - a_2(t)\cos(\lambda(t))\dot{\lambda}(t) + b_1\ddot{y}(t) \tag{5.23}$$

or

$$\dot{x}_1 = x_2$$

$$\dot{x}_2 = x_2^2 \tan x_1 - a_1(t)\tan x_1 - a_2(t)x_2 - \frac{b(t)}{\cos x_1}u + \frac{b(t)}{\cos x_1}f \tag{5.24}$$

where $u(t)$ is a commanded missile acceleration, $x_1 = \lambda(t)$, $x_2 = \dot{\lambda}(t)$, and the coefficients $a_1(t)$, $a_2(t)$, and $b(t)$ are determined by equations (5.3)–(5.5).

It is of importance to mention that considering a linear approximation of the trigonometric functions in equation (5.24) we will not obtain the linear system (5.2). There will be the additional nonlinear term $x_2^2 x_1$ (for small x_1, $x_2^2 \tan x_1 \approx x_2^2 x_1$). The linearization for small LOS angles at this stage is more rigorous than linearization (2.9) and sequential differentiation, as it was shown in many publications. The main reason for using equations (5.1) and (5.2) is the difficulty in dealing with nonlinear differential equations.

The derivative of the Lyapunov function (5.6) along any trajectory of equation (5.24) is

$$\dot{Q} = cx_2(x_2^2 \tan x_1 - a_1(t)x_1 \tan x_1 - a_2(t)x_2 - (b(t)u - b(t)f)/\cos x_1)$$

or

$$\dot{Q} = c(x_2^3 \tan x_1 - a_1(t)x_1x_2 \tan x_1 - a_2(t)x_2^2 - (b(t)x_2u - b(t)x_2f)/\cos x_1) \tag{5.25}$$

The negative definiteness of equation (5.25) can be guaranteed by the control-guidance law

$$u(t) = Nv_{cl}\cos(\lambda(t))\dot{\lambda}(t) + N_1\cos(\lambda(t))\dot{\lambda}^3(t) \tag{5.26}$$

$$-N_2\sin(\lambda(t))\ddot{r}(t) - N_0 r(t)\dot{\lambda}^2(t)\sin(\lambda(t)) + N_3 a_T(t)$$

$$N > 2,\ N_1 > 0,$$

$$N_0 \begin{matrix}\ge 1\\ \le 1\end{matrix} \quad \text{if } \ sign(\dot{\lambda}(t)\lambda(t)) \begin{matrix}\le 0\\ \ge 0\end{matrix}$$

$$N_2 \begin{matrix}\ge 1\\ \le 1\end{matrix} \quad \text{if } \ sign(\ddot{r}(t)\dot{\lambda}(t)\lambda(t)) \begin{matrix}\le 0\\ \ge 0\end{matrix}$$

$$N_3 \begin{matrix}\le 1\\ \ge 1\end{matrix} \quad \text{if } \ sign(a_T(t)\dot{\lambda}(t)) \begin{matrix}\le 0\\ \ge 0\end{matrix}$$

The guidance law (5.26) can be presented as the sum of the main PN law and additional correcting controls

$$u = Nv_{cl}\cos(\lambda(t))\dot{\lambda}(t) + \sum_{k=0}^{3} u_k \tag{5.27}$$

where

$$u_0 = -N_0 r(t)\dot{\lambda}^2(t)\sin(\lambda(t)) \tag{5.28}$$

$$u_1 = N_1 \cos(\lambda(t))\dot{\lambda}^3(t) \quad (5.29)$$

$$u_2 = -N_2 \ddot{r}(t)\sin(\lambda(t)) \quad (5.30)$$

$$u_3 = N_3 a_T(t) \quad (5.31)$$

For small LOS angles and short homing ranges (the case that was mostly discussed in the guidance literature) the term $x_2^3 \tan x_1$ in equation (5.25) is smaller than a dominant x_2^2 component. That is why the analysis of the linear system (5.2) is justified if such conditions are satisfied. For a larger spectrum of LOS angles the u_0 component is needed.

The effectiveness of the u_1 correction was discussed earlier for the linearized model. The u_2 correction is needed for maneuvering targets and when the second derivative of range is not small enough. The augmented proportional navigation term (5.31) differs from the well-known one [see also equation (2.53)] that was obtained rigorously for step maneuvers but was recommended to be used for all types of maneuvers. The $sign(a_T(t)\dot{\lambda}(t))$ factor reflects the dependence of the correction on the target behavior. Each of the controls u_k (k = 0,1,2,3) increases the effectiveness of the PN navigation law with respect to the criterion chosen. The number of controls applied in practice should depend on the problem under consideration (target distances, LOS angles, maneuvering or nonmaneuvering targets, and so forth, as well as the system's ability to realize the correction control in practice).

Taking into account that we consider a class of the modified PN laws, the control-corrections equations (5.28)–(5.31) are considered as the means of improving the PN law (2.49), extending its area of applicability. The coefficients $N_0 - N_3$ (constant or time-varying) can be determined based on simulation results of the whole missile system taking into account the autopilot limits on a missile acceleration, airframe dynamics, and some other factors (i.e., the same way as the most appropriate values $N = 3 - 4$ were established). A certain approach to their selection is given below.

The considered nonlinear planar model of engagement can be enhanced by specifying a missile-target impact achieved at a fixed LOS angle λ_0, as in the case of the linearized planar model, by introducing the state variables

$$z_1 = \sin(\lambda(t)) - \sin\lambda_0,\ x_2 = \dot{z}_1 = \dot{\lambda}(t)\cos(\lambda(t)) \quad (5.32)$$

and considering the Lyapunov function (5.19).

Analogous to equations (2.29)–(2.33) we can obtain

$$\dot{z}_1 = \frac{\dot{y}(t)}{r(t)} - \frac{\sin(\lambda(t))\dot{r}(t)}{r(t)} \quad (5.33)$$

$$\dot{x}_2 = \frac{\ddot{y}(t)}{r(t)} - \frac{\dot{z}_1\dot{r}(t)}{r(t)} - \frac{\dot{y}(t)\dot{r}(t)}{r^2(t)} - \frac{\ddot{r}(t)\sin(\lambda(t))}{r(t)} + \frac{\dot{r}^2(t)\sin(\lambda(t))}{r^2(t)} - \frac{\dot{r}(t)\dot{\lambda}(t)\cos\lambda(t)}{r(t)} \quad (5.34)$$

$$= \frac{\ddot{y}(t)}{r(t)} - \frac{2\dot{z}_1\dot{r}(t)}{r(t)} - \frac{z_1\ddot{r}(t)}{r(t)} - \sin\lambda_0 \frac{\ddot{r}(t)}{r(t)}$$

so that instead of equation (5.18) we have

$$\dot{z}_1 = x_2$$

$$\dot{x}_2 = -a_1(t)z_1 - a_2(t)x_2 - a_1(t)\sin\lambda_0 - b(t)u + b(t)a_T \quad (5.35)$$

Acting analogous to equation (5.20), we can derive the following guidance law:

$$u(t) = Nv_{cl}\cos(\lambda(t))\dot{\lambda}(t) + \sum_{k=1}^{3} u_k \tag{5.36}$$

where u_k (k = 1,3) coincides with equations (5.29) and (5.31), respectively, and

$$u_2 = N_2(\ddot{r}(t) - \frac{c_0}{c} r(t))(\sin(\lambda(t)) - \sin\lambda_0) - \ddot{r}(t)\sin\lambda_0 \tag{5.37}$$

The modified Lyapunov function, which contains trigonometric functions of the LOS, enables us to reduce the guidance problem with an impact angle constraint for the nonlinear planar model to the analogous one for the linearized model and the Lyapunov function (5.19). The modified Lyapunov function “eliminates” the quadratic term u_0 [see equation (5.28)] in the guidance law of the enhanced nonlinear model of engagement.

The guidance laws with the impact angle constraints (5.21) and (5.36) differ insignificantly from the corresponding laws obtained without the impact angle constraints. Their realization does not present any difficulties.

5.6 THREE-DIMENSIONAL ENGAGEMENT MODEL

For the three-dimensional case and the Earth-based coordinate system we rewrite equation (2.45)

$$\ddot{\lambda}_s(t) = -a_1(t)\lambda_s(t) - a_2(t)\dot{\lambda}_s(t) + b(t)(a_{Ts}(t) - u_s) \tag{5.38}$$

where $a_{Ts}(t)$ are the coordinates of the target acceleration vector and $u_s(t)$ (s = 1, 2, 3) are the coordinates of the missile acceleration vector, which are considered as controls.

As in equation (2.46), the Lyapunov function is chosen as the sum of squares of the LOS derivative components that corresponds to the nature of parallel navigation, i.e.,

$$Q = \frac{1}{2}\sum_{s=1}^{3} d_s\dot{\lambda}_s^2 \tag{5.39}$$

where d_s are positive coefficients.

Its derivative can be presented in the following form

$$2\dot{Q} = \sum_{s=1}^{3} d_s(-a_1(t)\lambda_s\dot{\lambda}_s - a_2(t)\dot{\lambda}_s^2 + b(t)\dot{\lambda}_s(a_{Ts}(t) - u_s)) \tag{5.40}$$

so that the three-dimensional guidance problem is similar to the linearized planar guidance problem.

Analogous to equation (5.16), the controls $u_s(t)$ that guarantee $\lim\|\dot{\boldsymbol{\lambda}}\| \to 0,\ t \to \infty$ can be presented as

$$u_s = Nv_{cl}\dot{\lambda}_s + \sum_{k=1}^{3} u_{sk} \tag{5.41}$$

where

$$u_{s1}(t) = N_1 \dot{\lambda}_s^3(t),\ N_1 > 0 \tag{5.42}$$

$$u_{s2}(t) = N_{2s}\lambda_s(t)\ddot{r}(t) \qquad N_{2s} \begin{matrix}\geq 1\\ \leq 1\end{matrix} \quad \text{if } sign(\ddot{r}(t)\dot{\lambda}_s(t)\lambda_s(t)) \begin{matrix}\leq 0\\ \geq 0\end{matrix} \tag{5.43}$$

$$u_{s3}(t) = N_{3s}a_{Ts}(t) \qquad N_{3s} \begin{matrix}\leq 1\\ \geq 1\end{matrix} \quad \text{if } sign(a_{Ts}(t)\dot{\lambda}_s(t)) \begin{matrix}\leq 0\\ \geq 0\end{matrix} \tag{5.44}$$

$$(s = 1,2,3).$$

The expressions (5.41)–(5.44) can be obtained in a similar fashion to the linear planar case [see equation (5.16)]. However, for the three-dimensional engagement model, in the case $d_s = 1$, the term

$$\sum_{s=1}^{3} -a_1(t)\lambda_s\dot{\lambda}_s$$

in equation (5.40) equals zero. This means that controls $u_{s2}(t) = N_{2s}\lambda_s(t)\ddot{r}(t)$ are not needed to guarantee $\lim\|\dot{\boldsymbol{\lambda}}\| \to 0,\ t \to \infty$. Nevertheless, the above-mentioned controls are very important parts of the guidance law.

The commanded acceleration can be considered as consisting of two components—radial (along the LOS, also called longitudinal) and tangential (perpendicular to the LOS, also called lateral). It follows from equation (5.43), the components $u_{s2}(t)$ belong to the radial acceleration, i.e., they influence the closing velocity.

Usually, during a missile flight, only two LOS rate components are dominant, so that the case of equal d_s is not typical and then $u_{s2}(t)$ (s = 1-3) also influence the tangential acceleration. However, the radial component is dominant.

Controls $u_{s2}(t) = N_{2s}\lambda_s(t)\ddot{r}(t)$ (s = 1-3) do not influence the tangential component of a missile acceleration in the case of equal d_s; they change the radial acceleration component, which is important for guaranteeing an appropriate acceleration (force) at the moment of intercept.

It is important to mention that for many types of existing missiles (e.g., without throttlable engines) radial acceleration can not be used as a control action. Such missiles are not able to use thrust control as a part of a guidance law. Controls u_{s2} can influence missile trajectory only by decelerating its motion.

As seen from equations (5.40)–(5.44), the multidimensional PN law follows immediately as one of the possible solutions and as a component of a more complicated law with nonlinear terms.

The described guidance laws can be used for the midcourse and terminal guidance. During the midcourse stage the components of the LOS are obtained from equation (1.8). For the terminal stage these components are usually calculated based on measurements of azimuth and elevation angles. The vectors $\boldsymbol{\lambda}(t)$ and $\dot{\boldsymbol{\lambda}}(t)$ can be presented as [see equations (1.9) and (1.16)]

$$\boldsymbol{\lambda}(t) = \begin{bmatrix}\cos\alpha\cos\beta\\ \cos\alpha\sin\beta\\ \sin\alpha\end{bmatrix},\ \dot{\boldsymbol{\lambda}}(t) = \begin{bmatrix}-\sin\alpha\cos\beta\\ -\sin\alpha\sin\beta\\ \cos\alpha\end{bmatrix}\dot{\alpha} + \begin{bmatrix}-\cos\alpha\sin\beta\\ \cos\alpha\cos\beta\\ 0\end{bmatrix}\dot{\beta} \tag{5.45}$$

where α and β are elevation and azimuth angles.

By comparing the guidance law (5.41) using equation (5.45) with the guidance law for the nonlinear planar model (5.27), we can conclude that the guidance law (5.27) can be used to analyze the coordinate u_3 in the three-dimensional case (i.e., the three-dimensional Lyapunov-based guidance law embeds the Lyapunov-based guidance laws obtained for the planar case).

The established similarity between the equations determining the guidance law for the three-dimensional and linearized planar engagement models enables us to present the guidance law for the three-dimensional enhanced model of engagement with the specified missile–target impact achieved at a fixed LOS angle $\boldsymbol{\lambda}_0$ in the form (5.41) with the modified term $u_{s2}(t)$ [see equation (5.43)], i.e.,

$$u_{s2}(t) = N_{2s}(\ddot{r}(t) - \frac{c_0}{c}r(t))(\lambda_s(t) - \lambda_{0s}) \ -\ddot{r}(t)\lambda_{0s} \tag{5.46}$$

$$N_{2s} \begin{matrix} \geq 1 \\ \leq 1 \end{matrix} \quad \text{if } sign((\ddot{r}(t) - \frac{c_0}{c}r(t)\dot{\lambda}_s(t)(\lambda_s(t) - \lambda_{0s})) \begin{matrix} \leq 0 \\ \geq 0 \end{matrix} \quad (s = 1,2,3)$$

Many interceptors use a lethality enhancement device to improve their hit-to-kill capabilities. For example, endoatmospheric guided missiles typically employ a fusing system and fragmentation warhead to accomplish this. The performance of these lethality enhancement systems can be sensitive to endgame conditions. Suitably controlling the terminal interceptor body rates and interceptor-threat approach angles can help to maximize the performance and effectiveness of the lethality enhancement device.

5.7 GENERALIZED GUIDANCE LAWS

As indicated earlier, the guidance laws considered in this chapter were obtained under the assumption that both guidance components, radial and tangential, can be realized in practice. However, this is possible only for certain types of missiles. For missiles without throttleable engines only tangential component of the developed guidance laws can be implemented.

Unlike missiles without throttleable engines, missiles with axial control can employ thrust control as a part of guidance. Because of their superior guidance ability, for the purpose of the detailed analysis of this type of missile, we consider separately the longitudinal and lateral motions.

For the three-dimensional case and the Earth-based coordinate system the target-to-missile range vector $\boldsymbol{r}(t)$ and its derivatives are represented by equations (1.17)–(1.19), so that the dynamic equations of the three-dimensional engagement can be presented in the form (1.20)

$$\ddot{\boldsymbol{r}}(t) = \boldsymbol{a}_T(t) - \boldsymbol{a}_M(t) = \boldsymbol{a}_{Tr}(t) + \boldsymbol{a}_{Tt}(t) - \boldsymbol{a}_{Mr}(t) - \boldsymbol{a}_{Mt}(t) \tag{5.47}$$

where missile $\boldsymbol{a}_M(t)$ and target $\boldsymbol{a}_T(t)$ accelerations consist of two components—longitudinal and lateral, i.e.,

$$\boldsymbol{a}_M(t) = \boldsymbol{a}_{Mr}(t) + \boldsymbol{a}_{Mt}(t), \quad \boldsymbol{a}_T(t) = \boldsymbol{a}_{Tr}(t) + \boldsymbol{a}_{Tt}(t) \tag{5.48}$$

$\boldsymbol{a}_{Tr}(t)$, $\boldsymbol{a}_{Mr}(t)$, $\boldsymbol{a}_{Tt}(t)$, and $\boldsymbol{a}_{Mt}(t)$ are the target and missile longitudinal (radial) and lateral (tangential) accelerations with the coordinates $a_{Trs}(t)$, $a_{Mrs}(t)$, $a_{Tts}(t)$, and $a_{Mts}(t)$ (s = 1,2,3), respectively.

Combining equations (1.19), (1.20), and (5.47), we obtain the following system of equations describing the three-dimensional engagement

$$\ddot{\lambda}_s(t)r(t) + 2\dot{r}(t)\dot{\lambda}_s(t) + \ddot{r}(t)\lambda_s(t) = a_{Ts}(t) - a_{Ms}(t) \quad (s = 1,2,3) \tag{5.49}$$

where $a_{Ts}(t)$ and $a_{Ms}(t)$ are the coordinates of $\boldsymbol{a}_T(t)$ and $\boldsymbol{a}_M(t)$, respectively.

The last term of the left part of equation (5.49) corresponds to the vector directed along the LOS. The components $q\lambda_s$ of $h_s = \ddot{\lambda}_s(t)r(t) + 2\dot{r}(t)\dot{\lambda}_s(t)$ (s = 1,2,3) that correspond to the vector directed along the LOS are determined from the orthogonality of radial and tangential vectors, i.e.,

$$\sum_{s=1}^{3}(h_s - q\lambda_s)q\lambda_s = 0 \ .$$

Using the equalities, obtained from the sequential differentiation of

$$\sum_{s=1}^{3}\lambda_s^2 = 1 \ ,$$

the following expression for the factor q can be obtained

$$q = r(t)\sum_{s=1}^{3}\ddot{\lambda}_s(t)\lambda_s(t) = -r(t)\sum_{s=1}^{3}\dot{\lambda}_s^2(t) \tag{5.50}$$

The expressions for the missile longitudinal and lateral motions follow from equations (5.49) and (5.50). We analyze these motions in the Cartesian frame of coordinates of an inertial reference coordinate system, in contrast to the well-known presentation of the three-dimensional kinematics of guidance (see, e.g., Reference [9]) describing the longitudinal and lateral motions using a rotating frame of coordinates with axes along the unit vectors 1_r directed along $\boldsymbol{r}$, 1_w directed along $\boldsymbol{r} \times \dot{\boldsymbol{r}}$, and $1_t = 1_r \times 1_w$.

For the longitudinal motion we have

$$\ddot{r}(t)\lambda_s(t) - r(t)\sum_{s=1}^{3}\dot{\lambda}_s^2(t)\lambda_s(t) = a_{Trs}(t) - a_{Mrs}(t) \quad (s = 1,2,3) \tag{5.51}$$

By presenting the radial vectors $\boldsymbol{a}_{Tr}(t)$ and $\boldsymbol{a}_{Mr}(t)$ in the form

$$a_{Trs}(t) = a_{Tr}(t)\lambda_s(t) \quad a_{Mrs}(t) = a_{Mr}(t)\lambda_s(t) \quad (s = 1,2,3) \tag{5.52}$$

where $a_{Tr}(t)$ and $a_{Mr}(t)$ are the target and missile radial accelerations, respectively, equation (5.51) can be reduced to

$$\ddot{r}(t) - r(t)\sum_{s=1}^{3}\dot{\lambda}_s^2(t) = a_{Tr}(t) - a_{Mr}(t) \tag{5.53}$$

For the lateral motion we have

$$\ddot{\lambda}_s(t)r(t) + 2\dot{r}(t)\dot{\lambda}_s(t) + r(t)\sum_{s=1}^{3}\dot{\lambda}_s^2(t)\lambda_s(t) = a_{Tts}(t) - a_{Mts}(t) \quad (s = 1,2,3) \tag{5.54}$$

The system of equations (5.53) and (5.54) is equivalent to the system (5.49). The analysis of their specifics enables us to simplify the analysis of the original system (5.49).

As mentioned earlier, missiles without axial control are able to control only the lateral motion using information about a missile thrust, drag, and target acceleration and considering them as external factors with respect to control actions. The basic widespread philosophy behind controlling the lateral motion is that the lateral missile acceleration should nullify the LOS rate (i.e., the lateral acceleration as control is aimed at implementing parallel navigation). In the ideal case $\dot{\lambda}_s(t) = 0$ (s = 1,2,3) the system (5.53) and (5.54) is reduced to

$$\ddot{r}(t) = a_{Tr}(t) - a_{Mr}(t) \tag{5.55}$$

It can be easily observed from equations (5.53) and (5.54) that the dynamics of longitudinal and lateral motions can be decoupled by using a pseudo-acceleration $a_{Mr1}(t)$ in the radial direction

$$a_{Mr1}(t) = a_{Mr}(t) - r(t)\sum_{s=1}^{3}\dot{\lambda}_s^2(t) \quad (s = 1,2,3) \tag{5.56}$$

so that instead of equation (5.53) we can analyze equation (5.55), where $a_{Mr}(t)$ is changed for $a_{Mr1}(t)$.

The terms "lateral acceleration" and "lateral motion" were used above to characterize the motion in a plane orthogonal to the LOS. The true proportional navigation (TPN) law $a_{Mts}(t) = -N\dot{r}(t)\dot{\lambda}_s(t)$, $N > 2$ characterizes the motion belonging to this plane. However, the class of guidance laws implementing parallel navigation does not necessarily satisfy equation (5.54) because the acceleration vector required by the guidance law does not lie in this plane. For example, in the pure PN (PPN) law the commanded acceleration is applied normal to the missile velocity vector; in the generalized PN (GPN) the commanded acceleration forms a constant angle with the normal to the LOS [9]. Because these laws have a dominant tangential component of acceleration, we will use the term lateral acceleration to characterize them and the term longitudinal (radial) acceleration to characterize the motion satisfying equation (5.55). Instead of equations (5.53) and (5.54), we will consider the system

$$\ddot{\lambda}_s(t)r(t) + 2\dot{r}(t)\dot{\lambda}_s(t) = a_{Tts}(t) - a_{Mts}(t) \quad (s = 1,2,3) \tag{5.57}$$

and equation (5.55).

In accordance with the Lyapunov-based control design approach, used earlier, the guidance problem can be formulated as the problem of choosing controls $a_{Mr}(t)$ and $a_{Mts}(t)$ (s = 1,2,3) to guarantee $\dot{r}(t) < 0$ and the asymptotic stability of the system of (5.57) with respect to $\dot{\lambda}_s(t)$ (s = 1,2,3). Because in reality we deal with a finite problem, for simplicity and a more rigorous use of the term "asymptotic stability" we assume, as earlier, disturbance (target acceleration) to be a vanishing function , i.e., contains a factor $e^{-\varepsilon t}$, where ε is an infinitely small positive number; moreover, if t_F is the time of intercept then $\lim_{t\to t_F} r(t) \to 0$ and $a_T(t) = 0$ for $t > t_F$.

From equation (5.55) the conditions $\dot{r}(t) < 0$ and $\lim_{t\to t_F} r(t) \to 0$ can be achieved by choosing $a_{Mr1}(t) > a_{Tr}(t)$ for $t \le t_F$ and $a_{Mr1}(t) = 0$ for $t > t_F$, i.e.,

$$a_{Mr1}(t) = k_1(t)a_{Tr}(t), \quad k_1(t) \ge 1 \tag{5.58}$$

This follows from the condition of negative definiteness of the derivative of the Lyapunov function $r^2(t)$ along any trajectory of equation (5.55), i.e., $r(t)\dot{r}(t) < 0$ where

$$\dot{r}(t) = \dot{r}(t_0) + \int_{t_0}^{t}(a_{Tr}(t) - a_{Mr1}(t))dt < 0;$$

t_0 is the initial moment of guidance.

The system described by equation (5.55) has been examined thoroughly in the literature; various optimal problems have been considered and solved (see, e.g., References [1,6]). Without considering concrete optimal problems here (their practical application is limited because of lack of information about future values of a target acceleration), we indicate only that a pseudoacceleration $a_{Mr1}(t)$ in the radial direction should exceed the radial target acceleration, so that the larger their difference the faster the decrease in range.

The asymptotic stability of equation (5.54) with respect to $\dot{\lambda}_s(t)$ $(s = 1,2,3)$ is guaranteed by the guidance law

$$a_{Mts}(t) = Nv_{cl}\dot{\lambda}_s(t) + \sum_{k=1,3} u_{sk}(t) \tag{5.59}$$

where $v_{cl} = -\dot{r}(t)$,

$$u_{s1}(t) = N_{1s}\dot{\lambda}_s^3(t), \quad N_{1s} > 0 \tag{5.60}$$

$$u_{s3}(t) = N_{3s}\, a_{Tts}(t), \quad N_{3s} \begin{matrix} \le 1 \\ \ge 1 \end{matrix} \quad \text{if } sign(a_{Tts}(t)\dot{\lambda}_s(t)) \begin{matrix} \le 0 \\ \ge 0 \end{matrix} \tag{5.61}$$

$$(s = 1,2,3)$$

The expressions (5.59)–(5.61) follow immediately from the procedure based on the Lyapunov approach described in the previous sections of this chapter, if the Lyapunov function has the form (5.39). In contrast to the terms u_{3s} in equation (5.44), the terms u_{3s} in equation (5.61) contain only the lateral component of the target acceleration.

Based on equations (5.57)–(5.61), the guidance law can be presented in the following form

$$a_{Ms}(t) = Nv_{cl}\dot{\lambda}_s(t) + r(t)\sum_{s=1}^{3}\dot{\lambda}_s^2(t) + N_1\dot{\lambda}_s^3(t) + k_1(t)a_{Trs}(t) + N_{3s}a_{Tts}(t) \quad (s = 1,2,3) \tag{5.62}$$

The first term of equation (5.62) corresponds to the traditional PN law. The third component of equation (5.62), with a properly chosen N_1, as discussed earlier, reacts to significant values of the LOS rate and should not influence the missile acceleration when the LOS rate is small. The coefficient $k_1(t)$ is chosen to guarantee fast decrease of $r(t)$. It can be constant or time-varying depending on available information about a target. The term $N_{3s}a_{Tts}(t)$ is different from the corresponding term in the augmented proportional navigation law because the parameter N_{3s} is time-varying and of a bang-bang type. The $sign(a_{Tts}(t)\dot{\lambda}_s(t))$ factor reflects the dependence of the correction on the target behavior. The case $N_{3s} = 1$ corresponds to the cancellation of the effect of the target maneuver on the Lyapunov function derivative $\dot{Q}$ (5.40) by forward-compensating the component of $\boldsymbol{a}_{Tr}(t)$ normal to the LOS. The coefficients N_1, N_2, and k_1 (constant or time-varying) can be determined based on simulation results of the whole missile system taking into account the autopilot limits on missile acceleration, airframe dynamics, and some other factors (i.e., the same way as the most appropriate values N = 3-4 were established).

The guidance law (5.62) assumes that a missile is able to control all three-dimensional space. For missiles enabled to control only their lateral acceleration, instead of equations (5.55) and (5.57) the initial equation (5.49) should be examined. This equation is analogous to equation (5.38), and the guidance law corresponding to this case is presented by equations (5.41)–(5.44). Comparison of equation (5.62) and equation (5.41) shows that in the case of missiles with uncontrollable thrust

the $u_{3s}(t)$ terms depend upon the total target acceleration rather than its tangential component and that instead of the radial components

$$k_1(t)a_{Trs}(t) + r(t)\lambda_s(t)\sum_{s=1}^{3}\dot{\lambda}_s^2(t)$$

the guidance law contains the radial component $u_{2s}(t)$ (s = 1,2,3). As mentioned earlier, $u_{2s}(t)$ in equation (5.41) influence the derivative $\dot{Q}$ (5.40) only in the case of unequal coefficients d_s (s = 1,2,3). Moreover, only negative $u_{2s}(t)$ (s = 1,2,3) (i.e., deceleration) can be realized in practice.

In our simplified model of engagement we assumed that the missile and target are point masses and considered the radial acceleration acting along the LOS. In reality, the radial acceleration acts along a missile's body and the tangential acceleration acts in the orthogonal direction, so that the real tangential acceleration obtained by projecting the acceleration (5.41) on the axis perpendicular to a missile's body axis may reflect the influence of the $u_{2s}(t)$ components (s = 1,2,3).

The obtained guidance laws assume that current information about target acceleration is available. Usually, we operate only with the estimated target acceleration, so that a result worse than in the ideal estimation case can be expected. Many missiles are unable to measure target acceleration and use it in a guidance law. In this case, the components $u_{3s}(t)$ (s = 1,2,3) are not present in the guidance law, and its performance is worse compared to the case when a target acceleration can be measured.

5.8 EXAMPLES

First, we consider a realistic example of a tail-controlled aerodynamic missile operating at high altitude to illustrate the effectiveness of the described guidance laws and compare it to PN guidance results.

The flight control dynamics are assumed to be presented by a third-order transfer function

$$W(s) = \frac{1 - \dfrac{s^2}{\omega_z^2}}{(1+\tau s)(1 + \dfrac{2\zeta}{\omega_M}s + \dfrac{s^2}{\omega_M^2})} \tag{5.63}$$

with damping ζ and natural frequency ω_M similar to Reference [18] ($\zeta = 0.7$ and $\omega_M = 20$ *rad/s*), the flight control system time constant $\tau = 0.5$ *s*, and the right-half plane zero $\omega_z = 5$ *rad/s*.

As it was mentioned in Reference [18], at high altitudes, where the airframe zero frequency ω_z can be low, optimal guidance, similar to Reference [2] for the single-lag model, has no advantage when compared to proportional navigation and can produce even worse results. Miss distance, when using optimal guidance, increases as the airframe zero frequency decreases. A new optimal guidance law that accounts for the presence of airframe zeroes was developed and tested in Reference [18]. It works better than a proportional navigation law but cannot be presented as a closed-form solution and is developed numerically and stored as a tabulated function of time depending on several factors.

The performance of the guidance laws (5.16) is compared to proportional navigation. We assume that the effective navigation ratio $N = 4$ and the closing velocity $v_{cl} = 1219.2$ *m/s* and consider the homing stage when the LOS angle is relatively small, so that the expression (5.16) can be used. As in Reference [18], two error sources are considered: a 3-g constant target maneuver and 1*mr* of range-independent angle measurement noise. The acceleration limit is 10 g.

A simplified model of the missile engagement is presented in Figure 5.1. Here R_{TM} is the range r between a missile and a target and $\hat{R}_{TM}$ is its estimate. The measurement of the LOS angle λ_k^*

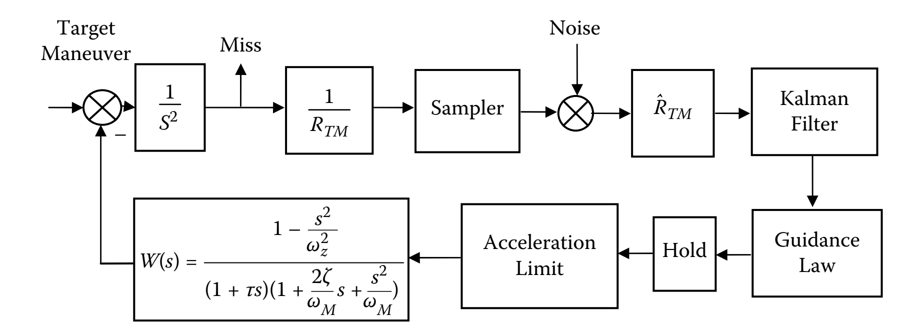


FIGURE 5.1 Missile guidance model.

is corrupted by noise. A pseudomeasurement of relative position y_k^* is created by a multiplication of λ_k^* by $\hat{R}_{TM}$. The Kalman filter then provides optimal estimates of relative position, relative velocity, and a target acceleration [17,18]. Three guidance laws are considered: proportional navigation; nonlinear guidance, discussed in the previous sections, without measurements of target acceleration; and nonlinear guidance using measurements of target acceleration.

The nonlinear guidance law has the form

$$u(t) = 4v_{cl}\dot{\lambda}(t) + N_1\dot{\lambda}^3(t) + N_3 a_T(t) \tag{5.64}$$

(For the linearized engagement model in Figure 5.1 we assume a constant closing velocity, so that the term with the second derivative $\ddot{r}(t)$ in equation (5.16) equals zero.)

We use the discrete form of the nonlinear guidance law and the estimates of $\dot{\lambda}$ in the form (symbol "^" denotes estimates)

$$\hat{\dot{\lambda}}_k = \frac{\hat{y}_k + \hat{\dot{y}}_k t_{go}}{v_{cl} t_{go}^2} \tag{5.65}$$

The results of a Monte Carlo simulation for a step target maneuver and zero initial conditions are presented in Figure 5.2. The mean absolute value of the resultant miss distances is given based on 50 simulation trials. The nonlinear term with gain N_1 = 40000 v_{cl} (data with symbol "*") significantly improves the performance of a missile when compared to the PN guidance law (data with symbol "--"). A further improvement is reached by measuring target acceleration: by using a constant gain N_3 = 1 (solid curve) or a time-dependent gain N_3 = 0.75; 1.25 [data with symbol "ооо"; see also equation (5.16)]. Each component of the guidance law (5.16) increases $|\dot{Q}(t)|$. This fact enables us to choose the gains N_i (i = 1–3) sequentially.

In the above example, N_1 was chosen based on value of the LOS angle rate estimates for the case of the PN guidance law [i.e., when only the first component of equation (5.64) was used], which was about 0.006 *rad/s* at the beginning of the homing stage and significantly less (three times and more) at the end of the homing stage. For the given N_1 value, we as if indirectly increased N in the PN law at the beginning of the homing stage [according to equation (5.14), about 30%]. However, the "cubic term" has a negligible influence at the end of the homing stage [see equation (5.14)].

Now we consider an example of a tail-controlled aerodynamic missile guided by the guidance laws discussed earlier and compare their effectiveness against a weaving maneuvering target with the acceleration $a_T(t)$ = 5g sin(1.75t). The flight control dynamics are assumed to be presented by equation (5.63) with damping ζ = 0.65 and natural frequency ω_M = 5 *rad/s*, the flight control system time constant τ = 0.1 *s* and the right-half plane zero ω_z = 30 *rad/s*.

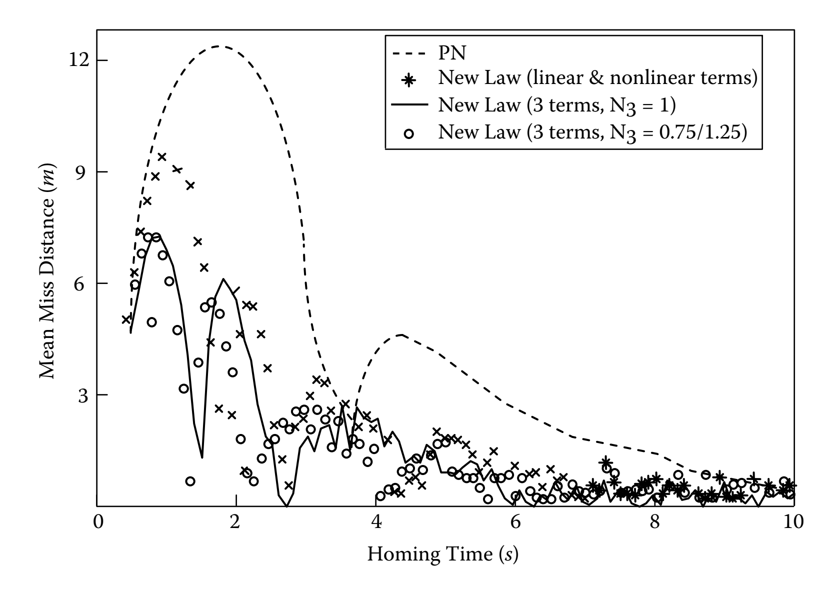


FIGURE 5.2 Comparative analysis of guidance laws performance.

The following guidance laws are analyzed (the effective navigation ratio $N = 3$, the closing velocity $v_{cl} = 7000\ m/s$):

1. The PN law $u(t) = 3v_{cl}\dot{\lambda}(t)$
2. The APN law $u(t) = 3v_{cl}\dot{\lambda}(t) + 1.5\ a_T(t)$
3. $u(t) = 3v_{cl}\dot{\lambda}(t) + N_1\dot{\lambda}^3(t)$
4. $u(t) = 3v_{cl}\cos(\lambda(t))\dot{\lambda}(t) + N_1\cos(\lambda(t))\dot{\lambda}^3(t) + N_3 a_T(t),$

$$(N_1 = 30000\ v_{cl};\quad N_3 = \begin{cases} 0.75 \\ \\ 1.75 \end{cases} \text{if } sign(a_T(t)\dot{\lambda}(t)) \begin{matrix} \le 0 \\ \ge 0 \end{matrix})$$

Simulation results are shown in Figure 5.3. Miss distances for the PN and APN guidance are shown by dashed and dash-dot lines, respectively. The effectiveness of the "cubic" term for the linearized planar model, together with the PN law, is shown by the dotted line. This term, as well as other additional terms, in the guidance law for the nonlinear planar model (solid line) significantly decreases the miss distance.

In conclusion, the guidance laws are tested on an example of the engagement model with the parameters close to those considered in Reference [7]: the effective navigation ratio $N = 3$; target initial conditions $R_{T1} = 4500\ m$, $R_{T2} = 2500\ m$, $R_{T3} = 0$; $V_{T1} = -350\ m/s$, $V_{T2} = 30\ m/s$; $V_{T3} = 0$; missile initial conditions $R_{M1} = R_{M2} = R_{T3} = 0$; $V_{M1} = 165\ m/s$, $V_{M2} = 475\ m/s$; $V_{T3} = 0$; target acceleration $a_{T1} = 0$, $a_{T2} = 3g\ \sin(1.31t)$, $a_{T3} = 0$; missile acceleration limit 5g. In contrast to Reference [7], the missile dynamics are taken into consideration: the missile flight control system right half-plane airframe zero frequency $\omega_z = 30\ rad/s$, damping $\zeta = 0.7$, natural frequency $\omega_M = 20\ rad/s$, and time constant $\tau = 0.5\ s$. A target weaving frequency is chosen according to Reference [12].

Figure 5.4 corresponds to the guidance law (5.62) and the case when the missile dynamics are ignored. It shows the trajectories of the target (crossed solid line) and missile for the PN law and the laws considered in this chapter. The time of intercept for the APN and PN laws equals 8 s. The APN does not improve the PN guidance in this case. However, the additional terms in equation (5.62) enable us to improve the PN performance. The symbol "ATN" indicates the components

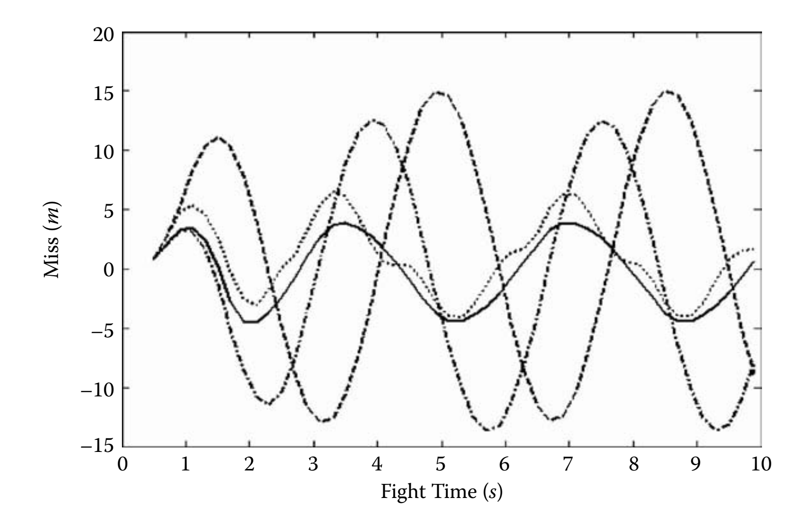


FIGURE 5.3 Miss distance comparison.

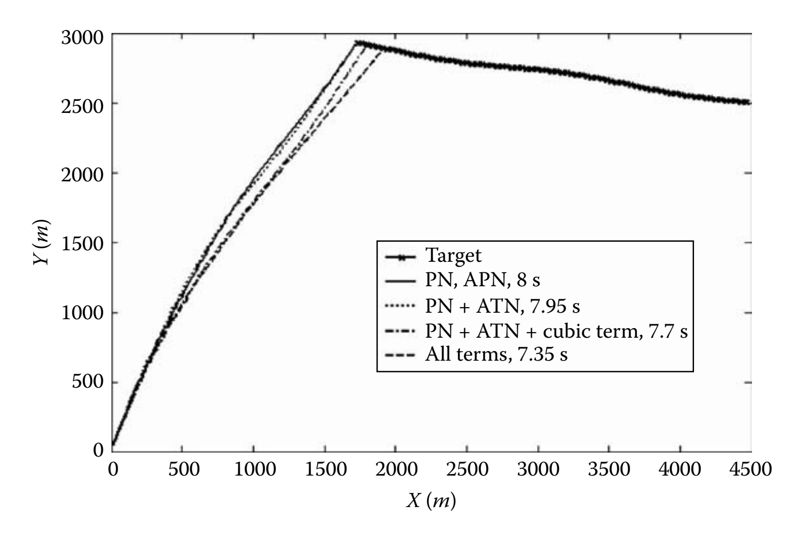


FIGURE 5.4 Comparison of the new guidance laws with PN and APN guidance (engagement model without missile dynamics).

$N_{3s}a_{Tts}(t)$ of equation (5.62) ($N_{31} = N_{32} = \{0.5; 3.5\}$, $N_{33} = 0$). The "cubic" term corresponds to $u_{s1}(t)$ components with gains $N_{11} = 20000v_{cl}$, $N_{12} = 2000v_{cl}$, $N_{13} = 0$. The guidance law with all terms of equation (5.62) ($k_1(t) = 7$) gives the best results. The time of intercept equals 7.35 *s*. As expected, inability to measure the target acceleration and absence of axial control decreases the missile performance. The time of intercept equals 7.8 *s* for the guidance law of equation (5.41), where $u_{2s}(t) = 0$, $N_{31} = N_{32} = \{1;3.5\}$, $N_{33} = 0$.

Figure 5.5 repeats the numerical simulations of Figure 5.4 taking into account the missile dynamics. In Figure 5.5 the miss distance and the time of intercept correspond to the moment of time when the closing velocity becomes positive. In the case of "PN + ATN" $N_{31} = \{0;1.5\}$, $N_{32} = 1$, and $N_{33} = 0$. In the case of "PN + ATN + cubic term" $N_{11} = 28000v_{cl}$, $N_{12} = 4000v_{cl}$, and $N_{13} = 0$. As in the case when the missile dynamics were ignored, the guidance law with all terms of equation (5.62) gives the best results. The parameters of the guidance law are $k_1(t) = 2.8$; $N_{11} = 400000v_{cl}$, $N_{12} = 19400v_{cl}$, $N_{13} = 0$; and $N_{31} = \{0;1.5\}$, $N_{32} = 1$, $N_{33} = 0$. The time of intercept and miss distance

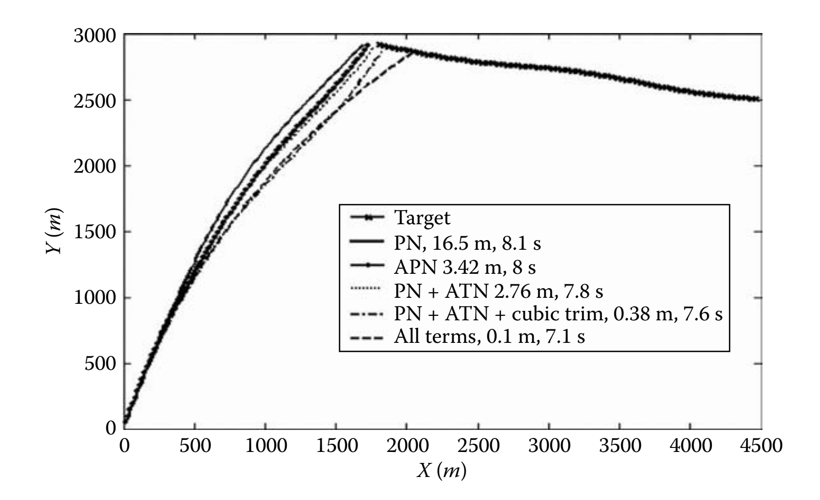


FIGURE 5.5 Comparison of the new guidance laws with PN and APN guidance (engagement model includes missile dynamics).

are significantly better than obtained under the PN and APN guidance laws. High gains N_{11} and N_{12} in the above example are chosen because of very small initial LOS rates.

The examples show the effectiveness of the guidance laws against maneuvering targets considered in this chapter and their superiority to PN and APN guidance. In addition to showing better performance, these laws can be easily implemented in practice because they use the same parameters as the PN and APN laws.

REFERENCES

1. Balakrishnan, S.N., Analytical missile guidance laws with a time-varying transformation, *Journal of Guidance, Control, and Dynamics*, 19, 2, 496–499, 1996.
2. Ben-Asher, J.Z. and Yaesh, I., Advances in missile guidance theory, *Progress in Astronautics and Aeronautics*, 180, American Institute of Astronautics and Aeronautics, Inc., Washington, DC, 1998.
3. Ghose, D., True proportional navigation with maneuvering target, *IEEE Transactions on Aerospace and Electronic Systems*, 30, 1, 229–237, 1994.
4. Guelman, M., A qualitative study of proportional navigation, *IEEE Transactions on Aerospace and Electronic Systems*, 7, 4, 637–643, 1971.
5. Kim, K.B., Kim, M.J., and Kwon, W.H., Receding horizon guidance laws with no information on the time-to-go, *Journal of Guidance, Control, and Dynamics*, 23, 2, 193–199, 2000.
6. Lee, E.B. and Markus, L., *Foundations of Optimal Control Theory*, John Wiley & Sons, Inc., New York, London, Sydney, 1986.
7. Moon, J., Kim, K., and Kim, Y., Design of missile guidance law via variable structure control, *Journal of Guidance, Control, and Dynamics*, 24, 4, 659–664, 2001.
8. Rumyantsev, V.V., On asymptotic stability and instability of motion with respect to a part of the variables. *Journal of Applied Mathematics and Mechanics*, 35 , 1, 19–30, 1971.
9. Shneydor, N.A., *Missile Guidance and Pursuit*, Horwood Publishing, Chichester, 1998.
10. Yanushevsky, R. and Boord, W., New approach to guidance law design, *Journal of Guidance, Control, and Dynamics*, 28, 1, 162–166, 2005.
11. Yanushevsky, R., Concerning Lyapunov-based guidance, *Journal of Guidance, Control, and Dynamics*, 29, 2, 509–511, 2006.
12. Yanushevsky, R., Analysis of optimal weaving frequency of maneuvering targets, *Journal of Spacecraft and Rockets*, 41, 3, 477–479, 2004.
13. Yanushevsky, R., An approach to design on control systems with parametric-coordinate feedback, *IEEE Transactions on Automatic Control*, 36, 11, 1293–1295, 1991.

14. Yanushevsky, R., Lyapunov approach to guidance laws design, in *Proceedings of the WCNA 2004*, Orlando, Florida, June 29–July 7, 2004.
15. Yanushevsky, R., Generalized missile guidance laws against maneuvering targets, *Proceedings of the Institute of Mechanical Engineers, Part I: Journal of Systems and Control Engineering*, 221, I3, 2007.
16. Yanushevsky, R., Methods and systems for guiding an object to a target using an improved guidance law. US Patent 7185844, issued March 2007.
17. Zarchan, P., Tactical and strategic missile guidance, *Progress in Astronautics and Aeronautics*, 176, American Institute of Astronautics and Aeronautics, Inc., Washington, DC, 1997.
18. Zarchan, P., Greenberg, E., and Alpert, J., Improving the high altitude performance of tail-controlled endoatmospheric missiles, *AIAA Guidance, Navigation and Control Conference*, AIAA Paper 2002-4770, August, 2002.

6 Design of Guidance Laws Implementing Parallel Navigation. Frequency-Domain Approach

6.1 INTRODUCTION

The classic approach to missile guidance is usually based on applying a guidance law obtained from certain line-of-sight (LOS) geometrical rules. The guidance law is the algorithm by which the desired geometrical rule is implemented. According to the well-known proportional navigation law, widely used in military applications, the missile acceleration is proportional to the measured LOS rate. However, acting as the commanded missile acceleration, this law produces the missile real acceleration, which differs from the desired commanded acceleration. Usually, kinematics of proportional navigation (PN) are analyzed without taking into account missile dynamics, and most recommendations concerning guidance law parameters are made based on this analysis. In the previous chapters, we acted the same way. As shown in Chapter 3 [see equation (3.6)], the miss distance due to a step target maneuver is exactly zero for an idealized, linearized, inertialess, two-dimensional PN missile–target engagement model. The influence of missile dynamics was examined analytically for single-lag models of guidance systems by using the method of adjoints [see equation (3.22)]. As indicated, the single-lag models, as well as the binomial models, do not quite match reality and do not accurately reflect flight control system dynamics. The analytical approach to analysis of the effectiveness of PN for more realistic models of guidance systems, reflecting airframe and autopilot dynamics, against weaving targets was considered in Chapter 4.

It is known that PN demonstrates good performance for nonmaneuvering or moderately maneuvering targets. For highly maneuvering targets the so-called optimal guidance laws (based on optimal control or game theory) can theoretically get significantly better results. However, as indicated earlier, these laws require complete and detailed information about missile dynamics and future behavior of a target. They are too complicated and the closed-form solution is obtained only for simple guidance system models [12,14].

As mentioned above, actual missile acceleration differs from the commanded acceleration because of the flight control system dynamics. On the one hand, its transient response may make the difference significant. For weaving targets, the frequency response of the flight control system determines the steady-state amplitude and phase shift of the real acceleration compared to the commanded acceleration. On the other hand, external disturbances usually ignored in many engagement models (e.g., drag) contribute to the difference between the actual and commanded accelerations and increase the miss distance.

The PN guidance law acted as a simple proportional controller that was used at the initial stage of control systems development. Now the PID (proportional-integral-differential) controllers are widely used in practice. Usually, the instruction of using these controllers contains the following: a proportional controller will have the effect of reducing the rise time and will reduce, but never eliminate, the steady-state error; an integral control will have the effect of eliminating the steady-state error, but it may make the transient response worse; a derivative control will have the effect

of increasing the stability of the system, reducing the overshoot, and improving the transient response. Can these recommendations be applied to the PN guidance law?

Over the years, control theory has made enormous progress, and various types of control laws have been developed and used in practice. Nevertheless, the guidance laws used in the aerospace field have not changed significantly and PN continues to dominate research and development. The so-called neoclassical approach, which, to a certain degree, is similar to the use of proportional-differential controllers (that have been used since the 1940s) was considered only in 2001 [1].

Taking into account that both transient and frequency responses can be improved by using feedback/feedforward control signals, we will consider how to use the classic control theory approach to improve the performance of missile systems with PN guidance. The approach to significantly decrease the miss distance by modifying the PN guidance and using in the guidance law the actual missile acceleration signals is discussed. New guidance laws and the conditions for choosing their parameters are considered.

6.2 NEOCLASSICAL MISSILE GUIDANCE

Let us again consider the missile guidance system discussed in Chapter 4 (see Figures 4.6 and 6.1). The relative separation $y(t)$ between a missile and a target is obtained by integrating the missile acceleration a_M subtracted from the target acceleration a_T. A division by range (closing velocity v_{cl} multiplied by time-to-go t_{go} until intercept) yields the geometric line-of-sight (LOS) angle λ, where the time-to-go is defined as $t_{go} = t_F - t$. Analogous to Figure 4.6, the missile seeker is presented formally as a perfect differentiator; the filter and seeker dynamics are represented by a transfer function

$$G_1(s) = \frac{\tau_z s + 1}{\tau_2 s + 1},$$

where τ_z and τ_2 are constant coefficients. An estimation of the LOS rate generates a guidance command a_c based on the proportional navigation law with the effective navigation ratio N. The flight control system dynamics, which combine its airframe and autopilot dynamics, are represented by the transfer function (4.12).

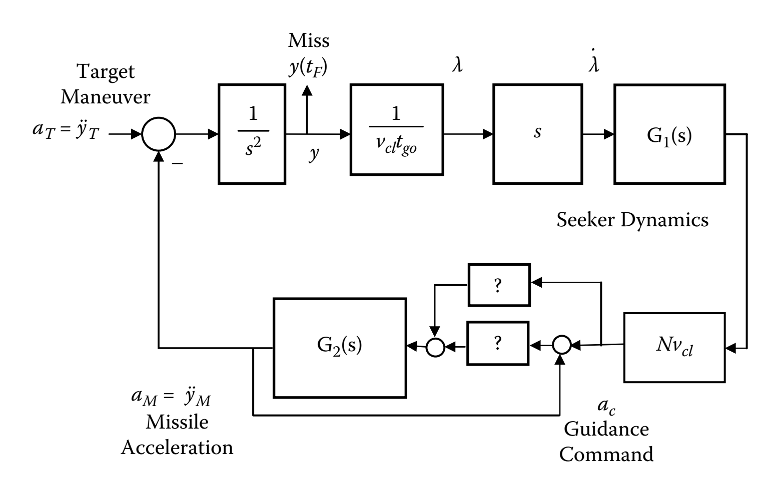


FIGURE 6.1 Modified missile guidance model.

We rewrite here the main relationships (4.13)–(4.15) of Chapter 4 [for simplicity we do not consider here $G_1(s)$ of higher order and do not use equation (4.29) for $W(s)$]:

$$Y(t_F, s) = \exp(N \int_{\infty}^{s} H(\sigma)d\sigma)Y_T(s) \tag{6.1}$$

where $Y_T(s)$ is the Laplace transform of a target vertical position $y_T(t)$, $Y(t_F,s)$ is the Laplace transform of $y(t_F)$,

$$H(s) = \frac{W(s)}{s} \tag{6.2}$$

$$W(s) = G_1(s) * G_2(s) = \frac{1 + r_1 s + r_2 s^2 + r_3 s^3}{(1+\tau_1 s)(1+\tau_2 s)(1+\frac{2\zeta}{\omega_M}s + \frac{s^2}{\omega_M^2})} \tag{6.3}$$

where r_k ($k = 1,\ldots,3$) are constant coefficients.

In contrast to Figure 4.6, Figure 6.1 contains the feedforward and feedback units, which should be determined in order to improve the performance of the PN guidance law.

The problem of obtaining small miss distance is similar to the problem of reaching high accuracy with conventional feedback systems. It is known that high accuracy can be achieved by increasing the controller gain in conventional feedback systems. However, the controversy between accuracy and stability makes the problem of designing high-accuracy systems difficult [3].

A special class of linear systems admitting infinite gains was considered in Reference [4], and the link between this class of linear structures and a class of linear optimal systems was discussed in Reference [9]. The class of linear structures examined in References [4,9], described by the n-order differential equations, requires n-1 "pure" differentiators. As shown in References [10,11], their practical realization can make the system nonrobust.

For an idealized, linearized, inertialess, two-dimensional PN missile–target engagement model, discussed in Chapter 3 [see equation (3.6)], $W(s) = 1$, so that an intuitive approach to achieve zero miss distance for the PN guided missile systems with the transfer function $W(s)$ described by function (6.3) consists of using the feedforward sequential unit with the transfer function $1/W(s)$, so that the transfer function (6.3) of the modified system (see Figure 6.1) would equal 1. Such a "naïve" approach was used in the inverse operator method applied to control systems admitting infinitely high gain [9]. Offered in the 1960s, this method suffers significant drawbacks. First, it ignores the transient response, which cannot be eliminated. As the result, it cannot be applied to systems with unstable zeroes, because the whole system with the inverse operator is nonrobust; it becomes unstable [9]. Finally, its realization usually requires multiple differentiation operations that make the real system susceptible to noise.

It looks like the similar idea to decrease the miss distance in the PN guided systems by including additional differentiating units in the "acceleration channel" was used in Reference [1]. The approach of achieving zero miss distance (ZMD) was called neoclassical guidance. The main result is stated by the following theorem of Reference [1]:

Theorem: Consider a strictly proper rational function

$$H(s) = \frac{W(s)}{s}$$

of the form

$$H(s)=\frac{b(s)}{a(s)}=\frac{b_1s^{n-1}+b_2s^{n-2}+\ldots+b_n}{s^n+a_1s^{n-1}+\ldots+a_{n-1}s},\qquad b_1\geq 0$$

where $a(s)$ and $b(s)$ are coprime polynomials.

Denote by r the relative order of $H(s)$, that is, $r = \deg[a(s)] - \deg[b(s)]$.

Under these conditions, if $s = \mathrm{Re}s + i\omega$,

$$F(\infty)=\lim_{\omega\to\infty}F(s)=\lim_{\omega\to\infty}\left[\int H(s)ds\right]\to\begin{cases}0 & iff \quad r\geq 2\\ \infty & iff \quad r=1\end{cases}$$

Proof: By presenting $H(s)$ in the form

$$H(s)=\frac{b_1}{s}+\sum_{j=2}^{\infty}h_js^{-j},$$

where h_j are coefficients of this series, and integrating the above expression, we obtain for $b_1 \neq 0$ (when $r = 1$) the integral tends to infinity, since $\ln(\infty)\to\infty$. For $b_1 = 0$, the result of integration gives the components $h_js^{1-j}/(1-j)$, $j > 1$, which tend to zero.

Since the infinite value of the above integral corresponds to the lower limit of function (6.1), that is, the corresponding exponent factor equals zero, the condition $r = 1$ gives zero $Y(t_F,s)$.

As stated in Reference [1], if the guidance system is linear, the degree of the numerator of $W(s)$ equals the degree of the denominator [the biproper transfer function $W(s)$] and $b_1 > 0$, then ZMD is obtained for any bounded target maneuver.

It is important to indicate that expression (6.1) was obtained based on the impulse response presentation by using the method of adjoints, so it is assumed that the planar model of the PN guided missile system has zero initial conditions. Hence, ZMD can be achieved only for the mentioned zero initial conditions.

Although the guidance systems operate on a finite interval of time, so that $y(t_F)$ is limited, to conclude only based on equation (6.1) that the ZMD property is attainable for the linearized models, satisfying the condition of the above theorem and improving missle performance, means ignoring the missile system dynamics. This is inadmissible and, as a result, the neoclassical approach can significantly worsen, rather than improve, the missile system performance.

The biproper transfer function can be obtained only if a compensator contains a "pure" differential operator. In practice, operations of differentiation can be performed only approximately, so that instead of the case $r = 1$ we have the case $r = 2$.

Using the analytical expressions (4.16)–(4.21), we obtain the expression for the miss distance for these two cases and compare the results for the "ideal" guidance system and the system with very close characteristics (with a real differentiation operator). The miss distance due to a weaving target will be evaluated by determining the magnitude of the steady-state component when the input, target acceleration, is a unit harmonic signal of frequency ω (e.g., $n_T = 1\ g\ sin\omega t$; g is acceleration of gravity), that is, from the expression (4.26).

The case of the "ideal" neoclassical guidance, we discuss, considers an example of a tail-controlled missile with

$$G_2(s) = \frac{1 - \frac{s^2}{\omega_z^2}}{(1+\tau_1 s)(1 + \frac{2\zeta}{\omega_M} s + \frac{s^2}{\omega_M^2})} \tag{6.4}$$

and the compensator

$$G_1(s) = -\tau_1 s + 1 \tag{6.5}$$

The negative sign of derivative $-\tau_1 s$ is stipulated by the condition $b_1 > 0$. According to the theorem this type of correction gives the zero miss distance.

Now, instead of equation (6.5) we consider a physically realizable unit

$$G_1(s) = \frac{-\tau_1 s + 1}{\varepsilon s + 1} \tag{6.6}$$

where ε is a small parameter.

The expression for the amplitude characteristic [see equations (4.17)–(4.19), and (4.26)] has the form

$$|P(t_F, \omega)| = g\omega^{N-2}(\omega^2 + \varepsilon^{-2})^{\frac{B_2 N}{2\varepsilon}}(\omega^2 + 1/\tau_1^2)^{B_1 N/2\tau_1}((\omega_M^2 - \omega^2)^2 + 4\omega_M^2\zeta^2)^{CN\omega_M^2/4}\exp(.) \tag{6.7}$$

where exp(.) is given by equation (4.27).

For $N = 3$, $\omega_M = 20$ *rad/s*, $\omega_z = 5$ *rad/s*, $\tau_1 = 0.5$ *s*, and $\zeta = 0.7$ the maximum miss distance (peak miss) of 234 *m* corresponds to a target maneuver with the frequency of 1.4 *rad/s* (i.e., with the period of 4.48 *s*). For $\tau_1 = 0.2$ *s* and $\varepsilon = 0.01$ *s* we obtain the miss distances of order $O(10^{-6})$ (i.e, a very good accuracy). However, the step response of the flight control system with the transfer function $W(s) = G_1(s)\,G_2(s)$ (see Figure 6.2) shows that the dynamic characteristics of the flight control system do not correspond to the design requirements. The signal generated by the negative derivative amplifies the "wrong-way tail effect," so that the dynamics of the modified system become inadmissible.

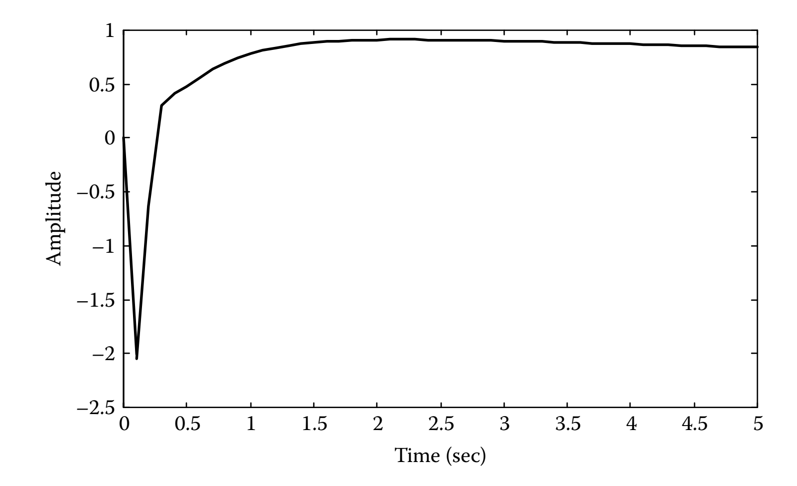


FIGURE 6.2 Step response for $\tau_1 = 0.2$ *s* and $\varepsilon = 0.01$ *s*.

Remark: In Reference [2] the nonlinear planar missile guidance system model was considered taking into account saturation due to aerodynamic or structural constraints. The positive realness (PR) condition was imposed to prevent saturation. Since the PR condition is widely used in nonlinear control theory as a stability condition, its relationship with finite time stability was established [1], so its combination with the accuracy condition [1] enables us to obtain appropriate dynamic characteristics of the flight control system. However, the PR condition significantly restricts the class of missile systems where, theoretically and under zero initial conditions, ZMD can be applied. The important class of tail-controlled missiles does not satisfy the PR condition.

6.3 PSEUDOCLASSICAL MISSILE GUIDANCE

The proportional navigation guidance law is so popular that it is considered as classic. Below we describe its modification by using the results of classic control theory. The approach offered is based on using feedforward/feedback control signals to make the real missile acceleration close to the commanded acceleration generated by the PN law. The performance of the modified guidance law is equivalent to the performance of the PN law applied to a fictitious flight control system with better dynamic characteristics.

We will consider the modified PN guidance law based on analysis of the following structure widely used in control theory (see Figure 6.3). Figure 6.3 presents in detail the part of the structure in Figure 6.1 that contains the symbol "?". Here the new commanded acceleration a_A (a new guidance law) is formed as a sum of the feedforward signal $G_4(D)a_c$ and the feedback signal $G_3(D)(a_c - a_M)$, i.e.,

$$a_A = G_4(D)a_c + G_3(D)(a_c - a_M) \tag{6.8}$$

(D is the differential operator; transfer functions $G_3(s)$ and $G_4(s)$ characterize the feedback and feedforward channels, respectively).

The transfer functions $W_\Sigma(s)$ characterizing the input–output relations between a_c and a_M can be presented as

$$W_\Sigma(s) = \frac{G_2(s)(G_3(s) + G_4(s))}{1 + G_2(s)G_3(s)} \tag{6.9}$$

where $G_4(0) = 1$ (it follows from the condition $W_\Sigma(0) = 1$, which is similar to $W(0) = 1$).

We will consider the fictitious flight control system $W_\Sigma(s)$ with better dynamic characteristics than the original flight control system $W(s)$ with respect to the commanded acceleration (the PN law).

The analysis of the guidance system with the new guidance law (6.8) is equivalent to the analysis of the guidance system in Figure 6.1 with the commanded acceleration a_c and the fictitious flight control system with the transfer function $W_\Sigma(s)$.

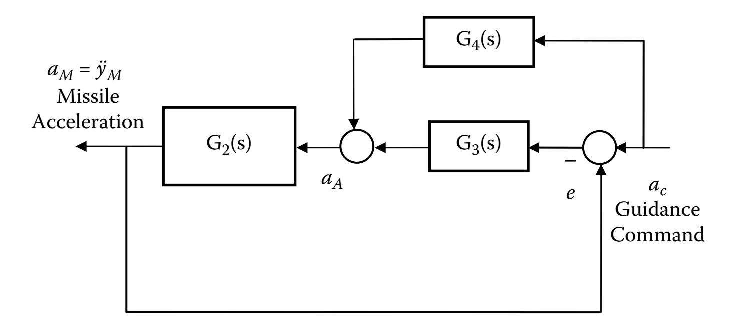


FIGURE 6.3 Modified guidance law.

The problem of designing the new guidance law, the performance of which is better than the performance of the PN guidance law, reduces to determining $W_\Sigma(s)$ [the transfer functions of the feedback and feedforward channels $G_3(s)$ and $G_4(s)$], which gives a smaller miss distance $y(t_F)$ than in the case of the initial $W(s)$, and has the transient response satisfying the design specifications.

According to equation (6.1), the miss distance due to a weaving target is evaluated by determining its steady-state component when the input is a unit harmonic signal of target acceleration with frequency ω, i.e., from the expression

$$P\ (t_F, i\omega) = \exp(N \textstyle\int_\infty^{i\omega} H(\sigma)d\sigma)\dfrac{g}{(i\omega)^2} \tag{6.10}$$

where $P(t_F, i\omega)$ is the frequency response relating the miss distance at moment t_F to the target acceleration a_T.

We will evaluate the steady-state component of equation (6.1), when the input is a sinusoidal signal; the peak miss distance characterizes its amplitude.

The integral in equation (6.10) can be presented in the following form:

$$\int_{i\infty}^{i\omega} H(\sigma)d\sigma = \int_\infty^{\omega} i(\operatorname{Re} H(i\omega) + i \operatorname{Im} H(i\omega))d\omega = \int_\omega^{\infty} (-i \operatorname{Re} H(i\omega) + \operatorname{Im} H(i\omega))d\omega \tag{6.11}$$

Since the absolute value of $\exp(N \int_\infty^{i\omega} H(\sigma)d\sigma)$ equals $\exp(N \int_\omega^\infty \operatorname{Im} H(i\omega)d\omega)$, we will analyze the expression for $\int_\omega^\infty \operatorname{Im} H(i\omega)d\omega$. Taking into account equation (6.2), we have

$$H(i\omega) = \frac{\operatorname{Re} W(i\omega)}{i\omega} + i\frac{\operatorname{Im} W(i\omega)}{i\omega} = \frac{\operatorname{Im} W(i\omega)}{\omega} - i\frac{\operatorname{Re} W(i\omega)}{\omega} \tag{6.12}$$

so that

$$\exp(N \textstyle\int_\omega^\infty \operatorname{Im} H(i\omega)d\omega) \ = \ \exp(-N \textstyle\int_\omega^\infty \dfrac{\operatorname{Re} W(i\omega)}{\omega} d\omega) \tag{6.13}$$

Theorem: The peak miss distance under the new guidance law a_A of equation (6.8) is less than under the PN guidance law if $W_\Sigma(s)$ of equation (6.9) has no poles in the right half-plane of the complex variable s and

$$\exp(\textstyle\int_\omega^\infty \dfrac{\operatorname{Re} W_\Sigma(i\omega)}{\omega} d\omega) \ > \ \exp(\textstyle\int_\omega^\infty \dfrac{\operatorname{Re} W(i\omega)}{\omega} d\omega) \tag{6.14}$$

Proof: The first condition is required for the existence of the integral in equation (6.10). The inequality (6.14) follows immediately from equations (6.10) and (6.13).

Corollary 1 of Theorem: If $W_\Sigma(s)$ is not a strictly proper rational function and its nominator and denominator are polynomials of the same order, then the peak miss distance equals zero.

Proof: In the case where the nominator and denominator have the same order, $W_\Sigma(s)$ and, hence, $\operatorname{Re} W_\Sigma(i\omega)$ contain a positive constant term, so that the integral in the left part of equation (6.14) equals infinity (i.e., the exponential term of equations (6.10) and (6.13) equals zero). Therefore, the peak miss equals zero.

Zero miss distance for a nonstrictly proper rational transfer function was discussed in the previous section. Here the conditions of ZMD were proved in a different way. Moreover, the above

statement relates only to the steady-state component of the miss distance. As mentioned earlier, the class of nonstrictly proper rational transfer functions is very sensitive to noise and its realization requires “pure” differential units, which can not be realized in practice. That is why we will consider only strictly proper rational functions $W_\Sigma(s)$.

Corollary 2 of Theorem: The peak miss distance under the new guidance law a_A [see equation (6.8)] is less than under the PN guidance law for target maneuver frequencies ω_T, if $W_\Sigma(s)$ has no poles in the right half-plane of the complex variable s and

$$\mathrm{Re}W_\Sigma(i\omega) > \mathrm{Re}W(i\omega), \quad \omega \geq \omega_T \tag{6.15}$$

Proof: Because the denominator of the integrand of equation (6.14) is positive, the condition proof of (6.14) is satisfied if the condition (6.15) holds.

In practice, it is easier to use the condition (6.15) than the condition (6.14). However, it is difficult (in the general case, simply impossible) to find physically realizable units $G_3(s)$ and $G_4(s)$ to satisfy the condition (6.15) for all $\omega \geq \omega_T$. That is why it is reasonable, first, to try to choose $G_3(s)$ and $G_4(s)$ from the condition (6.15) for $\omega \in [0,\omega_c]$, where ω_c characterizes the guidance system $W(i\omega)$ bandwidth, and then check whether equation (6.14) is satisfied. If equation (6.14) is not satisfied, $G_3(i\omega)$ and $G_4(i\omega)$ should be chosen from condition (6.15) for a higher range of ω.

The conditions (6.14) and (6.15) were obtained for the steady-state mode. Because of the correlation between the transient and frequency responses, it is plausible to assume that the new guidance laws satisfying these conditions will decrease the miss distance for small times of flight as well. Below, the described approach is demonstrated by using simple enough control structures, so that the new guidance laws can be easily realized in practice. Both transient and frequency responses are considered.

6.4 EXAMPLE SYSTEMS

Bounded input–bounded output (BIBO) stability conditions for considering the class of PN guidance structures were discussed in the Chapter 4. The transfer functions $G_3(s)$ and $G_4(s)$ should be chosen so that $W_\Sigma(s)$ is asymptotically stable.

6.4.1 Planar Model of Engagement

For the missile guidance model in Figure 6.1, $G_1(s) = 1$ and $G_2(s)$ is described by equation (4.12). The feedforward and feedback units in Figure 6.2 are chosen as

$$G_3(s) = \frac{k_1(\tau_{10}s + \mu)}{\tau_2 s + 1} \tag{6.16}$$

$$G_4(s) = k_2 \tag{6.17}$$

where τ_{10}, τ_2, and k_1 are constant parameters, $\mu = 1$ or 0, and $k_2 = 1$ or 0.

Based on equation (6.9) the transfer function $W_\Sigma(s)$ equals

$$W_\Sigma(s) = \frac{((k_1\tau_{10} + k_2\tau_2)s + k_1\mu + k_2)a(s)}{(\tau_2 s + 1)(\tau_1 s + 1)(1 + \frac{2\zeta}{\omega_M}s + \frac{s^2}{\omega_M^2}) + k_1(\tau_{10}s + \mu)a(s)} \tag{6.18}$$

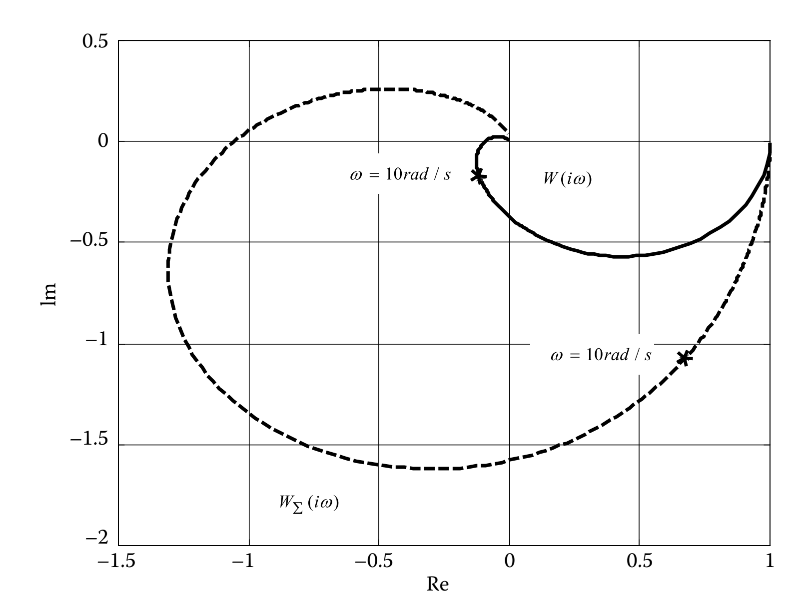


FIGURE 6.4 Frequency response $W(i\omega)$ and $W_\Sigma(i\omega)$ for $\omega_z = 30$ *rad/s*.

The procedure for finding $G_3(s)$ and $G_4(s)$ is demonstrated for examples of tail-controlled missiles where the right half-plane airframe zero can significantly influence the dynamics of the flight control system. Two cases, $\omega_z = 30$ *rad/s* and $\omega_z = 5$ *rad/s*, will be considered. As mentioned earlier, the last case corresponds to high altitudes of missile flight. The other parameters of $G_2(s)$ are chosen as $\zeta = 0.7$, $\omega_M = 20$ *rad/s*, and $\tau_1 = 0.5$ *s*. The effective navigation ratio $N = 3$; it can be changed, as shown below.

Formally, it is possible to present the condition (6.15), accompanied by the conditions for the poles of $W_\Sigma(i\omega)$ to guarantee a certain transient response, as a part of a mathematical programming problem to determine the unknown parameters of $W_\Sigma(i\omega)$. However, we will employ a standard engineering approach using elements of control theory and MATLAB software.

The frequency response of $W(i\omega)$ for $\omega_z = 30$ *rad/s* is given in Figure 6.4 (solid line). The dynamic properties of a system with such a response are satisfactory and the system has a sufficient margin of stability. According to control theory, the increase of gain k_1 (see Figure 6.3) decreases the steady-state error $e = a_c - a_M$. As seen from Figure 6.4, for $\omega \geq 10$ *rad/s*, $W(i\omega) << 1$ and $\mathrm{Re}W(i\omega) < 0$, so that the condition (6.14) should be checked for the range of frequencies $\omega \in [0,10]$.

First, we consider the case of $G_3(s) = k_1$. Analysis of equation (6.9) shows that by choosing, for example, $k_1 = 5$, we decrease significantly $e = n_c - n_1$ (i.e., make a_M closer to a_c). There exist two realizations of $W_\Sigma(i\omega)$ for $k_1 = 5$: $k_2 = 0$ and $k_2 = 1$. In the second case, the gain of $W_\Sigma(i\omega)$ equals 5/6, so that to satisfy the condition $W_\Sigma(0) = 1$ the effective navigation ratio should be increased by a factor of 6/5. In the future, we assume the corresponding increase (if necessary) of N, so that the gain of $W_\Sigma(s)$ equals 1. The frequency response $W_\Sigma(i\omega)$ in Figure 6.4 (dashed line) shows that $\mathrm{Re}W_\Sigma(i\omega) > \mathrm{Re}W(i\omega)$ for $\omega \in [0,10]$ (see also Figure 6.5). The real frequency response in Figure 6.5, as well as the step response in Figure 6.6, shows that the modified system $W_\Sigma(i\omega)$ has better dynamic characteristics than the original one.

Comparing the peak miss characteristics for a missile system with the PN guidance law and the modified guidance law, given in Figure 6.7, we can conclude that the guidance laws [see equation (6.8)]

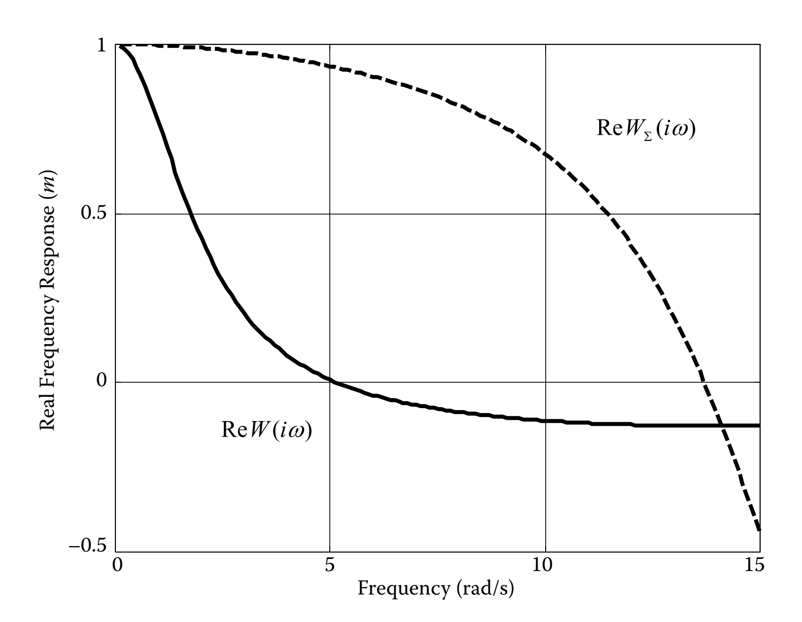


FIGURE 6.5 Real frequency response $W(i\omega)$ and $W_\Sigma(i\omega)$ for $\omega_z = 30$ *rad/s*.

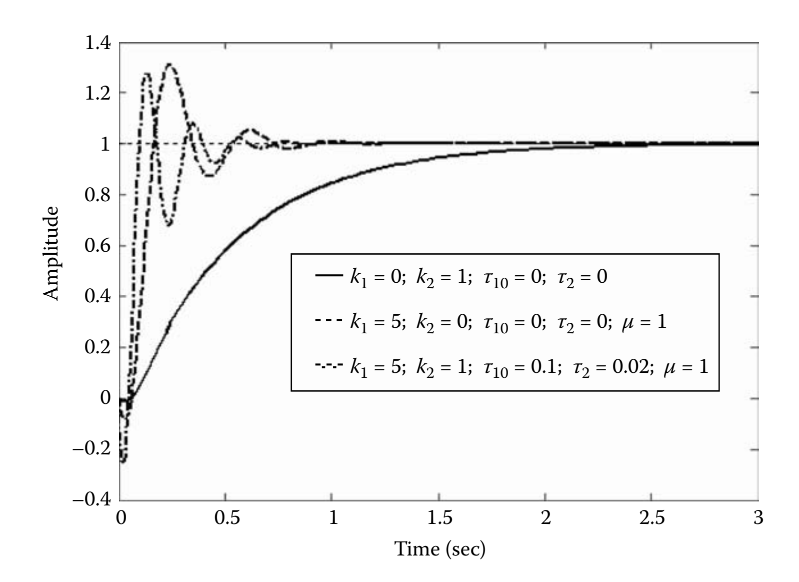


FIGURE 6.6 Step response of $W(s)$ and $W_\Sigma(s)$ for $\omega_z = 30$ *rad/s*.

$$a_A = 5(a_c - a_M), \quad N = 3*6/5,\ a_c = Nv_{cl}\dot{\lambda} \tag{6.19}$$

or

$$a_A = a_c + 5(a_c - a_M), \quad N = 3, \quad a_c = Nv_{cl}\dot{\lambda} \tag{6.20}$$

significantly decrease the miss distance.

By using a phase-lead network with parameters τ_{10} and τ_2 that increases Re$W_\Sigma(i\omega)$ more and, as a result, by using a more complicated guidance law (see Figures 6.6 and 6.7; the case $k_2 = 1$;

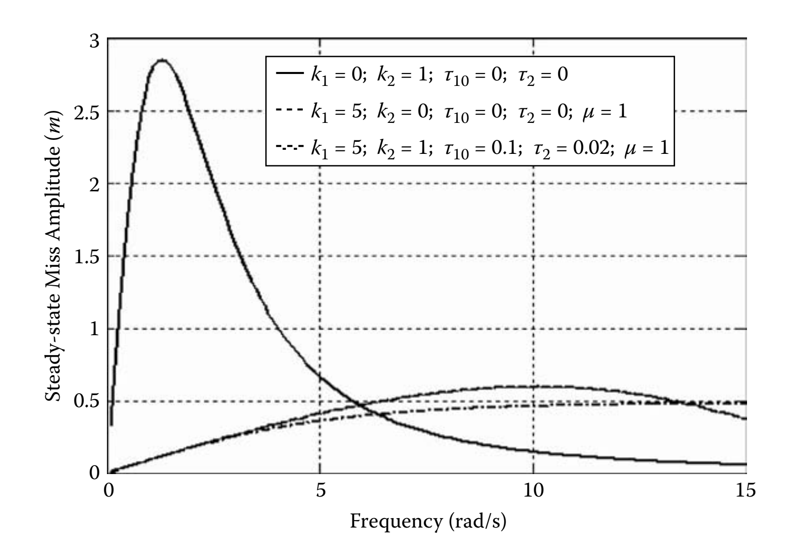


FIGURE 6.7 Comparison of the peak miss for the PN and modified guidance law for $\omega_z = 30$ *rad/s*.

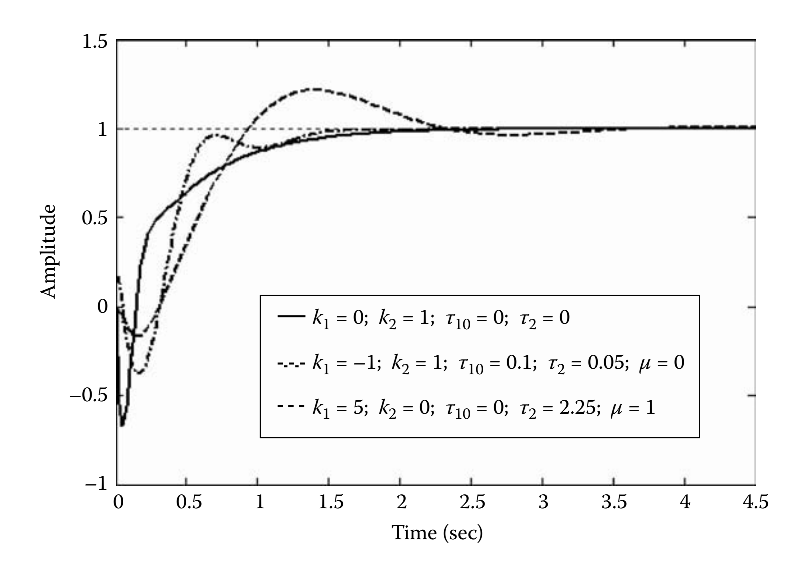


FIGURE 6.8 Step response of $W(s)$ and $W_\Sigma(s)$ for $\omega_z = 5$ *rad/s*.

$\tau_{10} = 0{,}1\ s$; $\tau_2 = 0.02\ s$; $\mu = 1$) we get an additional decrease of the miss distance. However, the additional change is not significant.

The step and frequency responses of the flight control system for $\omega_z = 5$ *rad/s* are given in Figures 6.8 and 6.9. At high altitudes the "wrong-way tail effect" of tail-controlled endoatmospheric interceptors is substantial, so that their dynamic characteristics at high altitudes are significantly worse than at lower altitudes. The amplitude characteristic of the frequency response for the missile with the PN guidance law given in Figure 6.10 shows that the peak miss for $\omega_z = 5$ *rad/s* is significantly higher than for the case $\omega_z = 30$ *rad/s* (see Figure 6.6). The analysis of the frequency response $W(i\omega)$ in Figure 6.9 (solid line) shows that gains $k_1 > 0.8$ would make the flight control system $W_\Sigma(s)$ unstable. Moreover, compared to the case $\omega_z = 30$ *rad/s*, here $W(i\omega)$ has a wider bandwidth and domain, where $\mathrm{Re}W(i\omega) < 0$.

Creating a feedback system with a gain k_1, similar to the case $\omega_z = 30$ *rad/s*, would require $G_3(s)$ to significantly narrow the bandwidth (i.e., $\tau_1 = 0$ and the time constant τ_2 should be big

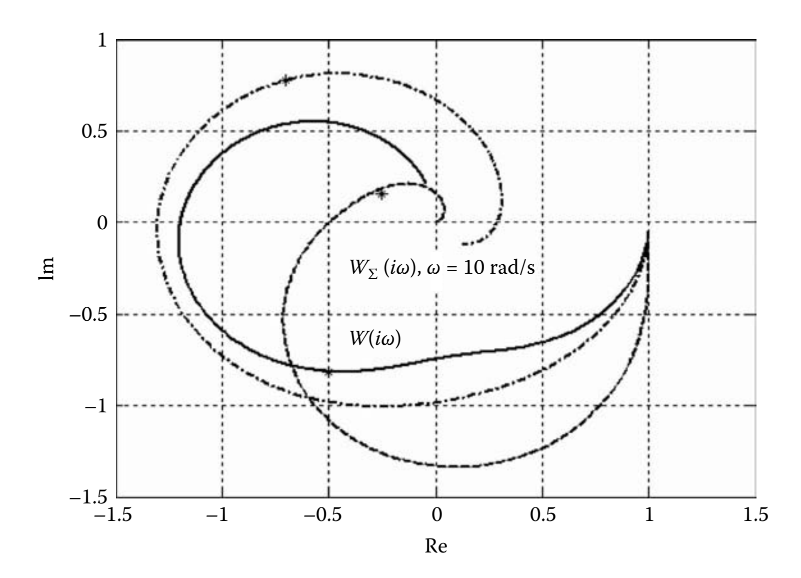


FIGURE 6.9 Frequency response $W(i\omega)$ and $W_\Sigma(i\omega)$ for $\omega_z = 5$ *rad/s*.

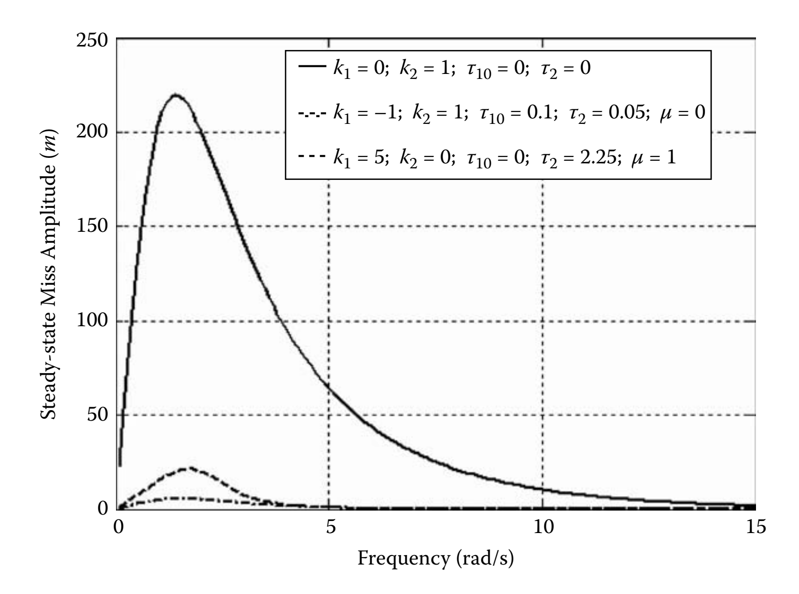


FIGURE 6.10 Comparison of the peak miss for the PN and modified guidance law for $\omega_z = 5$ *rad/s*.

enough). The analysis similar to the case of $\omega_z = 30$ *rad/s* shows that $\tau_2 = 2.25$ *s* enables us to decrease significantly the miss distance (see Figures 6.8–6.10; dashed lines). The guidance law has the following form:

$$2.25\dot{a}_A + a_A = 5(a_c - a_M), \quad N = 3*6/5, \quad a_c = Nv_{cl}\dot{\lambda} \tag{6.21}$$

As seen from the step response (Figure 6.8), the wrong-way tail effect acts as a "negative force" that can be compensated for by an opposite directed force, which can be realized by a positive feedback unit with a transfer function $\tau_{10}s/(\tau_2 s + 1)$.

The frequency and step responses and the amplitude characteristic of the frequency response for the parameters $k_1 = -1$; $k_2 = 1$; $\tau_{10} = 0{,}1$ *s*; $\tau_2 = 0.05$ *s*; $\mu = 0$, chosen from the condition (6.15), are given in Figures 6.8–6.10 (dash-dot lines). It follows that the guidance law

$$0.05\dot{a}_A + a_A = -0.05\dot{a}_c + a_c + 0.1\dot{a}_M, \quad a_c = Nv_{cl}\dot{\lambda} \tag{6.22}$$

enables us to obtain a lower peak miss than under the guidance law (6.21).

6.4.2 Multidimensional Model of Engagement

The above results were obtained and tested for the considered linear planar model assuming zero initial conditions of the flight control system coordinates and a constant closing velocity. The new guidance laws are tested also on a more precise multidimensional nonlinear model of engagement, similar to that considered in Chapter 5, with the following parameters: target initial conditions $R_{T1} = 4500\ m, R_{T2} = 2500\ m, R_{T3} = 0; V_{T1} = -350\ m/s, V_{T2} = 30\ m/s; V_{T3} = 0$; missile initial conditions $R_{M1} = R_{M2} = R_{M3} = 0;\ V_{M1} = 165\ m/s,\ V_{M2} = 475\ m/s;\ V_{M3} = 0$; target acceleration $a_{T1} = 0$, $a_{T2} = 3g\ \sin 1.31t,\ a_{T3} = 0$; missile acceleration limit $\|a_c\| \le 10g$ (R_i, V_i, $i = 1–3$, are distance and velocity coordinates). The flight control system has the same parameters as in the linear planar model.

The simulation results are presented in Table 6.1. The miss distance and the time of intercept correspond to the moment of time when the closing velocity becomes positive.

As seen from the table, the new guidance laws under consideration significantly decrease the miss distance (i.e., increase missile performance).

In Chapter 5, the class of guidance laws developed based on the Lyapunov method was discussed. Below we consider as the commanded acceleration the guidance law containing the "cubic" power of the LOS rate components λ_i (i = 1-3), i.e.,

$$a_{ci} = Nv_{cl}\dot{\lambda}_i + N_{1i}\dot{\lambda}_i^3, \quad N > 2, N_{1i} > 0 \quad (i = 1–3) \tag{6.23}$$

where N_{1i} is chosen as in the example in Chapter 5.

As mentioned earlier, even from a purely physical consideration we can assume that the missile guidance system with a variable gain, which is bigger when the LOS rate is big and smaller when the LOS rate is small, would act better than the traditional PN system. The component (6.23) with a properly chosen N_{1i} serves this purpose.

Because of the different "ideology" of the guidance laws considered in this and the previous chapters, we will test the effectiveness of the "cubic" term by considering the commanded acceleration in equation (6.23) and the guidance laws (6.19)–(6.22), that is, instead of the PN law with $N = 3$ the commanded acceleration has the form of equation (6.23). Formally, the nonlinear term in equation (6.23) does not allow us to rely on the analytical expressions (6.14) and (6.15) because they were obtained for the linear model of the missile guidance system. However, the basic idea of making the actual acceleration closer to the commanded acceleration enables us to assume that the guidance laws (6.19)–(6.22) can be used with the "cubic" term in equation (6.23). The simulation results are presented in Table 6.2.

TABLE 6.1
Comparative Analysis of Guidance Laws

Case #	Parameters	Time of intercept (*s*)	Miss (*m*)
1	$\omega_z = 30\ rad/s;\ N = 3;\ k_1 = 0;\ k_2 = 1;\ \tau_{10} = 0;\ \tau_2 = 0$	8.0	2.01
2	$\omega_z = 30\ rad/s;\ N = 3*6/5;\ k_1 = 5;\ k_2 = 0;\ \tau_{10} = 0;\ \tau_2 = 0;\ \mu = 1$	8.0	0.52
3	$\omega_z = 5\ rad/s;\ N = 3;\ k_1 = 0;\ k_2 = 1;\ \tau_{10} = 0;\ \tau_2 = 0$	8.0	5.58
4	$\omega_z = 5\ rad/s;\ N = 3*6/5;\ k_1 = 5;\ k_2 = 0;\ \tau_{10} = 0;\ \tau_2 = 2.25;\ \mu = 1$	8.0	0.81
5	$\omega_z = 5\ rad/s;\ N = 3;\ k_1 = -1;\ k_2 = 1;\ \tau_{10} = 0.1s;\ \tau_2 = 0.05s;\ \mu = 0$	8.0	0.29

TABLE 6.2
Analysis of Influence of Nonlinear "Cubic" Term

Case #	Parameters	Time of intercept (s)	Miss (m)
1	$\omega_z = 30\ rad/s;\ N = 3;\ k_1 = 0;\ k_2 = 1;\ \tau_{10} = 0;\ \tau_2 = 0$	7.2	2.01
2	$\omega_z = 30\ rad/s;\ N = 3*6/5;\ k_1 = 5;\ k_2 = 0;\ \tau_{10} = 0;\ \tau_2 = 0;\ \mu = 1$	6.1	0.5
3	$\omega_z = 5\ rad/s;\ N = 3;\ k_1 = 0;\ k_2 = 1;\ \tau_{10} = 0;\ \tau_2 = 0$	7.0	0.59
4	$\omega_z = 5\ rad/s;\ N = 3*6/5;\ k_1 = 5;\ k_2 = 0;\ \tau_{10} = 0;\ \tau_2 = 2.25s;\ \mu = 1$	6.0	0.29
5	$\omega_z = 5\ rad/s;\ N = 3;\ k_1 = -1;\ k_2 = 1;\ \tau_{10} = 0.1s;\ \tau_2 = 0.05s;\ \mu = 0$	6.0	0.28

The simulation results show that the guidance laws (6.8), (6.19)–(6.22) can work successfully with other guidance laws that contain the PN law as their component.

In contrast to the acceleration feedback used in autopilot systems [its influence is reflected in $G_2(s)$], the additional acceleration feedback described above is used to generate the new guidance law (6.8). It is assumed that the new guidance would work with existing autopilots. However, the expression of (6.8) and, especially, the acceleration operator $G_4(s)$ can also be used for the design of integrated guidance and autopilot systems.

The traditional approach to missile guidance and control system design has been to neglect interactions between these systems. Usually, individual missile systems are designed separately and then they are assembled. If the whole system performance is unsatisfactory, the individual subsystems are redesigned to improve the system performance. Because of its iterative nature, the design process can be highly time consuming and expensive. The approach discussed in this chapter can be considered as an important component of design methods for integrated guidance–autopilot systems.

REFERENCES

1. Gurfil, P., Jodorkovsky, M., and Guelman, M., Neoclassical guidance for homing missiles, *Journal of Guidance, Control, and Dynamics*, 24, 3, 452–459, 2001.
2. Gurfil, P., Jodorkovsky, M., and Guelman, M., Design of nonsaturating guidance systems, *Journal of Guidance, Control, and Dynamics*, 23, 4, 693–700, 2000.
3. Dorf., R.C., *Modern Control Systems*, Addison-Wesley, Inc., New York, 1989.
4. Meerov, M.V., *Structural Synthesis of High Accuracy Automatic Control Systems*, Nauka, Moscow, 1965.
5. Smith , O., *Feedback Control Systems*, McGraw-Hill, Inc., New York, 1958.
6. Shneydor, N.A., *Missile Guidance and Pursuit*, Horwood Publishing, Chichester, 1998.
7. Yanushevsky, R., Analysis of optimal weaving frequency of maneuvering targets, *Journal of Spacecraft and Rockets*, 41, 3, 477–479, 2004.
8. Yanushevsky, R., Frequency domain approach to guidance system design, *IEEE Transactions on Aerospace and Electronic Systems*, 43, 2007.
9. Yanushevsky, R., *Theory of Linear Optimal Multivariable Control Systems*, Nauka, Moscow, 1973.
10. Yanushevsky, R., On the robustness of the solution of the problem of the analytical construction of controls, *Automation and Remote Control*, 3, 356–363, 1966.
11. Yanushevsky, R., Robust stabilizability of linear differential-difference systems with unstable D-operator, *IEEE Transactions on Automatic Control,* 37, 6, 652–653, 1992.
12. Zarchan, P., Tactical and strategic missile guidance, *Progress in Astronautics and Aeronautics*, 176, American Institute of Astronautics and Aeronautics, Inc., Washington, DC, 1997.

13. Zarchan, P., Proportional navigation and weaving targets, *Journal of Guidance, Control, and Dynamics*, 18, 5, 969–974, 1995.
14. Zarchan, P., Greenberg, E., and Alpert, J., Improving the high altitude performance of tail-controlled endoatmospheric missiles, *AIAA Guidance, Navigation and Control Conference*, AIAA Paper 2002–4770, Aug. 2002.

7 Guidance Law Performance Analysis Under Stochastic Inputs

7.1 INTRODUCTION

The guidance laws analysis in the previous chapters was strictly deterministic. It was assumed that the information about their parameters contains no errors and the components of the missile guidance system have fixed parameters, so that no uncertainties exist. This approach is very useful at the initial stage of design.

The realization of the discussed guidance laws requires information about the line-of-sight (LOS) rate, closing velocity, and target acceleration. This information is received from the sensors that measure the variables that are present in the guidance laws. As with any measurements, these measurements are accompanied by noises, which can significantly increase the miss distance if the necessary means are not taken to decrease their influence on missile performance.

Here we consider noises that distort the guidance laws and their influence on the miss distance. As to the evaluation of the effect of uncertainties induced by the autopilot and airframe parameters, this type of problem is considered in control theory [1,5,10]. The appropriate results can be used when designing autopilot systems.

Because of the random nature of noises, the analysis of their influence on the miss distance requires the utilization of the mathematical apparatus of random functions, analysis of random processes driven by noise.

Random processes related to guidance problems can also be stipulated by the random character of target maneuvers.

Below we present basic facts for the theory of stochastic processes, which are necessary for understanding the following material. The characterization of the main sources of noise that influence proportional navigation (PN) guidance law performance is given. The effect of random disturbances (measurement noise and random maneuvers) on guided missile system performance is evaluated by the root-mean-square miss distance. The analytical expressions of the miss distance under the above-mentioned stochastic inputs will be obtained. Analytical expressions for the root-mean-square miss are examined in detail for a simple first-order model of the missile guidance system. For the higher-order models, the computational procedure and corresponding algorithms based on the obtained analytical expressions (see also References [7–9]) are discussed. The advantage of the approach considered is that it excludes the necessity for simulating the adjoint system to analyze the miss distance under the stochastic inputs (see e.g., References [3,11]) and, as a result, significantly simplifies the computational process.

Analytical expressions and related computational algorithms are given for proportional navigation (PN) guided missiles. However, the same expressions can be used for analysis of the more sophisticated guidance laws considered in Chapter 6 if instead of the real flight control system we operate with a fictitious one [see equation (6.9)].

7.2 BRIEF DISCUSSION OF STOCHASTIC PROCESSES

The theory of stochastic signals in its most general form is extremely abstract, and a rigorous presentation requires a degree of mathematical sophistication beyond the scope of this book. Our

main objective here is to present a specific set of results related to random signals that will be used later. Although the material related to random signals cannot be considered rigorous, we will summarize the important results and the mathematical assumptions accompanying them. We assume that the reader is familiar with fundamental concepts of the theory of probability such as random variables, probability distributions, and averages.

The general concept of a stochastic process can be stated in the following way. Let U be a set of elementary events and t a continuous parameter. A stochastic process $\eta(t)$ is defined as the function of two arguments

$$\eta(t) = f(e,t), \quad e \in U, t \in T \tag{7.1}$$

For every moment of time t, the function $f(e,t)$ is a function of e only and, consequently, is a random variable. For every fixed value of the argument e (i.e., for every elementary event), $f(e,t)$ depends only on t (i.e., is a function of time). Every such function is called a realization, or sample function, of the stochastic process $\eta(t)$. A stochastic process can be regarded either as a collection of random variables $\eta(t)$ that depend on the parameter t, or as a collection of the realizations of the process $\eta(t)$. To define a process it is necessary to specify a probability measure (e.g., a set of probability distribution functions) in the functional space of its realizations.

The probability law of a random variable η can always be specified by stating its distribution function or the probability density function $p(\eta)$.

The average or mean of a random variable η is defined by

$$m_\eta = E[\eta] = \int_{-\infty}^{\infty} \eta p(\eta) d\eta \tag{7.2}$$

The variance of η is defined by

$$Var[\eta] = E[(\eta - E[\eta])^2] = \sigma^2[\eta] = E[\eta^2] - E^2[\eta] \tag{7.3}$$

The standard deviation of η is defined by

$$\sigma[\eta] = \sqrt{Var[\eta]} \tag{7.4}$$

It can be shown that, if random variables η_i are independent, the mean m_0 and the variance σ_0^2 of the sum are the sum of the means and variances, respectively, i.e.,

$$m_0 = E[\sum \eta_i] = \sum E[\eta_i] = \sum m_{\eta_i} \tag{7.5}$$

$$\sigma_0^2 = E[(\sum \eta_i - m_0)^2] = \sum E[(\eta_i - m_{\eta_i})^2] = \sum \sigma^2_{\eta_i} \tag{7.6}$$

Below we present two important probability density functions: the uniform distribution $p_{uniform}(\eta)$ and the Gaussian or normal distribution $p_{normal}(\eta)$.

For the uniform distribution we have

$$p_{uniform}(\eta) = \frac{1}{b-a}, \qquad m_{uniform} = \frac{1}{b-a}\int_a^b \eta d\eta = \frac{b+a}{2}, \tag{7.7}$$

$$\sigma^2_{uniform} = E\left[\eta^2\right] - m^2_{uniform} = \frac{b^3 - a^3}{3(b-a)} - \left(\frac{b+a}{2}\right)^2 = \frac{(b-a)^2}{12} \tag{7.8}$$

where the variable $\eta \in [a,b]$.

For the normal distribution we have

$$p_{normal}(\eta) = \frac{1}{\sqrt{2\pi}\sigma_{normal}} \exp\left[-\frac{(\eta - m_{normal})^2}{2\sigma_{normal}}\right] \tag{7.9}$$

where m_{normal} and σ^2_{normal} are the mean and variance, respectively.

Analogous to the averages that characterize a random variable, the ensemble averages such as the average or mean of a process

$$m(t) = E[\eta(t)] = \int_{-\infty}^{\infty} \eta(t) p(\eta, t) d\eta, \tag{7.10}$$

the mean square value

$$E[\eta^2(t)] = \int_{-\infty}^{\infty} \eta^2(t) p(\eta, t) d\eta, \tag{7.11}$$

the root-mean-square (rms) value

$$rms = \sqrt{E[\eta^2(t)]}, \tag{7.12}$$

and the variance

$$\sigma^2_\eta(t) = E[(\eta(t) - E[\eta(t)])^2] = E[\eta^2(t)] - E^2[\eta(t)] \tag{7.13}$$

are introduced for stochastic processes, where $p(\eta,t)$ is the probability density function of a stochastic process introduced formally analogous to the probability density function of a random variable.

The square root of the variance $\sigma^2_\eta(t)$ is also known as the standard deviation. For random processes with zero mean the rms value coincides with the standard deviation.

The role played for a random variable η by its mean and variance is played for a stochastic process by its mean value function and its covariance kernel

$$Cov[(\eta(\tau), \eta(t)] = E[(\eta(\tau) - E[(\eta(\tau)])(\eta(t) - E[\eta(t)])] \tag{7.14}$$

A stochastic process $\eta(t)$ is called stationary if the probability distribution functions for two finite groups of variables $\eta(t_1), \eta(t_2), \ldots, \eta(t_n)$ and $\eta(t_1 - k), \eta(t_2 - k), \ldots, \eta(t_n - k)$ coincide and, hence, are independent of k.

Clearly, any numerical characteristic of a stationary process $\eta(t)$ is independent of the time t, that is, for the expectation and variance we have

$$E[\eta(t_i)] = m_\eta, \quad Var[\eta(t_i)] = \sigma_\eta^2 \quad (-\infty < t_i < \infty) \tag{7.15}$$

The covariance kernel $Cov[(\eta(\tau),\eta(t)]$ of a stationary process is a function of the absolute difference $|t - \tau|$, i.e.,

$$Cov[\eta(\tau),\eta(t + \tau)] = R_\eta(\tau) \tag{7.16}$$

where $R_\eta(\tau)$ is called the covariance function.

The stochastic process $\eta(t)$ was defined as the function of two arguments. It can be shown that for a class of stochastic processes, called the ergodic processes, which includes the stationary processes (a more rigorous formulation can be found, e.g., in Reference [2]), averages computed from a sample of a stochastic process can be identified with corresponding ensemble averages.

Given a finite sample $\{\eta(t), 0 \le t \le T\}$ of the process, we define the sample covariance function for stationary stochastic processes with zero mean as

$$R_{\eta T}(\tau) = \frac{1}{T}\int_{t_0}^{t_0+T} \eta(t)\eta(t+\tau)dt \tag{7.17}$$

Based on the ergodic property,

$$\lim_{T\to\infty} R_{\eta T}(\tau) = R_\eta(\tau) \tag{7.18}$$

where $R(\tau)$ is called the autocorrelation function.

Frequency-domain methods, based on the Fourier transform, are widely used for analysis of deterministic signals. The Fourier transform of the autocorrelation function also plays a significant role in the analysis of stationary random signals.

The Fourier transform of the function $(1/2\pi)R_\eta(\tau)$

$$\Phi_\eta(\omega) = \frac{1}{2\pi}\int_{-\infty}^{\infty} R_\eta(\tau)e^{-i\omega\tau}d\tau \tag{7.19}$$

of the stationary random function $\eta(t)$ is called the power spectral density of $\eta(t)$ or simply the spectral density.

Using the expression of the inverse Fourier transform and equations (7.13), (7.17), and (7.18), we can obtain

$$\sigma_\eta^2 = \int_{-\infty}^{\infty} |\eta(t)|^2\, dt = R_\eta(0) = \int_{-\infty}^{\infty} \Phi_\eta(\omega)d\omega \tag{7.20}$$

This expression is widely used to determine the mean square value of a stationary random function.

The spectral density of a signal exists if and only if the signal is a wide-sense stationary [2]. If the signal is not stationary, then the same methods used to calculate the spectral density can still be used, but the result cannot be called the spectral density. Based on the above expression, it can be shown that the power spectral density $\Phi_\eta(\omega)$ of the signal $\eta(t)$ is the square of the magnitude of the Fourier transform $\Pi(\omega)$ of the signal (Parseval's theorem), i.e.,

$$\Phi_\eta(\omega) = \frac{\Pi(\omega)\Pi^*(\omega)}{2\pi} = \left| \frac{1}{2\pi} \int_{-\infty}^{\infty} \eta(t) e^{-i\omega t} dt \right|^2 \tag{7.21}$$

where the symbol "*" indicates the complex conjugate operation.

The random process is said to be a white noise process if it possesses a constant power spectral density Φ_η. White noise is so called as an analogy with white light, which contains all frequencies. An infinite-bandwidth white noise signal is purely a theoretical construct. By having power at all frequencies, the total power of such a signal is infinite. White noise is the abstract, physically unrealizable, random process with autocorrelation function equal to a delta-function (as mentioned, it is equivalent to a constant spectral density). Despite its abstract nature, white noise is widely used for analysis of real systems when the real noise bandwidth significantly exceeds the system bandwidth (i.e., in practice, a signal can be "white" with a flat spectrum over a defined frequency band).

The above definition of white noise states only that it has equal energy at all frequencies and refers to correlations at two distinct times, which are independent of the noise amplitude distribution. While the frequency distribution may be the same, the amplitude distribution can be different. Noise with a Gaussian amplitude distribution (normal distribution) is called Gaussian noise. This says nothing of the correlation of the noise in time or of the spectral density of the noise. It is often incorrectly assumed that Gaussian noise is necessarily white noise. Gaussianity refers to the way signal values are distributed, while the term "white" refers to correlations at two distinct times, which are independent of the noise amplitude distribution. Gaussian white noise (white noise with a Gaussian amplitude distribution, also called the pseudowhite noise) is a good approximation of many real-world situations and generates mathematically tractable models. A useful relationship between the desired white noise spectral density Φ_η and the standard deviation σ of the pseudowhite noise (white noise has infinite standard deviation) (i.e., the Gaussian random numbers generated every interval Δ, is given by Reference [11]).

$$\Phi_\eta = \sigma^2 \Delta \tag{7.22}$$

The output $y(t)$ of a linear system with the impulse response $P(t,\tau)$, when the input signal $\eta(t)$ is white noise with the spectral density Φ_η, equals

$$y(t) = \int_{-\infty}^{t} P(t,\tau)\eta(\tau)d\tau \tag{7.23}$$

The mean square value of $y(t)$ can be presented as

$$E[y^2(t)] = \int_{-\infty}^{t}\int_{-\infty}^{t} P(t,\tau_1)P(t,\tau_2)E[\eta(\tau_1)\eta(\tau_2)]d\tau_1 d\tau_2 \tag{7.24}$$

Taking into account that the autocorrelation function (7.17) of white noise equals

$$E[\eta(\tau_1)\eta(\tau_2)] = \Phi_\eta \delta(\tau_1 - \tau_2) \tag{7.25}$$

the previous expression can be simplified as

$$E[y^2(t)] = \Phi_\eta \int_{-\infty}^{t} P^2(t,\tau)d\tau \tag{7.26}$$

It follows from equation (7.26) that the mean square response of a linear system influenced by white noise with the spectral density Φ_η is proportional to the integral of the square of the impulse response.

7.3 RANDOM TARGET MANEUVERS

In Chapter 3 we obtained the analytical expression for the miss distance for a constant maneuver a_T. This type of maneuver is convenient for analysis but is far from reality. In Chapter 4 we considered sinusoidal target maneuvers and determined the miss peak for the various times of flight t_F. The shape of this maneuver policy is deterministic and quite realistic. It corresponds to the so-called "barrel roll" strategy, which, in contrast to the sinusoidal deterministic maneuver, is random. The miss peak enables us to evaluate, to a certain degree, the worst case. A more realistic scenario corresponds to sinusoidal target maneuvers with random starting times of the maneuver, that is, with a random phase.

The result of Reference [3], showing how to use the concept of a shaping filter for the statistical representation of signals with known form but random starting time, is used here to write the expressions for the random step and sinusoidal signals, if their starting time is uniformly distributed over the flight time.

The ability to use shaping filters excited by white noise to generate random signals follows from equations (7.23)–(7.26) and (7.21) and is based on the fact that random processes that have the same mean and autocorrelation functions are mathematically equivalent for problems dealing with the mean square values of random signals.

A signal $x(t)$ of a known form $a(t)$ with random starting time T can be presented as

$$x(t) = a(t - T)s(t - T) \tag{7.27}$$

where $s(t)$ is the unit step function, i.e., $s(t) = 0$, $t < 0$ and $s(t) = 1$, $t \geq 0$.

In the case of a uniformly distributed starting time over the flight time t_F the probability density function $p_T(t)$ of T is given by

$$p_T(t) = \begin{cases} 1/t_F, & 0 \leq t \leq t_F \\ 0, & t > t_F \end{cases} \tag{7.28}$$

Hence, the autocorrelation function of equation (7.27) with a random starting time is

$$R_x(t_1, t_2) = E[x(t_1)x(t_2)] = \int_{-\infty}^{\infty} x(t_1)x(t_2)p_T(T)dT \tag{7.29}$$

For a random step signal a_T we have

$$R_x(t_1, t_2) == \int_0^{t_F} a_T^2 s(t_1 - T)s(t_2 - T))dT \,/\, t_F \tag{7.30}$$

Assuming $0 \leq t_1 \leq t_2 \leq t_F$, the above expression can be simplified to

$$R_x(t_1, t_2) = \frac{a_T^2}{t_F} \int_0^{t_1} s(t_1 - T)s(t_2 - T)dT \tag{7.31}$$

The autocorrelation function of the output $y(t)$ of the linear time-invariant system with the impulse response $P(t)$, when the input signal $\eta(t)$, $0 \le t \le t_F$, is white noise with the spectral density Φ_η, equals [see equations (7.17), (7.18), (7.23), and (7.25)]

$$R_y(t_1,t_2) = \int_0^{t_1}\int_0^{t_2} P(t_1-\tau_1)P(t_2-\tau_2)\Phi_\eta\delta(\tau_1-\tau_2)d\tau_1 d\tau_2 \tag{7.32}$$

Assuming $0 \le t_1 \le t_2 \le t_F$, the above expression becomes

$$R_y(t_1,t_2) = \Phi_\eta \int_0^{t_1} P(t_1-\tau_1)P(t_2-\tau_1)d\tau_1 \tag{7.33}$$

Equations (7.31) and (7.33) are equivalent if

$$\Phi_\eta = a_T^2 / t_F \text{ and } P(t) = 1 \tag{7.34}$$

For the sinusoidal target maneuver that starts at time T, we have

$$x(t) = a_T \sin(\omega_T t - T)s(t - T) \tag{7.35}$$

so that, instead of equation (7.30), the autocorrelation function of this signal with random starting time is

$$R_x(t_1,t_2) == \int_0^{t_F} a_T^2 \sin(\omega_T t_1 - T)\sin(\omega_T t_2 - T)s(t_1-T)s(t_2-T))dT / t_F \tag{7.36}$$

or, assuming $0 \le t_1 \le t_2 \le t_F$,

$$R_x(t_1,t_2) = \frac{a_T^2}{t_F}\int_0^{t_1} \sin(\omega_T t_1 - T)\sin(\omega_T t_2 - T)dT \tag{7.37}$$

Equations (7.33) and (7.37) are equivalent if

$$\Phi_\eta = a_T^2 / t_F \text{ and } P(t) = \sin\omega_T t \tag{7.38}$$

The above consideration shows that step and sinusoidal maneuvers of amplitude a_T, whose starting time is uniformly distributed over the flight time t_F, that is, the probability density function is given by equation (7.28), have the same autocorrelation function as a linear network, driven by white noise with spectral density $\Phi_\eta = a_T^2 / t_F$, with transfer functions

$$W_{filter}(s) = \frac{1}{s} \tag{7.39}$$

$$W_{filter}(s) = \frac{1/\omega_T}{s^2/\omega_T^2 + 1} \tag{7.40}$$

respectively.

7.4 ANALYSIS OF INFLUENCE OF NOISES ON MISS DISTANCE

As mentioned earlier, the ability to use the adjoint system to obtain the analytical expression (4.13) for the miss distance is stipulated by specifics of the considered model of the missile guidance system. Its state matrix [see, e.g., equation (3.8)] is a function of $t_F - t$. Its impulse response as a function of t_F can be analyzed as a function of σ ($0 \le \sigma \le t_F$), where σ is the impulse application time, by varying $t_F - \sigma$. The relationship between the impulse responses of the adjoint (more precisely, modified adjoint system) and original systems $P_{ma}(t_F - \sigma, t_F - t_0) = P(t_0,\sigma)$, where t_0 is the impulse observation time, enables us to examine $P(t_F,\sigma)$ as a function of t_F by considering $P_{ma}(t_F - \sigma, t_F - t_F) = P_{ma}(t_F - \sigma,0)$ as a function of $\sigma(0 \le \sigma \le t_F)$.

Here the adjoint system impulse response is used for statistical analysis of the original system in the presence of stochastic inputs.

The rms response $y(t_F)$ of a linear time-varying system with the impulse function $P_0(t,\sigma)$ at the finite time t_F, stipulated by the white noise input with the spectral density Φ_n, is presented [see equation (7.26)] by

$$rms = \{E[y^2(t_F)]\}^{1/2} = \sqrt{\Phi_n \int_0^{t_F} P_0^2(t_F,\sigma)d\sigma} \tag{7.41}$$

The analytical expressions for $P_0(t_F,\sigma)$ will be obtained by the method of adjoints. If earlier we used the method of adjoints to obtain analytical expressions of the miss distance assuming that the target acceleration is a deterministic function of time, here we will evaluate the effect of random disturbances (measurement noise and random target maneuvers) on the guided missile system performance, choosing the rms miss criterion. Assuming the linearized engagement planar model, the PN law and the linear guidance system dynamics (see Figure 4.3) we will use the expressions (4.10) and (4.34) to analyze the influence of the random disturbances on the miss distance.

Figure 7.1 is similar to Figure 4.1. It contains only additional stochastic inputs, which will be discussed in detail.

Target tracking represents estimation of position, velocity, and acceleration of a target. The estimation must handle different perturbations.

One of the perturbations is glint noise. Glint noise occurs, when radar is used in target tracking, because of interference between the reflected radar waves. In real radar target tracking systems, changes in the target aspect with respect to the radar can cause the apparent center of radar reflections (direction "seen" by the antenna) to wander significantly. The random wandering of the apparent

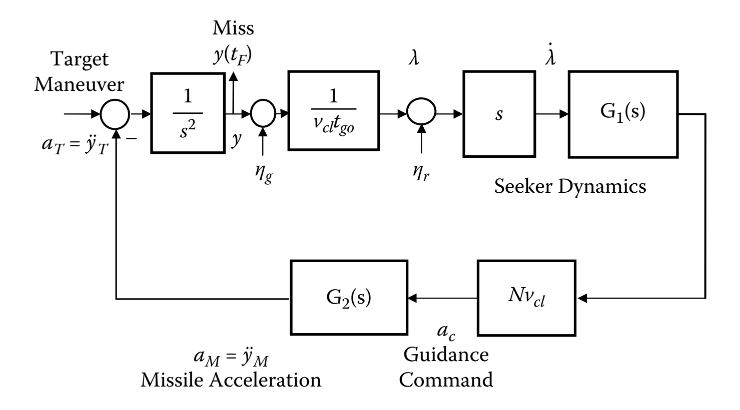


FIGURE 7.1 Missile guidance model.

radar reflecting center gives rise to noisy or jittered angle tracking. This form of measurement noise is called angle fluctuations or target glint. Glint noise mainly affects the performance of radar-guided missiles and to a smaller extent the performance of missiles with electro-optical seekers, where infrared radiance fluctuations are smaller than radar reflection fluctuations.

Glint affects measurement components (mostly the angles) by producing heavy-tailed non-Gaussian disturbances, which may severely affect the tracking accuracy. Glint noise is non-Gaussian, which makes the estimation more difficult. One of the most common target tracking methods today is the Kalman filter. This method assumes the perturbations to be Gaussian, but this will not be true for glint noise. In target tracking, the measurement noise is usually assumed to be Gaussian. However, as mentioned above, the distribution of glint noise is non-Gaussian long tailed. Moreover, it may be highly correlated, so that, to be rigorous, it cannot be modeled as white noise.

Nevertheless, to get the analytical expression that enables us to evaluate approximately the rms due to glint noise η_g (see Figure 7.1) we assume that η_g is white noise with the power density Φ_{gn}.

The model of the system adjoint to the system in Figure 7.1 is presented in Figure 7.2. The output $P_g(t_F,T)$ corresponds to the impulse response of the PN missile guidance system to the white noise input $\eta_g(t)$. The analytical expression for $P_g(t_F,s)$ can be written based on the expression obtained earlier of

$$P_T(t_F,s) = \exp(\int_{\infty}^{s} NH(\sigma)d\sigma)$$

[see equation (4.10)]. For the structure in Figure 7.2, with the input $\delta(t)$ and the output $P_g(t_F,t)$ we have

$$P_g(t_F,t) = \delta(t) - P_T(t_F,t)$$

or

$$P_g(t_F,s) = 1 - P_T(t_F,s) \tag{7.42}$$

Hence, based on equation (7.41), the rms miss distance due to glint noise can be obtained from the equation

$$\frac{rms^2}{\Phi_{gn}} = \frac{E\left[y^2(t_F)\right]_{gl\,\mathrm{int}}}{\Phi_{gn}} = \int_0^{t_F} \{L^{-1}\left[1 - P_T(t_F,s)\right]\}^2\,dt \tag{7.43}$$

where L^{-1} is the symbol of the inverse Laplace transform.

Noises that accompany range measurements are usually divided between range independent and range dependent. Within the structure in Figure 7.1, we will link the range-independent and

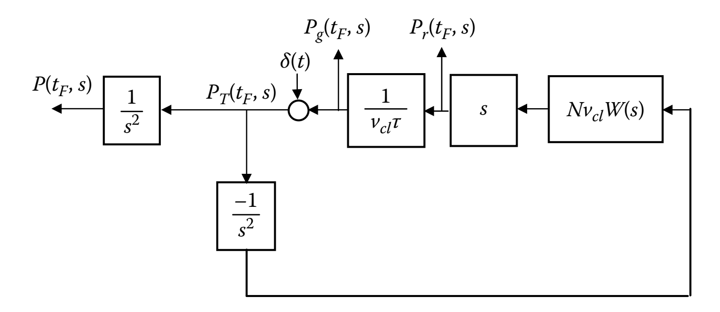


FIGURE 7.2 Modified block-diagram of adjoint system.

range-dependent noise with the LOS measurements. For midcourse guidance, when the missile is guided by radar, the information concerning LOS is transmitted based on measurements of the range components (equation 1.8). During the terminal stage, for semiactive systems, in which the target is illuminated by a transmitter (illuminator) not situated on the missile, range-dependent noise is the terminal noise produced in the missile receiver and also caused by various factors, for example, by signal processing effects or a source independent of the radar, such as a jammer. For active systems, in which the missile has its own radar, range-dependent noise, also called receiver noise, is also the terminal noise produced in the missile receiver. In both cases the noise dependence on range follows from the radar range equation, which shows that the signal noise ratio (SNR = $\sigma^2_{signal} / \sigma^2_{noise}$) is inversely proportional to the fourth power of range r [4]. The factor r^{-4} in the radar equation characterizes the divergence of the electromagnetic radiation with range r (on the outward and return pass). In contrast to active systems, semiactive systems operate only with the return pass. In this case, a received signal power is inversely proportional to the second power of range. That is why the active-receiver noise for active systems is proportional to the square of the distance between the missile and the target, and the passive-receiver noise for semiactive systems is proportional to the distance between the missile and the target.

The output $P_r(t_F,t)$ in Figure 7.1 corresponds to the impulse response of the PN missile guidance system to the white noise input $\eta_r(t)$, which models the range-independent LOS angular noise. The analytical expression for $P_r(t_F,s)$ is given based on the earlier-obtained expression of $P_T(t_F,s)$ and follows the rules of operations with transfer functions in control theory [1,5]. We have

$$P_r(t_F,s) = P_T(t_F,s)(-\frac{1}{s^2})Nv_{cl}W(s)s \tag{7.44}$$

It is easy to check that the absolute value of the above expression equals the absolute value of the product of the derivative of $P_T(t_F,s)$ and the closing velocity [see also equation (4.14) describing the relationship between $H(s)$ and $W(s)$]:

$$\frac{dP_T(t_F,s)}{ds} = \exp(\int_{\infty}^{s} NH(\sigma)d\sigma)NH(s) = \exp(\int_{\infty}^{s} NH(\sigma)d\sigma)N\frac{W(s)}{s} = P_T(t_F,s)N\frac{W(s)}{s} \tag{7.45}$$

By comparing equations (7.44) and (7.45) we can obtain the rms miss distance due to range-independent noise from

$$\frac{rms^2}{\Phi_{fn}} = \frac{E\left[y^2(t_F)\right]_{independent\ \ noise}}{\Phi_{fn}} = \int_0^{t_F} \{L^{-1}\left[v_{cl}\frac{dP_T(t_F,s)}{ds}\right]\}^2 dt \tag{7.46}$$

where Φ_{fn} is the power spectral density of range-independent noise.

As seen from equation (7.46), the rms value is proportional to the closing velocity, i.e., higher closing velocity yields more miss distance due to range-independent noise.

The block diagram of the missile guidance system for the case of range-dependent noise is given in Figure 7.3. Usually spectral density of range-dependent noise is given for a certain reference range r_0, so that the noise level is estimated with respect to the chosen reference level. The white noise signal $\eta_r(t)$ inputs the unit with the gain equal to the range $(r/r_0)^i$ of power i, where $i = 1$ for semiactive systems and $i = 2$ for active systems.

Using the known expression $r = v_{cl}(t_F - t)$, we present the system, adjoint to the one given in Figure 7.3, with the output $P_{ri}(t_F,s)$ in the form shown in Figure 7.4.

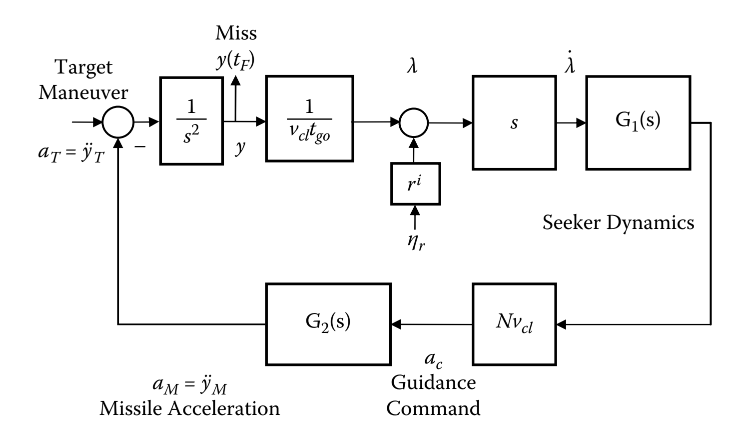


FIGURE 7.3 Missile guidance model with range-dependent noise.

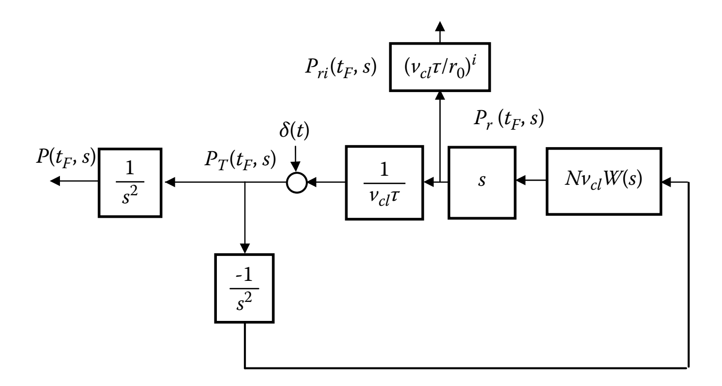


FIGURE 7.4 Modified block diagram of adjoint system with range-dependent noise.

Taking into account that

$$P_r(t_F, s) = -v_{cl}\frac{dP_T(t_F, s)}{ds} \tag{7.47}$$

and that for a function $f(t)$ the Laplace transform

$$L\{t^i f(t)\} = (-1)^i \frac{d^i L\{f(t)\}}{ds^i},$$

using equation (7.46) we can write the expression for the rms miss distance due to passive-receiver noise

$$\frac{rms^2}{\Phi_{pn}} = \frac{E\left[y^2(t_F)\right]_{passive}}{\Phi_{pn}} = \int_0^{t_F} \{L^{-1}\left[\frac{v_{cl}^2}{r_0}\frac{d^2P_T(t_F, s)}{ds^2}\right]\}^2 dt \tag{7.48}$$

and for the rms miss distance due to active-receiver noise equals

$$\frac{rms^2}{\Phi_{an}} = \frac{E\left[y^2(t_F)\right]_{active}}{\Phi_{an}} = \int_0^{t_F} \{L^{-1}\left[\frac{v_{cl}^3}{r_0^2}\frac{d^3P_T(t_F, s)}{ds^3}\right]\}^2 dt \tag{7.49}$$

where Φ_{pn} and Φ_{an} are the power spectral density of the passive-receiver noise and the active-receiver noise, respectively.

As seen from the above expressions (7.47)–(7.49), for the passive- and active-receiver noise the rms value is proportional to the square and cube of the closing velocity, respectively (i.e., higher closing velocity yields more miss distance due to range-dependent noise).

Neoclassical guidance discussed in the previous chapter is based on the structure of the missile guidance system that corresponds to $P_T(t_F,s) = 0$ [see equations (4.10), (6.1), (6.4), and (6.5)]. As follows from equation (7.46), (7.48), and (7.49), neoclassical guidance suppresses range-independent and -dependent noises (i.e., eliminates their influence on the miss distance). The case of glint noise is different. For long flight times the right part of equation (7.43) is close to 1 (for $t_F \to \infty$ it tends to 1), so that neoclassical guidance does not reduce the influence of glint on the miss distance. However, even the "theoretical ability" of the neoclassical guidance to nullify the influence of range-independent and -dependent noises is difficult to realize in practice, especially for fin-controlled missiles. As indicated earlier, the neoclassical guidance structure requires proportional-derivative controllers, which are sensitive to noise, that is, they create additional noise sources whose effect on miss distance can be significant.

7.5 EFFECT OF RANDOM TARGET MANEUVERS ON MISS DISTANCE

It was shown above that step maneuvers of amplitude a_T, whose starting time is uniformly distributed over the flight time t_F, and the random-phase sinusoidal maneuvers $a_T(t) = a_T \sin_T(\omega_T t + \varphi_T)$, where φ_T is a uniformly distributed random variable, can be represented as a white noise process with the power spectral density $\Phi_\varphi = a_T^2 / t_F$ passing through the shaping filter with the transfer functions $W_{filter}(s) = 1/s$ and $W_{filter}(s) = (s^2/\omega_T + \omega_T)^{-1}$, respectively [see equations (7.39) and (7.40)]. The missile guidance model that reflects random target maneuvers is shown in Figure 7.5. The adjoint model is given in Figure 7.6.

It follows immediately from Figure 7.6 and expressions (7.34) and (7.38)–(7.40) that for the step maneuvers with starting time uniformly distributed over the flight time t_F the rms miss distance is given by

$$\frac{rms^2}{\Phi_\varphi} = \frac{E\left[y^2(t_F)\right]_\varphi}{\Phi_\varphi} = \int_0^{t_F} \{L^{-1}\left[\frac{P_T(t_F,s)}{s^3}\right]\}^2 dt \tag{7.50}$$

and for the random-phase sinusoidal maneuvers the rms miss distance is

$$\frac{rms^2}{\Phi_\varphi} = \frac{E\left[y^2(t_F)\right]_\varphi}{\Phi_\varphi} = \int_0^{t_F} \{L^{-1}\left[(s^2/\omega_T + \omega_T)^{-1}\frac{P_T(t_F,s)}{s^2}\right]\}^2 dt \tag{7.51}$$

Since for neoclassical guidance $P_T(t_F,s) = 0$, based on equations (7.50) and (7.51) we can conclude that such guidance is the best remedy against maneuvering targets. However, as mentioned in the previous chapter and in the previous section, the seeming simplicity of neoclassical guidance is deceptive.

The rms miss distance in equations (7.50) and (7.51) corresponds to the steady-state miss, i.e., when the transient response of the missile guidance system has disappeared. The expressions (7.43), (7.46), and (7.48)–(7.51) enable us to analyze the influence of random disturbances on the miss distance and to design filters and components of the flight control system as well as guidance law [see Chapter 6] that would decrease this influence.

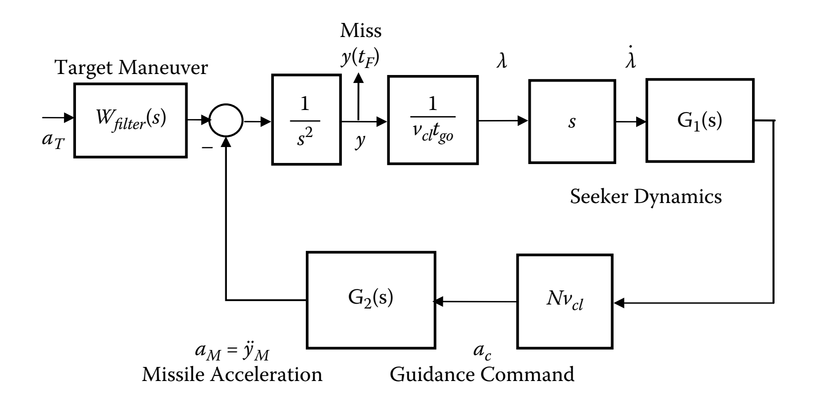


FIGURE 7.5 Missile guidance model with random target maneuvers.

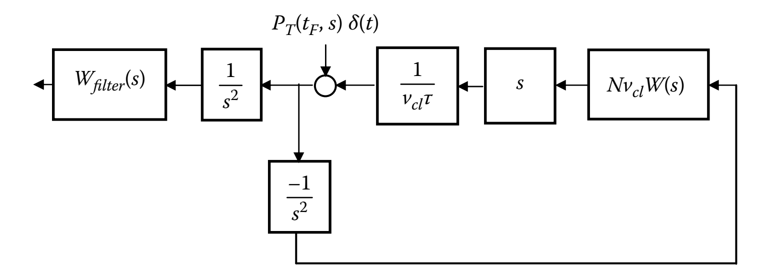


FIGURE 7.6 Block diagram of adjoint system for random maneuvers.

7.6 COMPUTATIONAL ASPECTS

The analytical expressions obtained for the rms miss distance can easily be transformed into computational algorithms. It is important to mention that the computational programs based on these algorithms are more compact and the time of computing is less (nowadays computers are very fast, so the time factor does not play a dominant role) than by using the existing modeling procedure of the method of adjoints in the time domain. Moreover, computational programs can be flexible enough to serve as a tool to analyze the influence of various parameters of the missile guidance system on its performance.

In Chapter 4 we showed that the impulse response $P(t_F,t)$ can be calculated based on the real part of the frequency response $\mathrm{Re}[P(t_F,i\omega)]$ [see equation (4.60)]. Analogous to equation (4.60), the expression of the impulse response $P_T(t_F,t)$ can be obtained, i.e.,

$$P_T(t_F,t) = \frac{2}{\pi}\int_0^{\infty} \mathrm{Re}[P_T(t_F,i\omega)]\cos\omega t d\omega \tag{7.52}$$

Multiplying

$$\mathrm{Re}[P_T(t_F,i\omega)],\ \mathrm{Re}[\frac{dP_T(t_F,i\omega)}{ds}],\ \mathrm{Re}[\frac{d^2P_T(t_F,i\omega)}{ds^2}],\ \mathrm{Re}[\frac{d^3P_T(t_F,i\omega)}{ds^3}]$$

by cos ωt and integrating similarly to equation (7.52), we can obtain the expressions of the impulse responses corresponding to the expressions in parentheses in equations (7.43), (7.46), (7.48), and

(7.49), respectively. It is impossible to obtain analogously the expressions of the inverse Laplace transform of equations (7.50) and (7.51) because the Fourier transform corresponding to the Laplace transform of equations (7.50) and (7.51) does not exist. However, taking into account that [see equations (4.10) and (4.11)]

$$\frac{P_T(t_F,s)}{s^3} = \frac{P(t_F,s)}{s} \tag{7.53}$$

the inverse Laplace transform of

$$\frac{P_T(t_F,s)}{s^3}$$

can be obtained analogous to the step miss using equation (4.62). The approximation of equation (7.51) will be discussed later.

The numerical integration of the modified equations (7.43), (7.46), and (7.48)–(7.51) does not present any difficulties.

The above computational procedure can be simplified if in all operations we operated with the real and imaginary parts of $P_T(t_F,i\omega)$. Taking into account that

$$\left.\frac{dP_T(t_F,s)}{ds}\right|_{s=i\omega} = -i\frac{dP_T(t_F,i\omega)}{d\omega}$$

$$\left.\frac{d^2P_T(t_F,s)}{ds^2}\right|_{s=i\omega} = (-i)^2\frac{d^2P_T(t_F,i\omega)}{d\omega^2}$$

$$\left.\frac{d^3P_T(t_F,s)}{ds^3}\right|_{s=i\omega} = (-i)^3\frac{d^3P_T(t_F,i\omega)}{d\omega^3}$$

and presenting $P_T(t_F,i\omega) = \mathrm{Re}[P_T(t_F,i\omega)] + i\mathrm{Im}[P_T(t_F,i\omega)]$, after simple operations we can write

$$\mathrm{Re}\left[\frac{d^kP_T(t_F,i\omega)}{ds^k}\right] = (-i)^{k-1}\frac{d^k\,\mathrm{Im}[P_T(t_F,i\omega)]}{d\omega^k}, \quad k=1,3$$

$$\mathrm{Re}\left[\frac{d^2P_T(t_F,i\omega)}{ds^2}\right] = -i\frac{d^2\,\mathrm{Re}[P_T(t_F,i\omega)]}{d\omega^2}, \quad k=2 \tag{7.54}$$

Since the expressions (7.43), (7.46), and (7.48)–(7.51) include the squares of the inverse Laplace transform values, we can ignore the signs in the above expressions.

Expressions (7.43), (7.46), and (7.48)–(7.49) can be reduced to

$$\frac{E\left[y^2(t_F)\right]_{gl\,\mathrm{int}}}{\Phi_{gn}} = \int_0^{t_F}\{\frac{2}{\pi}\int_0^{\infty}\mathrm{Re}[1-P_T(t_F,i\omega)]\cos\omega t d\omega\}^2\,dt \tag{7.55}$$

for the rms miss distance due to glint noise;

$$\frac{E\left[y^2(t_F)\right]_{independent\ \ noise}}{\Phi_{fn}} = \int_0^{t_F} \{\frac{2}{\pi} v_{cl} \int_0^{\infty} \frac{d\, \mathrm{Im}[P_T(t_F, i\omega)]}{d\omega} \cos \omega t d\omega\}^2\, dt \qquad (7.56)$$

for the rms miss distance due to range-independent noise;

$$\frac{E\left[y^2(t_F)\right]_{passive}}{\Phi_{pn}} = \int_0^{t_F} \{\frac{2}{\pi} \frac{v_{cl}^2}{r_0} \int_0^{\infty} \frac{d^2\, \mathrm{Re}[P_T(t_F, i\omega)]}{d\omega^2} \cos \omega t d\omega\}^2\, dt \qquad (7.57)$$

for the rms miss distance due to passive-receiver noise; and

$$\frac{E\left[y^2(t_F)\right]_{active}}{\Phi_{pn}} = \int_0^{t_F} \{\frac{2}{\pi} \frac{v_{cl}^3}{r_0^2} \int_0^{\infty} \frac{d^3\, \mathrm{Im}[P_T(t_F, i\omega)]}{d\omega^3} \cos \omega t d\omega\}^2\, dt \qquad (7.58)$$

for the rms miss distance due to active-receiver noise.

It is important to underline that the above expressions are valid because the Fourier transform exists (see Chapter 4 and Appendix B). As mentioned earlier, the expressions for the rms miss distance due to random maneuvers (7.50) and (7.51) cannot be written analogously because the Fourier transform of functions having the Laplace transform

$$\frac{P_T(t_F, s)}{s^3} \text{ and } (s^2 / \omega_T + \omega_T)^{-1} \frac{P_T(t_F, s)}{s^2}$$

does not exist. Based on equation (7.53), we can present equation (7.50) analogous to expression (4.62) for the step miss, that is, for the step maneuvers with starting time uniformly distributed over the flight time t_F the rms miss distance is

$$\frac{E\left[y^2(t_F)\right]_{\varphi}}{\Phi_{\varphi}} = \int_0^{t_F} \{\frac{2}{\pi} \int_0^{\infty} \frac{\mathrm{Re}[P(t_F, i\omega)]}{\omega} \sin \omega t d\omega\}^2\, dt \qquad (7.59)$$

For the random-phase sinusoidal maneuvers, the simplified form of equation (7.51) can be written only under the assumption that we can neglect the transient of $P(t_F,s)$, so that only the stationary term of the inverse Laplace transform is considered. The approximate value of the rms miss distance (in some cases the mistake can be significant) is given by

$$\frac{E\left[y^2(t_F)\right]_{\varphi}}{\Phi_{\varphi}} = \int_0^{t_F} \{\left|P(t_F, i\omega_T)\right| \sin(\omega_T t + \varphi(t_F, i\omega_T))\}^2\, dt \qquad (7.60)$$

where the amplitude $|P(t_F,i\omega_T)|$ and phase $\varphi(t_F,i\omega_T)$ are determined from equations (4.26) and (4.28), respectively.

The described approach is used below to analyze the rms miss distance for missile guidance systems with parameters similar to those considered in previous chapters.

7.7 EXAMPLES

For the first-order model of a missile guidance system the expressions (7.43), (7.46), and (7.48)–(7.51) can be obtained in analytical form. We will write and compare them with the results obtained based on the algorithmic procedure described below. This procedure will be applied to more realistic models of the missile guidance system to demonstrate how misleading the results obtained from the analysis of a simple first-order model can be. For this model we have [see equations (3.19) and (4.21)]

$$P_T(t_F, s) = (\frac{s}{s + 1/\tau})^N$$

so that

$$1 - P_T(t_F, s) = 1 - (\frac{s}{s + 1/\tau})^N \tag{7.61}$$

$$\frac{dP_T(t_F, s)}{ds} = \frac{N}{\tau} \frac{s^{N-1}}{(s + 1/\tau)^{N+1}} \tag{7.62}$$

$$\frac{d^2 P_T(t_F, s)}{ds^2} = \frac{N}{\tau} \frac{s^{N-2}(-2s + (N-1)/\tau)}{(s + 1/\tau)^{N+2}} \tag{7.63}$$

$$\frac{d^3 P_T(t_F, s)}{ds^3} = \frac{N}{\tau} \frac{s^{N-3}(4s^2 - 6s(N-1)/\tau + (N-1)(N-2)/\tau^2)}{(s + 1/\tau)^{N+3}} \tag{7.64}$$

$$\frac{P_T(t_F, s)}{s^3} = \frac{s^{N-3}}{(s + 1/\tau)^N} \tag{7.65}$$

$$(s^2/\omega_T + \omega_T)^{-1} \frac{P_T(t_F, s)}{s^2} = (s^2/\omega_T + \omega_T)^{-1} \frac{s^{N-2}}{(s + 1/\tau)^N} \tag{7.66}$$

The calculations below are made for an effective navigation ratio $N = 3$ and a guidance time constant $\tau = 0.5\ s$; random quantities are assumed to have zero mean.

The inverse Laplace transform of equation (7.61) equals

$$L^{-1}_{gl\,\text{int}} = (4t^2 - 12t + 6)e^{-2t}$$

Integrating the square of the above expression, from equation (7.43) we obtain the rms miss distance due to glint noise with spectral density 0.4 m^2/Hz shown in Figure 7.7 (solid line).

The inverse Laplace transform of equation (7.62) equals

$$L^{-1}_{independent} = (6t - 12t^2 + 4t^3)e^{-2t}$$

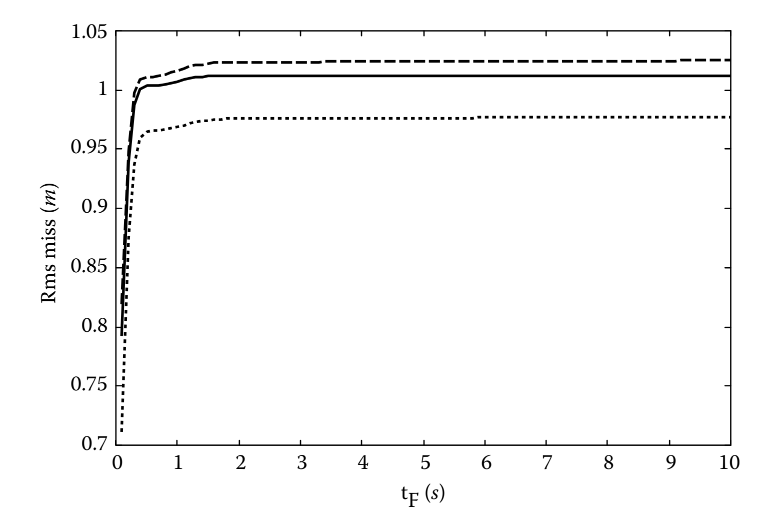


FIGURE 7.7 The rms miss distance due to glint noise.

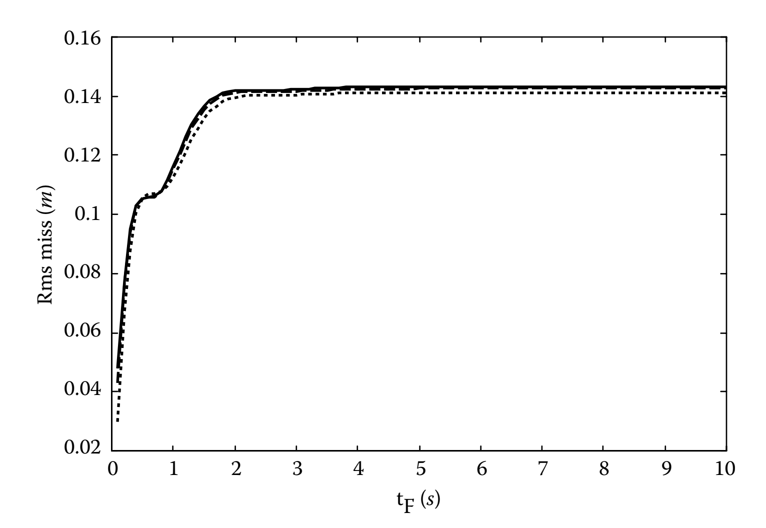


FIGURE 7.8 The rms miss distance due to independent angle noise.

Integrating the square of the above expression and assuming a closing velocity of 1,500 *m/s*, from equation (7.46) we obtain the rms miss distance due to independent-range noise with spectral density $6.5*10^{-8}$ rad^2/Hz, as shown in Figure 7.8 (solid line).

The inverse Laplace transform of equation (7.63) equals

$$L^{-1}_{passive} = (-4t^4 + 12t^3 - 6t^2)e^{-2t}$$

Integrating the square of the above expression and assuming a closing velocity of 1,500 *m/s*, from equation (7.48) we obtain the rms miss distance due to passive-receiver noise with spectral density $6.5*10^{-4}$ rad^2/Hz at a reference range of 10,000 *m*, as shown in Figure 7.9 (solid line).

The inverse Laplace transform of equation (7.64) equals

$$L^{-1}_{active} = (6t^3 - 12t^4 + 4t^5)e^{-2t}$$

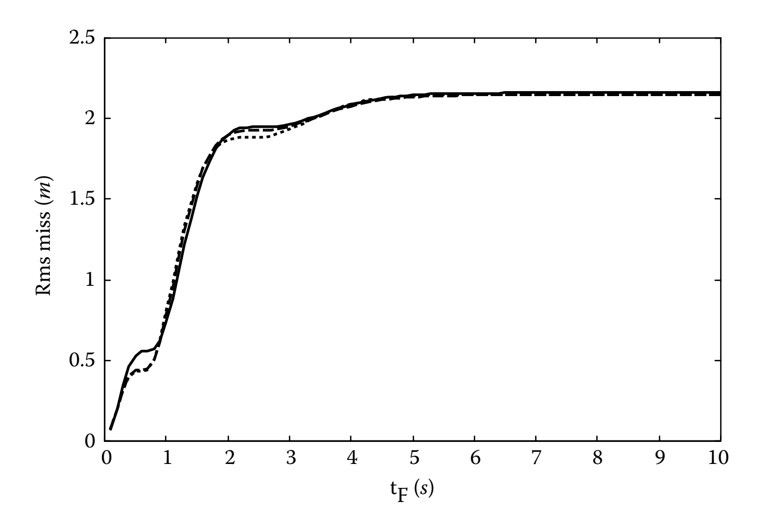


FIGURE 7.9 The rms miss distance due to passive-receiver noise.

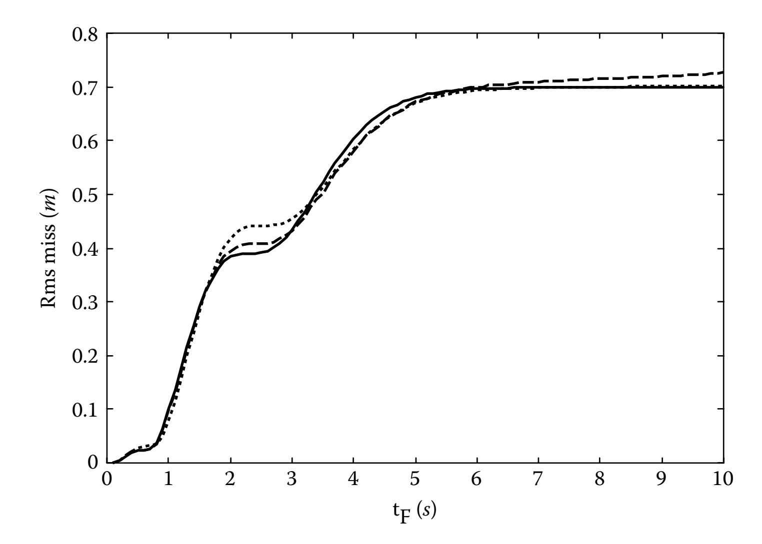


FIGURE 7.10 The rms miss distance due to active-receiver noise.

Integrating the square of the above expression and assuming a closing velocity of 1,500 *m/s*, from equation (7.49) we obtain the rms miss distance due to active-receiver noise with spectral density $6.5*10^{-4}$ rad^2/Hz at a reference range of 10,000 *m*, as shown in Figure 7.10 (solid line).

The inverse Laplace transform of equation (7.65) equals

$$L_{\varphi 1}^{-1} = 0.5t^2 e^{-2t}$$

Integrating the square of the above expression and assuming a 3-g step maneuver with a uniformly distributed starting time, from equation (7.50) we obtain the rms miss distance, as shown in Figure 7.11 (solid line).

The inverse Laplace transform of equation (7.66) for $\omega_T = 1.4$ *rad/s* equals

$$L_{\varphi 2}^{-1} = -0.025\cos 1.4t + 0.093\sin 1.4t + (-0.235t^2 - 0.08t + 0.025)e^{-2t}$$

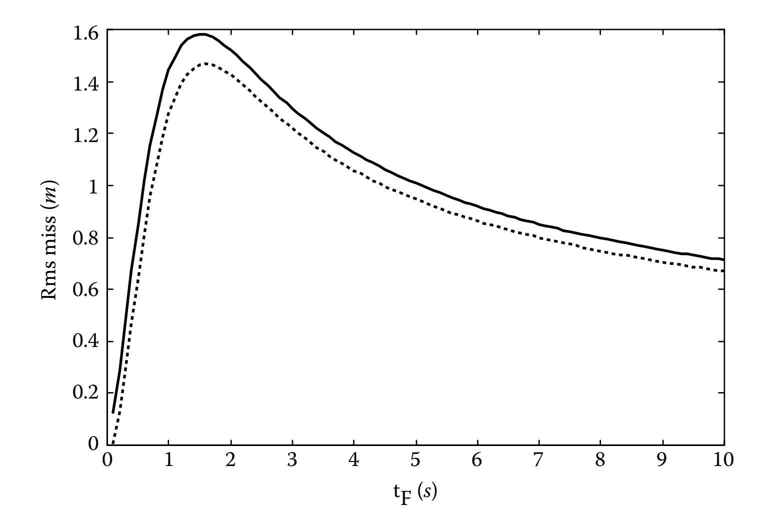


FIGURE 7.11 The rms miss for uniformly distributed 3-g step maneuver.

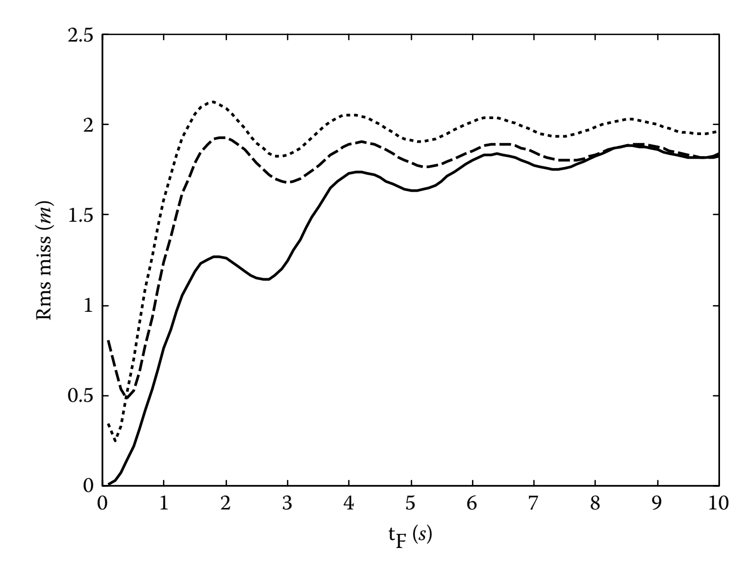


FIGURE 7.12 The rms miss for 3-g random-phase sinusoidal maneuver.

Integrating the square of the above expression and assuming a 3-g amplitude of a target acceleration, from equation (7.51) we obtain the rms miss distance due to the uniformly distributed random-phase sinusoidal maneuver with the frequency $\omega_T = 1.4$ *rad/s*, as shown in Figure 7.12 (solid line).

The above analytical expressions and the corresponding relationships between the rms miss and the time of flight t_F can be obtained by using the Laplace transform tables or MAPLE software. However, even this sophisticated software cannot help in a case of more realistic models of the missile guidance system, which contain complex-conjugated poles stipulated by the flight-control system damping and natural frequency [see equation (4.21)].

The precise solution (solid lines in Figures 7.7–7.12) for the first-order model was compared with the results of a simulation based on equations (7.55)–(7.60) and the analytical expressions (4.35), (4.37), (4.42), and (4.43) for $P_T(t_F,i\omega)$ and $P(t_F,i\omega)$ (dashed lines in Figures 7.7–7.12). In most cases the error does not exceed 1–3%. For the uniformly distributed step maneuver

(Figure 7.11) the simulation result is very close to the precise solution, so that the solid and dashed lines coincide. The largest error is obtained for the random-phase distributed maneuver (Figure 7.12). As expected, it becomes smaller after the transient (i.e., $t_F > 3$ s).

Below we present the results of a MATLAB rms miss simulation based on expressions (4.35), (4.37), (4.42), (4.43), and (7.55)–(7.60). Parallel with the simple model considered above with a time constant 0.5 *s*, more realistic models will be considered:

1. $\omega_z = 30$ *rad/s*, $\zeta = 0.7$, $\omega_M = 20$ *rad/s*, $\tau = 0.5$ *s*;
2. $\omega_z = 5$ *rad/s*, $\zeta = 0.7$, $\omega_M = 20$ *rad/s*, $\tau = 0.5$ *s*;
3. $\omega_z = 30$ *rad/s*, $\zeta = 0.7$, $\omega_M = 20$ *rad/s*, $\tau = 0.1$ *s*;
4. $\omega_z = 5$ *rad/s*, $\zeta = 0.7$, $\omega_M = 20$ *rad/s*, $\tau = 0.5$ *s*.

Comparative analysis of the rms distance for the missile guidance systems due to glint noise is given in Figure 7.13. The solid line, which coincides with the solid line in Figure 7.7, corresponds to the case of a first-order system. The dotted and dashed lines correspond to the case of a tail-controlled missile system with the airframe zero frequency $\omega_z = 30$ *rad/s*.

In both cases, the rms miss distance is more than for the simple first-order model. The larger is the flight control system time constant, the smaller is the rms miss distance.

The significant increase of the rms miss distance for the airframe zero frequency $\omega_z = 5$ *rad/s* (see Figure 7.14), which corresponds to high-altitude endoatmospheric interceptors, is stipulated by the "wrong-way tail effect."

As mentioned in previous chapters, because of the "wrong-way tail effect" the dynamic characteristics of tail-controlled missiles operating at high altitude are significantly worse than at low frequencies. However, if in the deterministic case the decrease of the flight control system time constant decreases the miss distance at low altitudes (high values of ω_z) and increases it at high altitudes (low values of ω_z), the rms miss distance due to glint noise increases with the decrease of the flight control system time constant for all considered cases.

The above-mentioned effect of glint noise may look "strange," especially for the first-order model, because the decrease of the time constant makes it closer to the ideal inertialess case. However, the described effect can be predicted by analyzing equation (7.55) and the expression given above of the first-order system $P(t_F,s)$ [see also (3.19)] as a function of τ.

Although the results shown in Figure 7.14 are far from reality, because glint noise may be highly correlated and should not be modeled as white noise, they are very informative. As seen

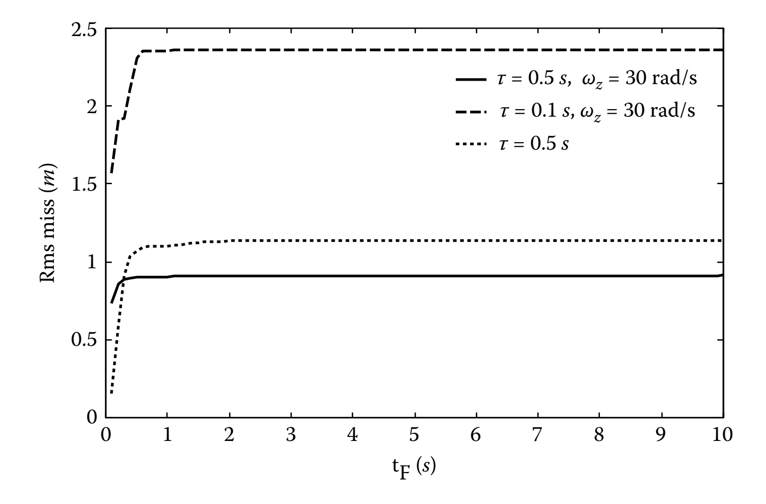


FIGURE 7.13 Comparative analysis of the rms miss due to glint noise.

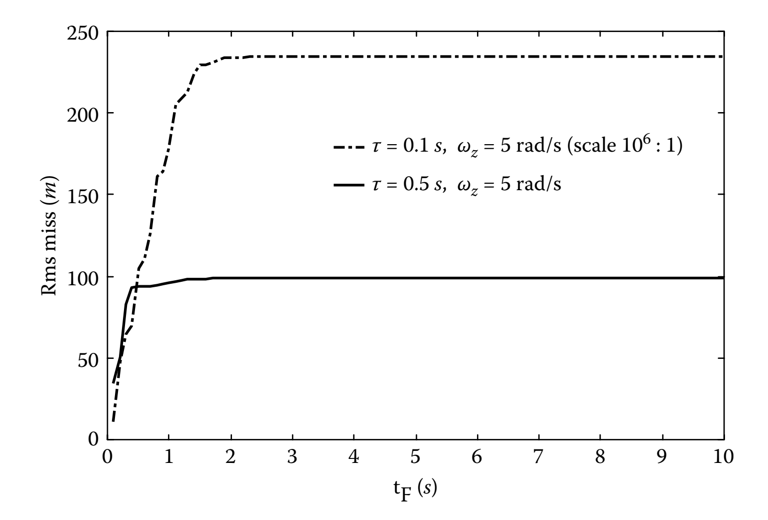


FIGURE 7.14 Comparative analysis of the rms miss due to glint noise.

from Figure 7.13 and Figure 7.14, the rms miss distance increases substantially at high altitude (by double digits) and the decrease of the flight control system time constant brings an additional drastic increase. As seen from equations (4.13) and (7.43), the rms miss due to glint noise increases with the increase of the effective navigation ratio.

Analysis of the influence of independent-range noise is presented in Figure 7.15 and Figure 7.16. The solid line in Figure 7.15 coincides with the solid line in Figure 7.8, built based on the analytical expression for the first-order guidance system model. The dotted and dashed lines correspond to the case of a tail-controlled missile system with the airframe zero frequency $\omega_z = 30$ *rad/s*. In contrast to the case of glint noise, the decrease of the flight control system time constant decreases the rms miss distance due to independent noise at low altitudes (high values of ω_z) and increases it at high altitudes (low values of ω_z) (i.e., analogous to the deterministic case).

The correlation between the above-considered cases for range-independent noise is not changed qualitatively for passive- and active-range dependent noises. As follows from Figure 7.17 and Figure 7.18, the rms miss distance for active-receiver noise is less than the passive-receiver noise miss. In the case of range-dependent noise, the decrease of the flight control system time constant at high altitude increases the rms miss significantly less than due to range-independent noise.

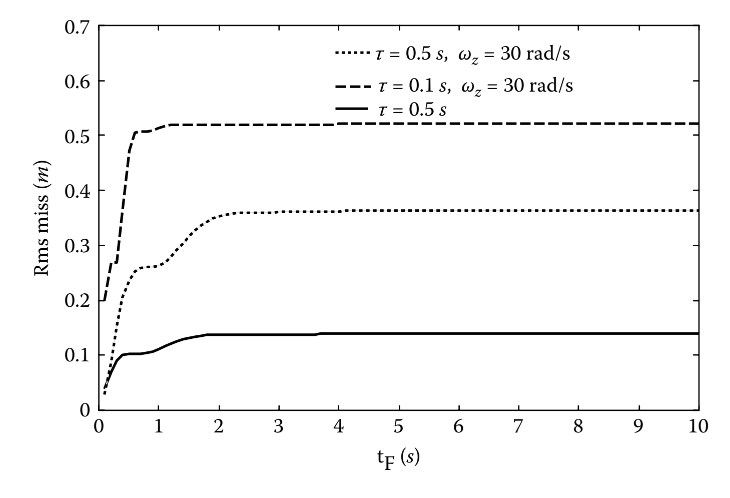


FIGURE 7.15 Comparative analysis of the rms miss due to independent noise.

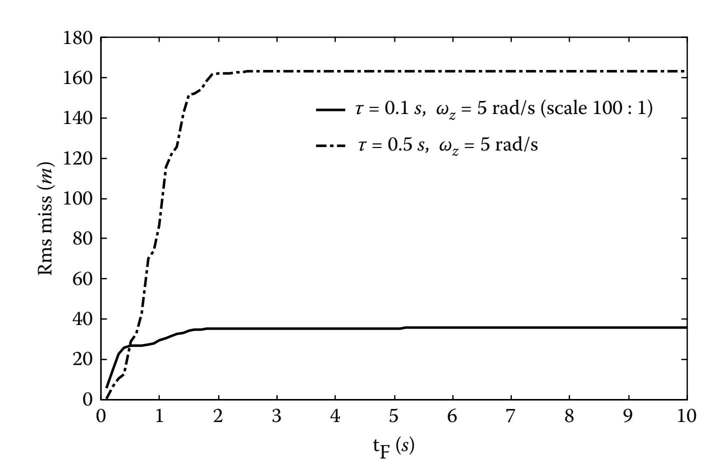


FIGURE 7.16 Comparative analysis of the rms miss due to independent noise.

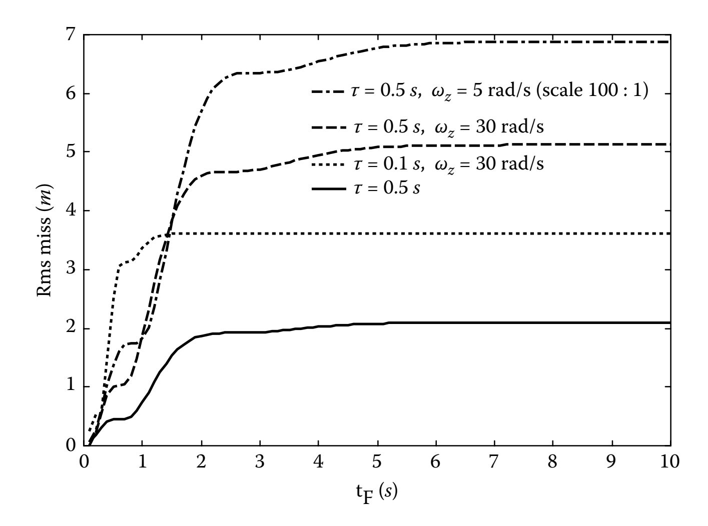


FIGURE 7.17 Comparative analysis of the rms miss due to passive-receiver noise.

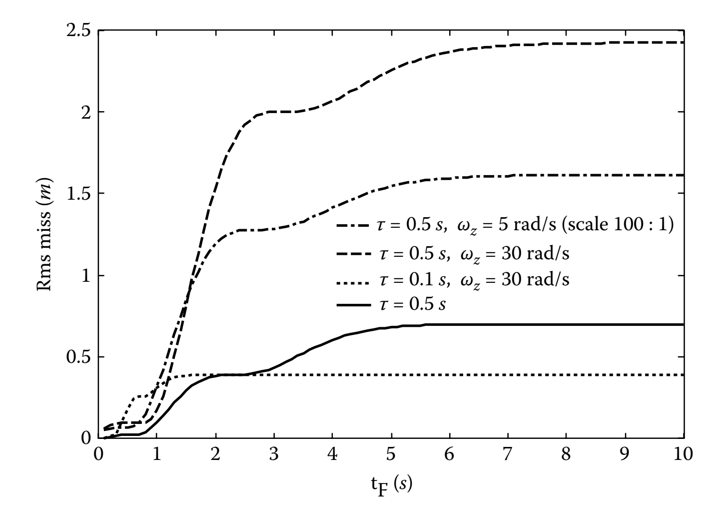


FIGURE 7.18 Comparative analysis of the rms miss due to active-receiver noise.

Since the range-independent and -dependent noise miss distances depend on a closing velocity, they can be significant for ballistic missiles.

Comparative analysis of the rms distance for the step maneuvers with starting time uniformly distributed over the flight time, according to equation (7.59), and for the random-phase sinusoidal maneuvers, based on equation (7.60), is presented in Figures 7.19 and 7.20.

As seen from Figure 7.19 and Figure 7.20, the rms miss distance is very sensitive to the flight-control system time constant. The solid lines in Figure 7.19 and Figure 7.20 correspond to the precise solution for the first-order model.

By choosing an appropriate quantization in the time h and frequency h_0 domains the operations of integration and differentiation are approximated by the summation and difference operations, respectively. In practice, the upper infinite limit of integration in equations (7.55)–(7.60) is changed to ω_{c0}, the frequency being chosen so that for $\omega \geq \omega_{c0}$ the values of the integrands of equations (7.55)–(7.60) are less than 5–10% of their maximum values, respectively. In the above examples, $\omega_{c0} = 19$ *rad/s*, $h_0 = 0.1$ *rad/s*, and $h = 0.1$ *s*.

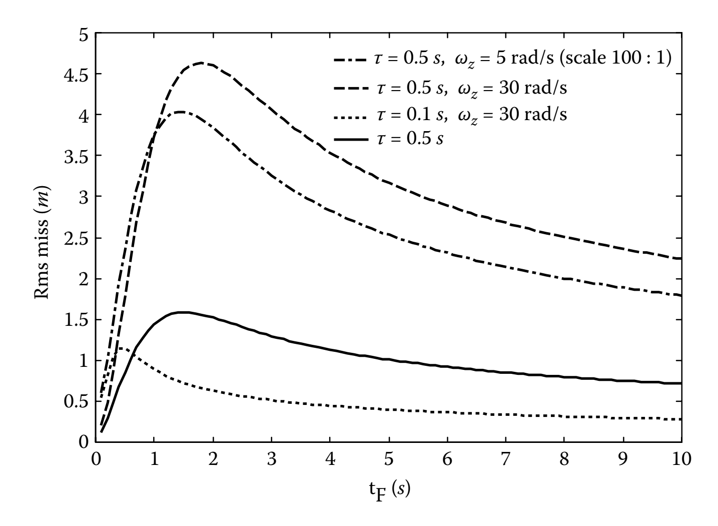


FIGURE 7.19 Comparative analysis for uniformly distributed 3-g step maneuver.

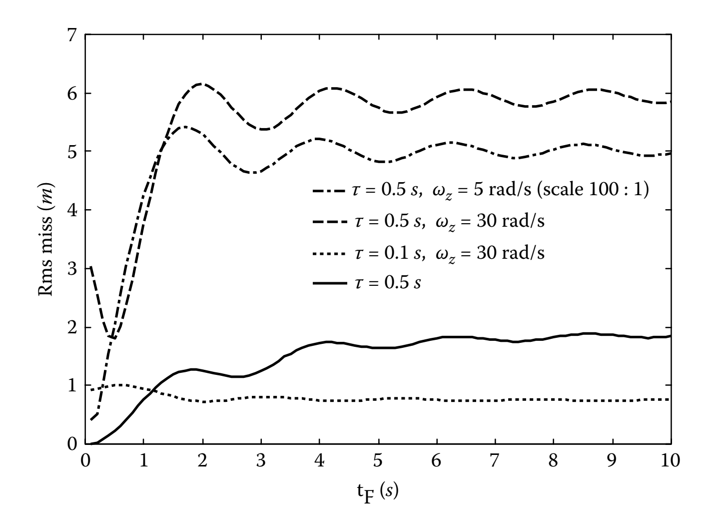


FIGURE 7.20 Comparative analysis for 3-g random-phase sinusoidal maneuver.

The methods of computational mathematics enable us to increase accuracy of the operations of integration and differentiation. It is known that the first, second, and third derivatives of a continuous function $y(t_0)$ at t_0 can be approximated by

$$h\dot{y}(t_0) = Diff(y_0,1) - \frac{1}{2}Diff(y_0,2) + \frac{1}{3}Diff(y_0,3) - ...$$

$$h^2\ddot{y}(t_0) = Diff(y_0,2) - Diff(y_0,3) + \frac{11}{12}Diff(y_0,4) - ...$$

$$h^3\dddot{y}(t_0) = Diff(y_0,3) - \frac{3}{2}Diff(y_0,4) + \frac{7}{4}Diff(y_0,5) - ...$$

where h is a quantization step size and $Diff\,(y_0, i)$ denotes the i-th order difference of $y(t_0)$ at t_0.

The approximation of the third derivative by the third-order difference (i.e., by using only the first term of the $h^3\dddot{y}(t_0)$ approximation), can give a tangible error. Instead of using the high-order differences, the expression (7.58) can be transformed into

$$\frac{E\left[y^2(t_F)\right]_{active}}{\Phi_{pn}} = \int_0^{t_F}\{\frac{2}{\pi}\frac{v_{cl}^3}{r_0^2}t^2\int_0^{\infty}\frac{d\,\mathrm{Im}[P_T(t_F,i\omega)]}{d\omega}\cos\omega t d\omega\}^2\,dt \tag{7.67}$$

This expression is easily obtained by using integration by parts of equation (7.58) and taking into account that $\mathrm{Im}^{(i)}[P_T(t_F,0)] = \mathrm{Im}^{(i)}[P_T(t_F,\infty)] = 0$, $i = 0,1,2$, where i is the order of derivative. The above equation, as well as equations (7.56) and (7.57), can be simplified analogously, taking into account $\mathrm{Re}^{(1)}[P_T(t_F,0)] = 0$.

Instead of equation (7.56), we can use

$$\frac{E\left[y^2(t_F)\right]_{independent\ \ noise}}{\Phi_{fn}} = \int_0^{t_F}\{\frac{2}{\pi}v_{cl}t\int_0^{\infty}\mathrm{Im}[P_T(t_F,i\omega)]\sin\omega t d\omega\}^2\,dt \tag{7.68}$$

Instead of equation (7.57), we can use

$$\frac{E\left[y^2(t_F)\right]_{passive}}{\Phi_{pn}} = \int_0^{t_F}\{\frac{2}{\pi}\frac{v_{cl}^2}{r_0}t\int_0^{\infty}\frac{d\,\mathrm{Re}[P_T(t_F,i\omega)]}{d\omega}\sin\omega t d\omega\}^2\,dt \tag{7.69}$$

However, the accuracy of the computational procedure based on equations (7.67)–(7.69) is very sensitive to ω_{c0}, especially for big t_F because of t factors in equations (7.67)–(7.69).

The expressions of $\mathrm{Re}[P_T(t_F,i\omega)]$ and $\mathrm{Im}[P_T(t_F,i\omega)]$ can be obtained directly from equations (4.42) and (4.43) or from equation (4.10) [see also (6.10)–(6.13)]

$$P_T(t_F,i\omega) = \exp(-N\int_{\omega}^{\infty}\frac{W(i\omega)}{\omega}d\omega) = \exp(-N\int_{\omega}^{\infty}\frac{\mathrm{Re}[W(i\omega)]}{\omega}d\omega)\exp(-iN\int_{\omega}^{\infty}\frac{\mathrm{Im}[W(i\omega)]}{\omega}d\omega)$$

so that the amplitude $|P_T(t_F,i\omega)|$ and phase $\varphi(P_T(t_F,i\omega))$ of $P_T(t_F,i\omega)$ equal

$$|P_T(t_F, i\omega)| = \exp(-N \int_{\omega}^{\infty} \frac{\text{Re}[W(i\omega)]}{\omega} d\omega) \tag{7.70}$$

$$\varphi(P_T(t_F, i\omega)) = -N \int_{\omega}^{\infty} \frac{\text{Im}[W(i\omega)]}{\omega} d\omega \tag{7.71}$$

The computational procedure based on equations (7.70) and (7.71) is simpler than the procedure described above using the analytical expressions for the frequency response (4.35), (4.37), (4.42), and (4.43). It only requires knowledge of the frequency response $W(i\omega)$ of the missile guidance system. Moreover, $W(i\omega)$ can be presented approximately based on experimental data. The results of simulation for the first-order model based on equations (7.70) and (7.71), instead of equations (4.42) and (4.43) (see dotted lines in Figures 7.7–7.12), show that the accuracy of this procedure is a little bit lower than the procedure described above employing the analytical expressions $P(t_F, i\omega)$ and $P_T(t_F, i\omega)$. The accuracy can be improved by increasing the upper limit ω_{c0} of integration in equations (7.70) and (7.71).

In all considered cases the first-order system analysis gives a significantly lower miss estimate than a more realistic model with a high airframe zero frequency ω_z. The first-order model gives absolutely unacceptable results in the case of small values of the airframe zero frequency.

7.8 FILTERING

The noises described above corrupt seeker measurements. To get reliable information for the line-of-sight rate required by the PN guidance law or its modifications considered in the previous chapters, it is necessary to use a filter that would decrease the rms miss distance contributed by all noise sources. Assuming independence of the random variable considered, the total rms miss distance can be determined as the square root of the sum of the variances of the miss distances from glint, independent, and dependent noises.

Considering $G_1(s)$ as the filter transfer function [see Figures 7.1 to 7.3], the filtering problem can be formulated as the problem of finding $G_1(s)$, which would decrease the total rms miss distance. Such formulation has a certain drawback, because it ignores the miss distance stipulated by the target maneuver. Dynamic characteristics of the filter influence this component of the total miss distance.

For highly maneuvering targets, the assumption that the phase angle of target weave, which is associated with initial conditions at the start of of the missile's terminal guidance, can be treated as a random variable uniformly distributed between 0 and 2π over a set of engagement is quite realistic, and the corresponding rms miss distance can be considered as the measure of effectiveness in analyzing missile performance against weaving targets. It means that the transfer function $G_1(s)$ of a filter should be chosen to minimize the total rms miss including the rms for the random-phase sinusoidal maneuvers.

Below we describe an engineering approach to choosing a filter with the transfer function $G_1(s)$ to improve the performance of a tail-controlled missile with $\omega_z = 30$ *rad/s*, $\zeta = 0.7$, $\omega_M = 20$ *rad/s*, and $\tau = 0.5$ *s*. From the comparative analysis of the rms miss due to range-independent and -dependent noises and the rms for the random-phase sinusoidal maneuvers (see Figures 7.15, 7.17, 7.18, and 7.70) for the given missile guidance system and the system with parameters $\omega_z = 30$ *rad/s*, $\zeta = 0.7$, $\omega_M = 20$ *rad/s*, and $\tau = 0.1$ *s* we can conclude that the decrease of τ significantly decreases all rms miss components but the component due to glint, and the total rms miss is significantly

less for the missile guidance system with $\tau = 0.1\ s$. Based on this analysis, it is easy to conclude that by applying the filter with the transfer function

$$G_1(s) = \frac{0.5s + 1}{0.1s + 1}$$

we would significantly improve the performance of the given missile guidance system at low altitudes. As indicated, at high altitudes its dynamic parameters are changed, so that the filter parameters should be changed as well.

We will not consider here any optimal filtering problems. Simple constant gain and optimal digital filters widely utilized in practice will be discussed in the next chapter.

REFERENCES

1. Chen, C., *Linear System Theory and Design,* CBS College Publishing, New York, 1984.
2. Gihman, I.I. and Skorohod, A.V., *The Theory of Stochastic Processes I*, Springer, New York, 1974.
3. Fitzgerald, R.J., Shaping filters for disturbances with random starting times, *Journal of Guidance and Control*, 2, 152–154, 1979.
4. Skolnik, M.I., *Radar Handbook*, McGraw-Hill, New York, 1990.
5. Smith, O., *Feedback Control Systems*, McGraw-Hill, Inc., New York, 1958.
6. Shneydor, N.A., *Missile Guidance and Pursuit*, Horwood Publishing, Chichester, 1998.
7. Yanushevsky, R., Analysis of optimal weaving frequency of maneuvering targets, *Journal of Spacecraft and Rockets*, 41, 3, 477–479, 2004.
8. Yanushevsky, R., Analysis and design of missile guidance systems in frequency domain, 44th AIAA Space Sciences Meeting, paper AIAA 2006-825, Reno, Nevada, 2006.
9. Yanushevsky, R., Frequency domain approach to guidance system design, *IEEE Transactions on Aerospace and Electronic Systems*, 43, 2007.
10. Yanushevsky, R., *Theory of Linear Optimal Multivariable Control Systems*, Nauka, Moscow, 1973.
11. Zachran, P., Complete statistical analysis of nonlinear missile guidance systems, *Journal of Guidance and Control*, 12, 1, 71–78, 1979.

8 Testing Guidance Laws Performance

8.1 INTRODUCTION

There are generally three phases to the engagement and interception of a target. The first launch phase is usually uncontrolled. During this stage, the rocket motor is initiated and the missile is boosted up to its operating velocity in the direction of a target. This is followed by the midcourse phase if the missile is not locked onto the target. Usually, during this phase the missile is guided by radar into an area that allows it to lock onto the target with its own sensor. During the terminal (homing) guidance phase, the missile is guided onto the target using its local sensor measurements. Depending on the interceptor and mission, the terminal phase can begin anywhere from tens of seconds down to a few seconds before intercept. The purpose of the terminal phase is to remove the residual errors accumulated during the prior phases and ultimately to reduce the final distance between the interceptor and threat below some specified level. For systems that use a fuze and fragmentation warhead, this final miss distance must be less than the warhead lethal radius. A direct-hit missile can tolerate only very small "misses" relative to a selected aimpoint. In either case, during the terminal phase of flight the interceptor must have a high degree of accuracy and a quick reaction capability. Moreover, near the very end of the terminal phase (often referred to as the endgame), the interceptor may be required to maneuver to maximum capability in order to converge on and hit a fast-moving evasive target.

Threat missile systems continue a steady evolution in technical sophistication leading to increased capability and, consequently, the ability to perform a wider range of missions. For example, tactical ballistic missiles can have high velocity and, upon reentry, can exhibit complex coning motion and slowdown as they move through the atmosphere. Likewise, high-performance cruise missiles can fly at supersonic speeds, have high lateral acceleration capability, and can execute maneuvers that are difficult to anticipate. The diversity of these threat missile systems and missions poses a significant challenge to missile interceptor design.

Modern missiles operate over a wide range of flight conditions, which vary with altitude, speed, and engine thrust. Aerodynamic missiles use aerodynamic forces to maintain their flight path. Ballistic missiles contain a part of their trajectory that is not influenced by propulsion or control. Ballistic missiles are categorized according to their range—the maximum distance measured along Earth's surface from the point of launch to the point of impact of the last element of the payload.

The United States divides missiles into five range classes [15]. Battlefield short-range ballistic missiles (BSRBM) have a range of up to 150 km. Short-range ballistic missiles (SRBM) have a range of up to 1,000 km. Medium-range ballistic missiles (MRBM) have a range of 1,000–2,400 km. The operational range of intermediate-range ballistic missiles (IRBM) is 2,400–5,500 km. Intercontinental ballistic missiles (ICBM) operate at distances over 5,500 km. Cruise missiles present a special class of missiles that targets mostly surface objects and possesses a very high accuracy. The computer that guides a cruise missile is programmed prior to launch with information about the ground terrain between the point where the missile is launched and its intended destination. Using sensors on the missile, it uses various terrain references to find the target. A cruise missile has sophisticated tracking equipment, including various sensors such as cameras and satellite data receivers that allow it to determine its position. Thus a cruise missile can sense its environment, process that information, decide what to do next, and execute that decision.

Various types of missiles have specific features, which should be reflected in simulation models. Usually the six degree simulation models (6-DOF) are used to imitate the engagement scenarios and to test the effectiveness of guidance laws. When nonlinear guidance laws and nonlinearities in a missile guidance system (e.g., acceleration saturation) as well as the uncertainties in missile dynamics are considered, it becomes necessary to resort to Monte Carlo techniques (repeated simulation trials) to arrive at the rms miss distance.

Proportional navigation (PN) is known to be an optimal solution, which, under the assumption of a constant closing velocity, absence of autopilot lags, and absence of target maneuvers, minimizes the linear quadratic cost functional of the missile acceleration. More advanced guidance laws depend on more detailed models of the target and missile and assumptions concerning the intercept scenario. The more realistic optimal problems have been investigated, and optimal guidance laws were developed. However, their performance is dependent on the estimation of the time-to-go, which is assumed to be known and commonly approximated as the range between the target and missile divided by the closing velocity. Typically, the estimates of the range and closing velocity are obtained from radar or other ranging devices. In reality, these data are contaminated by noise from radar-jamming devices or the processing electronics. This affects the accuracy of the estimation of the time-to-go, which causes errors in the terminal miss distance.

The linear approach, based on the assumption that the deviations from a nominal collision course are small, fails when the interception kinematics are highly nonlinear. Guidance system saturation occurs when the system demands (e.g., a commanded lateral acceleration 40 g) exceed the missile capability (e.g., the missile is only capable of 30 g). This situation arises in short-range engagements, where the missile is far from the nominal collision course, and in the case of highly maneuvering targets.

We considered the case of 2-DOF sinusoidal maneuvers, also known as weave maneuvers. This type is a useful starting point for analysis of intercept scenarios that involve ballistic missiles, although the ballistic target dynamics may involve an arbitrary periodic motion in three dimensions when re-entering the atmosphere. Instead of considering the 3-DOF PN problem, in many cases we assumed that lateral and longitudinal maneuver planes were decoupled by the means of roll-control, so that the consideration of the 2-DOF problem was justified. It was assumed also that the gravitational component of the total missile lateral acceleration is negligible. Such simplifications are possible only on the initial stage of analysis and design. Moreover, just after booster burnout, axial acceleration, center of gravity, and mass moment of inertia characteristics are changed. These variations should be incorporated in aerodynamic models.

8.2 FORCES ACTING ON MISSILES

Thrust is the main forward force acting on a missile and generated by a propulsion system. It is produced by the expulsion of a reaction mass, such as the hot gas products of a chemical reaction. Thrust T equals the sum of two terms, the momentum thrust and the pressure thrust

$$T = m_p v_e + (p_e - p_a)A_e \tag{8.1}$$

where m_p is the mass expelled in unit time (the propellant mass flow rate), v_e is the exhaust velocity (the average actual velocity of the exhaust gases), p_e is the exhaust pressure, p_a the ambient pressure, and A_e the area of the exit of the motor nozzle.

Even when the propellant flow rate and exhaust velocity are constant, so that the thrust force is constant, a rocket will accelerate at an increasing rate because the missile's overall mass decreases as propellant is used up. The change in velocity depends on the missile's initial total weight, glide weight (its final weight after the propellant is expended), thrust magnitude, and the rate at which the propellant is burning.

If the missile is launched from the air, it already possesses a large initial speed. In contrast to this type of missile, missiles launched from the ground (ground-based missiles) (i.e., having zero

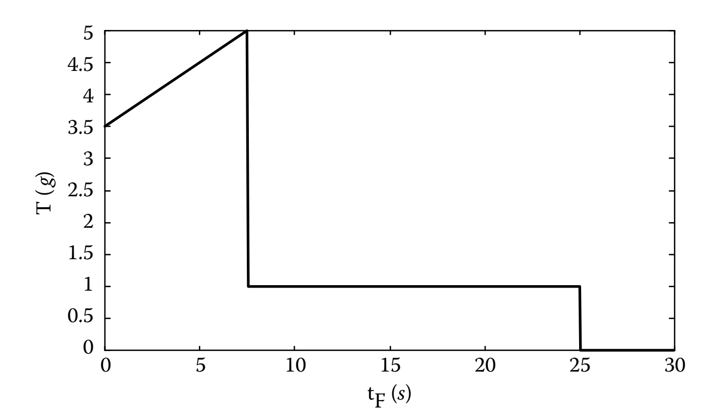


FIGURE 8.1 Thrust acceleration.

initial speed) need more propellant to reach the same speed. Ground-based strategic interceptors with a large operational range consist of one or two boost-stage boosters.

The thrust acceleration profile of a single boost stage missile is given in Figure 8.1. Here the boost phase lasts about 7.5 *s*. Next, the so-called sustain phase continues until 25 *s*. The last glide phase corresponds to $T = 0$.

The thrust force of many types of existing missiles (without throttleable engines) is uncontrolled and directed along the **x** axis of the missile's body (see Figure 8.2). Missiles with thrust vector control are able to change the direction of thrust. Their autopilots change the actuator angle and, as a result, influence the components of the thrust vector. Thrust is used to control the flight of these missiles.

Gravity, which was neglected in the previous chapters, significantly influences the missile range capability and should be included in more rigorous models than considered earlier. Usually, the gravity term is presented by the vertical coordinate of the ESF coordinate system, which equals *g*. However, for the IRBM and ICBM missiles the gravity force $\boldsymbol{G}$ is distributed along three ESF coordinates as

$$G_E = magG\frac{R_E}{\sqrt{R_E^2 + R_N^2 + (R_U + RE)^2}}, \quad G_N = magG\frac{R_N}{\sqrt{R_E^2 + R_N^2 + (R_U + RE)^2}}$$

$$G_U = magG\frac{R_U + RE}{\sqrt{R_E^2 + R_N^2 + (R_U + RE)^2}}, \quad magG = g\frac{RE}{\sqrt{R_E^2 + R_N^2 + (R_U + RE)^2}} \tag{8.2}$$

where RE is the Earth's radius and R_E, R_N, and R_U are the missile coordinates. For small altitudes, $magG = g$, $G_U = g$, and $G_E = G_N = 0$.

Drag and lift belong to the so-called aerodynamic forces. Drag acts along the velocity vector (see the wind axis in Figure 8.2) and impedes the missile's motion. It reduces missile speed, so reducing its acceleration capability. Lift is directed perpendicularly up with respect to drag and is the main force controlling the flight of a missile. The lift and drag forces are presented as

$$Lift = C_L QS, \quad Drag = C_D QS \tag{8.3}$$

where S is a reference area; C_L and C_D are the lift and drag coefficients, respectively; Q is the dynamic pressure, which depends on the atmospheric pressure $PRESS$ and $Mach$ number

$$Q = 0.7\ PRESS\ (Mach)^2 \tag{8.4}$$

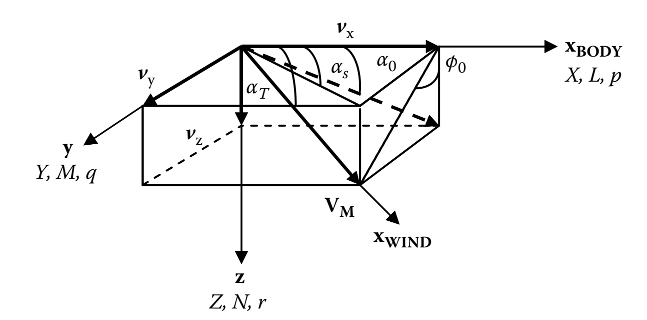


FIGURE 8.2 Coordinate systems used in missile dynamics.

In the body coordinate system (see Figure 8.2; the **x** axis is directed along the missile's body), instead of equation (8.3), the normal and axial forces generated by lift and drag are considered.

8.3 MISSILE DYNAMICS

Assuming a rigid body, constant mass, and inertia, and taking the origin of the body-fixed **x**, **y**, and **z** coordinate system at the missile center of gravity, the standard body axis six-degree-of-freedom equation of motion for a wide class of missiles can be presented as [3]

$$\begin{aligned}
\dot{v}_x &= rv_y - qv_z + X + G_x + T_x \\
\dot{v}_y &= -rv_x + pv_z + Y + G_y + T_y \\
\dot{v}_z &= qv_x - pv_y + Z + G_z + T_z \\
\dot{p} &= -L_{pq}pq - L_{qr}qr + L + L_T \\
\dot{q} &= -M_{rp}rp - M_{r^2p^2}(r^2 - p^2) + M + M_T \\
\dot{r} &= -N_{pq}pq - N_{qr}qr + N + N_T
\end{aligned} \tag{8.5}$$

where v_x, v_y, and v_z are the components of velocity along the **x**, **y**, and **z** axes (see Figure 8.2), respectively; p, q, and r denote the roll, pitch, and yaw rates, respectively; G_x, G_y, and G_z are the gravity components; X, Y, and Z model accelerations produced by the aerodynamic forces; L, M, and N model angular accelerations produced by the aerodynamic moments; T_x, T_y, and T_z model propulsion system forces; and L_T, M_T, and N_T model the moments produced by the propulsion system. All variables on the right part of equation (8.5) have units of acceleration.

The coefficients L_{pq}, L_{qr}, M_{rp}, $M_{r^2p^2}$, N_{pq}, and N_{qr} are obtained as a result of simplification of a more general form of moment (m_x, m_y, and m_z) equations [3]

$$\begin{aligned}
I_{xx}\dot{p} - (I_{yy} - I_{zz})qr + I_{yz}(r^2 - q^2) - I_{xz}(pq + \dot{r}) + I_{xy}(rp - \dot{q}) &= m_x \\
I_{yy}\dot{q} - (I_{zz} - I_{xx})rp - I_{xz}(r^2 - p^2) - I_{xy}(qr + \dot{p}) + I_{yz}(pq - \dot{r}) &= m_y \\
I_{zz}\dot{r} - (I_{xx} - I_{yy})pq + I_{xy}(q^2 - p^2) - I_{yz}(rp + \dot{q}) + I_{xz}(qr - \dot{p}) &= m_z
\end{aligned} \tag{8.6}$$

where I_{xx}, I_{yy}, and I_{zz} denote the mass moments of inertia about the **x**, **y**, and **z** axes; I_{xy}, I_{xz}, and I_{yz} denote the mass product of inertia about the **x** and **y**, **x** and **z**, and **y** and **z** axes, respectively.

It is desirable for the **x**, **y**, and **z** axes to coincide with the principal axes of inertia, so that the product-of-inertia terms vanish. For symmetry about the **xz** plane $I_{yz} = 0$ and $I_{xy} = 0$, so that instead of equation (8.6) we have

$$
\begin{aligned}
&I_{xx}\dot{p} - (I_{yy} - I_{zz})qr - I_{xz}(pq + \dot{r}) = m_x \\
&I_{yy}\dot{q} - (I_{zz} - I_{xx})rp - I_{xz}(r^2 - p^2) = m_y \\
&I_{zz}\dot{r} - (I_{xx} - I_{yy})pq + I_{xz}(qr - \dot{p}) = m_z
\end{aligned}
\tag{8.7}
$$

In the case of a cruciform configuration, which is symmetrical about both the **xy** and **xz** planes, $I_{xz} = 0$ as well, so that equation (8.7) is reduced to

$$
\begin{aligned}
&I_{xx}\dot{p} - (I_{yy} - I_{zz})qr = m_x \\
&I_{yy}\dot{q} - (I_{zz} - I_{xx})rp = m_y \\
&I_{zz}\dot{r} - (I_{xx} - I_{yy})pq = m_z
\end{aligned}
\tag{8.8}
$$

Based on the expressions for the lift and drag equations (8.2)–(8.4), the aerodynamic forces coefficients C_x, C_y, and C_z are modeled as nondimensional quantities and are scaled to units of force, so that

$$
\begin{bmatrix} X \\ Y \\ Z \end{bmatrix} = \frac{QS}{m} \begin{bmatrix} C_x \\ C_y \\ C_z \end{bmatrix}
\tag{8.9}
$$

where m is the mass of the missile.

The system of equations (8.7) can be presented in the form of the moment equations of (8.5), where the aerodynamic moments acting on the body are modeled as

$$
\begin{aligned}
&L = \frac{QSl}{I_{xx}I_{zz} - I_{xz}^2}(C_l I_{zz} + C_n I_{xz}) \\
&M = \frac{QSl}{I_{yy}} C_m \\
&N = \frac{QSl}{I_{xx}I_{zz} - I_{xz}^2}(C_n I_{xx} + C_l I_{xz})
\end{aligned}
\tag{8.10}
$$

where C_l, C_m, and C_n model nondimensional aerodynamic moment coefficients, rolling, pitching, and yawing, and l is a reference length (usually a missile diameter); the cross-axis inertia symmetry term couples the roll–yaw moment equations; the coefficients L_{pq}, L_{qr}, M_{rp}, $M_{r^2p^2}$, N_{pq}, and N_{qr} in equation (8.5) equal

$$
L_{pq} = \frac{I_{xz}(I_{xx} - I_{yy} - I_{zz})}{I_{xx}I_{zz} - I_{xz}^2}, \quad I_{qr} = \frac{I_{zz}(I_{zz} - I_{yy}) - I_{xz}^2}{I_{xx}I_{zz} - I_{xz}^2}, \quad M_{pr} = \frac{I_{xx} - I_{zz}}{I_{yy}},
\tag{8.11}
$$

$$
M_{r^2p^2} = \frac{I_{xy}}{I_{yy}}, \quad N_{qr} = \frac{I_{xz}(I_{zz} - I_{xx} - I_{yy})}{I_{xx}I_{zz} - I_{xz}^2}, \quad N_{pq} = \frac{I_{xx}(I_{xx} - I_{yy}) - I_{xz}^2}{I_{xx}I_{zz} - I_{xz}^2}
$$

The above equations (8.5), (8.10), and (8.11) are written for missile configurations possessing the **xz** plane of symmetry, so that $I_{yz} = 0$ and $I_{xy} = 0$. Both geometrical and mass symmetry are assumed here, although it is possible that slight mass asymmetries may exist in a real missile configuration.

If the mass distribution is such that $I_{yy} = I_{zz}$ (for missiles with circular body cross sections), the above expressions can be simplified. In the case of a cruciform configuration, which is symmetrical about both the **xy** and **xz** planes, $I_{xz} = 0$ as well, so that equations (8.5), (8.10), and (8.11) can be further simplified.

The gravitational forces are modeled as

$$\begin{bmatrix} G_x \\ G_y \\ G_z \end{bmatrix} = g \begin{bmatrix} -\sin\theta \\ \cos\theta\sin\phi \\ \cos\theta\cos\phi \end{bmatrix} \tag{8.12}$$

where the above angles are the Euler angles of rotation by which the $\bar{x},\bar{y},\bar{z}$ space-fixed system of coordinates, with its origin at the center of gravity, comes into coincidence with the **x**, **y**, **z** body-fixed system of coordinates [3]. The Euler angles ψ, θ, and ϕ correspond to the following order of rotation [3]: rotation about the $\bar{z}$ axis through angle ψ; rotation about the new position of the $\bar{y}$ axis through angle θ, putting the $\bar{x}$ axis into coincidence with the **x** axis; rotation about the **x** axis through angle ϕ (see Figure 8.3).

The angles α_0, α_s, and ϕ_0 are determined as [see Figure (8.1)]

$$\alpha_0 = \tan^{-1}(v_z/v_x),\ \alpha_s = \tan^{-1}(v_y/v_x),\quad \phi_0 = \tan^{-1}(v_y/v_z) \tag{8.13}$$

and the total angle α_T, determined as the angle between the missile **x** axis and the magnitude of the missile velocity vector $V_M = \sqrt{v_x^2 + v_y^2 + v_z^2}$ (see Figure 8.2), can be expressed as

$$\tan^2\alpha_T = (v_y^2 + v_z^2)/v_x^2 = \tan^2\alpha_0 + \tan^2\alpha_s \tag{8.14}$$

For small angles of attack and sideslip $\alpha_0 \approx v_z/v_x$, $\alpha_s \approx v_y/v_x$ and $v_x \approx V_M$. Assuming insignificant changes of speed (i.e., $\dot{v}_x \approx 0$), the accelerations $\dot{v}_y$ and $\dot{v}_z$ can be presented as $\dot{v}_y \approx v_x\alpha_s$ and $\dot{v}_z \approx v_x\alpha_0$. Under the above assumptions, the force equations of (8.5) can be simplified to give

$$\begin{aligned} V_M(q\alpha_0 - r\alpha_s) &= X + G_x + T_x \\ V_M(\dot{\alpha}_s + r - p\alpha_0) &= Y + G_y + T_y \\ V_M(\dot{\alpha}_0 - q + p\alpha_s) &= Z + G_z + T_z \end{aligned} \tag{8.15}$$

These equations are widely used in the preliminary studies to test autopilot design and guidance laws.

The missile's aerodynamic coefficients C_x, C_y, and C_z related to the aerodynamic forces and C_l, C_m, and C_n related to the aerodynamic moments are typically modeled as functions of the pitch-plane angle of attack α_0, the yaw-plane sideslip angle α_s, the aerodynamic roll angle ϕ_0 (see Figure 8.2), Mach number, body rates (p, q, and r), $\dot{\alpha}_0, \dot{\alpha}_s$, the aerodynamic control surface deflections in pitch, yaw, and roll (δP, δY, δR), center-of-gravity changes, and whether the main propulsion system is on or off.

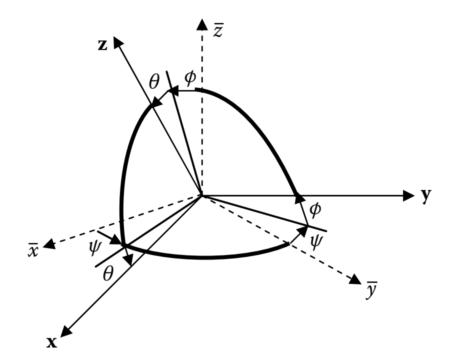


FIGURE 8.3 Euler angles.

According to equation (8.5), the body axis accelerations A_x, A_y, and A_z, the components of $\boldsymbol{A} = (A_x, A_y, A_z)$, are

$$\begin{bmatrix} A_x \\ A_y \\ A_z \end{bmatrix} = \begin{bmatrix} X + G_x + T_x \\ Y + G_y + T_y \\ Z + G_z + T_z \end{bmatrix} \tag{8.16}$$

Based on equation (8.9), this equation can be transformed in

$$\begin{bmatrix} A_x \\ A_y \\ A_z \end{bmatrix} = \frac{QS}{m} \begin{bmatrix} C_x(\alpha_0, \alpha_s, \delta P, \delta Y, \delta R) \\ C_y(\alpha_0, \alpha_s, \delta P, \delta Y, \delta R) \\ C_z(\alpha_0, \alpha_s, \delta P, \delta Y, \delta R) \end{bmatrix} + \begin{bmatrix} G_x \\ G_y \\ G_z \end{bmatrix} + \begin{bmatrix} T_x \\ T_y \\ T_z \end{bmatrix} \tag{8.17}$$

The functions C_x, C_y, and C_z are linearized and presented as

$$\begin{aligned} C_x &= C_{x0} + C_{xa_0}\alpha_0 + C_{xa_s}\alpha_s + C_{xV}V + C_{x\delta P}\delta P + C_{x\delta Y}\delta Y + C_{x\delta R}\delta R \\ C_y &= C_{y0} + C_{ya_0}\alpha_0 + C_{ya_s}\alpha_s + C_{yV}V + C_{y\delta P}\delta P + C_{y\delta Y}\delta Y + C_{y\delta R}\delta R \\ C_z &= C_{z0} + C_{za_0}\alpha_0 + C_{za_s}\alpha_s + C_{zV}V + C_{z\delta P}\delta P + C_{z\delta Y}\delta Y + C_{z\delta R}\delta R \end{aligned} \tag{8.18}$$

where the meaning of the coefficients of the Taylor's first-order approximation is obvious.

Analogous approximation can be done for C_l, C_m, and C_n [see equation (8.10)]

$$\begin{aligned} C_l &= C_{l0} + C_{la_0}\alpha_0 + C_{la_s}\alpha_s + C_{lV}V + C_{l\delta P}\delta P + C_{l\delta Y}\delta Y + C_{l\delta R}\delta R \\ C_m &= C_{m0} + C_{ma_0}\alpha_0 + C_{ma_s}\alpha_s + C_{mV}V + C_{m\delta P}\delta P + C_{m\delta Y}\delta Y + C_{m\delta R}\delta R \\ C_n &= C_{n0} + C_{na_0}\alpha_0 + C_{na_s}\alpha_s + C_{nV}V + C_{n\delta P}\delta P + C_{n\delta Y}\delta Y + C_{n\delta R}\delta R \end{aligned} \tag{8.19}$$

A more precise approximation also includes terms with coefficients depending on ϕ_0, $\dot{\alpha}_0$, $\dot{\alpha}_s$, p, q, and r [3]. The aerodynamic coefficients are an important part of a typical aerodynamic database for a missile that returns the aerodynamic forces and moments for a given missile orientation (α_0,

α_s, ϕ_0, Mach, and altitude), the aerodynamic control surface deflections (δP, δY, δR), and the mode of the propulsion system. The aerodynamic coefficients are presented here in a general form. In practice, depending on the type of missile, the stage of autopilot design, and the requirements for accuracy, many terms of equations (8.18) and (8.19) can be excluded from consideration.

8.4 AUTOPILOT AND ACTUATOR MODELS

An autopilot task is to control the motion of the missile. Maximizing missile performance requires choosing the appropriate autopilot structure for each stage of flight. Usually, during the midcourse phase, where a long flyout is required, and the terminal phase, where terminal homing maneuvers are necessary, autopilots that control the missile acceleration are used. At the end of terminal homing, during a guidance integrated fuze maneuver, the missile attitude may be controlled to improve the lethality of the warhead.

The missile dynamics model (8.5) [(8.6)–(8.10), (8.12), (8.15)–(8.19)] enables us to determine the desired values of controlled parameters. Their comparison with the real measured values of these parameters creates the error signals, which are used by autopilot controllers. Usually, instead of one autopilot, three autopilots are designed and used in practice: a pitch autopilot, a roll autopilot, and a yaw autopilot. Each of them is designed for individual channels, pitch, roll, and yaw, ignoring coupling between them. The effect of coupling is taken into account in the sophisticated design by creating interaction between the autopilots (i.e., by creating coupled autopilot channels).

Pitch rate dynamics were considered in equations (8.5), (8.10), and (8.15). Ignoring roll–yaw dynamics and considering only the components $C_{z\alpha_0}\alpha_0$, $C_{z\delta P}\delta P$, $C_{m\alpha_0}\alpha_0$, and $C_{m\delta P}\delta P$ in equations (8.18) and (8.19), we can obtain the transfer function characterizing the relationship between A_z and δP. As shown in [3], for tail-controlled missiles it has the form (4.12), i.e.,

$$\frac{A_z(s)}{\delta P(s)} = \frac{-Bs^2 + K(AE - BC)}{s^2 + AKs - C} \tag{8.20}$$

where

$$A = QSC_{z\alpha_0}/m, \quad B = QSC_{z\delta P}/m, \quad C = QSlC_{m\alpha_0}/I, \quad E = QSlC_{m\delta P}/I, \quad K = 1/V_{\mathrm{M}}$$

The corresponding expressions for the pitch rate and the angle of attack are [3]

$$\frac{q(s)}{\delta P(s)} = \frac{Es + K(AE - BC)}{s^2 + AKs - C}, \quad \frac{\alpha_0(s)}{\delta P(s)} = \frac{-BKs + E}{s^2 + AKs - C} \tag{8.21}$$

Expressions (8.20) and (8.21) are used in the pitch autopilot design. As mentioned earlier, for tail-controlled missiles the transfer function (8.20) is nonminimum phase. As the elevator δP deflects, the fin force accelerates the missile in the wrong direction. However, this force creates a pitching moment that rotates the missile. As the missile rotates, the body force accelerates the missile in the correct direction. One of the possible autopilot structures is given in Figure 8.4 (A_{z0} is a real missile acceleration; τ_1 is a time constant of the actuator, which is usually modeled as a first-order lag).

The pitch control law given in Reference [3] has the form

$$\delta P_c(s) = W_{P1}(s)e_z(s) + W_{P2}(s)q(s) \tag{8.22}$$

where $W_{P1}(s)$ and $W_{P2}(s)$ are the transfer functions with respect to the error between the measured and desired acceleration $e_z(s)$ and with respect to the measured pitch $q(s)$.

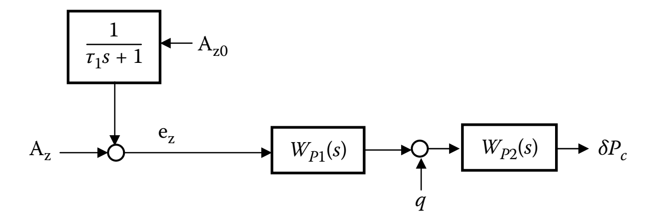


FIGURE 8.4 Pitch control.

These transfer functions are determined to guarantee autopilot stability with the desired response and ability to operate over a broad range of aerodynamic parameters (i.e., over a broad range of aerodynamic conditions). More sophisticated autopilots have time-varying parameters to compensate for changes in the missile dynamics. (In the examples of the previous chapters we considered guidance laws for various ω_z, which characterized changes in the missile dynamics for low and high altitudes.)

The yaw control law can be chosen in a similar way to the pitch control law, only in this case we operate with the components $C_{ya_s}\alpha_s$, $C_{y\delta Y}\delta Y$, $C_{na_s}\alpha_s$, and $C_{n\delta Y}\delta Y$. Some realizations of the roll control law are based on measured roll position and roll rate [3]. A constant p decouples the pitch and yaw channels [see equation (8.5)].

Over the past decades many techniques have been applied to autopilot design. They include classical multivariable, modern, and optimal approaches. Integrated design methodologies that combine guidance, estimation, and autopilot control systems have potential for increasing missile efficiency. Testing the guidance law should be linked with a certain structure of autopilot with appropriate parameters.

Since in this book the main focus is on tail-controlled missiles, we consider here only the widely used fin actuator model. Usually, fin actuator dynamics are modeled with a first- or second-order differential equation. The nonlinearities related to position and rate limits, as well as mechanical backlash of electromechanical actuators, should be included in the model. The autopilot pitch, yaw, and roll fin commands (δP, δY, δR) are distributed to the four fins producing real deflections δ_i ($i = 1,\ldots,4$). The above-mentioned nonlinearities relate to δ_i ($i = 1,\ldots,4$). The relationship between the actuator commands δP, δY, δR and individual fin deflections depends upon whether the missile has a "+" or "x" tail (i.e., whether the control surfaces are in line with the wings or in planes midway between the wings).

For "+" and "x" tails we have, respectively [3]

$$\delta P = \frac{\delta_2 - \delta_4}{2}, \quad \delta Y = \frac{\delta_1 - \delta_3}{2}, \quad \delta R = \frac{\delta_1 + \delta_2 + \delta_3 + \delta_4}{4}$$

and

$$\delta P = \frac{-\delta_1 + \delta_2 + \delta_3 - \delta_4}{4}, \quad \delta Y = \frac{\delta_1 + \delta_2 - \delta_3 - \delta_4}{4}, \quad \delta R = \frac{\delta_1 + \delta_2 + \delta_3 + \delta_4}{4} \tag{8.23}$$

To obtain the unique solution of equation (8.23) with respect to the actual fin deflections δ_i ($i = 1,\ldots,4$), the additional condition, the so-called "squeeze mode (SM) condition"

$$\delta SM = \frac{\delta_1 - \delta_2 + \delta_3 - \delta_4}{4} \tag{8.24}$$

should be satisfied. The actual fin deflection should be chosen to make the axial force resulting from deflections as small as possible [3].

The restrictions related to the fin deflections are transformed into the autopilot limits (δP, δY, δR), which, in turn, impose constraints on the missile acceleration.

8.5 REFERENCE SYSTEMS AND TRANSFORMATIONS

A reference frame (coordinate axes) determines the origin and direction of measurement of the motion states of a dynamic model. The origin is the point from which the states are measured. The axes of the reference frame define the directions of measurement. Common reference frames in simulation are body frames, navigation frames, and inertial frames. The inertial frame is the nonaccelerating reference frame used for calculating the Newtonian equations of motion. The navigation frame is generally located at a convenient position in space; for simulation of missiles, the navigation frame may be located on the Earth's surface at a given latitude and longitude. The navigation frame may be fixed, rotating, accelerating, or moving with respect to the inertial frame. In practice, it is difficult to define a reference frame that is not accelerating with respect to inertial space. For example, an Earth-fixed reference frame is suitable for some low-fidelity situations. However, in high-fidelity situations the rotation and movement of the Earth need to be accounted for in the definition of the inertial frame. The body-fixed frame has its position and orientation fixed to the vehicle body. The body-carried frame has its position fixed to the vehicle body and its orientation fixed to the navigation frame. Different simulations (or phases of a single simulation) may require different inertial reference frames for the fidelity requirements. The choice of reference frames affects the numerical error incurred in the simulation. This suggests that the reference frames used by dynamic models could be chosen to reduce numerical errors.

As mentioned in Chapter 1, the flight dynamics problems require a number of reference frames for specifying relative positions, velocities, and accelerations. The equations of motion can be written with respect to any reference plane, the choice usually being a matter of convenience and accuracy requirements. The motion states of aerospace vehicles are commonly expressed using the navigation frame and the body frame. The vehicle position is commonly expressed as the position of the body frame with respect to the navigation frame, and the vehicle velocity is commonly expressed as the velocity of the body frame with respect to the navigation frame. The body frame is a convenient reference frame to express many forces and moments generated on the body.

Three orthogonal reference systems are used in the six-degree-of-freedom simulation model described below: the Earth-fixed reference system (ESF), the missile body system, and the seeker reference system. In Chapter 1, we described the NED vehicle-carried coordinate system. As mentioned earlier, in many applications the ESF origin is near enough to the vehicle that Earth's curvature is negligible, so that the NED axes are parallel to the ESF axes.

The orientation of any reference frame relative to another can be characterized by three angles (the Euler angles), which are the consecutive rotations about the **z**,**y**,**x** axes, respectively, that carry one reference frame into coincidence with the other (see Figure 8.3).

The sequence of rotations that carry the NED frame into coincidence with the missile body frame are known as the body Euler angles transformation. The transformation matrices are given by

$$L_1(\psi) = \begin{bmatrix} \cos\psi & \sin\psi & 0 \\ -\sin\psi & \cos\psi & 0 \\ 0 & 0 & 1 \end{bmatrix}, \quad L_2(\theta) = \begin{bmatrix} \cos\theta & 0 & -\sin\theta \\ 0 & 1 & 0 \\ \sin\theta & 0 & \cos\theta \end{bmatrix}, \quad L_3(\phi) = \begin{bmatrix} 1 & 0 & 0 \\ 0 & \cos\phi & \sin\phi \\ 0 & -\sin\phi & \cos\phi \end{bmatrix} \tag{8.25}$$

so that the transformation from the NED to the missile body system can be described by

$$L_{EB} = L_3(\phi)L_2(\theta)L_1(\psi) = \begin{bmatrix} \cos\theta\cos\psi & \cos\theta\sin\psi & -\sin\theta \\ \sin\phi\sin\theta\cos\psi & \sin\phi\sin\theta\sin\psi & \sin\phi\cos\theta \\ -\cos\phi\sin\psi & +\cos\phi\cos\psi & \\ \cos\phi\sin\theta\cos\psi & \cos\phi\sin\theta\sin\psi & \cos\phi\cos\theta \\ +\sin\phi\sin\psi & -\sin\phi\cos\psi & \end{bmatrix} \quad (8.26)$$

It is easy to conclude that equation (8.12) corresponds to the transformation of the vector (0, 0, g).

Taking into account that the vector of the angular velocity of the missile body frame relative to the NED frame with coordinates $\dot{\phi}$, $\dot{\theta}$, $\dot{\psi}$ equals the difference between the angular velocities of the missile body frame (p, q, r) and the NED frame, and assuming the angular velocity of the NED frame to be equal to zero, we can use transformations (8.25) to present the rate of change of the Euler angles between the Earth axes and the missile body axes in terms of the body rotational rates p, q, and r [5]

$$\begin{bmatrix} \dot{\phi} \\ \dot{\theta} \\ \dot{\psi} \end{bmatrix} = \begin{bmatrix} 1 & \sin\phi\tan\theta & \cos\phi\tan\theta \\ 0 & \cos\phi & -\sin\phi \\ 0 & \sin\phi\sec\theta & \cos\phi\sec\theta \end{bmatrix} \begin{bmatrix} p \\ q \\ r \end{bmatrix} \quad (8.27)$$

If the missile is assumed to be roll stabilized (many simulation models are built based on this assumption, i.e., $p = 0$), the simplified Euler rate equations (8.27) are used.

The Euler angles are obtained by integrating these rates and including initial values of the angles at the initiation of the simulation process, i.e.,

$$\phi(t) = \int_0^t \dot{\phi}(t)dt + \phi_0, \quad \theta(t) = \int_0^t \dot{\theta}(t)dt + \theta_0, \quad \psi(t) = \int_0^t \dot{\psi}(t)dt + \psi_0 \quad (8.28)$$

The above relations relate to the case of nonrotating spherical Earth, i.e., the rotation of the NED frame relative to the ECI frame can be neglected. A more precise model should take into account Earth's rotation and its oblateness effect [5].

8.6 SEEKER MODEL

During the terminal phase of flight target tracking is performed by a seeker that detects a target and tracks it within its field of view. Usually, seekers are mounted on gimbals. Mostly they are equipped with two mutually perpendicular yaw and pitch gimbals. Sometimes a third gimbal, the so-called roll gimbal, is added. Seekers are always stabilized, that is, their axes remain fixed in space. To achieve stabilization and pointing control, the gimbals are controlled by torque motors, using signals from rate gyros, as well as sensor information of the target position. Infrared (IR) imaging sensors are used in optical seekers; an antenna is used as the sensor in radar seekers.

Analogous to the Euler body angles defined for the missile body frame with respect to the NED frame, the Euler angles between the missile body axes and the seeker axes can be defined. As indicated earlier, the **x** axis of the missile body coordinate system is coincident with the longitudinal axis of the missile; the **y** axis points out of the right side of the missile's body and the **z** axis is

orthogonal to both the **x** and **y** axes and defined by the right-hand rule, so that positive is defined as down. The $\mathbf{x}_s$ axis for the seeker onboard the interceptor missile coincides with the boresight of the seeker. The $\mathbf{y}_s$ and $\mathbf{z}_s$ axes are referred to as the yaw and pitch seeker axes. When the seeker boresight axis $\mathbf{x}_s$ coincides with the missile body **x** axis and the seeker gimbal angles are zero, the $\mathbf{y}_s$ and $\mathbf{z}_s$ axes coincide with the missile body **y** and **z** axes, respectively. The rotational sequence from the **x**, **y**, **z** axes to the $\mathbf{x}_s$, $\mathbf{y}_s$, $\mathbf{z}_s$ axes L_{BS} is yaw, pitch, and zero roll (ψ_s, θ_s, 0). This corresponds to such a seeker's platform that it tracks the target in azimuth and elevation.

For this case,

$$L_{BS} = L_2(\theta_s)L_1(\psi_s) = \begin{bmatrix} \cos\theta_s \cos\psi_s & \cos\theta_s \sin\psi_s & -\sin\theta_s \\ -\sin\psi_s & \cos\psi_s & 0 \\ \sin\theta_s \cos\psi_s & \sin\theta_s \sin\psi_s & \cos\theta_s \end{bmatrix} \tag{8.29}$$

Taking into account that the seeker angular velocity vector in the NED frame equals the sum of the seeker angular velocity vector with respect to the missile and the missile angular velocity vector in the NED, this relationship can be redefined in terms of the seeker body rates (p_s, q_s, r_s), the seeker Euler angle rates $(\dot{\psi}_s, \dot{\theta}_s, 0)$, and the missile body rates (p, q, r), i.e.,

$$p_s\mathbf{x}_s + q_s\mathbf{y}_s + r_s\mathbf{z}_s = \dot{\psi}_s\mathbf{z} + \dot{\theta}_s(-\sin\psi_s\mathbf{x} + \cos\psi_s\mathbf{y}) + p\mathbf{x} + q\mathbf{y} + r\mathbf{z} \tag{8.30}$$

and solved for the seeker Euler angle rates (here we assume the unit coordinate vectors).

Using equation (8.29) and assuming zero missile body and seeker roll rate ($p = p_s = 0$), equation (8.30) can be written in the seeker coordinate system

$$\begin{bmatrix} q_s \\ r_s \end{bmatrix} = \begin{bmatrix} -\sin\psi_s & \cos\psi_s & 0 \\ \sin\theta_s \cos\psi_s & \sin\theta_s \sin\psi_s & \cos\theta_s \end{bmatrix} \begin{bmatrix} -\dot{\theta}_s \sin\psi_s \\ q + \dot{\theta}_s \cos\psi_s \\ r + \dot{\psi}_s \end{bmatrix} \tag{8.31}$$

The seeker Euler angle rates equations follow immediately from equation (8.31)

$$\dot{\psi}_s = \frac{r_s - q\sin\theta_s \sin\psi_s}{\cos\theta_s} - r \tag{8.32}$$

$$\dot{\theta}_s = q_s - q\cos\psi_s \tag{8.33}$$

The seeker Euler angles are obtained by integrating the rate equations.

Typically, the line-of-sight (LOS) error is sensed in two orthogonal components measured along the $\mathbf{y}_s$ and $\mathbf{z}_s$ axes. The elevation error $\theta_{es} = \tan^{-1}(-R_{z_s} / R_{x_s})$, measured along the $\mathbf{z}_s$ axis, and the azimuth error $\alpha_{es} = \tan^{-1}(R_{y_s} / R_{x_s})$, measured along the $\mathbf{y}_s$ axis, are used as the input signals to the seeker head control system that, after filtering these signals, produces torques about the axes perpendicular to the sensed error axes, which causes a gyroscopic precession of the seeker head to reduce the LOS error (the seeker Euler angle rates tend to zero). A block diagram of the seeker dynamics loop is presented in Figure 8.5.

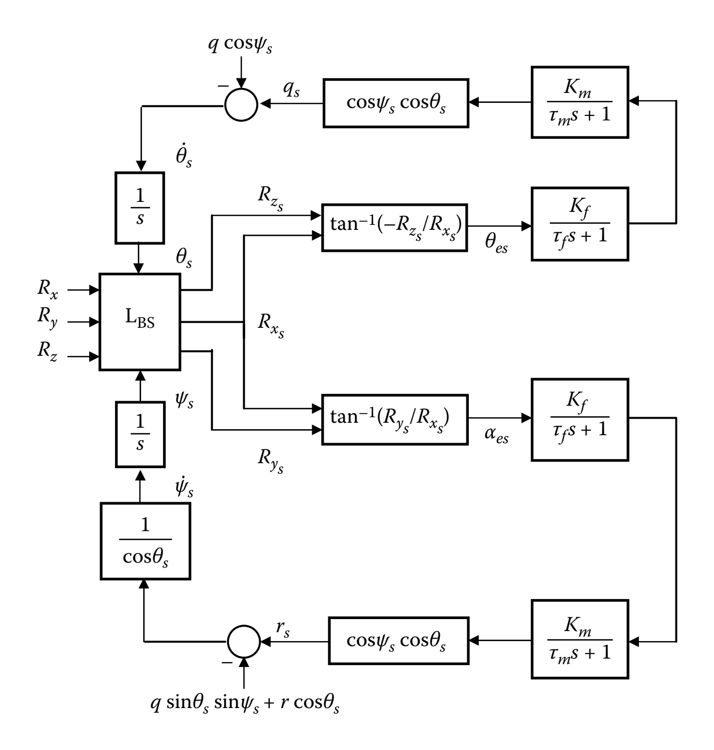


FIGURE 8.5 Seeker dynamics loop.

Here the motor and filter are characterized by the first-order transfer functions with the time constants τ_m and τ_f and gains K_f and K_m, respectively; the purpose of cosines of the gimbal angles $\cos\psi_s \cos\theta_s$ is to reduce the torque of the motor, as the gimbal angles increase. The closed-loop dynamics correspond to equations (8.32) and (8.33).

One of the factors that degrade performance of radar-guided missiles is the radome, which is designed to protect the missile from airflow and reduce drag. A nonhemispheric radome causes a refraction of the incoming electromagnetic wave, thus giving a wrong indication of the target location. The radome reflection has a destabilizing effect on the missile guidance system, especially at high altitudes [18,19]. The radome effect couples the missile LOS angles to the body dynamics through the gimbal angles and causes the aberration of the measured LOS angles. One of the ways of compensating the radome effect is described in References [14,19]. It combines filtering with use of nondestructive dither on the acceleration command signal. The LOS angles measured by the seeker are not equal to the true LOS angles. They depend nonlinearly on the horizontal and vertical gimbal angles ψ_s and θ_s, respectively. The first-order approximation gives the additional error terms $\rho_\psi \psi_s$ and $\rho_\theta \theta_s$, respectively. Following Reference [10], in the simulation model the radome slope coefficients can be described by random processes

$$\dot{\rho}_\psi = w_{\rho\psi}, \quad \dot{\rho}_\theta = w_{\rho\theta} \tag{8.34}$$

where $w_{\rho\psi}$ and $w_{\rho\theta}$ are zero-mean Gaussian white noise stochastic processes.

Seekers may saturate because they operate only within their field-of-view limits. The limits on ψ_s and θ_s should be incorporated into the simulation model. The detailed seeker model including the stabilization loop enables us to obtain more accurate estimates of the LOS and its derivative. It should be included in very sophisticated models. This is beyond the scope of this book, which

is focused primarily on guidance problems. For the purpose of testing guidance laws, a simplified seeker model can be considered [4]. It includes the unit determining the LOS and LOS rate and a filter. The seeker dynamics can be presented by the first- or second-order (for some types of seekers) differential equation. Noise and errors because of the radome effect can be incorporated directly into the LOS rate expression.

8.7 FILTERING AND ESTIMATION

Information required by guidance laws is obtained based on measurements provided by various sensors. It is known that any measurement is accompanied by noise that distorts, to a certain degree, the result of measurement. Special measures are used to increase the accuracy. Until recently, most measurements have been typically carried out using analog equipment. Now we are living in the digital era, when digital devices are dominating. The so-called weapon control system (WCS), a computerized program, operates missiles during the launch and midcourse phases, and microprocessors (controllers) guide missiles during the homing stage. Even if some sensors and simple filters remain analog, the information from them is input in digital form. That is why we describe below digital filters that are used in the guidance process that can be easily incorporated in the simulation model.

The α,β and α,β,γ filters are widely used in target tracking [1]. Tracking radar systems are used to measure the target's relative position in range, azimuth angle, elevation angle, and velocity. The α,β filter produces, on the *n*th observation, smoothed estimates for the position and velocity $x_s(n) = x_s(n,n)$ and $\dot{x}_s(n) = \dot{x}_s(n,n)$, respectively, as well as a predicted position for the $(n + 1)$th observation $x_p(n + 1,n)$, i.e.,

$$x_s(n) = x_p(n) + \alpha(x_m(n) - x_p(n)) \tag{8.35}$$

$$\dot{x}_s(n) = \dot{x}_s(n-1) + \frac{\beta}{T}(x_m(n) - x_p(n)) \tag{8.36}$$

$$x_p(n+1) = x_p(n+1,n) = x_s(n) + T\dot{x}_s(n) \tag{8.37}$$

where α,β are the filter gains, T is the sampling period, x_m is the measured position sample, and initial conditions are defined as

$$x_s(1) = x_p(2) = x_m(1), \quad \dot{x}_s(1) = 0, \quad \dot{x}_s(2) = (x_m(2) - x_m(1))/2$$

The recommendations concerning the choice of the parameters α and β

$$\beta = \frac{\alpha^2}{2-\alpha} \tag{8.38}$$

are motivated by the goals of reducing the measurement noise and minimizing the tracking error (i.e., so the filter should be able to track maneuvering targets).

The fading memory filters are a subclass of the α,β filters. The filter parameters depend upon the so-called smoothing factor $0 \le \xi \le 1$ and are given by

$$\alpha = 1 - \xi^2, \quad \beta = (1 - \xi)^2 \tag{8.39}$$

where heavier smoothing corresponds to larger values of the smoothing factor.

Most of the guidance laws considered earlier require some knowledge of the target's acceleration. The target's acceleration cannot be estimated accurately enough using only angle measurements made by imaging sensors on the interceptor; usually range information is required. It can be supplied either by off-board passive sensors or by on-board active sensors.

The α,β,γ filter produces, on the nth observation, smoothed estimates for the position, velocity, and acceleration $\ddot{x}_s(n) = \ddot{x}_s(n,n)$, as well as a predicted position for the $(n + 1)$th observation, i.e.,

$$x_s(n) = x_p(n) + \alpha(x_m(n) - x_p(n)) \tag{8.40}$$

$$\dot{x}_s(n) = \dot{x}_s(n-1) + T\ddot{x}_s(n-1) + \frac{\beta}{T}(x_m(n) - x_p(n)) \tag{8.41}$$

$$\ddot{x}_s(n) = \ddot{x}_s(n-1) + \frac{2\gamma}{T^2}(x_m(n) - x_p(n)) \tag{8.42}$$

$$x_p(n+1) = x_s(n) + T\dot{x}_s(n) + \frac{T^2}{2}\ddot{x}_s(n) \tag{8.43}$$

where initial conditions are

$$x_s(1) = x_p(2) = x_m(1), \quad \dot{x}_s(1) = \ddot{x}_s(1) = \ddot{x}_s(2) = 0, \quad \dot{x}_s(2) = \frac{x_m(2) - x_m(1)}{2},$$

$$\ddot{x}_s(3) = \frac{x_m(1) + x_m(3) - 2x_m(2)}{T^2}$$

The analog of equation (8.38) for the α,β,γ filter is given as

$$2\beta - \alpha(\alpha + \beta + \gamma/2) = 0 \tag{8.44}$$

and for the fading memory α,β,γ filters analog of equation (8.39) is

$$\alpha = 1 - \xi^3, \quad \beta = 1.5(1 - \xi)^2(1 + \xi), \quad \gamma = (1 - \xi)^3 \tag{8.45}$$

As in the case of the α,β filters, $\xi = 0$ means that there is no smoothing.

The Kalman filter is considered as a more sophisticated filtering and estimation tool than the above-described filters. It is known to be optimal in the white Gaussian noise environment. The optimal filtering problem is formulated in the following way. For the system of difference equations

$$\boldsymbol{x}(n + 1) = A_n\boldsymbol{x}(n) + B_n w(n), \quad x_m(n) = H_n\boldsymbol{x}(n) + v(n) \tag{8.46}$$

where $w(n)$ and $v(n)$ are independent Gaussian random processes with zero means and covariances Q_n and R_n, respectively, based on the measurements $x_m(k)$ $(k = 1,2,\ldots,n)$, find the estimates $\boldsymbol{x}(n,n)$ of $\boldsymbol{x}(n)$ that minimize the sum of squares of the measurement errors

$$\sum_{i=1}^{n} (x_m(i) - H_i\boldsymbol{x}(i,i))^T R_i (x_m(i) - H_i\boldsymbol{x}(i,i))$$

where $w(n)$ and $v(n)$ are scalars describing the process and measurement noises, respectively; A_n, B_n, and H_n are the matrices of appropriate dimensions.

The solution of the filtering problem is given as (see e.g., Reference [9])

$$\boldsymbol{x}(n+1,n+1 = A_n\boldsymbol{x}(n,n)+ \tag{8.47}$$

$$P(n+1,n)H_{n+1}^T[H_{n+1}P(n+1,n)H_{n+1}^T + R_{n+1}]^{-1}[\boldsymbol{x}_m(n+1) - H_{n+1}A_n\boldsymbol{x}(n,n)]$$

where the matrix $P(n,n)$ is the solution of the matrix Riccati equation

$$P(n+1,n) = A_n P(n,n) A_n^T + B_n Q_n B_n^T \tag{8.48}$$

$$P(n+1,n+1) = P(n+1,n) - P(n+1,n)H_{n+1}^T[H_{n+1}P(n+1,n)H_{n+1}^T + R_{n+1}]^{-1}H_{n+1}P(n+1,n) \tag{8.49}$$

$P(n,n-1)$ and $P(n,n)$ are interpreted as covariance matrices representing errors in the state estimates before and after an update, respectively.

The Kalman filter equation can be presented in a form close to equations (8.35), (8.36), and (8.40)–(8.42) that describe the α,β and α,β,γ filters. By introducing the state prediction vector $\boldsymbol{x}(n+1,n)$ that satisfies the state prediction equation

$$\boldsymbol{x}(n+1,n) = A_n\boldsymbol{x}(n,n) \tag{8.50}$$

and the filter gain K_n

$$K_n = P(n,n-1)H_n^T[H_n P(n,n-1)H_n^T + R_n]^{-1} \tag{8.51}$$

equation (8.47) can be rewritten as

$$\boldsymbol{x}(n+1,n+1) = \boldsymbol{x}(n+1,n) + K_{n+1}[x_m(n+1) - H_{n+1}\boldsymbol{x}(n+1,n)] \tag{8.52}$$

It looks similar to equations (8.35), (8.36), (8.40)–(8.42), which were obtained based on an intuitive approach. In contrast to the α,β and α,β,γ filters, the Kalman filter gain is time-varying. It depends on $P(n,n)$, that is, the solution of equations (8.48) and (8.49). The solution of equations (8.48) and (8.49) depends on the initial conditions $P(0,0)$. This presents the separate and most difficult part of the filtering problem. Nevertheless, Kalman filters are very popular and widely used in practice. The interpretation of $P(n,n\text{-}1)$ and $P(n,n)$ as covariance matrices helps choose $P(0,0)$. The justification of this interpretation is based on the following.

Subtracting equation (8.50) from equation (8.46) yields the state prediction error

$$\boldsymbol{e}(n+1,n) = A_n\boldsymbol{e}(n,n) + B_n w(n) \tag{8.53}$$

so that the state prediction covariance $P(n+1,n) = E[\boldsymbol{e}(n+1,n)\,\boldsymbol{e}(n+1,n)^T]$ satisfies equation (8.48); $P(n,n) = E[\boldsymbol{e}(n,n)\,\boldsymbol{e}(n,n)^T]$, called the updated covariance, and $\boldsymbol{e}(n,n)$ is the updated error in the state estimates [see (8.52)].

Subtracting equation (8.52) from the state equation (8.46) and acting in a manner similar to equation (8.53), we can obtain equation (8.49), which can be rewritten as

$$P(n+1,n+1) = P(n+1,n) - K_{n+1}S(n+1)K_{n+1}^T \tag{8.54}$$

where

$$S(n+1) = H_{n+1}P(n+1,n)H_{n+1}^T R_{n+1} \tag{8.55}$$

is called the measurement prediction covariance; $S(n+1) = E[\boldsymbol{e}_m(n+1,n)\,\boldsymbol{e}_m(n+1,n)^T]$; $\boldsymbol{e}_m(n+1,n)$ is the measurement prediction error

$$\boldsymbol{e}_m(n+1,n) = \boldsymbol{x}_m(n+1) - H_{n+1}\boldsymbol{x}(n+1,n) = H_{n+1}\boldsymbol{e}(n+1,n) + v(n+1) \tag{8.56}$$

The widespread tracking models (nearly constant velocity $\ddot{x}(t) = w_0(t)$ and near-constant acceleration $\dddot{x}(t) = w_0(t)$ models [1]; $w_0(t)$ is the zero-mean white noise process) are analyzed based on the above expressions. For these models, the matrices $A_n = A$, $B_n = B$, and $H_n = H$ are

$$A_n = \begin{bmatrix} 1 & T \\ 0 & 1 \end{bmatrix},\ B_n = \begin{bmatrix} 0 \\ 1 \end{bmatrix},\ H_n = \begin{bmatrix} 1 \\ 0 \end{bmatrix} \text{ for the nearly constant velocity model} \tag{8.57}$$

$$A_n = \begin{bmatrix} 1 & T & 0.5T^2 \\ 0 & 1 & T \\ 0 & 0 & 1 \end{bmatrix},\ B_n = \begin{bmatrix} 0 \\ 0 \\ 1 \end{bmatrix},\ H_n = \begin{bmatrix} 1 \\ 0 \\ 0 \end{bmatrix} \text{ for the nearly constant acceleration model} \tag{8.58}$$

In the discretized state equations with the sampling period T, the discrete time process noise relates to the continuous time zero-mean white noise process $w_0(t)$ with the spectral density Q_0 as

$$w(n) = \int_0^T e^{A_c(T-\tau)} B w_0(nT+\tau)\,d\tau \tag{8.59}$$

where A_c is the state matrix of the equations $\ddot{x}(t) = w_0(t)$ and $\dddot{x}(t) = w_0(t)$, respectively. Then $Q = E[w(n)w(n)^T]$ equals

$$Q = \begin{bmatrix} \frac{T^3}{3} & \frac{T^2}{2} \\ \frac{T^2}{2} & T \end{bmatrix} Q_0 \text{ for the nearly constant velocity model} \tag{8.60}$$

$$Q = \begin{bmatrix} \frac{T^5}{20} & \frac{T^4}{8} & \frac{T^3}{6} \\ \frac{T^4}{8} & \frac{T^3}{3} & \frac{T^2}{2} \\ \frac{T^3}{6} & \frac{T^2}{2} & T \end{bmatrix} Q_0 \text{ for the nearly constant acceleration model} \tag{8.61}$$

Based on the steady-state solution of the Riccati equations (8.48) and (8,49), for these two models the relationship between the parameters of the α,β and α,β,γ filters and the steady-state

parameters of the corresponding Kalman filters is established [1]. The position gain α, velocity gain coefficient β, and acceleration gain γ are the functions of the so-called target maneuverability index

$$\lambda = \frac{\sigma_w T^2}{\sigma_v},$$

where σ_w and σ_v, the variances of the process and measurement noise, characterize the motion and observation uncertainty, respectively.

The described target state estimators are important subsystems in advanced missile guidance systems. Target state estimators are required for two reasons. First, the measurements provided by on-board seekers such as LOS angles and its rates, as well as range and range rate, are often contaminated by noise and are not in a form usable by the guidance laws. Second, advanced guidance laws require additional information about the target such as its acceleration, which cannot be provided by the on-board sensors. The PN guidance law has been used most widely in the homing phase. However, there exist many situations (highly maneuvering targets), where the PN law performs unsatisfactorily. This fact has given rise to various modifications of the PN guidance law; some of them were considered in the previous chapters. The augmented PN guidance law and other guidance laws considered in the previous chapters need information about the target acceleration for their implementation. The optimal guidance laws are based on information about target acceleration and the predicted intercept point or time-to-go, so that their implementation needs the estimates of the corresponding parameters. Even in the case of the classic PN law, the LOS rate and closing velocity need to be estimated, since the corresponding measurements are noisy. In the example of Chapter 5, the Kalman filter was used to produce a smoothed LOS rate estimate for use in the PN law.

In general, the use of the Kalman filter can be rigorously justified, when the missile–target engagement dynamics are considered to be linear. Moreover, although various elegant expressions have been obtained, the application of the above-described Kalman filters requires certain skills and experience. 9-DOF and 6-DOF filters are used for estimating the position, velocity, and acceleration of the target. There exist algorithms that operate with both models and determine when to switch from one model to another.

Although Kalman filters are based on the theory developed for linear models, they are applied also for nonlinear models. The kinematics of the target are modeled, usually, in the NED coordinate system, but the target position measurements are assumed to be made in the spherical system, consisting of range, azimuth, and elevation angles [see equations (1.4) and (1.5)]. The transformation from the spherical coordinate system to the Cartesian coordinate system is nonlinear. The so-called extended Kalman filters are used to increase the accuracy of estimations. The approach used in the extended Kalman filter is based on the linearization of nonlinear functions by using a first-order Taylor series expansion (ignoring the second- and higher-order terms). The resulting approximate measurement equation becomes linear, but the measurement matrix should be calculated in every iteration. Despite a lack of rigorous mathematical justification (in contrast to the Kalman filter), the extended Kalman filter is widely used in attitude estimation (e.g., Euler angles). The Kalman filters (original and extended) require complete prior covariance information on the initial state, process noise, and measurement noise.

In numerous applications, essential statistical information concerning the process and measurement noise may either be missing or may be poorly defined. The filter operation is further affected by modeling errors, linearization approximations, and, as a result, the covariance matrix, computed from the Riccati equation of the extended Kalman filter, may not resemble the true covariance matrix of errors in the estimated state.

The so-called unscented filters, developed as an improvement on the extended Kalman filters, are also used in attitude estimation [16]. However, the above-mentioned filters and their tuning require extensive experimental data.

The filters included in the simulation model used for testing guidance laws should contain well-tested parameters. The accuracy and robustness of state estimators have been some of the limiting factors for improving guidance performance against maneuvering targets. The filters considered above must be tuned to the most stressing threat expected. If the threat is less stressing, performance will be worse than optimal compared to a Kalman filter tuned to a less stressing threat. This leads to the consideration of adaptive estimation techniques that give robust performance over a wide class of maneuvering targets. A survey of numerous estimation techniques can be found in Reference [2].

8.8 KAPPA GUIDANCE

The Kappa algorithm [7] dominates midcourse guidance in the endoatmosphere and can be interpreted as maximization of the terminal missile velocity, i.e., Kappa guidance is an optimal guidance law that maximizes missile speed at the beginning of the terminal phase of flight. This requirement is essential against a target at a far distance or at low altitude. When engaging a target at long range or at low altitude, missile velocity is the prime factor. Kappa guidance is applied also for targets at close distances. When engaging a close-in target, the time line is most important because the missile must destroy the target before it reaches within the minimum range of intercept.

The Kappa algorithm is based on knowledge of the predicted intercept point. As indicated in the introduction of Chapter 5, the accuracy of prediction or estimation significantly influences the accuracy of the engagement. Because the Kappa guidance law is obtained as the solution of the terminal optimal problem, it requires complete information (current and future) about the missile and target, as well as the external conditions during the engagement. However, the missile dynamic equations including drag and lift can only be implemented approximately, and it is impossible to estimate analytically the influence of incomplete information on the outcome of the engagement. Moreover, the predicted intercept point and time-to-go are important parameters that dominate the accuracy of the optimal solution. These parameters can only be estimated, and it is difficult to evaluate the influence of the errors on the engagement final results.

It is difficult to reflect all factors when formulating the optimal guidance problem, so that many optimal problems discussed in the literature have not been implemented in practice. All optimal problems are also rather complex for real-time on-board implementation. In many publications, target maneuvers were either neglected or assumed to be well-defined, mostly constant. In guidance laws that explicitly include the target maneuver, the estimation of related variables, which cannot be measured directly, becomes critical. Formally, the optimal problem that generates the Kappa algorithm ignores target behavior. Indirectly, it is taken into account in the estimate of the predicted intercept point. The optimal problem is accompanied by many assumptions. However, and very importantly, the Kappa midcourse guidance algorithm is successfully used in the SM2 (U.S. Standard Missile 2) missiles. That is why it deserves to be included in the simulation software and is considered below.

Let the vector $\boldsymbol{r}_{PIP}$ indicate the position of the predicted intercept point and the vector $\boldsymbol{r}_M$ characterize the current missile position. Then the PN law (2.24) can be rewritten as

$$\boldsymbol{a}_c = \frac{N}{t_{go}^2}(\boldsymbol{r}_{PIP} - \boldsymbol{r}_M - \boldsymbol{v}_M t_{go}) - \frac{N}{t_{go}}(\boldsymbol{v}_{PIP} - \boldsymbol{v}_M)$$

where the missile velocity $\boldsymbol{v}_M$ terms were added with opposite signs to the right part of equation (2.24) and $\boldsymbol{v}_{PIP}$ is the missile terminal velocity at the intercept point.

The above equations can be presented in a more general form

$$\boldsymbol{a}_c = \frac{K_1}{t_{go}^2}(\boldsymbol{r}_{PIP} - \boldsymbol{r}_M - \boldsymbol{v}_M t_{go}) - \frac{K_2}{t_{go}}(\boldsymbol{v}_{PIP} - \boldsymbol{v}_M) \tag{8.62}$$

where K_1 and K_2 are some coefficients.

Assuming that the predicted intercept point can be evaluated during the missile flight and that $\boldsymbol{v}_{PIP}$ is a desired terminal missile velocity, the problem of finding the optimal guidance law can be formulated as a problem of finding the optimal values K_1 and K_2 that maximize the terminal value of $\boldsymbol{v}_M$. As shown in Reference [7], the optimal values are

$$K_1 = \frac{w^2 r^2 (\cosh(wr) - 1)}{wr \sinh(wr) - 2(\cosh(wr) - 1)} \tag{8.63}$$

$$K_2 = \frac{w^2 r^2 - wr \sinh(wr)}{wr \sinh(wr) - 2(\cosh(wr) - 1)} \tag{8.64}$$

where

$$w^2 = \frac{D_0 L_\alpha (T / L_\alpha + 1)^2}{m^2 v^4 (2C_{L_\alpha} + T / L_\alpha)} \tag{8.65}$$

$$D_0 = C_{D0} QS, \quad Lift = QSC_{L_\alpha}\,\alpha = L_\alpha \alpha$$

(D_0 is the drag component stipulated by the component C_{D0} of $C_D = C_{D0} + C_{L_\alpha}\alpha^2$ assuming that the so-called drag curve is a parabola [11] and L_α is the lift factor [see equation (8.3)]; T is thrust, m is the mass, and v is the speed of the missile.)

The first term of equation (8.62) is called the proportional term and presented as

$$\boldsymbol{a}_{c1} = \frac{K_1}{t_{go}^2}(\boldsymbol{r}_{tgo} - \boldsymbol{v}_M t_{go}) \tag{8.66}$$

where $\boldsymbol{r}_{tgo}$ is the range-to-go vector.

The second term of equation (8.62) is called the shaping term and presented as

$$\boldsymbol{a}_{c2} = \frac{K_2}{t_{go}}(\boldsymbol{v}_{PIP} - \boldsymbol{v}_M) \tag{8.67}$$

The desired terminal velocity vector $\boldsymbol{v}_{PIP} = (V_{PIPN}, V_{PIPE}, V_{PIPD})$ is given as

$$\begin{aligned} V_{PIPN} &= V_M \cos\mu_v \cos\mu_h \\ V_{PIPE} &= V_M \cos\mu_v \sin\mu_h \\ V_{PIPD} &= -V_M \sin\mu_v \end{aligned} \tag{8.68}$$

where the angles μ_v and μ_h are the vertical and horizontal trajectory shaping angles.

For tactical ballistic missiles $\mu_v \approx 45°$, for cruise missiles $\mu_v \approx -75°$.

A slightly different presentation of the proportional and shaping terms can be found in Reference [13].

8.9 SIMULATION MODELS

Modern threats have become faster, stealthier, and more maneuverable. Successfully engaging such threats will require a system approach that implements a combination of advanced sensor processing

algorithms, guidance algorithms, and control processing techniques. Missile defense interceptor flight control system design requirements are generally driven by high maneuver rates that are needed for terminal homing. These requirements must be met while retaining stability and robustness throughout a large possible engagement envelope.

In the previous section, we described the main missile system elements that should be included in the simulation model. Depending on the accuracy requirements and the guidance laws under consideration, some of the elements may not be needed in the model, and some equations can be simplified.

The simulation model should analyze the performance of guidance laws in a realistic simulation environment, which accounts for the effects of drag and flight control system dynamics on the missile's performance. Analysis of the missile's kinematic boundary and other criteria should be used as the measure of effectiveness and basis of comparison. The engagement envelope or kinematic boundary is of paramount importance. The kinematic boundary represents the maximum range at which the missile will achieve a hit, when there is no noise in the system. It can, therefore, be used as a criterion for comparing the performance of guidance laws. Among other significant features of guidance system performance are the miss distance, the time of intercept, maximum rate of turn, and maximum lateral acceleration. The comparative analysis of guidance laws is more restrictive. It includes some of these features (the engagement envelope and miss distance, the time of intercept), as well as specific features, such as the missile terminal speed and impact angle.

The PN guidance law and the Kappa guidance law can be used as the baseline against which the other guidance laws will be tested. The candidate guidance laws include the guidance laws considered in this book and their combination (i.e., hybrid guidance laws, as well as other guidance laws considered in the literature). The guidance laws should be tested against nonmaneuvering and maneuvering targets.

The simulation model should be built based on the module principle, which is the most efficient way to create simulation models that can be enhanced in the future or simplified if necessary. Separate modules serve as building blocks. If needed, some of them can be deleted without damaging the structure, or new ones can be added to make the structure more sophisticated.

Normally the design of models could be developed using a computer-aided software engineering (CASE) tool supporting an object-oriented methodology such as the Unified Modeling Language, an object-based methodology such as HOOD, or a structured design methodology such as Yourdon. These tools generate the model stubs, and the models would then typically be implemented in C++, ADA, or C. Simulink and MATLAB developed software based on six-degrees-of-freedom dynamics and simplified aerodynamics that can be used in the aerospace industry.

Building a simulation model is an art. Despite the existing design tools, deep knowledge of specific problems enables one to create more sophisticated programs than by using the existing "general use" tools. Below we describe the structure of a hypothetical simulation model that, in our opinion, best meets the research requirements. The simulation model is focused on analyzing various intercept problems in the endoatmosphere. It can be realized by using, for example, Visual FORTRAN.

8.9.1 6-DOF Simulation Model

The simulation model should properly reflect two stages of the missile flight, its midcourse and homing stages. As mentioned earlier, in certain scenarios the mission requirements call for the payload to impact the target from a specific direction. These requirements are of importance during the so-called endgame, the final part of the homing stage.

The simulation process usually starts from the midcourse phase. It means that the missile prehistory (its uncontrolled boost stage) should be presented by the missile position and velocity at the beginning of the midcourse stage (see Figure 8.6). The launch parameters, which define the direction of the missile flight, are determined by the predicted intercept point (PIP). The initial

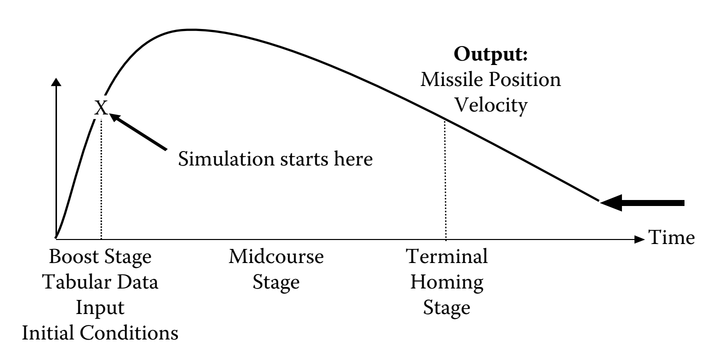


FIGURE 8.6 Stages of the simulation process.

unguided boost stage is strictly programmable depending on the target position at the launch time and some other external measurable factors.

Typically, there exist tables that enable us to find, depending on the intercept point, the position and velocity of the missile up to about 6 *s* after its launch (i.e., at the beginning of the midcourse phase). They have been obtained from various experiments combined with analytical analysis. For missiles launched from ships, corrections should be calculated for ship movement, ballistic wind influence, and launch cell parallax. These data and related equations should be incorporated into the model.

As indicated earlier, during the midcourse phase the missile is guided by the weapon control system. The most sophisticated simulation models should be able to model the main WCS operations that include: (1) algorithms to determine the predicted intercept point and time-to-go; (2) filtering that provides the midcourse guidance with inputs characterizing the target position, velocity, and, if needed, acceleration; (3) midcourse guidance commands. The predicted intercept point and time-to-go are also used in some versions of the PN law in the terminal guidance phase. As mentioned, the difficulties in predicting target position stem from uncertainty in interception time because of unpredictability of the target's future behavior. Factors contributing to uncertainties in the intercept point are (1) random and systematic errors in the defense detection and tracking system's measurement of the position and velocity and estimate of acceleration of the attacking missile; (2) lack of knowledge of the attacking missile's target; and (3) intentional trajectory shaping and intentional evasive maneuvers. A reasonable assumption is that at long ranges the missile need only travel in approximately the right direction. Hence, at long range the time to intercept needs to be found only roughly. As interception approaches, the need for accuracy increases. The time-to-go can be estimated roughly as $t_{go} = -\dot{r}/r$. In practice, a more detailed scenario-specific analysis is used to determine PIP and the time-to-go. This topic is beyond the scope of this book.

Absence of the PIP module in the simulation model would require certain homework to determine the missile initial position and velocity at the beginning of the midcourse stage. If the simulation process deals only with the terminal stage, the missile position and velocity should be determined separately based on specifics of the scenario under consideration.

The filtering module should contain the set of equations discussed earlier. During the midcourse, the interceptor receives frequent updates on its position from off-board tracking sensors, so that formally the estimates of the position and velocity (as well as acceleration, for some guidance algorithms) not only of the target but also the missile are needed. In the less sophisticated simulation models, the filtering operations are applied to the relative position and velocity of the missile with respect to the target. This relates also to the terminal stage. The filtering module realizes signal processing algorithms to provide smoothed data that are used in the guidance law. It is very important to model the errors expected in tracking using infrared sensors and surface- and air-based radars based on the analysis of these devices. Then the obtained filtering results are more realistic than under the assumption of Gaussian white noise.

The target module consists of a 3-DOF point-mass presentation of the target motion. The target model should be capable of executing a maneuver at a given time. The user should be able to adjust the time and extent of this maneuver. From an almost infinite variety of possible maneuvers, it is important to choose the most representative maneuvers for various types of missiles and the intercept scenarios.

In the previous chapters, we considered the so-called step and weave maneuvers. Within these two main classes, special types of maneuvers are specified. For example, analyzing boost-phase intercept systems (attacking ballistic missiles should be disabled in their boosting phase during the first few minutes of flight), it is reasonable to model a sudden increase or decrease in the target's missile angle of attack and a switchback maneuver, in which the target switches from a positive to negative angle of attack. Maneuvers like these (lunge maneuvers) might be performed either to shape the attacking missile trajectory or to try to evade an anticipated interceptor. In the simulation model, a lunge maneuver should be executed during the last few seconds before the predicted intercept time. Another kind of maneuver, a jinking maneuver, is a periodic maneuver, usually a sinusoidal modulation of the acceleration that would produce a fish-tail-like motion of the missile during the last few seconds before the predicted intercept. Such maneuvers are likely to be within the capabilities of the attacker's missiles. Cruise missiles that possess a very "smart" guidance system can perform various maneuvers. The most typical are "diving" maneuvers, when a cruise missile significantly changes its altitude, and weave maneuvers in a horizontal plane, when it approaches the target at a very low altitude.

Optimal control and game theories were used to formulate precisely and solve the problem of optimal pursuit and evasion. Unfortunately, this approach cannot work because it is difficult to build an analytical model that closely matches reality and can be used in practice. Deterministic optimal problems require ideal information, which cannot be obtained, about the target and missile flight parameters. However, the optimal approach does enable an evaluation of the best possible scenario for the evader that can be used for comparison with strategies that can be realized in practice. The optimal evader's maneuver, if *a priori* information concerning the missile guidance system is available, is described in Reference [18]. An intuitive evasive maneuver, which is formulated as the reverse PN, is given in Reference [8]. It is expected, although it is yet to be proved, that the target would be able to avoid the pursuing missile by turning its velocity vector reversely proportional to the LOS rate. Based on analysis of the optimal maneuvers for various scenarios, practical periodic target evasive maneuvers were considered [18]. Random target maneuvers were discussed in Chapter 7.

Evasive maneuver design parameters include magnitude, weave period (for weaving evasion), initiation time, and duration. The maximum achievable maneuver magnitude–period combination is a function of initiation and duration times and may vary within the established flight envelope of interest. Offensive missile design information, including airframe configuration, mass properties parameters, and aerodynamic and propulsion parameters needs to be used. Based on this information, flight performance can be evaluated and the maximum achievable maneuver, as well as the region within the vehicle's flight profile, where the maneuver is most likely to occur, can be determined. Missile Datcom, a widely used semiempirical datasheet component build-up method for preliminary design of missile aerodynamics and performance, can be used to build a dynamic model [see, e.g., equation (4.65)] of an offensive missile and establish the maximum achievable maneuver magnitude. The optimal weaving frequency can be determined as described in Chapter 4 (see Figure 4.13).

The midcourse guidance module contains algorithms realizing the guidance law under consideration. Based on smoothed data from the filtering module, the commanded acceleration is calculated in the NED coordinate system and transferred to the missile model. Taking into account that the missile trajectory of the model, formally deterministic and generated by the guidance law, differs from the real one, it is reasonable to use in the model as the missile data the deterministic signal plus noise depending on the missile data accuracy requirements. Usually, the calculation of the commanded acceleration is accompanied by the calculation of the gravity acceleration

(equation 8.2). However, depending on taste, a separate missile gravity module can be created that calculates the acceleration in the NED coordinates according to equation (8.2), or in the missile body coordinate system according to equation (8.12). The WCS operates with a certain frequency (usually, 4–10 *Hz*). The acceleration commands are transferred with this frequency to the missile model that operates with a significantly higher frequency.

Typically the missile model includes (1) the thrust module, (2) the aerodynamic module, (3) the missile dynamics module, (4) the autopilot module, (5) the fin/actuator module, (6) the seeker module, (7) the missile trajectory module, and (8) the coordinate transformation module.

The thrust module contains data to obtain a certain thrust profile. One of its components is the pressure table. It is used to calculate the second term in equation (8.2). The aerodynamic module contains the aerodynamic forces and aerodynamic moment coefficients (8.9), (8.10), and (8.17)–(8.19) used in the missile dynamics module. The missile dynamics module models the missile dynamics from the aerodynamic forces (aerodynamic module), thrust and gravity (thrust module) [see equations (8.4), (8.5)–(8.10), and (8.15)]. It contains tables of mass, center of gravity, and moment of inertia that are used to determine the missile dynamics [see equations (8.5) and (8.11)]. The autopilot module calculates the required fin deflection, within admissible limits. The fin/actuator module receives the fin commands from the autopilot module and translates these commands from roll, pitch, and yaw commands to the required input to each actuator. The fin configuration must match the aerodynamic data used in the missile aerodynamic module. As mentioned earlier, the autopilot equations (8.20)–(8.22) correspond only to one channel of control and a certain type of autopilot. They are given as an illustration without detailed consideration (see details, e.g., in [3,17]). It is desirable for the simulation model to be oriented on a concrete type of autopilot used in specific missiles. The real missile acceleration is described by equation (8.17). Based on equation (8.5) it is possible to determine the components of the missile velocity that correspond to the determined fin deflection. The missile trajectory module integrates the equations of motion [see equations (1.1), (1.2), and (1.20)]. Initially, the missile velocity or acceleration vectors in the missile body coordinate system are transferred into the NED coordinate frame by the L_{BE} operator; $L_{BE} = L_{EB}^{-1} = L_{EB}^{T}$ [see equation (8.26)]. This operation is produced in the coordinate transformation module. If system (8.5) is used, and the missile position $\boldsymbol{r}_{M,k\text{-}1}$ at $t_{k\text{-}1}$ is known, then at a moment t_k

$$\boldsymbol{v}_{\boldsymbol{M}} = L_{EB}^{T}\, \boldsymbol{V}_{\mathrm{M}}, \quad \boldsymbol{r}_{\boldsymbol{M,k}} = \int_{t_{k-1}}^{t_k} \boldsymbol{v}_M\, dt + \boldsymbol{r}_{M,\,k-1} \tag{8.69}$$

The less precise expression follows from

$$\ddot{\boldsymbol{r}}_M = L_{EB}^{T}\ \boldsymbol{A}, \quad \boldsymbol{v}_{M,\,k} = \int_{t_{k-1}}^{t_k} \ddot{\boldsymbol{r}}_M\, dt + \boldsymbol{v}_{M,\,k-1} \tag{8.70}$$

where $\boldsymbol{v}_{M,k-1}$ and $\boldsymbol{v}_{M,k}$ are the missile velocity in the NED frame at $t_{k\text{-}1}$ and t_k, respectively.

For small time increments Δ, we can use the approximation

$$\boldsymbol{v}_{M,\,k} = \ddot{\boldsymbol{r}}_{M,\,k}\Delta + \boldsymbol{v}_{M,\,k-1}, \quad \boldsymbol{r}_{M,\,k} = \ddot{\boldsymbol{r}}_{M,\,k-1}\Delta^2/2 + \boldsymbol{v}_{M,\,k-1}\Delta + \boldsymbol{r}_{M,\,k-1} \tag{8.71}$$

where the notations are obvious.

During the homing stage the target information is received by a seeker. However, since we use a 3-DOF point-mass presentation of the target motion, this motion is presented initially in the NED coordinate frame. Then using the transformations $L_{EB}L_{BS}$ from the coordinate transformation module,

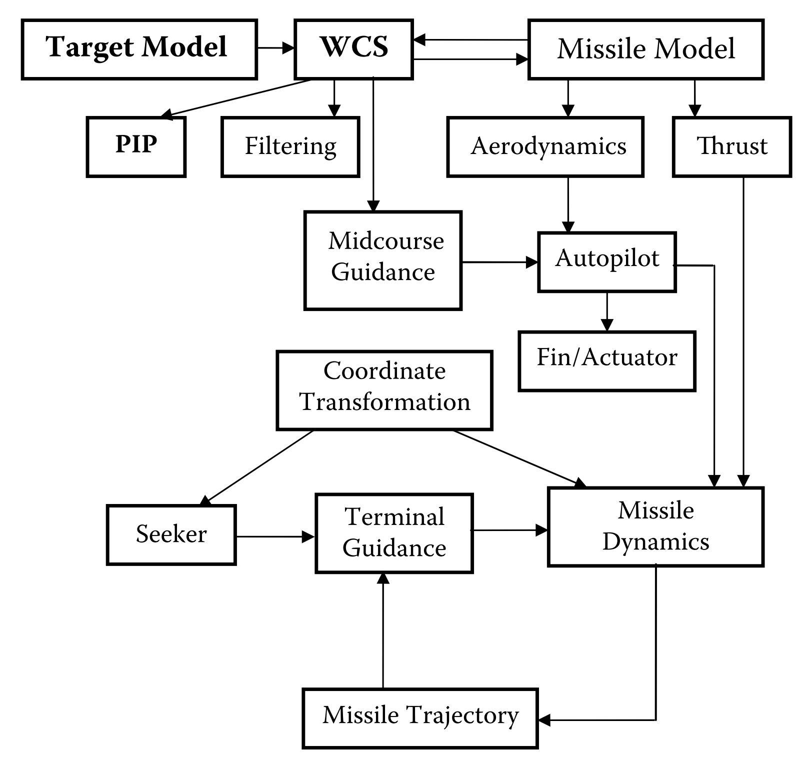


FIGURE 8.7 6-DOF simulation model structure.

the target position $\boldsymbol{r}_T$, velocity $\dot{\boldsymbol{r}}_T$, and acceleration $\ddot{\boldsymbol{r}}_T$ (if needed) vectors are transformed into the seeker coordinate system, together with $\boldsymbol{r}_M$ and $\dot{\boldsymbol{r}}_M$, and used in the seeker's module. The relative position of the target with respect to the missile is used to compute the actual LOS. Band-limited white noise is added to the LOS components to reflect the influence of noise on missile performance. The corrupted LOS vector is created by including noise, as described in the previous chapter, as well as the radome boresight errors [see equation (8.34)]. The estimated LOS rate is produced by a filter. The LOS and LOS rate vectors in the seeker coordinate frame are transformed into the missile body coordinate frame, where all operations are performed similarly to the midcourse phase.

The effectiveness of new guidance laws should be tested by comparing them with four commonly used guidance laws: the "pure" PN guidance [see equation (2.23)], the "predictive" PN guidance that requires knowledge of the time-to-go [see equation (2.24)], the APN guidance [see equation (2.28)], and the Kappa guidance. These laws should be contained in the guidance reference module. It is useful to also create the management module that would control all operations between all the above-mentioned modules.

Of course, the described structure of the 6-DOF simulation model (see Figure 8.7) is only one possible realization of the simulation model. The concise discussion above was focused on the main components that should be present in a sophisticated 6-DOF simulation model.

8.9.2 3-DOF Simulation Model

The 3-DOF simulation model is significantly simpler than the 6-DOF simulation model. However, it can be successfully used to test new guidance laws. All operations are performed in the NED coordinate system (below, the indices 1, 2, and 3 will indicate N, E, and D coordinates, respectively). There are no dynamic models of a seeker and autopilot. The flight control system is represented by the transfer function similar to the planar case considered in the previous chapters [see, e.g., equations (4.12), (4.15), (4.34), and (5.63)]. However, in the 3-DOF simulation model, the differential equations

corresponding to the transfer function mentioned above should describe the relationship between the coordinates of the commanded and actual accelerations (i.e., the dimension of the system of differential equations is three times higher than in the planar models).

The main difficulty in building the 3-DOF model relates to the presentation of the total missile acceleration. The thrust force is directed along to the missile's body; for missiles without throttleable engines the controlled part of the commanded acceleration acts orthogonal to the body; drag forces are directed along to the missile velocity vector. Without knowledge of the angle of attack, it is impossible to properly combine the corresponding components of missile acceleration. However, the 3-DOF missile model contains insufficient information to determine the angle of attack. Knowledge of the missile velocity vector enables us to determine the component of the target acceleration orthogonal to this vector. Assuming small angles of attack, more precisely, zero angle of attack, the above-mentioned components can be presented along and orthogonal to the velocity vector. Such models exist. However, their accuracy is not high enough, especially in the case of highly maneuvering targets.

The approximate values of the angle of attack can be obtained from the missile aerodynamic data. The aerodynamic module should contain the following regression models describing the relationship between the angle of attack α_T and the lift C_L, normal C_N, and axial C_A force coefficients [the expressions for normal and axial forces are analogous to equation (8.3)]

$$\alpha_T = k_{00} + k_{01}C_L + k_{02}C_L^2$$

$$\alpha_T = k_{10} + k_{11}C_N + k_{12}C_N^2$$

$$C_A = k_{20} + k_{21}\alpha_T + k_{22}\alpha_T^2 \tag{8.72}$$

which can be built based on the missile aerodynamic data available from experiments or generated, for example, by Missile Datcom (see Appendix C).

Here and below we will use the k-coefficients without any additional explanation. It is assumed that they are known or can be calculated. The coefficients k_{sl} ($s = 0,1,2$; $l = 0,1,2$) are determined for a set of Mach numbers $Mach(i)$ ($i = 1,2,\ldots,n_i$) and altitudes $Alt(j)$ ($j = 1,2,\ldots,n_j$) based on the missile aerodynamic data, so that a certain mesh $k_{sl}(i, j)$ ($s = 0,1,2$; $l = 0,1,2$) with known values in its nodes (i, j) should be created. For a concrete Mach number $Mach$ belonging to $[i_0, i_0 + 1)$ and a concrete altitude Alt belonging to $[j_0, j_0 + 1)$, the regression coefficients can be calculated by using various interpolation formulas [12], for example,

$$k_1 = k_{sl}(i_0, j_0) + \frac{k_{sl}(i_0+1, j_0) - k_{sl}(i_0, j_0)}{Mach(i_0+1) - Mach(i_0)}(Mach - Mach(i_0))$$

$$k_2 = k_{sl}(i_0, j_0+1) + \frac{k_{sl}(i_0+1, j_0+1) - k_{sl}(i_0, j_0+1)}{Mach(i_0+1) - Mach(i_0)}(Mach - Mach(i_0))$$

$$k_{sl} = k_1 + \frac{Alt - Alt(j_0)}{Alt(j_0+1) - Alt(j_0)}(k_2 - k_1) \tag{8.73}$$

Based on equations (8.72) and (8.73), the angle of attack and the drag-generated axial force can be calculated. Formally, angle of attack could be calculated from the first equation of (8.72) and (8.3), assuming that lift is created by the orthogonal (to the velocity) component of the

commanded acceleration. However, in this case we ignore acceleration limits imposed by the autopilot. That is why the first equation of (8.72) can be used only to calculate the initial condition $\alpha_T(0)$ of the computational procedure determining the angle of attack.

In the 3-DOF simulation model the autopilot module contains operations related to the computation of the angle of attack and the commanded acceleration affecting the missile trajectory. If $\boldsymbol{v}_M = (V_{M1}, V_{M2}, V_{M3})$ is the missile velocity vector, then the unit velocity vector $\boldsymbol{e}_M = (e_{M1}, e_{M2}, e_{M3})$ has components

$$e_{Mi} = V_{Mi} / \sqrt{V_{M1}^2 + V_{M2}^2 + V_{M3}^2} \quad (i = 1, 2, 3) \tag{8.74}$$

The projection a_L of the guidance law-commanded acceleration $\boldsymbol{a}_c = (a_{c1}, a_{c2}, a_{c3})$ on the velocity vector is

$$a_L = \boldsymbol{a}_c \boldsymbol{e}_M = \sum_{i=1}^{3} a_{ci} e_i ,$$

so that the coordinates of the vector-projection $\boldsymbol{a}_L = (a_{L1}, a_{L2}, a_{L3})$ are

$$a_{ci} = a_L e_i \quad (i = 1,2,3) \tag{8.75}$$

and the acceleration $\boldsymbol{a}_{cN} = (a_{cN1}, a_{cN2}, a_{cN3})$ normal to the velocity vector equals

$$a_{cNi} = a_{ci} - a_L e_i \quad (i = 1,2,3) \tag{8.76}$$

The unit vector $\boldsymbol{e}_{LN} = (e_{LN1}, e_{LN2}, e_{LN3})$ orthogonal to the velocity vector is given by

$$e_{LNi} = a_{cNi} / \sqrt{a_{cN1}^2 + a_{cN2}^2 + a_{cN3}^2} \quad (i = 1,2,3) \tag{8.77}$$

For the given angle of attack $\alpha_T = \alpha_T(0)$, the unit vector $\boldsymbol{e}_B = (e_{B1}, e_{B2}, e_{B3})$ along to the body axis can be presented as

$$\boldsymbol{e}_B = \boldsymbol{e}_M \cos \alpha_T + \boldsymbol{e}_{LN} \sin \alpha_T \tag{8.78}$$

Acting analogously to equations (8.75) and (8.76), we obtain the components of the commanded acceleration normal to the missile body $\boldsymbol{a}_{cBN} = (a_{cBN1}, a_{cBN2}, a_{cBN3})$

$$a_{cBNi} = a_{ci} - a_B e_{Bi} \quad (i = 1,2,3) \tag{8.79}$$

where

$$a_B = \boldsymbol{a}_c \boldsymbol{e}_B = \sum_{i=1}^{3} a_{ci} e_{Bi} .$$

The autopilot acceleration limit $a_{\lim}$ (pitch, roll/yaw) can be presented by half-empirical expressions $a_{\lim} = f(Q)$. They reflect the fact that during flight the missile is subjected to varying pressure depending on the altitude of the missile. This affects its fin displacement (which is limited), since less deflection is required when the missile is flying in dense atmosphere, and more deflection is needed in a rare atmosphere. If $a_{cBN} = \sqrt{a_{cBN1}^2 + a_{cBN2}^2 + a_{cBN3}^2} > a_{\lim}$, then

$$a_{cBNi} = a_{cBNi} \frac{a_{cBN}}{a_{\lim}} \quad (i = 1,2,3) \tag{8.80}$$

Based on the commanded acceleration (8.80) and (8.3), (8.4), the coefficient C_N can be calculated, and from the second equation of (8.72) the new value of the angle of attack $\alpha_T(1)$ is determined. If the difference between $\alpha_T(0)$ and $\alpha_T(1)$ is small enough, $\alpha_T = \alpha_T(1)$. Otherwise, a certain computational procedure $\alpha_T(j+1) = \alpha_T(j) + \Delta$ can be applied to make two consecutive $\alpha_T(j)$ close enough, where j is a step of iterations and Δ is an increment. The new value of the angle of attack $\alpha_T(j+1)$ is used in equation (8.78), and the operations described above should be repeated. Assuming the initial value of the angle of attack to be positive and evaluating its first difference (equivalent to the derivative for discrete time), it is possible to operate with positive and negative angles of attack. There is no rigorous proof that the computational procedure converges. However, the tests performed on a 3-DOF simulation model show that for quite accurate regression models (8.72) and an appropriate search procedure (see, e.g., Reference [6]), which we leave the reader to choose, the required iterations number only in tens.

The missile dynamics module sums up all components of acceleration (thrust $\boldsymbol{a}_{thrust} = T\mathbf{e_B}$, normal component of the guidance law $\boldsymbol{a}_{cBN}$, gravity, and drag-generated axial component $\boldsymbol{a}_{axial}$). The drag-generated axial component of acceleration is determined by computing the axial force coefficient C_A of equation (8.72), for a given angle of attack, and then using the expressions similar to equations (8.3) and (8.9).The total acceleration $\boldsymbol{a}_{MT} = (a_{\text{MT1}}, a_{\text{MT2}}, a_{\text{MT3}})$ [see also equations (8.16) and (8.17)]

$$\boldsymbol{a}_{MT} = \boldsymbol{a}_{cBN} + (\mathbf{T} - \frac{QS}{m} C_A)\boldsymbol{e}_B + \boldsymbol{G} \tag{8.81}$$

serves the input of the system of differential equations describing the flight-control system dynamics

$$\dot{x}_{1i} = x_{2i}, \qquad \dot{x}_{2i} = x_{3i},$$

$$\dot{x}_{3i} = -\frac{\omega_M^2}{\tau} x_{1i} - \frac{\omega_M^2 + 2\zeta\omega_M}{\tau} x_{2i} - \frac{2\zeta\omega_M \tau + 1}{\tau} x_{3i} + \frac{\omega_M^2}{\tau} a_{MTi}$$

$$\ddot{r}_j = x_{3j-2,i} - \frac{1}{\omega_z^2} x_{3j,i} \qquad (i, j = 1,2,3) \tag{8.82}$$

Here ω_M, ζ, ω_z, and τ are the flight control system natural frequency, damping, airframe zero frequency, and the actuator time constant, respectively. The indicated parameters are functions of time and depend on the dynamic pressure, missile aerodynamic characteristics, its variable mass, and other factors [see equation (8.20)]. Numerical integration of equation (8.82), as well as differential equations considered earlier, is performed using the Runge–Kutta method described in Appendix D. The use of numerical integration routines in the simulation introduces numerical error, which can be propagated during the course of the simulation. To keep results accurate over long simulation runs, controlling these numerical errors is essential. Higher-order methods, such as the Runge–Kutta series, express the derivative function as a power series to calculate a more accurate estimate of the incremental term. As shown in the previous chapters, the most "sensitive parameter" for tail-controlled missiles is the airframe zero frequency, which should be changed depending on the missile altitude. The first-order unit describing the actuator dynamics and included in equation (8.80) can be placed before the autopilot limiter (as a possible modification of the missile dynamics module).

The structure of the described 3-DOF missile model is shown in Figure 8.8. In addition to the modules considered earlier, this structure includes the aerodynamic limit unit. In reality, this unit

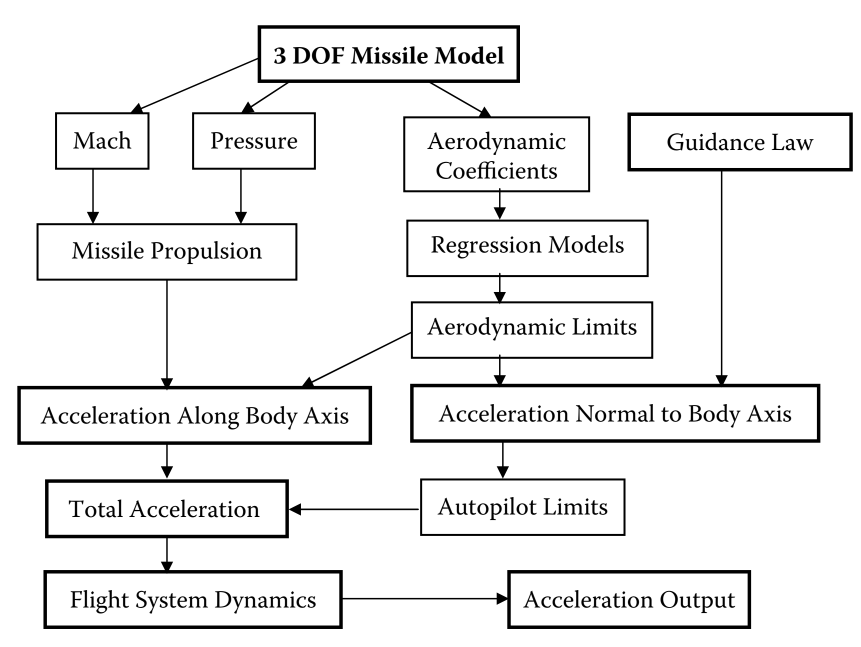


FIGURE 8.8 3-DOF missile model structure.

does not exist. It simply reflects the fact that the angle of attack in regression models (8.72) is limited. The models are obtained based on the aerodynamic data for the trim angles of attack, so that regression models (8.72) are valid for definite values of these angles below the upper limit, which depends on Mach number and altitude. Although the 3-DOF model does not describe missile dynamics precisely, and the angle of attack is determined only approximately, its relative simplicity makes it an effective tool for guidance laws performance analysis.

As in the case of the 6-DOF simulation model, the missile trajectory [equation (8.70)] and velocity [equation (8.71)] are obtained by integrating the actual missile acceleration [equation (8.82)]. Both models should calculate the closing velocity. Its negative value indicates the end of the simulation process. The range between the missile and the target at this moment presents the miss distance, and the time of flight is the estimate of the time of intercept.

It was mentioned before and it is essential to underscore that the miss distance is the most important but not the only important parameter characterizing missile performance. The miss distance should be considered together with the engagement envelope. The time of intercept and the missile terminal velocity (speed and impact angle) are also important factors in evaluating missile performance. This means that the comparative analysis of guidance laws should be based on vector criterion including the above-mentioned components.

Since it is impossible to be certain what specific missile threats we will face in the future or from where these threats will come, the long-term strategy is to strengthen and maximize the flexibility of missile defense capabilities. The development of new guidance laws, which are the “brains” of missiles, and testing them using sophisticated simulation models is an important component of this strategy.

REFERENCES

1. Bar-Shalom, Y. and Fortmann, T.E., *Tracking and Data Association*, Academic Press, Boston, 1988.
2. Cloutier, J., Evers, J., and Feeley, J., An assessment of air-to-air missile guidance and control technology, *IEEE Control Systems Magazine*, 9, 27–34, 1989.

3. Cronvich, L., Aerodynamic consideration for autopilot design, in *Tactical missile aerodynamics,* edited by M. Hemsch and J. Nielsen, *Progress in Aeronautics and Astronautics*, 124**,** AIAA, Washington, DC, 1986.
4. Ekstrand, B., Tracking filters and models for seeker applications, *IEEE Transactions on Aerospace and Electronic Systems,* 37, 3, 965–977, 2001.
5. Etkin, B., *Dynamics of Atmospheric Flight*, Dover, Mineola, NY, 2005.
6. Fletcher, R., *Methods of Optimization,* John Wiley & Sons, New York, 2000.
7. Grey, J.E. and Hecht, N.K., A derivation of Kappa guidance, *Naval Surface Warfare Center,* Dahlgren, 1–14, 1989.
8. Kuo, V., Evasive maneuver against a rogue aircraft in air traffic management, *AIAA Guidance, Navigation, and Control Conference*, AAIA 2003-5512, Monterey, CA, 2002.
9. Lee, R., *Optimal Estimation, Identification, and Control*, MIT Press, Cambridge, 1964.
10. Lin, J.M. and Chau, Y.F., Radome slope compensation using multiple-model Kalman filters, *Journal of Guidance, Control and Dynamics*, 18, 637–640, 1994.
11. Nielsen, J.N., *Missile Aerodynamics*, Nielsen Engineering & Research, Inc., Mountain View, CA, 1998.
12. Phillips, G.M., *Interpolation and Approximation by Polynomials*, Springer-Verlag, Heidelberg, 2003.
13. Serakov, D. and Lin, C-F., Three-dimensional mid-course guidance state equations, *Proceedings of American Control Conference*, San Diego, CA, 6, 3738–3742, 1999.
14. Shneydor, N.A., *Missile Guidance and Pursuit*, Horwood Publishing, Chichester, 1998.
15. Spencer, J., *The Ballistic Missile Threat Handbook*, The Heritage Foundation, Washington, DC, 2002.
16. Wan, E. and van der Merwe, R., The unscented Kalman filter. In *Kalman Filtering and Neural Networks*, edited by S. Haykin, Wiley, New York, 2001.
17. Wise, K. and Broy, D., Agile missile dynamics and control, *Journal of Guidance, Control and Dynamics*, 21, 441–449, 1998.
18. Zarchan, P., Tactical and strategic missile guidance*, Progress in Aeronautics and Astronautics*, 124, AIAA, Washington, DC, 1999.
19. Zarchan, P. and Gratt, H., Adaptive radome compensation using dither, *Journal of Guidance, Control and Dynamics*, 22, 51–57, 1999.

9 Integrated Missile Design

9.1 INTRODUCTION

The development of new missile systems starts from the formulation of their operational requirements. An operational requirement presents a document that describes the tactical need for a missile system and the area of its use. The operational requirements are then translated into performance specifications, which are given to contractors. In the case of a missile guidance system, the performance specifications may define the specific type of guidance to be employed. The tactical problem is the basis for the operational requirement and tactical considerations are the overriding considerations in all stages of the design of a missile guidance system.

The first problem faced by the designer of a missile guidance system is that of translating the missile tactical problem into specifications for the guidance system design. After that the mathematical model (i.e., the mathematical expressions that govern its behavior) is developed. The design process usually starts with simplified equations of missile motion, aerodynamic, kinematic, and inertial coupling being ignored. Then cross-coupling between the subsystems is taken into consideration, and the three-dimensional aerodynamic model is needed for the 6-DOF simulation. As an aid to the process of design, simulation of the system accompanies the design process. As the design progresses, complete simulation may give way to partial simulation by substituting some of the completed elements of the system (parts constituting actual "hardware") for the mathematical expressions previously employed. When the guidance system has been developed, the behavior of the equipment is proved by flight tests. Data collected during these tests provide the designer of the guidance system with additional information to conclude whether the design system meets the functional requirements formulated at the beginning of the design process or the system needs some corrections or maybe, in the worst case, it should be redesigned.

In Chapter 4, we presented a block diagram of an interceptor's main subsystems (see Figure 4.1) and described briefly their functions and the subsystems interconnection.

The traditional approach for missile guidance and control systems has been to design these subsystems separately, then to integrate them and after that to verify their performance. If the overall system performance is unsatisfactory, individual subsystems are redesigned to improve the whole system performance.

Integrated design of the flight vehicle systems is an emerging trend within the aerospace industry. Currently, there are major research initiatives within the aerospace industry, the department of defense, and NASA to attempt interdisciplinary optimization of the whole vehicle design, while preserving the innovative freedom of individual subsystem designers. Integrated design of guidance, control, and fuze/warhead systems represents a parallel trend in missile technology. There has been increasing interest in integrated synthesis of missile guidance and control systems in recent literature [3,4,7–11]. Proponents of the integrated approach state that missile performance can be enhanced by using methods exploiting the synergism between guidance and control (autopilot) subsystems. More cautious advocates of integrated missile design believe that because the traditional approach can lead to modifications subsequently made to each subsystem in order to achieve the desired weapon system performance, this approach can result in excessive design iterations and may not always exploit any synergism existing between the missile guidance, autopilot, and fuze/warhead subsystems. That is why methods for achieving tighter integration between the missile guidance, autopilot, and fuze/warhead subsystems have the potential to enhance missile performance and should be developed and tested in practice.

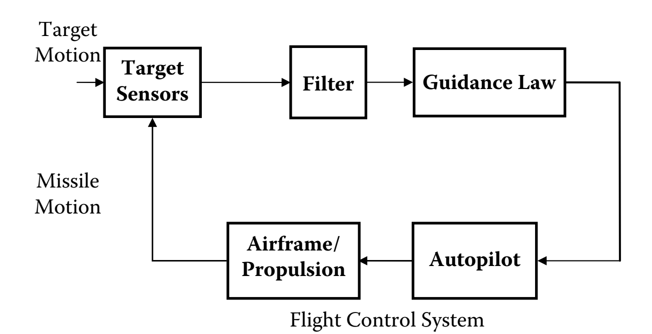


FIGURE 9.1 Traditional missile guidance and control design architecture.

Integrated design of missile guidance and control systems is considered as a first step toward the development of integrated missile design methodologies. As indicated in References [9–11], integrated guidance and control systems are expected to result in significant improvements in missile performance, leading to lower weight and enhanced lethality. Both of these factors will lead to a more effective, lower-cost weapon system.

Figure 9.1 presents a word form of Figure 4.4 and Figure 5.1. We analyzed the models in Figure 4.4 and Figure 5.1 assuming the guidance law is known. In traditional flight control systems, the guidance law uses the relative missile/target states to generate acceleration commands. More precisely, they were examined analytically in the case of the proportional navigation (PN) guidance law. The modifications of the PN law were offered based on the principle of parallel navigation, without any connection with the autopilot design. The guidance law's efficiency was tested for various parameters of airframe, which, as indicated, depend on the altitude of missile motion.

The autopilot design presents one of the most important parts of missile design. The autopilot control system makes the real missile acceleration follow the commanded acceleration created by the guidance law. It receives the guidance commands and issues the relevant aerodynamic (e.g., fin), thrust-vector, or divert control commands necessary to achieve the commanded acceleration. The autopilot tracks the acceleration commands by changing the missile attitude to generate angle of attack and angle of sideslip using fin deflections or moments generated using the reaction jet thrust.

Usually autopilot designers couple three autopilots: a roll autopilot provides roll stabilization while pitch and yaw autopilots provide controlled maneuvers in any desired direction relative to the stabilized position. As mentioned in Chapter 8, to maximize overall missile performance for each phase of flight the appropriate autopilot command structure should be chosen. This may include designing different autopilots for the boost, midcourse, and terminal phases [12].

The problems connected with autopilot design were stimulus for control theory in the 1940s. The development of nonlinear control theory is indebted to nonlinearity of autopilots (e.g., a limited fin angular position).

The autopilot serves as a controller of a nonlinear time-varying plant, the missile airframe. Without any doubt, technical advances in the various interceptor elements (e.g., airframe, actuation, sensor, and propulsion systems) enhance missile performance. However, any advances should be tested for the guidance law implemented in practice. It is natural to believe that the decrease of the autopilot time constant will result in improving missile performance; however, as we showed, for fin-controlled missiles guided by the PN law at high altitudes this can significantly decrease missile performance.

Traditional architecture separates guidance and flight control functions. Guidance laws are developed separately and tested for existing functioning autopilots, and autopilots are designed independently using methods of classic or modern control theory [2,5,6,12,14] and tested for

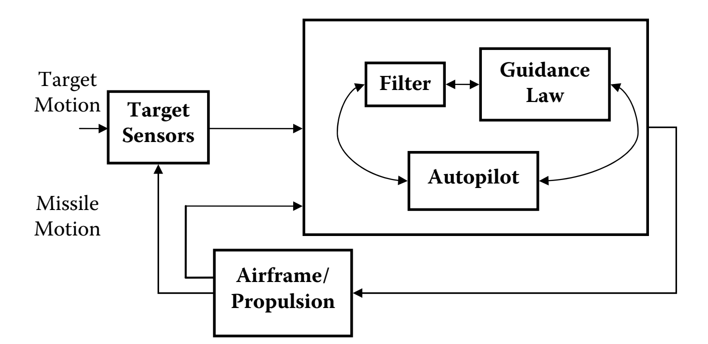


FIGURE 9.2 Integrated missile guidance and control design architecture.

existing functioning guidance laws. The models of the airframe considered in Chapters 1–7 are too simple compared with the detailed model given in Chapter 8, which is used in autopilot design.

Integrated guidance and control laws are supposed to combine guidance and control functions. Integrated missile design operates with a detailed missile model and considers the target states relative to the missile as a part of a generalized model. The guidance and control laws are obtained as a solution to a certain optimal problem, which must guarantee the internal stability of the missile dynamics. The architecture of the integrated guidance and control system is given in Figure 9.2.

Below we describe two basic models of the integrated missile and control system presented in References [9–11]. The integrated guidance-control law for homing missiles is obtained as a solution of finite-interval optimal control problems. The model of Reference [11] includes filter design as part of the integrated design process comprising design of a guidance filter, guidance law, and autopilot. The model of References [9,10] looks “more modest” and operates only with guidance law and fin deflections as control actions. Since the integrated guidance and control laws are linked with optimal problems, the Bellman equations for various performance indices are examined. Special performance indices are considered, which make it possible to simplify the Bellman functional equations and solve the optimal problems dealing with the Lyapunov equations. The integrated laws obtained based on modern control theory procedure are compared with the laws using the classic control theory approach. In contrast to the previous chapters, where the term *missile guidance system* combined the guidance and control units, here we will consider them separately. To emphasize this, we will use the terms *missile guidance* and *control system*.

9.2 INTEGRATED MISSILE GUIDANCE AND CONTROL MODEL

The integrated guidance and control model is usually presented in the form

$$\dot{\boldsymbol{x}}(t) = \boldsymbol{f}(\boldsymbol{x},t) + \boldsymbol{B}(\boldsymbol{x},t)\boldsymbol{u}(t) + \boldsymbol{D}(\boldsymbol{x},t)\boldsymbol{w}(t), \quad \boldsymbol{x}(t_0) = \boldsymbol{x}_0$$

$$\boldsymbol{y}(t) = \boldsymbol{c}(\boldsymbol{x},t) + \boldsymbol{D}_1(\boldsymbol{x},t)\boldsymbol{w}(t) \tag{9.1}$$

where $\boldsymbol{x}(t)$ is the $m \times 1$ state vector; $\boldsymbol{u}(t)$ is the $n \times 1$ control vector; $\boldsymbol{w}(t)$ is the $p \times 1$ vector of disturbances; $\boldsymbol{y}(t)$ is the $l \times 1$ vector of output variables; $\boldsymbol{f}(\boldsymbol{x},t)$, $\boldsymbol{c}(\boldsymbol{x},t)$, $\boldsymbol{B}(\boldsymbol{x},t)$, $\boldsymbol{D}(\boldsymbol{x},t)$, and $\boldsymbol{D}_1(\boldsymbol{x},t)$ are vector functions and matrices of appropriate dimensions.

Since we operate with the nonlinear system, the traditional approach uses the linearization technique and uses the solutions of the linearized problems sequentially. First a set of linearized models for a large number of flight conditions is developed and a control law is designed for each linearized model using an appropriate synthesis technique [5].

An alternative approach to control design is based on the so-called extended linearization concept, which requires a nonlinear system to be factored (when possible) so that it has a "linear-looking" structure, the so-called state-dependent coefficient form [3,4,9–11].

For example, the system

$$\begin{bmatrix} \dot{x}_1 \\ \dot{x}_2 \end{bmatrix} = \begin{bmatrix} x_1^2 - x_1 + x_1 x^2 + u_1 \\ x_1^2 x_2 - x_2 + x_2^2 + u_2 \end{bmatrix}$$

can be parameterized as

$$\begin{bmatrix} \dot{x}_1 \\ \dot{x}_2 \end{bmatrix} = \begin{bmatrix} x_1 - 1 & x_1 x_2 \\ x_1 x_2 & x_2 - 1 \end{bmatrix} \cdot \begin{bmatrix} x_1 \\ x_2 \end{bmatrix} + \begin{bmatrix} u_1 \\ u_2 \end{bmatrix}$$

However, this parameterization is not unique. There exists an infinite number of possible representations in the state-dependent coefficient form and, unfortunately, there is no criterion that would justify our choice as the best.

For the nonlinear system (9.1) the extended linearization representation has the following form

$$\dot{\boldsymbol{x}}(t) = \boldsymbol{A}(\boldsymbol{x},t)\boldsymbol{x}(t) + \boldsymbol{B}(\boldsymbol{x},t)\boldsymbol{u}(t) + \boldsymbol{D}(\boldsymbol{x},t)\boldsymbol{w}(t), \quad \boldsymbol{x}(t_0) = \boldsymbol{x}_0$$

$$\boldsymbol{y}(t) = \boldsymbol{C}(\boldsymbol{x},t)\boldsymbol{x}(t) + \boldsymbol{D}_1(\boldsymbol{x},t)\boldsymbol{w}(t) \tag{9.2}$$

where $\boldsymbol{A}(\boldsymbol{x},t)$ and $\boldsymbol{C}(\boldsymbol{x},t)$ are matrices of appropriate dimensions.

We rewrite the system (8.5), (8.8), and (8.16) assuming missile airframe **x**–**z** axis symmetry and that the mass distribution is such that $I_{yy} = I_{zz}$

$$\begin{aligned}
\dot{v}_x &= r v_y - q v_z + A_x \\
\dot{v}_y &= -r v_x + p v_z + A_y \\
\dot{v}_z &= q v_x - p v_y + A_z \\
I_{xx}\dot{p} &= m_x \\
I_{yy}\dot{q} - (I_{zz} - I_{xx}) r p &= m_y \\
I_{zz}\dot{r} - (I_{xx} - I_{yy}) p q &= m_z
\end{aligned} \tag{9.3}$$

where

$$\begin{bmatrix} A_x \\ A_y \\ A_z \end{bmatrix} = \begin{bmatrix} X + G_x + T_x \\ Y + G_y + T_y \\ Z + G_z + T_z \end{bmatrix} \tag{9.4}$$

v_x, v_y, and v_z are the components of velocity along the **x**, **y**, and **z** axes (see Figure 8.2), respectively; p, q, and r denote the roll, pitch, and yaw rates; A_x, A_y, and A_z are the body axis accelerations; G_x, G_y, and G_z are the gravity components; X, Y, and Z model accelerations produced by the aerodynamic forces; T_x, T_y, and T_z model propulsion system forces; m_x, m_y, and m_z model angular accelerations produced by the aerodynamic moments.

Differentiating the expressions for the angle of attack α_0 and the sideslip angle α_s [see equation (8.13)]

$$\tan\alpha_0 = v_z/v_x,\ \tan\alpha_s = v_y/y_x,$$

i.e.,

$$\dot{\alpha}_0 = \frac{\dot{v}_z v_x - v_z \dot{v}_x}{v_x^2}\cos^2\alpha_0,\ \dot{\alpha}_s = \frac{\dot{v}_y v_x - v_y \dot{v}_x}{v_x^2}\cos^2\alpha_s \tag{9.5}$$

and substituting the components of the derivative of the missile velocity vector V_M from equation (9.3), taking into account

$$V_M^2 = v_x^2 + v_y^2 + v_z^2 = v_x^2 + v_x^2\tan^2\alpha_s + v_x^2\tan^2\alpha_0 = \Lambda v_x^2 \tag{9.6}$$

where

$$\Lambda = 1 + \tan^2\alpha_s + \tan^2\alpha_0 \tag{9.7}$$

expressions (9.5) can be presented in the following form

$$\dot{\alpha}_0 = \frac{A_z\Lambda\cos^2\alpha_0}{V_M} - \frac{A_x\Lambda\cos\alpha_0\sin\alpha_0}{V_M} + q - (p + r\tan\alpha_0)\tan\alpha_s\cos^2\alpha_0 \tag{9.8}$$

$$\dot{\alpha}_s = \frac{A_y\Lambda\cos^2\alpha_s}{V_M} - \frac{A_x\Lambda\cos\alpha_s\sin\alpha_s}{V_M} - r - (p + q\tan\alpha_s)\tan\alpha_0\cos^2\alpha_s \tag{9.9}$$

The last three equations of (9.3) can be solved for $\dot{p}, \dot{q}$, and $\dot{r}$

$$\begin{aligned} \dot{p} &= \frac{m_x}{I_{xx}} \\ \dot{q} &= \frac{m_y}{I_{yy}} + \frac{I_{zz} - I_{xx}}{I_{yy}} rp \\ \dot{r} &= \frac{m_z}{I_{zz}} + \frac{I_{xx} - I_{yy}}{I_{zz}} pq \end{aligned} \tag{9.10}$$

To meet the requirements of the extended linearization representation, the expressions for the aerodynamic forces and moments are presented as [see also equations (8.17)–(8.19)]

$$\begin{bmatrix} X \\ Y \\ Z \\ m_x \\ m_y \\ m_z \end{bmatrix} = V_M^2 \begin{bmatrix} c_{X\alpha 0} & c_{X\alpha s} & c_{X\delta P} & c_{X\delta Y} & c_{X\delta R} \\ c_{Y\alpha 0} & c_{Y\alpha s} & c_{Y\delta P} & c_{Y\delta Y} & c_{Y\delta R} \\ c_{Z\alpha 0} & c_{Z\alpha s} & c_{Z\delta P} & c_{Z\delta Y} & c_{Z\delta R} \\ c_{m_x\alpha 0} & c_{m_x\alpha s} & c_{m_x\delta P} & c_{m_x\delta Y} & c_{m_x\delta R} \\ c_{m_y\alpha 0} & m_{y}\alpha s & c_{m_y\delta P} & c_{m_y\delta Y} & c_{m_y\delta R} \\ c_{m_z\alpha 0} & c_{m_z\alpha s} & c_{m_z\delta P} & c_{m_z\delta Y} & c_{m_z\delta R} \end{bmatrix} \cdot \begin{bmatrix} \alpha_0 \\ \alpha_s \\ \delta_P \\ \delta_Y \\ \delta_R \end{bmatrix} + V_M^2 \begin{bmatrix} c_X^0 \\ c_Y^0 \\ c_Z^0 \\ c_{mx}^0 \\ c_{my}^0 \\ c_{mz}^0 \end{bmatrix} \tag{9.11}$$

that is, the aerodynamic force and moment coefficients c_{kl}^s are described in polynomial form with respect to the angle of attack α_0, the sideslip angle α_s, the pitch fin deflection δP, the yaw fin deflection δY, and the roll fin deflection δR. The possible constant terms in the polynomial representation have the upper index "0." The most significant nonzero term is the drag component c_X^0. For simplicity, here and below we indicate the dependence of the aerodynamic forces and moments on the dynamic pressure only by the factor V_M^2 of equation (8.4); it is assumed that other components of the dynamic pressure, as well as the missile mass m and reference parameters S, l in equations (8.9) and (8.10), are reflected in the coefficients c_{kl}^s.

As an example, assuming $c_{mx}^0 = 0$, the roll rate expression (9.10) is parameterized as

$$\dot{p} = \frac{c_{m_x\alpha 0}\alpha_0 + c_{m_x\alpha s}\alpha_s + c_{m_x\delta P}\delta P + c_{m_x\delta Y}\delta Y + c_{m_x\delta R}\delta R}{I_{xx}} \tag{9.12}$$

The requirement for the missile aerodynamic model to be specified in polynomial form may not be acceptable in situations where the design has to be based on nonsmooth aerodynamic data obtained from wind tunnel tests.

Using the first equation of equation (8.27)

$$\dot{\phi} = p + q \sin\phi \tan\theta + r \cos\varphi \tan\theta \tag{9.13}$$

and comparing the commanded Euler roll angle rate $\dot{\phi}_c$ with $\dot{\phi}$ determined by equation (9.13) the expression for the roll error ε_ϕ can be presented as [11]

$$\dot{\varepsilon}_\phi = -\frac{1}{\tau_\phi}\varepsilon_\phi + \frac{1}{\tau_\phi}(\dot{\phi}_c - p - q \sin\phi \tan\theta - r \cos\varphi \tan\theta) \tag{9.14}$$

where τ_ϕ is an adjustable parameter.

Tail-fin actuators are modeled as having second-order dynamics [11], so that

$$\begin{aligned} \ddot{\delta}_P &= -2\xi_a\omega_a\dot{\delta}_P + \omega_a^2(\delta_1 - \delta_P) \\ \ddot{\delta}_Y &= -2\xi_a\omega_a\dot{\delta}_Y + \omega_a^2(\delta_2 - \delta_Y) \\ \ddot{\delta}_R &= -2\xi_a\omega_a\dot{\delta}_R + \omega_a^2(\delta_3 - \delta_R) \end{aligned} \tag{9.15}$$

where δ_i ($i = 1,2,3$) is the commanded pitch-yaw-roll angular tail-fin position, and ω_a and ξ_a represent the natural frequency and damping ratio of the tail-fin servo-actuator, respectively. The control

vector $\boldsymbol{u}(t) = (\delta_1, \delta_2, \delta_3)$ consists of the three tail-fin angular position commands. This is typical for tail-controlled missiles.

The expression for target–missile relative acceleration in the Earth-fixed inertial frame is similar to equation (1.20)

$$\ddot{r}_x = a_{Tx} - a_{Mx}, \quad \ddot{r}_y = a_{Ty} - a_{My}, \quad \ddot{r}_z = a_{Tz} - a_{Mz} \tag{9.16}$$

where r_x, r_y, and r_z are the components of the range vector.

In Reference [11] the target acceleration model is presented as the first-order lag process

$$\dot{a}_{Tx} = \frac{1}{\tau_T}(-a_{Tx} + w_T), \quad \dot{a}_{Ty} = \frac{1}{\tau_T}(-a_{Ty} + w_T), \quad \dot{a}_{Tz} = \frac{1}{\tau_T}(-a_{Tz} + w_T) \tag{9.17}$$

τ_T represents the target maneuver time constant and $w_T(t)$ is a disturbance input.

The equations considered above can be presented in the form (9.2) with the following state, output, and control vectors

$$\boldsymbol{x}(t) = \begin{bmatrix} r_x(t) \\ \dot{r}_x(t) \\ r_y(t) \\ \dot{r}_y(t) \\ r_z(t) \\ \dot{r}_z(t) \\ \alpha_0(t) \\ \alpha_s(t) \\ p(t) \\ q(t) \\ r(t) \\ \varepsilon_\phi(t) \\ \delta_P(t) \\ \dot{\delta}_P(t) \\ \delta_Y(t) \\ \dot{\delta}_Y(t) \\ \delta_R(t) \\ \dot{\delta}_R(t) \\ a_{Tx}(t) \\ a_{Ty}(t) \\ a_{Tz}(t) \end{bmatrix} \quad \boldsymbol{y}(t) = \begin{bmatrix} r_x(t) \\ r_y(t) \\ r_z(t) \\ a_{Mx}(t) \\ a_{My}(t) \\ a_{Mz}(t) \\ p(t) \\ q(t) \\ r(t) \\ \varepsilon_\phi(t) \\ \delta_P(t) \\ \delta_Y(t) \\ \delta_R(t) \\ a_{Tx}(t) \\ a_{Ty}(t) \\ a_{Tz}(t) \\ A_{x0}(t) \\ g(t) \end{bmatrix} \quad \boldsymbol{u}(t) = \begin{bmatrix} \delta_1(t) \\ \delta_2(t) \\ \delta_3(t) \end{bmatrix}$$

(The components of the output vector $A_{x0}(t)$ and $g(t)$ are defined as pseudomeasurements to account for axial thrust-minus-drag and gravity, respectively.)

In the model considered above the state variables $r_x, \dot{r}_x, r_y, \dot{r}_y, r_z, \dot{r}_z, a_{Tx}, a_{Ty}$, and a_{Tz} do not depend directly upon other state variables, so that system (9.2) consists of two separate subsystems. The dynamic equations were written separately for the guidance and control subsystems as if they are considered independently; however, this is not the case. The components of the missile acceleration in equation (9.16) written in the Earth-fixed inertial frame correspond to the components (9.4) presented in the missile body frame, so that all subsystems of the model are interconnected.

The linkage between the missile-target position coordinates and the state variables of equation (9.3) is more evident in the model considered in [9]

$$\begin{aligned} \dot{x}_b &= v_x + y_b r - z_b q \\ \dot{y}_b &= v_y - x_b r + z_b p \\ \dot{z}_b &= v_z + x_b q - y_b p \end{aligned} \tag{9.18}$$

where the missile-target position coordinates x_b, y_b, and z_b are presented in the missile body coordinate system.

However, equation (9.18) is valid under the assumption that the target velocity vector is negligible compared with the missile velocity vector. In the general case, the missile-target position coordinates r_x, r_y, and r_z in the Earth-fixed inertial frame should be transformed to the missile body frame [see equation (8.26)] and the relationship (8.27) between the Euler angles and the body rotational rates p, q, and r should be used. Of course, such a model will be more complicated.

To increase the accuracy of the aerodynamic model the aerodynamic forces and moments in equation (9.3) can be approximated by higher-order polynomials. Then instead of equation (9.11) we have

$$V_M^{-2}\begin{bmatrix} X \\ Y \\ Z \\ m_x \\ m_y \\ m_z \end{bmatrix} = \begin{bmatrix} c_{X\alpha 0} & c^1_{X\alpha 0} & c_{X\alpha s} & c^1_{X\alpha s} & c_{X\delta P} & c_{X\delta Y} & c_{X\delta R} \\ c_{Y\alpha 0} & c^1_{Y\alpha 0} & c_{Y\alpha s} & c^1_{Y\alpha s} & c_{Y\delta P} & c_{Y\delta Y} & c_{Y\delta R} \\ c_{Z\alpha 0} & c^1_{z\alpha 0} & c_{Z\alpha s} & c^1_{Z\alpha s} & c_{Z\delta P} & c_{Z\delta Y} & c_{Z\delta R} \\ c_{m_x\alpha 0} & c^1_{m_x\alpha 0} & c_{m_x\alpha s} & c^1_{m_x\alpha s} & c_{m_x\delta P} & c_{m_x\delta Y} & c_{m_x\delta R} \\ c_{m_y\alpha 0} & c^1_{m_y\alpha 0} & c_{m_y\alpha s} & c^1_{m_y\alpha s} & c_{m_y\delta P} & c_{m_y\delta Y} & c_{m_y\delta R} \\ c_{m_z\alpha 0} & c^1_{m_z\alpha 0} & c_{m_z\alpha s} & c^1_{m_z\alpha s} & c_{m_z\delta P} & c_{m_z\delta Y} & c_{m_z\delta R} \end{bmatrix} \cdot \begin{bmatrix} \alpha_0 \\ \alpha_0^3 \\ \alpha_s \\ \alpha_s^3 \\ \delta_P \\ \delta_Y \\ \delta_R \end{bmatrix} + \begin{bmatrix} c_X^0 \\ c_Y^0 \\ c_Z^0 \\ c_{mx}^0 \\ c_{my}^0 \\ c_{mz}^0 \end{bmatrix} \tag{9.19}$$

(Notation of additional coefficients is obvious.)

Substituting the aerodynamic forces and moments from equation (9.19) into equation (9.3) and considering the state vector $\boldsymbol{x}(t) = (p\ q\ r\ v_x\ v_y\ v_z\ x_b\ y_b\ z_b)^T$, we obtain the following components of the matrix $\boldsymbol{A}(\boldsymbol{x},t) = \left[A_{ij}\right]$ in equation (9.2)

$$A_{11} = A_{12} = A_{13} = A_{17} = A_{18} = A_{19} = 0$$

$$A_{14} = \frac{1}{I_{xx}}(c^0_{mx} + c_{m_x\alpha 0}\alpha_0 + c^1_{m_x\alpha 0}\alpha_0^3 + c_{m_x\alpha s}\alpha_s + c^1_{m_x\alpha s}\alpha_s^3)v_x$$

$$A_{15} = \frac{1}{I_{xx}}(c^0_{mx} + c_{m_x\alpha 0}\alpha_0 + c^1_{m_x\alpha 0}\alpha^3_0 + c_{m_x\alpha s}\alpha_s + c^1_{m_x\alpha s}\alpha^3_s)v_y$$

$$A_{16} = \frac{1}{I_{xx}}(c^0_{mx} + c_{m_x\alpha 0}\alpha_0 + c^1_{m_x\alpha 0}\alpha^3_0 + c_{m_x\alpha s}\alpha_s + c^1_{m_x\alpha s}\alpha^3_s)v_z$$

$$A_{21} = \frac{I_{zz} - I_{xx}}{I_{yy}}r, \quad A_{22} = A_{23} = A_{27} = A_{28} = A_{29} = 0$$

$$A_{24} = \frac{1}{I_{yy}}(c^0_{my} + c_{m_y\alpha 0}\alpha_0 + c^1_{m_y\alpha 0}\alpha^3_0 + c_{m_y\alpha s}\alpha_s + c^1_{m_y\alpha s}\alpha^3_s)v_x$$

$$A_{25} = \frac{1}{I_{yy}}(c^0_{my} + c_{m_y\alpha 0}\alpha_0 + c^1_{m_y\alpha 0}\alpha^3_0 + c_{m_y\alpha s}\alpha_s + c^1_{m_y\alpha s}\alpha^3_s)v_y$$

$$A_{26} = \frac{1}{I_{yy}}(c^0_{my} + c_{m_y\alpha 0}\alpha_0 + c^1_{m_y\alpha 0}\alpha^3_0 + c_{m_y\alpha s}\alpha_s + c^1_{m_y\alpha s}\alpha^3_s)v_z$$

$$A_{31} = \frac{I_{xx} - I_{yy}}{I_{zz}}q, \quad A_{32} = A_{33} = A_{37} = A_{38} = A_{39} = 0$$

$$A_{34} = \frac{1}{I_{zz}}(c^0_{mz} + c_{m_z\alpha 0}\alpha_0 + c^1_{m_z\alpha 0}\alpha^3_0 + c_{m_z\alpha s}\alpha_s + c^1_{m_z\alpha s}\alpha^3_s)v_x$$

$$A_{35} = \frac{1}{I_{zz}}(c^0_{mz} + c_{m_z\alpha 0}\alpha_0 + c^1_{m_z\alpha 0}\alpha^3_0 + c_{m_z\alpha s}\alpha_s + c^1_{m_z\alpha s}\alpha^3_s)v_y$$

$$A_{36} = \frac{1}{I_{zz}}(c^0_{mz} + c_{m_z\alpha 0}\alpha_0 + c^1_{m_z\alpha 0}\alpha^3_0 + c_{m_z\alpha s}\alpha_s + c^1_{m_z\alpha s}\alpha^3_s)v_z$$

$$A_{41} = A_{47} = A_{48} = A_{49} = 0, \; A_{42} = -v_z, \; A_{43} = v_y$$

$$A_{44} = -(c^0_X + c_{X\alpha 0}\alpha_0 + c^1_{X\alpha 0}\alpha^3_0 + c_{X\alpha s}\alpha_s + c^1_{X\alpha s}\alpha^3_s)v_x$$

$$A_{45} = -(c^0_X + c_{X\alpha 0}\alpha_0 + c^1_{X\alpha 0}\alpha^3_0 + c_{X\alpha s}\alpha_s + c^1_{X\alpha s}\alpha^3_s)v_y$$

$$A_{46} = -(c^0_X + c_{X\alpha 0}\alpha_0 + c^1_{X\alpha 0}\alpha^3_0 + c_{X\alpha s}\alpha_s + c^1_{X\alpha s}\alpha^3_s)v_z$$

$$A_{51} = v_z, \; A_{53} = -v_x, \; A_{52} = A_{57} = A_{58} = A_{59} = 0$$

$$A_{54} = (c_Y^0 + c_{Y\alpha 0}\alpha_0 + c_{Y\alpha 0}^1\alpha_0^3 + c_{Y\alpha s}\alpha_s + c_{Y\alpha s}^1\alpha_s^3)v_x$$

$$A_{55} = (c_Y^0 + c_{Y\alpha 0}\alpha_0 + c_{Y\alpha 0}^1\alpha_0^3 + c_{Y\alpha s}\alpha_s + c_{Y\alpha s}^1\alpha_s^3)v_y$$

$$A_{56} = (c_Y^0 + c_{Y\alpha 0}\alpha_0 + c_{Y\alpha 0}^1\alpha_0^3 + c_{Y\alpha s}\alpha_s + c_{Y\alpha s}^1\alpha_s^3)v_z$$

$$A_{61} = -v_y,\ A_{62} = v_x,\ A_{63} = A_{67} = A_{68} = A_{69} = 0$$

$$A_{64} = -(c_Z^0 + c_{Z\alpha 0}\alpha_0 + c_{Z\alpha 0}^1\alpha_0^3 + c_{Z\alpha s}\alpha_s + c_{Z\alpha s}^1\alpha_s^3)v_x$$

$$A_{65} = -(c_Z^0 + c_{Z\alpha 0}\alpha_0 + c_{Z\alpha 0}^1\alpha_0^3 + c_{Z\alpha s}\alpha_s + c_{Z\alpha s}^1\alpha_s^3)v_y$$

$$A_{66} = -(c_Z^0 + c_{Z\alpha 0}\alpha_0 + c_{Z\alpha 0}^1\alpha_0^3 + c_{Z\alpha s}\alpha_s + c_{Z\alpha s}^1\alpha_s^3)v_z$$

$$A_{72} = -z_b,\ A_{73} = y_b,\ A_{74} = 1,\ A_{71} = A_{75} = A_{76} = A_{77} = A_{78} = A_{79} = 0$$

$$A_{81} = z_b,\ A_{83} = -x_b,\ A_{85} = 1,\ A_{82} = A_{84} = A_{86} = A_{87} = A_{88} = A_{89} = 0$$

$$A_{91} = -y_b,\ A_{92} = x_b,\ A_{96} = 1,\ A_{93} = A_{94} = A_{95} = A_{97} = A_{98} = A_{99} = 0$$

(signs in A_{ij}, i = 4–6, j = 4–6, correspond to the direction of axial and normal forces).

For the control vector $\boldsymbol{u}(t) = (\delta_P, \delta_Y, \delta_R)^T$ the matrix $\boldsymbol{B}(\boldsymbol{x},t) = \left[B_{ij}\right] = V_M^2\left[B_{ij}^0\right]$ in equation (9.2) has the following form [the model can easily be enhanced by including tail-fin actuator dynamics similar to equation (9.15)]

$$B_{11}^0 = \frac{1}{I_{xx}}c_{m_x\delta P},\ B_{12}^0 = \frac{1}{I_{xx}}c_{m_x\delta Y},\ B_{13}^0 = \frac{1}{I_{xx}}c_{m_x\delta R}$$

$$B_{21}^0 = \frac{1}{I_{yy}}c_{m_y\delta P},\ B_{22}^0 = \frac{1}{I_{yy}}c_{m_y\delta Y},\ B_{23}^0 = \frac{1}{I_{yy}}c_{m_y\delta R}$$

$$B_{31}^0 = \frac{1}{I_{zz}}c_{m_z\delta P},\ B_{32}^0 = \frac{1}{I_{zz}}c_{m_z\delta Y},\ B_{33}^0 = \frac{1}{I_{zz}}c_{m_z\delta R}$$

$$B_{41}^0 = c_{X\delta P},\ B_{42}^0 = c_{X\delta Y},\ B_{43}^0 = c_{X\delta R}$$

$$B_{51}^0 = c_{Y\delta P},\ B_{52}^0 = c_{Y\delta Y},\ B_{53}^0 = c_{Y\delta R}$$

$$B_{61}^0 = -c_{Z\delta P},\ B_{62}^0 = -c_{Z\delta Y},\ B_{63}^0 = -c_{Z\delta R}$$

$$B_{71}^0 = B_{72}^0 = B_{73}^0 = B_{81}^0 = B_{82}^0 = B_{83}^0 = B_{91}^0 = B_{92}^0 = B_{93}^0 = 0.$$

The difference between the two models described above and offered for use in the integrated guidance and control system design is in choosing the state variables of the models. The state variables in Reference [11] combine the state variables of two separate designs, the guidance law and autopilot. The choice of the angle of attack and the sideslip angle as the state and output variables is physically justifiable and used in the current practice of autopilot design. However, the matrix $\boldsymbol{A}(\boldsymbol{x},t)$ of the extended linearization representation (9.2) is too complicated. It depends upon the Euler angles and the components of the missile velocity vector, that is, the first three equations of (9.3) are indirectly present in the model. The model of Reference [9] has a certain advantage over the model of Reference [11]. As an integrated model, it looks more logical than the model in Reference [11] because the coupling of guidance and control is more noticeable. However, as mentioned, it is obtained under the assumption that the target velocity vector is negligible compared with the missile velocity vector. Although the nonlinear models are considered, limits on missile acceleration and some other important parameters are not included in the models.

The models presented above in the state-space form required by modern control theory are used to formulate the integrated guidance and control problem as an optimal control problem. The authors of References [9–11] offer the solution of the integrated design problem using the existing solutions of linear optimal problems. Assuming first $\boldsymbol{w}(t) = 0$ and considering the linearized model (9.2) and the performance index [see (A7)–(A17)]

$$I = \frac{1}{2}(\boldsymbol{x}^T(t_F)\boldsymbol{C}_0\boldsymbol{x}(t_F) + \int_{t_0}^{t_F}(\boldsymbol{x}^T(t)\boldsymbol{R}\boldsymbol{x}(t) + \|\boldsymbol{u}(t)\|^2)dt) \tag{9.20}$$

we obtain the optimal solution in the form

$$u(t) = -\boldsymbol{B}^T W(t)x(t) \tag{9.21}$$

$$\dot{W} + \boldsymbol{A}^T W + W\boldsymbol{A} - W\boldsymbol{B}\boldsymbol{B}^T W + \boldsymbol{R} = 0,\ W(t_F)=\boldsymbol{C}_0 \tag{9.22}$$

Instead of the Riccati equation (9.22), the so-called state-dependent Riccati equation was considered in References [3,4,9–11]. The state-dependent Riccati equation technique is applied for the equations of motion in the extended linearized form (9.2) together with a state-dependent quadratic performance index. A state-dependent algebraic Riccati equation is formulated using the model (9.2) ignoring disturbances and assuming $\boldsymbol{A}(\boldsymbol{x},t) = \boldsymbol{A}(\boldsymbol{x})$ and $\boldsymbol{B}(\boldsymbol{x},t) = \boldsymbol{B}(\boldsymbol{x})$ and introducing the state-dependent weight matrix $\boldsymbol{R}(\boldsymbol{x})$ in the performance index. As shown in References [3,4] for the performance index

$$I = \int_{t_0}^{\infty}(\boldsymbol{x}^T(t)\boldsymbol{R}(x)\boldsymbol{x}(t) + \|\boldsymbol{u}(t)\|^2)dt \tag{9.23}$$

the state-dependent algebraic Riccati equation can be written as

$$\boldsymbol{A}^T(\boldsymbol{x})W(\boldsymbol{x}) + W(\boldsymbol{x})\boldsymbol{A}(x) - W(\boldsymbol{x})\boldsymbol{B}(\boldsymbol{x})\boldsymbol{B}^T(\boldsymbol{x})W(\boldsymbol{x}) + \boldsymbol{R}(\boldsymbol{x}) = 0 \tag{9.24}$$

For the performance index

$$I = \frac{1}{2}(\boldsymbol{x}^T(t_F)\boldsymbol{C}_0(\boldsymbol{x})\boldsymbol{x}(t_F) + \int_{t_0}^{t_F}(\boldsymbol{x}^T(t)\boldsymbol{R}(\boldsymbol{x})\boldsymbol{x}(t) + \|\boldsymbol{u}(t)\|^2)dt) \tag{9.25}$$

the modification of equation (9.24), similar to equation (9.22), can be obtained.

The linear quadratic dynamic games approach to model (9.2) allows us to find the control $\boldsymbol{u}(t)$ counteracting the disturbances $\boldsymbol{w}(t)$, i.e., the optimal solution for the functional

$$\min_{u(t)}\max_{w(t)} I = \frac{1}{2}(\boldsymbol{x}^T(t_F)\mathbf{C}_0(x)\boldsymbol{x}(t_F) + \int_{t_0}^{t_F}(\boldsymbol{x}^T(t)\boldsymbol{R}(x)\boldsymbol{x}(t) + \|\boldsymbol{u}(t)\|^2 + \gamma\|\boldsymbol{w}(t)\|^2)dt)$$

similar to equation (9.25), where γ is a constant coefficient, which is also obtained from the Riccati equation [11]. In all the above cases the control structure is the same

$$\boldsymbol{u}(t) = -\boldsymbol{B}^T(\boldsymbol{x})W(\boldsymbol{x})\boldsymbol{x}(t) \tag{9.26}$$

i.e., at each moment fin deflections depend on the current values of the state vector of the model chosen in the design process. If not all the system states are available from measurements, the procedure can be modified to synthesize state-dependent estimators.

The described method of the integrated guidance and control system design based on the modification of the optimal solution for linear optimal problems by using the nonlinear equations in the extended linearized form needs more rigorous mathematical justification. It looks too complicated to be used in practice despite the experimental results published in [9–11] supporting its efficiency.

Since the control laws used in [9–11] are obtained based on the procedure of dynamic programming, below we describe more general optimal control laws that do not require the extended linearized representation of guidance-control models.

9.3 SYNTHESIS OF CONTROL LAWS

9.3.1 MINIMIZATION OF STANDARD FUNCTIONALS

First we consider the optimal problem for the system presented in more general form than equation (9.1)

$$\dot{\boldsymbol{x}}(t) = \boldsymbol{f}(\boldsymbol{x},\boldsymbol{u},t), \quad \boldsymbol{x}(t_0) = \boldsymbol{x}_0 \tag{9.27}$$

and the generalized performance index

$$I = V_0(\boldsymbol{x}(t_F)) + \int_0^{t_F} L(\boldsymbol{x}(t),\boldsymbol{u}(t),t)dt \tag{9.28}$$

where the function $L(\boldsymbol{x}(t), \boldsymbol{u}(t), t)$ depends simultaneously on two variables, the state vector $\boldsymbol{x}(t)$ and the control vector $\boldsymbol{u}(t)$; $V_0(\boldsymbol{x}(t_F))$ is the function of the terminal state $\boldsymbol{x}(t_F)$.

The synthesis problem of a closed-loop optimal control system consists of finding the controller equations $\boldsymbol{u}(t) = \Gamma[\boldsymbol{x}(t),t]$ which, together with equation (9.27), form the stable system and minimize the functional (9.28). The procedure of obtaining the Bellman functional equation is described in Appendix A. For the performance index (9.28) and the system (9.27) it can be presented as

$$\frac{\partial V}{\partial t} + \min_{u(t)}\{L(\boldsymbol{x},\boldsymbol{u},t) + \frac{\partial V^T}{\partial x} f(\boldsymbol{x},\boldsymbol{u},t)\} = 0 \tag{9.29}$$

where the function $V(\boldsymbol{x}(t))$ should satisfy the condition $V(t_F) = V_0(\boldsymbol{x}(t_F))$ and

$$\frac{\partial V^T}{\partial x} = (\frac{\partial V}{\partial x_1},...,\frac{\partial V}{\partial x_m}).$$

Although equation (9.29) is presented in a compact form, in many practical cases it is difficult to find its solution. Assuming that $\boldsymbol{u}_0(t)$ minimizes the expression in braces of equation (9.29) and substituting $\boldsymbol{u}_0(t)$ in equation (9.29) we have

$$\frac{\partial V}{\partial t} + \frac{\partial V^T}{\partial x} f(\boldsymbol{x}, \boldsymbol{u}_0, t) = -L(\boldsymbol{x}, \boldsymbol{u}_0, t) \tag{9.30}$$

or

$$\frac{\partial}{\partial u_0} L(\boldsymbol{x}, \boldsymbol{u}_0, t) + \frac{\partial}{\partial u_0}\{\frac{\partial V^T}{\partial x} \boldsymbol{f}(\boldsymbol{x}, \boldsymbol{u}_0, t)\} = 0 \tag{9.31}$$

where the partial derivative is written with respect to the components of $\boldsymbol{u}_0 = (u_{01},\ldots,u_{0n})^T$.

The optimal synthesis problem can be solved only if we can obtain the solution of the system of nonlinear partial differential equations (9.31) and then present $\boldsymbol{u}_0$ as a function of $\boldsymbol{x}$ and t. Difficulties in solving this problem are demonstrated below.

Let us consider the model similar to equation (9.1)

$$\dot{\boldsymbol{x}}(t) = \boldsymbol{f}(\boldsymbol{x},t) + \boldsymbol{B}(\boldsymbol{x},t)\boldsymbol{u}(t), \quad \boldsymbol{x}(t_0) = \boldsymbol{x}_0 \tag{9.32}$$

For this model and the additive functional

$$I = V(\boldsymbol{x}(t_F)) + \int_{t_0}^{t_F} (R(\boldsymbol{x}(t),t) + Q(\boldsymbol{u}(t),t))dt \tag{9.33}$$

equations (9.30) and (9.31) have the form

$$\frac{\partial V}{\partial t} + \frac{\partial V^T}{\partial x}(\boldsymbol{f}(\boldsymbol{x},t) + \boldsymbol{B}(\boldsymbol{x},t)\boldsymbol{u}_0) + Q(\boldsymbol{u}_0,t) = -R(\boldsymbol{x},t) \tag{9.34}$$

$$\frac{\partial Q^T(\boldsymbol{u}_0,t)}{\partial u_0} + \frac{\partial V^T}{\partial x}\boldsymbol{B}(\boldsymbol{x},t) = 0 \tag{9.35}$$

Assuming that equation (9.35) can be resolved with respect to $\boldsymbol{u}_0 = (u_{01},\ldots,u_{0n})^T$, that is,

$$\boldsymbol{u}_0 = \Gamma[\boldsymbol{B}^T(\boldsymbol{x},t)\frac{\partial V}{\partial x},t] \tag{9.36}$$

and substituting equation (9.36) in equation (9.34) we obtain

$$\frac{\partial V}{\partial t}+\frac{\partial V^T}{\partial x}\boldsymbol{f}(\boldsymbol{x},t)+\frac{\partial V^T}{\partial x}\boldsymbol{B}(\boldsymbol{x},t)\Gamma[\boldsymbol{B}^T(\boldsymbol{x},t)\frac{\partial V}{\partial x},t]+Q(\Gamma[\boldsymbol{B}^T(\boldsymbol{x},t)\frac{\partial V}{\partial x},t],t)=-R(\boldsymbol{x},t) \tag{9.37}$$

The solution to this equation satisfying the boundary condition $V(t_F) = V_0(\boldsymbol{x}(t_F))$ should determine the optimal control based on equation (9.35). It is possible to prove that if

$$Q(\boldsymbol{u},t)-Q(\boldsymbol{u}_0,t)-\frac{\partial Q^T(\boldsymbol{u}_0,t)}{\partial u_0}(\boldsymbol{u}-\boldsymbol{u}_0)$$

is a positive definite function of $\boldsymbol{u}$ that equals zero only when $\boldsymbol{u} = \boldsymbol{u}_0$, then equation (9.36) is the optimal control [6,13].

Let the functional (9.33) have the form

$$I=V_0(\boldsymbol{x}(t_F))+\int_{t_0}^{t_F}(R(\boldsymbol{x}(t),t)+\frac{1}{2}\boldsymbol{u}^T(t)K^{-1}\boldsymbol{u}(t))dt \tag{9.38}$$

where $K = [k_{ii}]$ is a diagonal matrix with $k_{ii} > 0$.

In this case the function

$$Q(\boldsymbol{u},t)-Q(\boldsymbol{u}_0,t)-\frac{\partial Q^T(\boldsymbol{u}_0,t)}{\partial u_0}(\boldsymbol{u}-\boldsymbol{u}_0)$$

satisfies the above conditions of the existence of a unique optimal solution (9.36). The Bellman functional equation and the expression for the optimal control can be written as [see equations (9.30) and (9.31)]

$$\boldsymbol{u}=\boldsymbol{u}_0=-K\boldsymbol{B}^T(\boldsymbol{x},t)\frac{\partial V}{\partial x} \tag{9.39}$$

$$\frac{\partial V}{\partial t}+\frac{\partial V^T}{\partial x}\boldsymbol{f}(\boldsymbol{x},t)-\frac{1}{2}\frac{\partial V^T}{\partial x}\boldsymbol{B}(\boldsymbol{x},t)K\boldsymbol{B}^T(\boldsymbol{x},t)\frac{\partial V}{\partial x}=-R(\boldsymbol{x},t),\quad V(t_F)=V_0(\boldsymbol{x}(t_F)) \tag{9.40}$$

The solution of the functional Bellman equation even in the form of equation (9.40) is a matter of insurmountable difficulty even when we seek an approximate solution of Bellman functional equations. The analytical solution exists only for the linear-quadratic problems. The method of power series to solve equation (9.40) was offered in Reference [1]. The solution is sought as

$$V=\frac{1}{2}\sum_{i=1}^{m}\sum_{j=1}^{m}\gamma_{ij}x_ix_j+\frac{1}{3}\sum_{i=1}^{m}\sum_{j=1}^{m}\sum_{r=1}^{m}\gamma_{ijr}x_ix_jx_r+\ldots \tag{9.41}$$

where the unknown coefficients should be determined from the system of the ordinary differential equations. This approach can be useful for models similar to equation (9.2).

9.3.2 Minimization of Special Functionals

For the model described by equation (9.32) we consider the functional

$$I = V_0(\boldsymbol{x}(t_F)) + \int_{t_0}^{t_F} (R(\boldsymbol{x}(t),t) + Q(\boldsymbol{u}(t),t) + Q_0(\boldsymbol{u}_0(t),t))dt \tag{9.42}$$

where $Q(\boldsymbol{u}(t),t)$ and $Q_0(\boldsymbol{u}_0(t),t)$ are such functions that

$$Q(\boldsymbol{u},t) + Q_0(\boldsymbol{u}_0,t) - \frac{\partial Q^T(\boldsymbol{u}_0,t)}{\partial u_0}\boldsymbol{u}$$

is the positive definite, with respect to $\boldsymbol{u}$, function, which equals zero at $\boldsymbol{u} = \boldsymbol{u}_0$. The function $\boldsymbol{u}_0$ is an unknown optimal control. The functionals including unknown optimal controls were introduced and used for synthesis of control systems in Reference [6].

Following Reference [6] we will show that the optimal control for the functional (9.42) is determined from the expression

$$\frac{\partial Q^T(\boldsymbol{u}_0,t)}{\partial u_0} = -\frac{\partial V^T}{\partial x}\boldsymbol{B}(\boldsymbol{x},t) \tag{9.43}$$

where $V(\boldsymbol{x},t)$ is the solution of the Lyapunov equation for equation (9.32) when $\boldsymbol{u} \equiv 0$

$$\frac{\partial V}{\partial t} + \frac{\partial V^T}{\partial x}\boldsymbol{f}(\boldsymbol{x},t) = -R(\boldsymbol{x},t), \quad V(t_F) = V_0(\boldsymbol{x}(t_F)) \tag{9.44}$$

The Bellman equation for the optimal problem (9.42) and (9.32) has the form

$$\frac{\partial V}{\partial t} + \min_{u(t)}\{R(\boldsymbol{x}(t),t) + Q(\boldsymbol{u}(t),t) + Q_0(\boldsymbol{u}_0(t),t) + \frac{\partial V^T}{\partial x}(\boldsymbol{f}(\boldsymbol{x},t) + \boldsymbol{B}(\boldsymbol{x},t)\boldsymbol{u})\} = 0 \tag{9.45}$$

Minimization of the expression in braces immediately gives equation (9.43). Substituting equation (9.43) in the modified equation (9.45)

$$\frac{\partial V}{\partial t} + R(\boldsymbol{x}(t),t) + Q(\boldsymbol{u}_0(t),t) + Q_0(\boldsymbol{u}_0(t),t) + \frac{\partial V^T}{\partial x}(\boldsymbol{f}(\boldsymbol{x},t) + \boldsymbol{B}(\boldsymbol{x},t)\boldsymbol{u}_0) = 0 \tag{9.46}$$

and taking into account that

$$Q(\boldsymbol{u}_0,t) + Q_0(\boldsymbol{u}_0,t) - \frac{\partial Q^T(\boldsymbol{u}_0,t)}{\partial u_0}\boldsymbol{u}_0$$

equals zero, we obtain equation (9.44).

For the "modernized" functional (9.38)

$$I = V_0(\boldsymbol{x}(t_F)) + \int_{t_0}^{t_F} (R(\boldsymbol{x}(t),t) + \frac{1}{2}[\boldsymbol{u}^T(t)K^{-1}\boldsymbol{u}(t) + \boldsymbol{u}_0^T(t)K^{-1}\boldsymbol{u}_0(t)])dt \tag{9.47}$$

the optimal solution is

$$\boldsymbol{u} = \boldsymbol{u}_0 = -K\boldsymbol{B}^T(\boldsymbol{x},t)\frac{\partial V}{\partial x} \tag{9.48}$$

that is, it looks identical to equation (9.39).

However, if here $V = V(\boldsymbol{x},t)$ is the solution of the Lyapunov equation (9.44), for the performance index (9.38) and control law (9.39), $V(\boldsymbol{x},t)$ is the solution of more complicated nonlinear partial differential equation (9.40), that is, instead of the Bellman equation we operate with the Lyapunov equation (9.44) and the Lyapunov function $V(\boldsymbol{x},t)$. The existence of the Lyapunov function satisfying (9.44) assumes the uncontrolled ($\boldsymbol{u} \equiv 0$) process described by equation (9.32) to be stable. In the case of instability, it should be initially stabilized. Later the stabilization feedback should be included in the controller structure obtained by the above-considered method.

Similarly to equation (9.41) the method of power series can be used to solve the Lyapunov equation (9.44). Assuming that the components of $\boldsymbol{f}(\boldsymbol{x}(k)) = [f_i]$ in equation (9.32) can be presented by convergent power series in a certain domain χ, that is,

$$f_i = \sum_{j=1}^{m} a_{ij}x_j + \sum_{j=1}^{m}\sum_{k=1}^{m} a_{ijk}x_jx_k + \sum_{j=1}^{m}\sum_{k=1}^{m}\sum_{r=1}^{m} a_{ijkr}x_jx_kx_r + \ldots \tag{9.49}$$

and presenting the positive definite functions V_0 and R of the functional (9.47) as

$$V_0 = \frac{1}{2}\sum_{i=1}^{m}\sum_{j=1}^{m} \rho_{ij}x_ix_j + \frac{1}{3}\sum_{i=1}^{m}\sum_{j=1}^{m}\sum_{r=1}^{m} \rho_{ijr}x_ix_jx_r + \ldots \tag{9.50}$$

$$R = \frac{1}{2}\sum_{i=1}^{m}\sum_{j=1}^{m} \mu_{ij}x_ix_j + \frac{1}{3}\sum_{i=1}^{m}\sum_{j=1}^{m}\sum_{r=1}^{m} \mu_{ijr}x_ix_jx_r + \ldots \tag{9.51}$$

where a_* and μ_* are constant or time-dependent coefficients and ρ_* is a constant coefficient, we seek the solution of the Lyapunov equation in the form (9.41). It is supposed that the power series

$$\frac{\partial V}{\partial x_i} = \sum_{j=1}^{m} \gamma_{ij}x_j + \sum_{j=1}^{m}\sum_{k=1}^{m} \gamma_{ij}x_jx_k + \sum_{j=1}^{m}\sum_{k=1}^{m}\sum_{r=1}^{m} \gamma_{ijkr}x_jx_kx_r + \ldots \tag{9.52}$$

converges in χ.

For the functional (9.47) and the diagonal matrix $K(t) = [k_i(t)]$ the optimal control law (9.48) can be written as

$$u_i = -k_i(t)\sum_{j=1}^{m} B_{ij}\frac{\partial V}{\partial x_j} \tag{9.53}$$

where the coefficients of equation (9.52) satisfy the system of differential equations [6]

$$\dot{\gamma}_{\underbrace{i\ldots q}_{S}} - \sum_{S_1=1}^{S-1}\frac{S_1!(S-S_1)!}{(S-1)!}\sum_{s=1}^{m}\{\gamma_{\underbrace{si\ldots h}_{S_1}}a_{\underbrace{kj\ldots q}_{S-S_1}}\} = -\mu_{\underbrace{i\ldots q}_{S}} \tag{9.54}$$

with the boundary conditions

$$\gamma_{i,\ldots,q}(t_F) = \rho_{i,\ldots,q}, \quad i,\ldots,q = 1, 2,\ldots,m \tag{9.55}$$

(Here the symbol {*} denotes summation of the product in braces for each possible change of indices in γ and a.)

There exists one more very effective approach to solve the problem (9.47) of minimization of the performance index (9.47) subject to equation (9.32). Taking into account that the expression (9.48) corresponds to the derivative of V along any trajectory of the uncontrolled ($\boldsymbol{u} \equiv 0$) system (9.32), i.e.,

$$\dot{\boldsymbol{x}}_u(t) = \boldsymbol{f}(\boldsymbol{x}_u, t) \tag{9.56}$$

we can rewrite equation (9.44) as

$$\frac{dV}{dt} = -R(\boldsymbol{x}_u, t) \tag{9.57}$$

From this equation we have

$$V(\boldsymbol{x}_u(t_F), t_F) - V(\boldsymbol{x}_u(t), t) = -\int_t^{t_F} R(\boldsymbol{x}_u(t), t)dt \tag{9.58}$$

or, taking into consideration the terminal condition $V(t_F) = V_0(\boldsymbol{x}(t_F))$,

$$V(\boldsymbol{x}_u(t), t) = V_0(\boldsymbol{x}_u(t_F)) + \int_t^{t_F} R(\boldsymbol{x}_u(t), t)dt \tag{9.59}$$

Let $X(\boldsymbol{x},t,\sigma)$ be the solution of equation (9.56) for the initial condition $\boldsymbol{x}_t = \boldsymbol{x}(t)$, where $\boldsymbol{x}(t)$ is the current state of system (9.32). Then instead of equation (9.43) we can present the analytical expression of the optimal control in the form

$$\frac{\partial Q^T(\boldsymbol{u}_0, t)}{\partial u_0} = -\frac{\partial}{\partial x}\left[V_0(X(\boldsymbol{x}, t, t_F)) + \int_t^{t_F} R(X(x, t, \sigma))d\sigma\right]^T \boldsymbol{B}(\boldsymbol{x}, t) \tag{9.60}$$

For functional (9.47) we have

$$\boldsymbol{u} = \boldsymbol{u}_0 = -K\boldsymbol{B}^T(\boldsymbol{x}, t)\frac{\partial}{\partial x}\left[V_0(X(\boldsymbol{x}, t, t_F)) + \int_t^{t_F} R(X(\boldsymbol{x}, t, \sigma))d\sigma\right] \tag{9.61}$$

The performance indices considered in this section enable us to obtain the optimal control algorithms that require significantly fewer computational operations than the performance indices examined in the previous section. In turn, the control law (9.61) has a certain advantage over others considered in this section. The computational algorithm based on equation (9.61) should include the following operations in discrete time:

(i) at the beginning of each discrete moment of time $k = k_0, k_0 + 1,\ldots, k_F$, when the control values are determined, the current value of the state vector of equation (9.32) should be determined (or estimated);
(ii) the solution $X(\boldsymbol{x}, t, \sigma)$ of equation (9.56) on the interval $[k, k_F]$ for the initial conditions coinciding with the current (or close to it) state of equation (9.32) should be determined;
(iii) computation of the gradient of $V(\boldsymbol{x},t)$ for the current moment of time k [see equations (9.59) and (9.60)];
(iv) computation of the control actions according to equation (9.61).

Since computational operations are performed by a computer, the integration in equation (9.60) is changed to the summation. The discrete form of equation (9.60) is obvious.

Below we consider the discrete-time analogue of the problem (9.32) and (9.42)

$$\boldsymbol{x}(k+1) = \boldsymbol{f}(\boldsymbol{x}(k)) + \boldsymbol{B}(\boldsymbol{x}(k+1))\boldsymbol{u}(k), \quad \boldsymbol{x}(k_0) = \boldsymbol{x}_0 \tag{9.62}$$

$$I = V_0(\boldsymbol{x}(k_F)) + \sum_{k_0}^{k_F} R(\boldsymbol{x}(k)) + Q(\boldsymbol{u}(k)) + Q_0(\boldsymbol{u}_0(k)) \tag{9.63}$$

assuming that the function

$$Q(\boldsymbol{u}) + Q_0(\boldsymbol{u}_0) - \frac{\partial Q^T(\boldsymbol{u}_0)}{\partial u_0}\boldsymbol{u}$$

is positive definite with respect to $\boldsymbol{u}$ and equals zero at $\boldsymbol{u} = \boldsymbol{u}_0$.

The Bellman equation can be presented as

$$V_i[x(i)] = \min_{u(i)}\{R(\boldsymbol{x}(i)) + Q(\boldsymbol{u}(i)) + Q_0(\boldsymbol{u}_0(i)) + V_{i+1}^T[\boldsymbol{f}(\boldsymbol{x}(i)) + \boldsymbol{B}(\boldsymbol{x}(i))\boldsymbol{u}(i)]\}, \tag{9.64}$$

$$V(\boldsymbol{x}(k_F)) = V_0(\boldsymbol{x}(k_F)), \quad i = k_F - 1, k_F - 2,\ldots$$

Acting analogously to the continuous case, instead of equations (9.43) and (9.44) we have

$$\frac{\partial Q^T(\boldsymbol{u}_0(i))}{\partial u_0} = -\frac{\partial V_{i+1}^T}{\partial x(i+1)}\boldsymbol{B}(\boldsymbol{x}(i)) \tag{9.65}$$

$$V_{i+1}[\boldsymbol{f}(\boldsymbol{x}(i)) + \boldsymbol{B}(\boldsymbol{x}(i))\boldsymbol{u}_0(i)] - V_i(\boldsymbol{x}(i)) - \frac{\partial V_{i+1}^T}{\partial x(i+1)}\boldsymbol{B}(\boldsymbol{x}(i))\boldsymbol{u}_0(i) = -R(\boldsymbol{x}(i)) \tag{9.66}$$

The first-order approximation of $V_{i+1}[\boldsymbol{f}(\boldsymbol{x}(i)) + \boldsymbol{B}(\boldsymbol{x}(i))\boldsymbol{u}_0(i)]$ as

$$V_{i+1}[\boldsymbol{f}(\boldsymbol{x}(i)) + \boldsymbol{B}(\boldsymbol{x}(i))\boldsymbol{u}_0(i)] \approx V_{i+1}[\boldsymbol{f}(\boldsymbol{x}(i))] + \frac{\partial V_{i+1}^T}{\partial x(i+1)}\boldsymbol{B}(\boldsymbol{x}(i))\boldsymbol{u}_0(i) \tag{9.67}$$

makes it possible to simplify equation (9.66), so that it instead of equation (9.66) we can use the equation in the form similar to equation (9.44)

$$V_{i+1}[\boldsymbol{f}(\boldsymbol{x}(i))] - V_i[\boldsymbol{x}(i)] = -R(\boldsymbol{x}(i)), \quad V(\boldsymbol{x}(k_F)) = V_0(\boldsymbol{x}(k_F)) \tag{9.68}$$

As mentioned earlier, the optimal problems examined here have a certain computational advantage over the optimal problems considered in the previous section and can compete successfully with them in integrated guidance and control systems design.

9.4 INTEGRATION AND DECOMPOSITION

Decomposition means the disintegration, the division of the whole system into absolutely independent or weakly interconnected subsystems, which at certain stages can be treated separately. Solutions obtained for these subsystems are used later to obtain the solution for the whole problem. For many years, this approach was considered as natural and logical and in many cases as the only way to resolve complex problems. The decomposition methods formed a special part of computational mathematics. They were widely developed and used especially in the initial stage of the computer era, when the time of computation was the main restricting factor.

The term *integration* means an act of combining into an integral whole. Nowadays powerful computers enable us to solve problems we could only dream of solving several years ago. Does it mean that it is worth loading computers with huge models, containing many "fuzzy" parameters and relying upon the solutions obtained? Does it mean that we should not trust our intuition and rely upon common sense? Computers, however powerful they might be, need time for computations. Homing missiles use their on-board computers, and for them the time of computation, as well as the computer's weight, depending on its computational ability, are very important factors.

As shown in Figure 9.1, the guidance law and control units are connected in series. This means that, formally, each of these units, at least at the initial stage, can be designed separately. However, as seen from Figure 9.1, they are interconnected also by the existing feedback loop, and that is why the integrated approach to missile guidance and control has merit.

The system concept is paramount in all stages of design because a decision in one particular design area on one specific component may radically affect other parts of the missile system design. However, it does not contradict the necessity of thoroughly examining separate elements of the system.

As mentioned earlier, the natural approach to solving a complicated problem is to first consider simplified parts of the problem and solve them; later the problem is brought closer to reality by gradually including the complicating factors of the full problem. This enables the designers to appreciate all aspects and details of the problem.

This approach is used in autopilot design [5]. At the earliest stages of design, the behavior of servos and airframe is approximated by linear differential equations with constant coefficients, so that well-known analytical methods can be used to roughly evaluate some design parameters. Despite the approximate nature of the analytical solutions obtained, they make it possible to arrive at qualitative estimates of the most important effects of the missile system parameters on the system's accuracy. As mentioned earlier, at the preliminary stage of autopilot design, three rotational channels (roll, pitch, and yaw) are investigated separately. The flight control system must stabilize and control the attitude of a missile about the three body axes—roll, pitch, and yaw. As shown in Figure 8.2, roll is defined as being about the longitudinal axis; yaw is orthogonal to roll and is contained in the trajectory plane; pitch is orthogonal to both and completes the right-handed set. The three channels of the flight control system are similar, with pitch and yaw usually being nearly identical. Their separate consideration significantly simplifies the design procedure. Their aerodynamic coupling is taken into account later, and the control system is modified to meet additional requirements.

The item of prime importance to the designer is the accuracy of the missile system. However, accuracy requirements are linked to other important characteristics of the whole missile system. In addition, the autopilot should guarantee system stability over the missile operational range. The desired autopilot response is required to be fast with minimum overshoot to meet structural limitation. The autopilot should also provide attenuation of high frequencies, so that it does not

react to high-frequency aeroelastic behavior that can affect the sensor signals or to noise accompanying the acceleration commands [5].

The airframe parameters and structure significantly influence missile performance, and the guidance system designer should have full knowledge of the airframe response (e.g., its frequency response characteristics) to the guidance system commands. In turn, the dynamic characteristics of the airframe depend on the type of control chosen (e.g., jet, tail, canard, or wing) and the location of control devices.

The guidance designer is vitally interested in the weight admissible for the guidance equipment and the dimensions and locations of the space allocated for it. The location of some elements of the guidance system (e.g., gyros) may be quite critical. The designer should be involved in the airframe design and space allocation to properly place the motion-sensitive elements. During the preliminary design, the missile body is usually assumed to be rigid. However, taking elastic behavior of the structure and its effect on aerodynamics into account later, additional corrections can be made. For example, the accelerometers should be placed where the translational vibrations of the structure are minimal, and the pitch and yaw rate sensors should be placed where the rotational vibrations are minimal.

We described only some of the problems that should be resolved in the process of the missile guidance and control system design. Most of them relate to autopilot design, assuming that the guidance law has already been chosen.

Proponents of the integrated approach [3,4,7–11] offer to design the autopilot and to determine the guidance law based on certain criteria. However, the criteria chosen [see equations (9.25) and (9.30)] are closely linked with the generalized Riccati equation [see equations (9.22) and (9.24)]. As indicated in References [9–11], after transforming the missile model into the state-dependent coefficient form, the next major responsibility of the designer is to select the state-weighting matrices $C_0(\boldsymbol{x})$ and $R(\boldsymbol{x})$ positive semidefinite for all expected values of $\boldsymbol{x}$. As admitted in Reference [9], selecting matrix functions that meet these requirements for all values of the state vector is not generally practical. It is difficult to justify the choice of coefficients in the matrices indicated above for various engagement scenarios. Moreover, there is no rigorous proof that the closed-loop nonlinear system based on the procedure described in References [9–11] will be stable. That is why the optimal approach discussed in the previous section looks more encouraging. It is more rigorous and it is easier to solve the Lyapunov equations similar to equation (9.44) than the Bellman equations (9.20), (9.24), or (9.40).

The optimal methods described in this chapter belong to a class of analytical controller design and suffer the drawback pertaining to this class: the choice of the performance index coefficients presents a separate independent problem, and the realization of the optimal solution entails certain difficulties because the measurement of the whole-state vector is required.

The methods of analytical design of controllers based on the state-space models and optimal control theory have been extensively presented in the literature. During the last fifty years, thousands of papers and books have been dedicated to this problem. However, they were not widely used in engineering practice. Engineers, dealing with real physical systems, prefer to operate with the input–output relationships and frequency characteristics of separate elements of the systems. They feel better about the system potential, when they know, for example, its bandwidth. Frequency domain methods, developed in the United States many years ago, are still very popular and widely used in engineering practice because they are very physical. Following the traditional autopilot design procedure, as soon as the method of guidance has been determined, and the general bandwidth specifications for the main autopilot components have been developed, the design of the system then proceeds using analytical methods, modeling, and simulation.

Too much passion for mathematics, rather than the physics of a process under consideration, can be more dangerous than neglecting modern mathematical tools and relying on intuition based on deep physical understanding of the process.

It is worth remembering that traditionally, based on past experience, the guidance objective is formulated in terms of LOS. The widely used PN and pure pursuit guidance laws are based on

certain principles, the so-called geometrical rules. According to the pure pursuit rule, the pursuer should be directed at the target. According to the parallel navigation rule, the direction of the LOS should be kept parallel to the initial LOS. People adopted these rules from nature, observing the behavior of predators. The optimal law corresponding to PN, which is the simplest implementation of the parallel navigation rule, was obtained as a solution to a specially constructed optimal problem for an extremely simplified missile guidance model (2.54) and (2.44). The optimal solution requires information about future target behavior. Indirectly, it can be presented by the indication of the time-to-go or the predicted intercept point. It can be justified for midcourse guidance, where at least there is time to improve the situation. However, for homing guidance, a mistake in determining the time-to-go or the predicted intercept point can be crucial.

Classic control theory is based on the feedback principle. The optimal control theory supplies us with an optimal control law as a function of time. Only for a special class of optimal problems the optimal solution can be presented as a function of the system state vector (i.e., present controller equations similar to the closed-loop system examined in classic control theory).

Does it mean that the optimization methods of modern control theory are useless? Not at all. The optimal solutions (9.26), (9.48), (9.53), and (9.61) help engineers choose a rational structure for the control system. Although the measurements available on board the missile are limited, and the authors of References [9–11] assumed that all the measurements required for the implementation of the integrated guidance and control law were available, analyzing the structure in Figure 9.1 and the optimal solution (9.26) we can easily conclude that the autopilot input in Figure 9.1 lacks many components of the state vector of equation (9.2). Most of these components influence the missile actual acceleration a_{Mx}, a_{My}, and a_{Mz}, so it is logical to conclude that the structure with missile acceleration feedback [see Figure 6.3] is better than the structure in Figure 9.1. This is the same conclusion we came to in Chapter 6, supporting the necessity of the acceleration feedback as a measure to make the actual missile acceleration close to the commanded acceleration (in full accordance with the feedback principle).

Here we presented Figure 6.1 in a more general form. As seen from Figure 9.3, the autopilot input is considered as the commanded acceleration, that is, the real guidance law consists of two parts: the first component depends directly on an initially chosen guidance law; the second component presents a correction caused by the difference between the chosen guidance law and its realization. The same structure can be interpreted in a different way. We can consider it as consisting of the guidance part presented by a chosen guidance law and the autopilot, which includes the acceleration feedback; for many existing autopilots, which contain acceleration feedback, the structure in Figure 6.3 and in Figure 9.3 assumes the necessity of an additional acceleration feedback. The difference in terminology does not change the whole problem: to increase missile system accuracy.

Usually the design of a product, which has its "predecessors," does not start from zero. It uses components of the previous design and improves them. Should we ignore this approach?

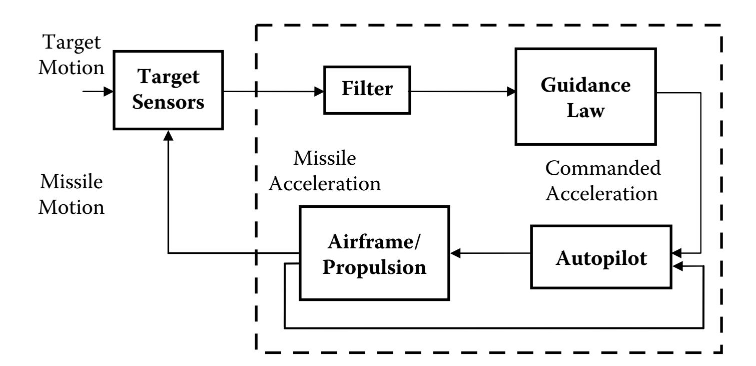


FIGURE 9.3 Integrated guidance control system.

The structure in Figure 9.3 and the procedure of determining its components can be considered as a modernization of the existing systems. Analysis of the relationship between the miss distance and the missile parameters (see Chapters 4 and 7) enables the designers to establish the "critical" parameters and to see the way of improving missile accuracy (to redesign certain components that would change these parameters). The design procedure to modernize the existing missile guidance and control systems will enable designers to modify the existing design procedure analyzing the influence of the missile main dynamic parameters on the miss distance and considering the new guidance laws and the new guidance-autopilot structure to improve missile performance.

As mentioned in Chapter 8, the design process is an art, and we hope the above material presents useful information for reflection.

REFERENCES

1. Albrekht, E., On optimal stability of nonlinear systems, *Journal of Applied Mathematics and Mechanics*, 25, 5, 836–844, 1961.
2. Blakelock, J., *Automatic Control of Aircraft and Missiles*, 2nd ed., Wiley-Interscience, New York, 1991.
3. Cloutier, J., D'Souza, C., and Mracek, C., Nonlinear regulation and nonlinear h•control via the state-dependent Riccati equation technique, *Proceedings of the International Conference on Nonlinear Problems in Aviation and Aerospace*, Daytona Beach, FL, May 1996.
4. Cloutier, J., Mracek, C., Ridgely, D., and Hammett, K., State dependent Riccati equation techniques: theory and applications, *ACC Workshop Tutorial*, 6, 1998.
5. Cronvich, L., Aerodynamic consideration for autopilot design, in *Tactical missile aerodynamics,* edited by M. Hemsch and J. Nielsen, *Progress in Aeronautics and Astronautics*, 124**,** AIAA, Washington, DC, 1986.
6. Krasovskii, A., *Systems of Automatic Control of Flight and Their Analytical Design*, Nauka, Moscow, 1973.
7. Lin, C., Wang, Q., Speyer, J., Evers, J., and Cloutier, J., Integrated estimation, guidance, and control system design using game theoretic approach, in *Proceedings of the American Control Conference*, 3220–3224, 1992.
8. Lin, C., Ohlmeyer, E., Bibel, J., and Malyevac, S., Optimal design of integrated missile guidance and control, *World Aviation Conference*, Anaheim, CA, AIAA-985519, 1998.
9. Menon, P. and Ohlmeyer, E., Integrated design of agile missile guidance and control systems, *Proceedings of the 7th Mediterranean Conference on Control and Automation (MED99),* Haifa, Israel, 1999.
10. Menon, P., Sweriduk. G., and Ohlmeyer, E., Optimal fix-interval integrated guidance-control laws for hit-to-kill missiles, *AIAA Guidance, Navigation, and Control Conference,* AIAA, 2003-5579, Austin, Texas, 2003.
11. Palumbo, N., Reardon, B., and Blauwkamp, R., Integrated guidance and control for homing missiles, *Johns Hopkins APL Technical Digest*, 25, 2, 121–130, 2004.
12. Wise, K. and Broy, D., Agile missile dynamics and control, *Journal of Guidance, Control and Dynamics*, 21, 441–449, 1998.
13. Yanushevsky, R., A controller design for a class of nonlinear systems using the Lyapunov-Bellman approach, *Transactions of the ASME, Journal of Dynamic Systems, Measurement, and Control,* 114, 390–393, 1992.
14. Yanushevsky, R., *Theory of Optimal Linear Multivariable Control Systems*, Nauka, Moscow, 1973.

10 Missile Guidance Software

10.1 INTRODUCTION

A well-structured and efficient program gives the programmer the same sort of pleasure that an artist feels when creating a new work or a mathematician gets from the elegant proof of a theorem. Although the programs presented in this chapter cannot be considered as highly sophisticated, they can be used to analyze and design various guidance laws and will help readers to develop their own programs. The programs presented are written using VISUAL FORTRAN and MATLAB [1–3].

Introduced in 1954, FORTRAN was the first high-level language. Its weakness, however, is its poor structure. In addition, the language has poor facilities for describing data and handling input and output. It was improved with more recent versions, FORTRAN 77 and FORTRAN 90. A language that came to be significant for the subsequent development of programming languages was ALGOL, which was released in 1960. The big advantage of this language is that it has a good structure. Nevertheless, ALGOL did not become very popular and widely used. In 1965, the language BASIC was introduced and became widespread. Although its advantages lie in its simplicity, its disadvantage lies in its lack of structure. Presented in 1971, Pascal has good program structure similar to ALGOL. However, its main weakness is that it lacks constructs for enabling larger programs to be built up in a modular way. This makes all the above-mentioned languages most suitable for developing small programs.

C is a language that has become very popular in spite of its age (it was developed at the beginning of the 1970s). Most of today's operating systems and other system programs (e.g., for handling windows and menus), are written in C. The most widely used of the object-oriented languages is an extension of C, C++, created in 1985. To write "good" programs—easily understandable, easily enhanced, and free from errors—a set of rules and recommendations were developed, and the concept of structured programming was introduced. During the 1970s, it became clear that even well-structured programs were not enough for mastering the complexity involved in developing large programs. It became obvious that it was necessary to support the division of the program into well-defined parts, or modules that could be developed and tested independently. Apart from being well structured, the new languages, such as Ada and Java, support the modular developments of programs. Moreover, they allow programs to communicate with users.

Similar to public libraries that enable us to learn and increase our level of knowledge, modern programming languages are supplied with libraries that enhance their programming ability. The most popular programming languages are constantly developing. Their new versions try to include features that are attractive in other languages. Moreover, interfaces are created so that various languages can communicate with each other.

It is obvious that programming languages oriented to special classes of problems are more efficient than general purpose languages. MATLAB is one such specialized language, which is very useful for scientific programming. The very first version of MATLAB was written in the late 1970s for use in courses in matrix theory, linear algebra, and numerical analysis. MATLAB is a high-performance language for technical computing. MATLAB is fundamentally built upon a foundation of sophisticated matrix software, in which the basic data element is a matrix that does not require dimensioning. This allows users to solve many technical computing problems, especially those with matrix formulations, spending a fraction of the time it would take to write programs in a scalar noninteractive language such as C or FORTRAN. MATLAB allows easy matrix manipulation, plotting of functions and data, implementation of algorithms, creation of user interfaces, and

interfaces with programs in other languages. Focused on various industry applications, MATLAB developed the so-called toolboxes, comprehensive collections of M-files, functions that extend the MATLAB environment to solve particular classes of problems in such areas as signal processing, control systems, neural networks, and so forth. The MATLAB mathematical function library includes a vast collection of computational algorithms. A software package for modeling, simulating, and analyzing dynamic systems is called SIMULINK. It supports linear and nonlinear systems, modeled in continuous time, sampled time, or a hybrid of the two, that is, it allows users to build new models or modify existing models. For modeling, SIMULINK provides a graphical user interface (GUI) for building models as block diagrams, using click-and-drag mouse operations. SIMULINK includes a comprehensive block library of sinks, sources, linear and nonlinear components, and connectors. Users can also customize and create their own blocks using S-functions. In recent years, SIMULINK has included blocks that can be used in the aerospace industry for process simulation and control system design.

The MATLAB programs presented in this chapter can compete with the programs that can be created using SIMULINK and MATLAB in the time domain to evaluate the miss distance. Their advantage is in using the frequency characteristics of the missile flight control system, which are more physical than the representation by a system of differential equations. Some of the VISUAL FORTRAN programs given below have common features with the FORTRAN programs in Zarchan [4]. Their structure, dictated by the common character of the problems considered, is similar. In contrast to Zarchan, more complicated models are considered. Readers who are familiar with Reference [4] do not need to spend a lot of time to understand these programs because, for the pieces of programs that are similar to Reference [4], labels were made analogous to Reference [4].

VISUAL FORTRAN includes FORTRAN 90 modules and libraries for doing Windows programming at the Win32 application program interface (API) level. It enables programmers to build source code into several types of programs and libraries using the visual development environment (also called Developer Studio), which organizes development into the so-called projects. A project consists of the source files required for an application, along with the specifications for building the project. Projects are contained in a *workspace*. The DFWIN.F90 module provides access to a full range of routines including window management, graphic device interface, system services, multimedia, and remote procedure calls. FORTRAN libraries are blocks of code kept separate from the main part of the program; they offer important advantages in organizing large programs and in sharing routines between several programs. VISUAL FORTRAN is well suited for the 3-DOF or 6-DOF engagement programs as well as for the more complicated models including a radar model.

The programs for the planar models written in MATLAB or FORTRAN can be written in other languages such as BASIC, Pascal, C, and so forth. However, for the multidimensional models of engagement VISUAL FORTRAN is preferable. The models including radar, weapon control system, and missile require more sophisticated languages such as Ada or Java.

10.2 SOFTWARE FOR FREQUENCY-DOMAIN APPROACH

The frequency domain approach to the analysis of the linearized PN guidance system models was considered in Chapter 4, where the analytical expressions for the transfer function of the guidance system with respect to target acceleration and related expressions for missile system performance were obtained. As indicated, the obtained analytical expressions need to employ simpler computational programs than by using existing time-domain methods.

Below we present some programs that demonstrate the effectiveness of the frequency domain approach in analyzing missile performance.

Listing 10.1 presents the MATLAB program to determine the peak miss distance for weave target maneuvers. The program corresponds to the example of the third-order model of the flight control system dynamics considered in Chapter 4. Its time constant, natural frequency, damping, and airframe zero frequency are denoted by *T*, *wm*, *damp*, and *wz*, respectively. The effective

navigation ratio is denoted as in the previous chapters. The expressions for coefficients B, C, and D are obtained from equations (4.17)–(4.19). The expression $y(i,1)$ for the amplitude characteristic (4.26) is presented as the product of $ac1(i,1)$, $ac2(i,1)$, $ac3(i,1)$, and $ac4(i,1)$ that equal the corresponding factors of equation (4.26).

LISTING 10.1
MATLAB Program to Determine the Peak Miss

```
function peak.miss
    T = 0.5;
    N = 3.;
    wz = 5.;
    wm = 20.;
    damp = 0.7;
    beta = sqrt(1.-damp^2);
    B = (T^2 - wz^(-2))/(2.*damp/wm -T-1./(T*wm^2));
    C = - 1./wm^2 - B/T/wm^2;
    D = -2.*damp/wm + C*T*wm^2 ;
    wt = 3.5;
    Tt = 0.15;
    wzt = 15.;
    dampt = 0.8;
for q = 1:150
    w(q,1) = q/10;
    ac1(q,1) = 0;
    ac2(q,1) = 0;
    ac3(q,1) = 0;
    ac4(q,1) = 0;
    G(q,1) = 0;
    GT(q,1)= 0;
    y (q,1) = 0;
end
for i = 1:150
    ac1(i,1) = w(i,1).^(N-2);
    ac2(i,1) = (w(i,1).^2.+ (1./T)^2).^(N*B/(T*2));
    ac3(i,1) = ((wm.^2-w(i,1).^2).^2 + 4.*(damp^2).*(w(i,1).^2)*wm.^2).^(C*N/4*wm^2);
    G(i,1) = atan((w(i,1)-wm*sqrt(1-damp^2))./wm/damp)-atan((w(i,1) +
             wm*sqrt(1-damp^2))./wm/damp);
    ac4(i,1) = exp(N*wm*(D-C*damp*wm)./(2.*sqrt(1.-damp^2)).*G(i,1));
%   GT(i,1) = (1.-(w(i,1)./wzt).^2)./sqrt((1.+Tt^2)*((1.-
%             (w(i,1)./wt).^2.)^2+4*((w(i,1)./wt).^2).*dampt^2));
    GT(i,1) = 1.;
    y(i,1) = 9.81*ac1(i,1).*ac2(i,1).*ac3(i,1).*ac4(i,1).*GT(i,1);
end
plot(w,y);grid; xlabel('Frequency (rad/s)'); ylabel('Steady-state miss
    amplitude (m)');
```

The *for* loop (i = 1:150) enables us to obtain the relationship between the amplitude of the steady-state miss distance $y(i,1)$ and the frequency $w(i,1)$, which is presented in Figure 4.7. Analyzing this relationship, the optimal maneuver policy, the optimal weaving frequency of a target, can be determined. This program enables us to examine the influence of the flight control system parameters on the missile system performance (see Table 4.1).

As indicated in Chapter 4, the generalized missile guidance model [see equations (4.65)–(4.70)] gives more accurate estimates of the miss distance (see Figure 4.13). Target missile dynamics are

presented by the time constant *Tt*, natural frequency *wt*, damping *dampt*, and airframe zero frequency *wzt*, respectively. Its amplitude characteristic *GT*(*i*,1) [see equation (4.67)] is written but is not used in the program (see the symbol "%" indicating that the line of the program is disabled). To use the generalized model program to determine the peak miss distance the symbol "%" should be deleted from the lines where *GT*(*i*,1) is determined, and placed on the line *GT*(*i*,1) = 1.

The MATLAB program of Listing 10.2 is more powerful than the program of Listing 10.1. It is written for the fourth-order model [see equation (4.17)]. Since we deal with two time constants *T*1 and *T*2, instead of the factor *ac*2(*i*,1) in Listing 10.1, here we have two factors *ac*21(*i*,1) and *ac*22(*i*,1). The program also contains the expression for the phase characteristic *f*(*i*,1) as well [see equation (4.28)]. As a result, the real *RE*(*i*,1) and imaginary *IM*(*i*,1) parts of the frequency response can be obtained (see Figure. 4.9 and Figure 4.10). The expression of *RE*(*i*,1) is used to obtain the miss step response *INT*(*j*,1) based on the procedure described in Chapter 4 [see equation (4.62)].

LISTING 10.2
MATLAB Program for Miss Analysis. Deterministic Case

```
function miss_analysis;
    T1 = 0.5;
    T2 = 0.1;
    wz = 5.;
    r1 =  0.;
    r2 = -wz^(-2);
    r3 = 0.;
    N = 3.;
    wm = 20.;
    damp = 0.7;
    wt = 3.5;
    Tt = 0.15;
    wzt = 15.;
    dampt = 0.8;
    beta = sqrt(1.-damp^2);
    B1 = (T1^2 -r1*T1 + r2-r3/T1)/(2.*damp/wm -T1-1./(T1*wm^2))/(1.-T2/T1);
    B2 = (T2^2 -r1*T2 + r2-r3/T2)/(2.*damp/wm -T2-1./(T2*wm^2))/(1.-T1/T2);
    BT2 = B2/T2;
    C = -1./wm^2 - B1/T1/wm^2 -BT2/wm^2;
    D = r1-B1-B2-(T1+T2) -2.*damp/wm;
for q = 1:150
    w(q,1) = q/10;
    t(q,1) = q/10;
    ac1(q,1) = 0;
    ac21(q,1) = 0;
    ac22(q,1) = 0;
    ac3(q,1) = 0;
    ac4(q,1) = 0;
    G(q,1) = 0;
    RE(q,1) = 0;
    IM(q,1) = 0;
    INT(q,1) = 0;
    f(q,1) = 0;
    y(q,1) = 0;
    z(q,1) = 0;
end
for i = 1:150
    ac1(i,1) = w(i,1).^(N-2.);
```

```
    ac21(i,1) = (w(i,1).^2.+ (1./T1)^2).^(N*B1/(T1*2));
    ac22(i,1) = (w(i,1).^2.+ (1./T2)^2).^(N*BT2/2);
    ac3(i,1) = ((wm.^2-w(i,1).^2).^2 +
               4.*(damp^2).*(w(i,1).^2)*wm.^2).^(C*N/4*wm^2);
    G(i,1) = atan((w(i,1)-wm*sqrt(1.-damp^2))./wm/damp)-atan((w(i,1) +
            wm*sqrt(1.- damp^2))./wm/damp);
    ac4(i,1) = exp(N*wm*(D-C*damp*wm)./(2.*sqrt(1.-damp^2)).*G(i,1));
    y(i,1) = 9.81*ac1(i,1).*ac21(i,1).*ac22(i,1).*ac3(i,1).*ac4(i,1);
    f(i,1) = -3.14 +N*(3.14/2. + B1/T1.*atan(w(i,1)*T1) + B2/T2.*atan(w(i,1)*T2)
            +C/2.*wm^2*atan(2.*w(i,1)*wm*damp/(wm^2-w(i,1)^2)-wm*(D-damp*wm*C)/
            4/sqrt(1.-damp^2)*log((w(i,1)^2+wm^2-2.*w(i,1)*wm*sqrt(1.-damp^2))/
            (w(i,1)^2+wm^2+2.*w(i,1)*wm*sqrt(1.-damp^2)))));
    RE(i,1) = y(i,1).*cos(f(i,1));
    IM(i,1) = y(i,1).*sin(f(i,1));
end
for j = 1:150
    for i = 1:150
        z(i,1) = RE(i,1).*sin(w(i,1).*t(j,1))./w(i,1);
    end
        INT(j,1) = 2./3.14*0.1*sum(z);
end
    plot(w, y);grid ; xlabel('Frequency (rad/s)');ylabel('Steady-state miss
    amplitude (m)');
%   plot(RE, IM); grid;xlabel(''RE (m)');ylabel('IM (m)');
%   plot(w, RE);grid;xlabel('Frequency (rad/s)');ylabel('Real frequency response
    (m)');
%   plot(t, INT);grid ; xlabel('Time (s)');ylabel('Step miss (m)');
```

In Chapter 6, the frequency approach was used to design new guidance laws that improve the performance of missile systems with PN guidance. Listing 10.3 presents the program that is based on the analytical expressions of Chapter 4 and Chapter 6 and the structure of the modified missile guidance model given in Figure 6.1. The modified guidance is characterized by the parameters *tau1* and *tau2*, K_1 and K_2 [see equation (6.16) and (6.17)]. Their initial values indicated in the program correspond to PN guidance without any modification. The figures in Chapter 6 and Table 6.1 are obtained by using this program [see **plot**(*RE*, *IM*), **plot** (*w*, *RE*), **plot**(*t*, *INT*)].

LISTING 10.3
MATLAB Program for Guidance Laws Analysis and Design

```
function guidance_design;
    N = 3.;
    wz = 5.;
    wm = 20.;
    damp = 0.7;
    T = 0.5;
    tau1 = 0.;
    tau2 = 0.;
    K1 = 0.;
    K2 = 1.;
    a0 = -wz^(-2);
    b0 = T/wm^2*tau2;
    b1 = T/wm^2 + (2.*T*damp/wm +1./wm^2)*tau2 + a0*tau1;
    b2 = 2.*T*damp/wm +1./wm^2+(2*damp/wm+T)*tau2 + a0*K1;
    b3 = 2.*damp/wm +T + tau1 + tau2;
    b4 = 1.+ K1;
```

```
    d0 = a0*(tau1 + tau2*K2);
    d1 = a0*(K2 + K1);
    d2 = tau1 + tau2*K2;
    d3 = K2+K1;
    X = [b0, b1, b2, b3, b4];
    roots(X)
    SYS = TF([d0 d1 d2 d3], [b0 b1 b2 b3 b4]);
    step(SYS)
    i1 = 1500.;
for q = 1: i1
    w(q,1) = q/10;
    p1(q,1) = 0.;
    p2(q,1) = 0.;
    p3(q,1) = 0.;
    p4(q,1) = 0.;
    RE(q,1) = 0;
    RE1(q,1) = 0;
    IM(q,1) = 0;
    IM1(q,1) = 0;
    INT(q,1) = 0.;
    INT1(q,1) = 0.;
    y(q,1) = 0.;
end
for q = 1:i1
    p1(q,1) = -d1.*w(q,1).^2 + d3;
    p2(q,1) = -d0.*w(q,1).^3 + d2.*w(q,1);
    p3(q,1) = b0.*w(q,1).^4 -b2.*w(q,1).^2 + b4;
    p4(q,1) = -b1.*w(q,1).^3 + b3.*w(q,1);
    RE(q,1) = (p1(q,1).*p3(q,1) + p2(q,1).*p4(q,1))./(p3(q,1).^2 + p4(q,1).^2);
    RE1(q,1) = RE(q,1)./w(q,1);
    IM(q,1) = (-p1(q,1).*p4(q,1) + p2(q,1).*p3(q,1))./(p3(q,1).^2 + p4(q,1).^2);
    IM1(q,1) = IM(q,1)./w(q,1);
end
for i = 1:i1
        INT1(i,1) = RE1(i,1);
    for q = i+1:i1
        INT1(q,1) = (INT1(q-1,1)+RE1(q,1));
    end
        INT(i,1) = 0.1*INT1(i1,1);
        y(i,1) = exp(-N*INT(i,1)).* 9.81./w(i,1)^2;
end
plot(w(1:150), y(1:150));grid ; xlabel('Frequency (rad/s)');ylabel('Steady-state
    miss amplitude (m)');
```

The transfer function of the modified system (6.9) is presented in the form

$$W_{\Sigma}(s) = \frac{d_3 + d_2 s + d_1 s^2 + d_0 s^3}{b_4 + b_3 s + b_2 s^2 + b_1 s^3 + b_0 s^4} \tag{10.1}$$

and the expressions for the coefficients of the nominator and denominator are obtained. Based on the values of these coefficients and using the statement **roots**(X), the roots of the characteristic equation can be calculated. The statements SYS = **TF**([d0 d1 d2 d3], [b0 b1 b2 b3 b4]), and **step**(SYS) enable us to obtain the step response corresponding to the transfer function $W_{\Sigma}(s)$.

In contrast to the programs of Listings 10.1 and 10.2, this program calculates the frequency response approximately [see equations (7.70) and (7.71)] rather than using the precise expressions (4.35) and (4.37). In the program the infinite integration limit in equations (4.13), (7.70), and (7.71) is changed to a large number and presented by the parameter *i*1. The real and imaginary parts of the nominator of $W_\Sigma(s)$ are presented by *p1*(*q*,1) and *p2*(*q*,1), respectively. The real and imaginary parts of the denominator of $W_\Sigma(i\omega)$ are presented by *p3*(*q*,1) and *p4*(*q*,1), respectively. *RE*(*q*,1) and *IM*(*q*,1) are the real and imaginary parts of $W_\Sigma(i\omega)$, respectively. Taking into account that $H(i\omega) = W_\Sigma(i\omega)/i\omega$ [see equation (4.14)], the expressions *RE*1(*q*,1) and *IM*1(*q*,1) for the real and imaginary parts of $H(i\omega)$ are given. For the chosen step of summation 1/10, the approximate value of the amplitude *y*(*i*,1) of the steady-state miss distance due to a weaving target with the frequency *w*(*q*,1) is calculated.

The influence of noises on the miss distance was analyzed in Chapter 7. Based on the analytical expressions (7.55)–(7.58) [see also equations (7.43), (7.46), (7.48), and (7.49)] the programs that calculate the root-mean-square (rms) miss distance due to glint noise, range-independent noise, and passive- and active-receiver noise are presented.

Listing 10.4 presents the program to determine the rms miss due to glint noise [see equation (7.55)] for the fourth-order guidance system model assuming the spectral density *glint* equals 0.4 m^2/Hz. The upper part of the program repeats the corresponding lines of Listing 10.2, only here the frequency characteristics *y*(*i*,1), *f*(*i*,1), *RE*(*i*,1), and *IM*(*i*,1) [see equations (4.42) and (4.43)] are presented with respect to a target vertical position $y_T(t)$ rather than a target acceleration. The parameter *i*1 presents the upper limit of the approximation of the inverse Fourier transform; its value should be chosen to calculate the improper integral of the inverse Fourier transform with high accuracy. The *for* loops are used to calculate the inverse Fourier transform *P*1(*j*,1), its square *P*2(*j*,1), and the definite integral *P*3(*j*,1) as a function of the time of flight t_F. The rms miss is given by *P*4(*j*,1) [2/π coefficient of the inverse Fourier transform is included in the expression *P*4(*j*,1); *w*(*i*,1) and *t*(*j*,1)) denote frequency and time, respectively].

LISTING 10.4
MATLAB Program for the rms Miss Due to Glint Noise

```
function rms_glint;
    i1 = 250.;
    glint = 0.4;
    N = 3.; T1 = 0.5;  T2 = 0.1; wm = 20; damp = 0.7;
    r1 = 0.;
    wz = 5.;  r2 = - wz^(-2) ;
    r3 = 0.;
    beta = sqrt(1.-damp^2);
    B1 = (T1^2 -r1*T1+ r2-r3/T1)/(2.*damp/wm-T1-1./(T1*wm^2))/(1.-T2/T1);
    B2 = (T2^2 -r1*T2 + r2-r3/T2)/(2.*damp/wm-T2-1./(T2*wm^2))/(1.-T1/T2);
    BT2 = B2/T2;
    C = -1/wm^2- B1/T1/wm^2-BT2/wm^2;
    D = r1-B1-B2-(T1+T2)-2*damp/wm;
for q = 1: i1
    w(q,1) = q/10; t(q,1) = q/10;
    ac1(q,1) = 0; ac2(q,1) = 0; ac3(q,1) = 0; ac4(q,1) = 0; G(q,1) = 0;
    RE(q,1) = 0; IM(q,1) = 0; RE1(q,1) = 0; f(q,1) = 0; y(q,1) = 0; z(q,1) = 0;
    P1(q,1) = 0; P2(q,1) = 0; P3(q,1) = 0; P4(q,1) = 0;
end
for i = 1: i1
    ac1(i,1) = w(i,1).^N;
    ac21(i,1) = (w(i,1).^2.+(1./T1)^2).^(N*B1/(T1*2));
```

```
    ac22(i,1) = (w(i,1).^2.+(1./T2)^2).^(N*BT2/2);
    ac3(i,1) = ((wm.^2-w(i,1).^2).^2 +
             4.*(damp^2).*(w(i,1).^2)*wm.^2).^(C*N/4*wm^2);
    G(i,1) = atan((w(i,1)-wm*sqrt(1.-damp^2))./wm/damp)-
             atan((w(i,1) +wm*sqrt(1.- damp^2))./wm/damp);
    ac4(i,1) = exp(N*wm*(D-C*damp*wm)./(2.*sqrt(1-damp^2)).*G(i,1));
    y(i,1) = ac1(i,1).*ac21(i,1).*ac22(i,1).*ac3(i,1).*ac4(i,1);
    f(i,1) = N*(3.14/2 + B1/T1.*atan(w(i,1)*T1) + B2/T2.*atan(w(i,1)*T2) +
            C/2*wm^2*atan(2*w(i,1)*wm*damp/(wm^2-w(i,1)^2) - wm*(D-
            damp*wm*C)/4./sqrt(1.-damp^2)*log((w(i,1)^2+wm^2-2.*w(i,1)*
            wm*sqrt(1-damp^2))/(w(i,1)^2+wm^2+2.*w(i,1)*wm*sqrt(1-damp^2)))));
    RE(i,1) = y(i,1).*cos(f(i,1));
    IM(i,1) = y(i,1).*sin(f(i,1));
end
for j = 1:100
    for i = 1: i1
            z(i,1) = (1.-RE(i,1)).*cos(w(i,1).*t(j,1));
        if  i == 1
            z0(i,1) = z(i,1);
        else
            z0(i,1) = z(i,1) + z0(i -1,1);
        end
    end
            P1(j,1) = 0.1*z0(i1,1);
    if  j == 1
            P2(j,1) = P1(j,1).^2;
    else
            P2(j,1) = P1(j,1).^2 + P2(j -1,1);
    end
       P3(j,1) = glint*0.1*P2(j,1);
       P4(j,1) = 2./3.14*sqrt(P3(j,1));
end
plot(w,P4);grid ; xlabel('Time (s)');ylabel('RMS miss (m)');
```

Listing 10.5 is the program to determine the rms miss due to range-independent noise for the fourth-order guidance system model assuming the spectral density *noise* equals $6.5*10^{-8}$ rad^2/Hz and the closing velocity $vcl = 1{,}500$ *m*/s. The program repeats most of the program of Listing 10.4. The expressions for $z(i,1)$ and $P3(j,1)$ are different and correspond to equation (7.56); $y1$ denotes the first difference of $IM(i,1)$.

LISTING 10.5
MATLAB Program for the rms Miss Due to Range Independent Noise

```
function rms_independent;
    i1 = 250.;
    noise = 6.5*10^(-8);
    vcl = 1500.;
    T1 = 0.5;  T2 = 0.1;
    r1 = 0.;
    wz = 5.;
    r2 = - wz^(-2) ;
    r3 = 0.;
    N = 3.;
    wm = 20;
```

```
    damp = 0.7;
    beta = sqrt(1.-damp^2);
    B1 = (T1^2 -r1*T1+ r2-r3/T1)/(2.*damp/wm-T1-1./(T1*wm^2))/(1.-T2/T1);
    B2 = (T2^2 -r1*T2 + r2-r3/T2)/(2.*damp/wm-T2-1./(T2*wm^2))/(1.-T1/T2);
    BT2 = B2/T2;
    C =-1/wm^2- B1/T1/wm^2-BT2/wm^2;
    D = r1-B1-B2-(T1+T2)-2*damp/wm;
for q = 1: i1
    w(q,1) = q/10; t(q,1) = q/10;
    ac1(q,1) = 0; ac2(q,1) = 0; ac3(q,1) = 0; ac4(q,1) = 0; G(q,1) = 0;
    RE(q,1) = 0; IM(q,1) = 0; f(q,1) = 0; y(q,1) = 0; z(q,1) = 0;
    P1(q,1) = 0; P2(q,1) = 0; P3(q,1) = 0; P4(q,1) = 0;
end
for i = 1: i1
    ac1(i,1) = w(i,1).^N;
    ac21(i,1) = (w(i,1).^2.+(1./T1)^2).^(N*B1/(T1*2));
    ac22(i,1) = (w(i,1).^2.+(1./T2)^2).^(N*BT2/2);
    ac3(i,1) = ((wm.^2-w(i,1).^2).^2 +
             4.*(damp^2).*(w(i,1).^2)*wm.^2).^(C*N/4*wm^2);
    G(i,1) = atan((w(i,1)-wm*sqrt(1.-damp^2))./wm/damp)-
             atan((w(i,1) +wm*sqrt(1.- damp^2))./wm/damp);
    ac4(i,1) = exp(N*wm*(D-C*damp*wm)./(2.*sqrt(1-damp^2)).*G(i,1));
    y(i,1) = ac1(i,1).*ac21(i,1).*ac22(i,1).*ac3(i,1).*ac4(i,1);
    f(i,1) = N*(3.14/2 + B1/T1.*atan(w(i,1)*T1) + B2/T2.*atan(w(i,1)*T2) +
             C/2*wm^2*atan(2*w(i,1)*wm*damp/(wm^2-w(i,1)^2) - wm*(D-
             damp*wm*C)/4./sqrt(1.-damp^2)*log((w(i,1)^2+wm^2-2.*w(i,1)*
             wm*sqrt(1-damp^2))/(w(i,1)^2+wm^2+2.*w(i,1)*wm*sqrt(1.-damp^2)))));
    RE(i,1) = y(i,1).*cos(f(i,1));
    IM(i,1) = y(i,1).*sin(f(i,1));
end
    y1 = diff(IM); y1(i1 ,1) = 0;
for j = 1:100
            z(i,1) = y1(i,1).*cos(w(i,1).*t(j,1));
    for i = 1: i1
        if  i == 1
            z0(i,1) = z(i,1);
        else
            z0(i,1) = z(i,1) + z0(i-1,1);
        end
    end
            P1(j,1) = 0.1*z0(i1,1);
    if  j == 1
            P2(j,1) = P1(j,1).^2;
    else
            P2(j,1) = P1(j,1).^2 + P2(j-1,1);
    end
            P3(j,1) = 0.1*noise*vcl^2*10^2*P2(j,1);
            P4(j,1) = 2./3.14*sqrt(P3(j,1));
end
plot(w,P4);grid ; xlabel('Time (s)');ylabel('RMS miss (m)');
```

Listing 10.6 presents the program to determine the rms miss due to range-dependent noise for the fourth-order guidance system model assuming the spectral density *noise* equals $6.5*10^{-4}$ rad^2/Hz, the closing velocity $vcl = 1{,}500$ m/s, and the reference range $r0 = 10{,}000$ m. The program combines the cases of passive-receiver (*factor* = 1) and active-receiver noises. The rms

miss distance due to passive-receiver noise is calculated based on equation (7.69) rather than equation (7.57). The rms miss distance due to active-receiver noise is calculated based on equation (7.67) rather than equation (7.58). Similar to Listing 10.5, the program repeats most of the program of Listing 10.4. The expressions for $z(i,1)$ and $P3(j,1)$ are different and correspond to equation (7.67) and equation (7.69); $y1$ denotes the first difference of $IM(i,1)$ and $y11$ denotes the first difference of $RE(i,1)$.

LISTING 10.6
MATLAB Program for the rms Miss Due to Receiver Noise

```
function rms_receiver;
    i1 = 250.;
    factor = 1.;
    noise = 6.5*10^(-4);
    vcl = 1500.;
    r0 = 10.^4;
    T1 = 0.5; T2 = 0.1;
    r1 = 0.;
    wz = 30.; r2 = - wz^(-2) ;
    r3 = 0.;
    N = 3.;
    wm = 20;
    damp = 0.7;
    beta = sqrt(1.-damp^2);
    B1 = (T1^2 -r1*T1+ r2-r3/T1)/(2.*damp/wm-T1-1./(T1*wm^2))/(1.-T2/T1);
    B2 = (T2^2 -r1*T2 + r2-r3/T2)/(2.*damp/wm-T2-1./(T2*wm^2))/(1.-T1/T2);
    BT2 = B2/T2;
    C = -1/wm^2- B1/T1/wm^2-BT2/wm^2;
    D = r1-B1-B2-(T1+T2)-2*damp/wm;
for q = 1: i1
    w(q,1) = q/10; t(q,1) = q/10;
    ac1(q,1) = 0; ac2(q,1) = 0; ac3(q,1) = 0; ac4(q,1) = 0; G(q,1) = 0;
    RE(q,1) = 0; IM(q,1) = 0; f(q,1) = 0; y(q,1) = 0; z(q,1) = 0;
    P1(q,1) = 0; P2(q,1) = 0; P3(q,1) = 0; P4(q,1) = 0;
end
for i = 1: i1
    ac1(i,1) = w(i,1).^N;
    ac21(i,1) = (w(i,1).^2.+(1./T1)^2).^(N*B1/(T1*2));
    ac22(i,1) = (w(i,1).^2.+(1./T2)^2).^(N*BT2/2);
    ac3(i,1) = ((wm.^2-w(i,1).^2).^2 +
                4.*(damp^2).*(w(i,1).^2)*wm.^2).^(C*N/4*wm^2);
    G(i,1) = atan((w(i,1)-wm*sqrt(1.-damp^2))./wm/damp)-
             atan((w(i,1) +wm*sqrt(1.- damp^2))./wm/damp);
    ac4(i,1) = exp(N*wm*(D-C*damp*wm)./(2.*sqrt(1-damp^2)).*G(i,1));
    y(i,1) = ac1(i,1).*ac21(i,1).*ac22(i,1).*ac3(i,1).*ac4(i,1);
    f(i,1) = N*(3.14/2 + B1/T1.*atan(w(i,1)*T1) + B2/T2.*atan(w(i,1)*T2) +
             C/2*wm^2*atan(2*w(i,1)*wm*damp/(wm^2-w(i,1)^2) - wm*(D-
             damp*wm*C)/4./sqrt(1.-damp^2)*log((w(i,1)^2+wm^2-2.*w(i,1)*
             wm*sqrt(1-damp^2))/(w(i,1)^2+wm^2+2.*w(i,1)*wm*sqrt(1-damp^2)))));
    RE(i,1) = y(i,1).*cos(f(i,1));
    IM(i,1) = y(i,1).*sin(f(i,1));
end
```

```
             y1 = diff(IM); y1(i1,1) =0; y11 = diff(RE); y11(i1,1) = 0;
for j = 1:100
             if factor == 1
                 z(i,1) = y11(i,1).*t(j,1).*sin(w(i,1).*t(j,1));
             else
                 z(i,1) = y1(i,1).*(t(j,1).^2).*cos(w(i,1).*t(j,1));
             end
        for i = 1: i1
             if  i == 1
                 z0(i,1) = z(i,1);
             else
                 z0(i,1) = z(i,1)+z0(i-1,1);
             end
        end
                 P1(j,1) = 0.1*z0(i1,1);
        if j == 1
                 P2(j,1) = P1(j,1).^2;
        else
                 P2(j,1) = P1(j,1).^2 + P2(j-1,1);
        end
            if factor == 1
                 PP3(j,1) = noise*(vcl^2/r0)^2*0.1*10^2*PP2(j,1);
            else
                 PP3(j,1) = noise*(vcl^3/r0^2)^2*0.1*10^2.*PP2(j,1);
            end
                 P4(j,1) = 2./3.14*sqrt(P3(j,1));
end
plot(w,P4);grid ; xlabel('Time (s)');ylabel('RMS miss (m)');
```

The above-described programs can be combined in a more complicated program that would enable us to analyze the rms miss distance for all types of noises acting separately or simultaneously.

The fourth-order model of the planar engagement is widely used in analysis of missile performance. For the higher-order models, the expressions similar to those given in Listings 10.4–10.6 can be obtained based on equations (4.32) and (4.33). It is possible to modify the programs of Listings 10.4–10.6 by using the approximate expression for the frequency characteristics as shown in the program of Listing 10.3 [see also equations (7.70) and (7.71)]. Readers can easily create such programs.

The above-described programs can be combined in a more sophisticated program that would combine the deterministic and stochastic cases.

In Chapter 7 we showed that the step maneuvers with uniformly distributed starting time and the random-phase sinusoidal maneuvers with uniformly distributed phase can be presented as white noise passing through the shaping filters [see equations (7.39) and (7.40)]. Listing 10.7 presents the program built based on equations (7.50) and (7.51). In contrast to the programs of Listings 10.4–10.6, here $y(i,1)$, f$(i,1)$, and $RE(i,1)$ correspond to the frequency response with respect to target acceleration [see equation (7.53)], so that we operate with factors $ac1(i,1)$, $ac21(i,1)$, $ac22(i,1)$, $ac3(i,1)$, and $ac4(i,1)$ as in Listings 10.2. The program combines the cases of the random step maneuvers (*factor* = 1) and random-phase sinusoidal maneuvers. The rms miss distance due to the random step maneuver with the 3-g amplitude (act = 3.*9.81) is calculated based on equation (7.59). The rms miss distance due to the 3-g random-phase maneuver with the frequency wt = 1.4 *rad/s* is calculated based on equation (7.60). Based on the above explanation of the previous programs

it is not difficult to understand this program. It is possible to modify the program of Listing 10.7 by using the approximate expression for the frequency characteristics as shown in the program of Listing 10.3 [see also equations (7.70) and (7.71)].

LISTING 10.7
MATLAB Program for the rms Miss Due to Random Maneuvers

```
function rms_maneuvers;
    i1 = 250.;
    factor = 1;
    act = 3.*9.81; wt=1.4;
    T1 = 0.5; T2 = 0.1;
    r1 = 0.;
    wz = 30.;
    r2 = - wz^(-2) ;
    r3 = 0.;
    N = 3.;
    wm = 20;
    damp = 0.7;
    beta = sqrt(1.-damp^2);
    B1 = (T1^2 -r1*T1+ r2-r3/T1)/(2.*damp/wm-T1-1./(T1*wm^2))/(1.-T2/T1);
    B2 = (T2^2 -r1*T2 + r2-r3/T2)/(2.*damp/wm-T2-1./(T2*wm^2))/(1.-T1/T2);
    BT2 = B2/T2;
    C = -1/wm^2- B1/T1/wm^2-BT2/wm^2;
    D = r1-B1-B2-(T1+T2)-2*damp/wm;
for q = 1: i1
    w(q,1) = q/10; t(q,1) = q/10;
    ac1(q,1) = 0; ac2(q,1) = 0; ac3(q,1) = 0; ac4(q,1) = 0; G(q,1) = 0;
    RE(q,1) = 0; f(q,1) = 0; y(q,1) = 0; z(q,1) = 0;
    P1(q,1) = 0; P2(q,1) = 0; P3(q,1) = 0; P4(q,1) = 0;
end
for i = 1: i1
    ac1(i,1) = w(i,1).^(N-2);
    ac21(i,1) = (w(i,1).^2.+(1./T1)^2).^(N*B1/(T1*2));
    ac22(i,1) = (w(i,1).^2.+(1./T2)^2).^(N*BT2/2);
    ac3(i,1) = ((wm.^2-w(i,1).^2).^2 +
              4.*(damp^2).*(w(i,1).^2)*wm.^2).^(C*N/4*wm^2);
    G(i,1) = atan((w(i,1)-wm*sqrt(1.-damp^2))./wm/damp)-
             atan((w(i,1) +wm*sqrt(1.- damp^2))./wm/damp);
    ac4(i,1) = exp(N*wm*(D-C*damp*wm)./(2.*sqrt(1-damp^2)).*G(i,1));
    y(i,1) = ac1(i,1).*ac21(i,1).*ac22(i,1).*ac3(i,1).*ac4(i,1);
    f(i,1) = - 3.14+ N*(3.14/2 + B1/T1.*atan(w(i,1)*T1) + B2/T2.*atan(w(i,1)*T2)
             + C/2*wm^2*atan(2*w(i,1)*wm*damp/(wm^2-w(i,1)^2) - wm*(D-
             damp*wm*C)/4./sqrt(1.-damp^2)*log((w(i,1)^2+wm^2-2.*w(i,1)*
             wm*sqrt(1-damp^2))/(w(i,1)^2+wm^2+2.*w(i,1)*wm*sqrt(1-damp^2)))));
    RE(i,1) = y(i,1).*cos(f(i,1));
end
for j = 1:100
        if factor == 1
            z(i,1) = RE(i,1)./w(i,1).*sin(w(i,1).*t(j,1));
        end
```

```
    for i = 1: i1
        if  i == 1
            z0(i,1) = z(i,1);
        else
            z0(i,1) = z(i,1) + z0(i-1,1);
        end
    end
        if factor == 1
            P1(j,1) = 0.1*z0(i1,1);
        else
            P1(j,1) = y(14,1).*sin(w(14,1).*t(j,1) + f(14,1));
        end
    if j == 1
            P2(j,1) = P1(j,1).^2;
    else
            P2(j,1) = P1(j,1).^2 + P2(j-1,1);
    end
            P3(j,1) = 0.1*act^2*P2(j,1)./ t(j,1);
        if factor == 1
            P4(j,1) = 2./3.14*act*P1(j,1);
        else
            P4(j,1) = sqrt(P3(j,1));
        end
end
plot (w,P4); grid; xlabel('Time (s)'); ylabel('RMS miss (m)');
```

10.3 SOFTWARE FOR TIME-DOMAIN METHODS

Simulation in the time domain dominates analysis and design of missile systems because it enables us to examine the missile and target trajectories in real time and to analyze the influence of main missile parameters on its behavior. Each organization related to the aerospace industry has its own software, simple and complicated software programs that are used depending on the specifics of the problems under consideration.

Since the models of dynamic systems are described by differential equations, we will consider first the program demonstrating a numerical integration technique widely used for solving differential equations. Listing 10.8 presents the flight-control system dynamics simulation using the fourth-order Runge–Kutta method with an integration step size $H = 0.01$ s. The system of differential equations describing the flight-control dynamics is presented by equation (8.75), and the corresponding Runge–Kutta expressions are given in Appendix D [see equations (D7)–(D9)]. The commanded and real missile acceleration are denoted by *TAM*1 and *AM*1*F*, respectively. For definiteness, here we assumed *TAM*1 to be constant and equal to 1-g. The time constant, natural frequency, damping, and airframe zero frequency are denoted by *TACT*, *OM*, *ZET*, and *ZERO*, respectively. *K*0(*NN*), *K*1(*NN*), *K*2(*NN*), and *K*3(*NN*) are the Runge–Kutta coefficients that are calculated based on equations (D7)–(D9). The coefficients equal the derivatives evaluated at various times on the interval $[T, T+H]$; the period of integration is *Tf*. Since each following coefficient depends on the previous one, the *SUBROUTINE KINEMAT*1(*X, XD, TAM*1) is used to determine the Runge–Kutta coefficients; *X* and *XD* denote the system coordinates and their derivatives, respectively. The transfer function corresponding to the system of differential equations (8.75) is the product of the transfer function (8.20) describing the airframe dynamics of tail-controlled missiles and the transfer function describing the autopilot as a single-lag unit.

LISTING 10.8
FORTRAN Program to Simulate Flight Control Dynamics

```
IMPLICIT NONE
INTEGER NN, M
PARAMETER (NN = 3)
REAL*8   T, Tf, H, ZERO, AM1F, TAM1
REAL*8 X(NN), XX(NN), XD(NN), K0(NN), K1(NN), K2(NN), K3(NN)
        AM1F = 0.
        XX(1) = 0.
        XX(2) = 0.
        XX(3) = 0.
        XD(1) = 0.
        XD(2) = 0.
        XD(3) = 0.
        H = 0.01
        T = 0.
        Tf = 10.
        ZERO = 5.
        TAM1 = 9.81
50  CONTINUE
        T = T+H
    IF(T>Tf) GOTO 60
  CALL KINEMAT1(XX,XD,TAM1)
    DO  M = 1,3
        K0(M) = XD(M)
        X(M) = XX(M) + 0.5*H*K0(M)
    END DO
  CALL KINEMAT1(X,XD,TAM1)
    DO  M = 1,3
        K1(M) = XD(M)
        X(M) = XX(M) + 0.5*H*K1(M)
    END DO
  CALL KINEMAT1(X, XD, TAM1)
    DO   M = 1,3
        K2(M) = XD(M)
        X(M) = XX(M) + H*K2(M)
    END DO
  CALL KINEMAT1(X, XD, TAM1)
    DO   M = 1,3
        K3(M) = XD(M)
        XX(M) = XX(M) + H*(K0(M) + 2*(K1(M) + K2(M)) + K3(M))/6
    END DO
        AM1F = XX(1) - ZERO**(-2)*XX(3)
GOTO 50
20  CONTINUE
    WRITE(*,*) T, AM1F
    END DO
60  CONTINUE
    PAUSE
    END
  SUBROUTINE KINEMAT (X, XD, TAM1)
    PARAMETER (NN=3)
    REAL*8 X(NN), XD(NN)
```

```
    REAL*4  OM, ZET, TACT
    REAL*8  TAM1
        OM = 20.
        ZET = 0.7
        TACT = 0.5
      XD(1) = X(2)
      XD(2) = X(3)
      XD(3) = -((OM**2/TACT)*X(1)) -((OM**2 + 2.*ZET*OM/TACT)*X(2))&
              -((2.*ZET*OM + (1./TACT))*X(3)) + (OM**2/TACT)*TAM1
RETURN
END
```

In the program, *NN* is the order of the system of differential equations, which is 3 in the considered case. The statements of the program before statement *label* 50 initialize the system (i.e., set initial conditions). The *CALL KINEMAT*1(*XX*,*XD*,*TAM*1) transfers the program to the *SUBROUTINE KINEMAT*1(*X, XD, TAM*1).

Listing 10.9 presents a planar missile–target engagement simulation corresponding to the model in Figure 4.4 and Figure 4.10. We do not use the method of adjoints in the program. Now computers are so powerful that it does not take a lot of time to run the program several times, especially for the deterministic cases. Moreover, the method of adjoints is valid only for linear models. The miss distance is determined directly as a result of simulation for each time of flight Tf $\in$ [0.5, 10] in increments of 0.5 *s*. The statements of the program before statement *label* 10 initialize the system, that is, set initial conditions, including the target acceleration *AT*1 and closing velocity *VC*. The *SUBROUTINE KINEMAT* (*X*, *XD*, *TAM*1, *AT*1) is built based on the generalized missile guidance model (see Figure 4.10), which is described by the ninth-order (*NN* = 9) system of differential equations. The missile and target are presented by the third-order system of differential equations, respectively, similar to the subroutine of Listing 10.8 (in contrast to the missile parameters, the target parameter notations start with the letter "*T*"). The relative missile displacement *Y* is described by the second-order differential equation [see, e.g., equation (1.20)]. Similar to Listing 10.8, here the system of differential equations is integrated by using the fourth-order Runge–Kutta method with an integration step size *H* = 0.01 s.

LISTING 10.9
FORTRAN Program to Examine Miss Distance. Deterministic Case

```
IMPLICIT NONE
INTEGER    NN, M, J, STEP, GL
PARAMETER (NN = 8)
REAL*8  T, T1, Tf, Tgo, H, RTM, LOS, LOSD, TAM1, AT1,VC, N1
REAL*8  X(NN), XX(NN), XD(NN), K0(NN), K1(NN), K2(NN), K3(NN), XXold(NN)
REAL*8  YD, Y, Y1
        GL = 1
        VC = 1219.2
        AT1 = 3*9.81
    DO 60  Tf  = 0.5, 10., 0.5
        TAM1 = 0.
        XX(1) = 0.
        XX(2) = 0.
        XX(3) = 0.
        XX(4) = 0.
        XX(5) = 0.
        XX(6) = 0.
```

```
        XX(7) = 0.
        XX(8) = 0.
        XD(1) = 0.
        XD(2) = 0.
        XD(3) = 0.
        XD(4) = 0.
        XD(5) = 0.
        XD(6) = 0.
        XD(7) = 0.
        XD(8) = 0.
        H = 0.01
        T = 0.
        Y = 0.
        YD = 0.
        LOSD = 0.
        LOS = 0.
        RTM = VC*Tf
10  IF(T>Tf -0.0001) GOTO 999
    DO 30 J = 1, NN
        XXold(J) = XX(J)
30  CONTINUE
        Y =  XX(7)
        YD = XX(8)
        T1 = T
    STEP = 1
    GOTO 200
40  STEP = 2
  CALL KINEMAT(XX,XD,TAM1,AT1)
    DO M = 1, 8
    K0(M) = XD(M)
        X(M) = XXold(M) + 0.5*H*K0(M)
    END DO
        Y = XX(7)
        YD = XX(8)
        T1 = T + 0.5*H
    GOTO 200
41  STEP = 3
  CALL KINEMAT(X,XD,TAM1,AT1)
    DO M = 1, 8
        K1(M) = XD(M)
        X(M) = XXold(M) + 0.5*H*K1(M)
    END DO
        T1 = T + 0.5*H
        Y = X(7)
        YD = X(8)
    GOTO 200
42  STEP = 4
  CALL KINEMAT(XX,XD,TAM1,AT1)
    DO M = 1, 8
        K2(M) = XD(M)
        X(M) = XXold(M) + H*K2(M)
    END DO
        T1 = T+H
        Y = XX(7)
        YD = XX(8)
```

```
    GOTO 200
43  STEP = 5
  CALL KINEMAT(X,XD,TAM1,AT1)
    DO M = 1, 8
        K3(M) = XD(M)
        X(M) = XXold(M) + H*(K0(M) +2.*(K1(M)+K2(M)) +K3(M))/6.
    END DO
        T = T1
        Y = X(7)
        YD = X(8)
200 CONTINUE
        Tgo = Tf -T1 + 0.00001
        RTM = VC*Tgo
        LOS = Y/VC/Tgo
        LOSD = (RTM*YD + Y*VC)/(RTM**2)
    IF (GL == 1) THEN
        TAM1 = 4.*VC*LOSD
    ENDIF
    IF (GL == 2) THEN
        TAM1 = 4.*VC*LOSD + 4.*(10**4)*VC*LOSD**3
    ENDIF
    IF (GL == 3) THEN
        IF(AT1*LOSD<0.) THEN
            N1 = 0.75
        ELSE
            N1 = 1.25
        ENDIF
        TAM1 = 4.*VC*LOSD + 4.*(10**4)*VC*LOSD**3 + N1*AT1
    ENDIF
    IF (ABS(TAM1)> = 10.*9.81) THEN
        TAM1 = 10.*9.81*TAM1/ABS(TAM1)
    ENDIF
    IF(STEP == 1) THEN
    GOTO 40
    ELSEIF (STEP == 2) THEN
    GOTO 41
    ELSEIF (STEP == 3) THEN
    GOTO 42
    ELSEIF (STEP == 4) THEN
    GOTO 43
    ELSE
    GOTO 10
    ENDIF
999 CONTINUE
    Y1 = ABS(Y)
    WRITE(*,*) Tf ,Y1
60  CONTINUE
    PAUSE
    END
  SUBROUTINE KINEMAT (X, XD, TAM1, AT1)
    PARAMETER(NN = 8)
    REAL*8 X(NN),XD(NN)
    REAL*4 OM, ZET, TACT, ZERO, TOM, TZET, TTACT, TZERO
    REAL*8 TAM1, AT1
        OM = 20.
```

```
        ZET = 0.7
        TACT = 0.5
        ZERO = 5.
        TOM = 20.
        TZET = 0.7
        TTACT = 0.5
        TZERO = 20.
    XD(1) = X(2)
    XD(2) = X(3)
    XD(3) = - ((OM**2/TACT)*X(1)) - ((OM**2 + 2.*ZET*OM/TACT)*X(2))&
            - ((2.*ZET*OM + (1/TACT))*X(3)) + (OM**2/TACT)*TAM1
    XD(4) = X(5)
    XD(5) = X(6)
    XD(6) = - ((TOM**2/TTACT)*X(4)) - ((TOM**2 + 2.*TZET*TOM/TTACT)*X(5))&
            - ((2.*TZET*TOM + (1./TTACT))*X(6)) + (TOM**2/TTACT)*AT1
    XD(7) = X(8)
    XD(8) = (X(4) - TZERO**(-2)*X(6)) - (X(1)-ZERO**(-2)*X(3))
    RETURN
    END
```

Several types of guidance laws can be analyzed. The factor $GL = 1$ corresponds to PN guidance with the effective navigation ratio $N = 4$; the guidance law with the factor $GL = 2$ also includes the "cubic" term [see equation (5.64)], and the guidance law with the factor $GL = 3$ also includes the target acceleration term with a time-dependent gain [see equations (5.61) and (5.64)]. The expressions for these guidance laws are written based on equations (2.9)–(2.12) and (5.41). The line-of-sight, its derivative, range, and time-to-go are denoted as *LOS*, *LOSD*, *RTM*, and *Tgo*, respectively. The chosen acceleration limit equals 10-g. For definiteness, the parameters of the guidance laws are chosen similarly to the example of Chapter 5.

Listing 10.10 presents a VISUAL FORTRAN simulation for the planar model in Figure 4.4 assuming that the LOS measurements are corrupted by noise. The LOS noise (*LOSNOISE*) is zero-mean Gaussian noise, with standard deviation *SIGNOISE* generated by the *FUNCTION* gasdev(idum). The noise inputs the model every *TS* seconds [see statement *IF* ($S < TS - 0.0001$) GOTO 10]. The α,β filter is used in the considered model ($R1 = 0.4$, $R2 = 0.1/TS$). Its equations are given between statement *labels* 75 *and* 77 [see equations (8.35)–(8.37)]. The measured LOS and its derivative are denoted *LOSH* and *LOSDH*, respectively. They are used in the guidance laws analogously to the program of Listing 10.9. The miss distance mean *Ymean*, its absolute value *Y*1, and standard deviation *SIGMA* are given for each flight time of interest *Tf* after 50 simulation trials (see *DO* 20; *RUN* = 50). The loop *DO* 60 enables us to obtain the above-mentioned miss distance estimates for different flight times ranging from 0.5 *s* to 10 *s* in increment of 0.5 *s*.

LISTING 10.10
FORTRAN Program to Examine Miss Distance. Stochastic Case

```
IMPLICIT NONE
INTEGER NN, M, I, STEP, RUN, idum, GL
PARAMETER (NN = 3)
REAL gasdev
DIMENSION Z(5000)
REAL*8   S, T, Tf, Tgo, H, TS, R1, R2, ZERO
REAL*8   LOS, LOSD, LOSH, LOSDH, RTM, VC, AT1, TAM1, AM1F, N1
REAL*8   X(NN), XX(NN), XD(NN), K0(NN), K1(NN), K2(NN), K3(NN)
REAL*8   SIGNOISE, LOSNOISE, RESLOS, Z1, SIGMA, Z
REAL*8   Ymean, YOLD,YDOLD, Y, YD, Y1, e
```

```
        GL = 1
        RUN = 50
        idum = 425001
        VC = 1219.2
        AT1 = 3*9.81
        ZERO = 5.
        SIGNOISE = 0.001
        TS = 0.1
        H = 0.001
    DO 60 Tf = 0.5, 10., 0.1
        Z1 = 0.
    DO 20  I = 1, RUN
        AM1F = 0.
        TAM1 = 0.
        XX(1) = 0.
        XX(2) = 0.
        XX(3) = 0.
        XD(1) = 0.
        XD(2) = 0.
        XD(3) = 0.
        T = 0.
        S = 0.
        YD =0.
        Y = 0.
        YOLD = 0.
        YDOLD = 0.
        e = 0.
        LOSD = 0.
10  IF(T > Tf - 0.0001) GOTO 999
        YOLD = Y
        YDOLD = YD
    STEP =1
    GOTO 200
66  STEP = 2
        Y = Y +H*YD
        YD = YD +H*e
        T = T+H
    GOTO 200
55  CONTINUE
        Y = 0.5*(YOLD + Y + H*YD)
        YD = 0.5*(YDOLD +YD + H*e)
        S = S + H
    IF (S < TS - 0.0001) GOTO 10
        S = 0.
        LOSNOISE = gasdev(idum)*SIGNOISE
75      R1 = 0.4
        R2 = 0.1/TS
        RESLOS = LOS + LOSNOISE  – (LOSH +TS*LOSDH)
        LOSH = LOSH + TS* LOSDH + R1*RESLOS
77      LOSDH = LOSDH + R2*RESLOS
    IF (GL == 1)THEN
        TAM1 = 4*VC*LOSDH
    ENDIF
    IF (GL == 2)THEN
        TAM1 = 4*VC*LOSDH  + 4*(10**4)*VC*LOSDH**3
    ENDIF
```

```
    IF (GL == 3)THEN
        IF(AT1*LOSDH<0.) THEN
            N1 = 0.75
        ELSE
            N1 = 1.25
        ENDIF
        TAM1 = 4.*VC*LOSDH   + 4.*(10**4)*VC*LOSDH**3 + N1*AT1
    ENDIF
    IF (ABS(TAM1)> = 10.*9.81) THEN
         TAM1 = 10.*9.81*TAM1/ABS(TAM1)
    ENDIF
33  CONTINUE
    CALL KINEMAT(XX,XD,TAM1)
    DO  M = 1, 3
        K0(M) = XD(M)
        X(M) = XX(M) + 0.5*H*K0(M)
    END DO
    CALL KINEMAT (X, XD,TAM1)
    DO  M = 1, 3
        K1(M) = XD(M)
        X(M) = XX(M) + 0.5*H*K1(M)
    END DO
    CALL KINEMAT (X, XD, TAM1)
    DO  M = 1, 3
        K2(M) = XD(M)
        X(M) = XX(M) + H*K2(M)
    END DO
    CALL KINEMAT(X,XD, TAM1)
    DO  M = 1, 3
        K3(M) = XD(M)
        XX(M) = XX(M) + H*(K0(M) + 2.*(K1(M) + K2(M)) + K3(M))/6
    END DO
        AM1F = XX(1) – ZERO**(-2)*XX(3))
        e = AT1-AM1F
    GOTO 10
200 CONTINUE
        Tgo = Tf - T + 0.00001
        RTM = VC *Tgo
        LOS = Y/VC/Tgo
        LOSD = (RTM*YD + Y*VC)/(RTM**2)
    IF(STEP - 1)66,66,55
999 CONTINUE
        Z(I) = Y
        Z1 = Z(I) + Z1
        Ymean = Z1/I
        Y1 = ABS(Ymean)
20  CONTINUE
        SIGMA = 0.
        Z1 = 0.
    DO  50 I = 1,RUN
        Z1 = (Z(I)-Ymean)**2 +Z1
    IF (I == 1) THEN
        SIGMA = 0.
    ELSE
        SIGMA = SQRT(Z1/(I-1))
    ENDIF
```

```
50  CONTINUE
    WRITE(*,*) Tf, Y1, SIGMA
60  CONTINUE
    PAUSE
    END
    SUBROUTINE KINEMAT (X, XD, TAM1)
    PARAMETER (NN = 3)
    REAL*8  X(NN), XD(NN)
    REAL*4 OM, ZET, TACT
    REAL*8  TAM1
        OM = 20.
        ZET = 0.7
        TACT = 0.5
        XD(1) = X(2)
        XD(2) = X(3)
        XD(3) = - ((OM**2/TACT)*X(1)) - ((OM**2 + 2.*ZET*OM/TACT)*X(2))&
                - ((2.*ZET*OM+ (1./TACT))*X(3)) + (OM**2/TACT)*TAM1
    RETURN
    END
    FUNCTION gasdev(idum)
    INTEGER idum
    REAL gasdev
    INTEGER iset
    REAL fac,gset,rsq,v1,v2,ran
    SAVE iset,gset
    DATA iset/0/
    IF (iset.eq.0) THEN
1           v1 =2.*ran(idum)-1.
            v2 =2.*ran(idum)-1.
            rsq = v1**2+v2**2
    IF(rsq.ge.1..or. rsq.eq.0.)GOTO 1
            fac = sqrt(-2.*log(rsq)/rsq)
            gset = v1*fac
            gasdev = v2*fac
            iset = 1
    ELSE
            gasdev = gset
            iset = 0
    ENDIF
    RETURN
    END
```

The deterministic part of the program is slightly different from the program of Listing 10.9. Instead of the generalized missile model (see Figure 4.10), here we ignore target dynamics (see Figure 4.4), so that we operate with the fifth-order system of differential equations. As an alternative of the fourth-order Runge–Kutta method to this system we use it with the third-order system of differential equations describing the missile dynamics, as presented in Listing 10.8, and use the second-order Runge–Kutta method for the double integration procedure [see equation (1.20)]. For small integration steps *H*, the error is negligibly small. Analogous to Listing 10.9, the statements of the program before statement *label* 10 initialize the system for each flight time *Tf*. The *SUBROUTINE KINEMAT*1(*X*, *XD*, *TAM*1) is similar to the subroutine of Listing 10.8. The LOS, its derivative, range, and time-to-go are denoted as *LOS*, *LOSD*, *RTM*, and *Tgo*, respectively; *e* is the difference between the target and missile accelerations. The chosen acceleration limit equals 10-g. For definiteness, the parameters of the guidance laws are chosen similarly to the example of Chapter 5.

Listing 10.11 presents a VISUAL FORTRAN simulation to calculate the miss distance for both deterministic and stochastic cases. It combines the programs of Listings 10.9 and 10.10. We give below only a part of the program that should combine the mentioned programs, indicating mostly the modified part of the new program. The parts that should be added from the programs of Listings 10.9 and 10.10 are obvious. The new feature of this program is the parameter *filter*. Its zero value corresponds to the deterministic case; in this case the integer *RUN* equals 1 (see statement *labels* 11 and 12).

LISTING 10.11
FORTRAN Program to Examine Miss Distance. General Case

```
IMPLICIT NONE
INTEGER  RUN, idum, GL, filter
REAL gasdev
DIMENSION Z(5000)
REAL*8  S,  TS,  R1, R2, ZERO
REAL*8  LOSH, LOSDH,  RESLOS
REAL*8  Ymean,  SIGNOISE, LOSNOISE, RES,  SIGMA, Z, Z1
11      RUN = 50
        idum = 425001
        SIGNOISE = 0.001
        TS = 0.1
        filter = 1
    IF( filter == 0.) THEN
        RUN = 1
    ENDIF
        .................................................................
    DO 60 Tf = 0.5, 10., 0.1
        Z1 = 0.
12  DO 20  I = 1, RUN
        .................................................................
        LOSDH = 0.
        LOSH = 0.
        RTM = VC*Tf
10  IF(T>Tf-0.0001) GOTO 999
        S=S+H
        .................................................................
95  CONTINUE
    IF(filter == 0.) GOTO 10
    IF(S<(TS - 0.0001)) GOTO 10
        S = 0.
        LOSNOISE = gasdev(idum)*SIGNOISE
        R1 = 0.4
        R2 = 0.1/TS
        LOS = Y/VC/Tgo
        LOSD = (RTM*YD+Y*VC)/(RTM**2)
        RESLOS = LOS+LOSNOISE-(LOSH+TS*LOSDH)
        LOSH = LOSH+TS*LOSDH+R1*RESLOS
        LOSDH = LOSDH+R2*RESLOS
    GOTO 10
200 CONTINUE
        Tgo = Tf-T1 + 0.00001
        RTM = VC*Tgo
```

```
        LOS = Y/VC/Tgo
        LOSD = (RTM*YD+Y*VC)/(RTM**2)
    IF( filter == 0.) THEN
        LOS = LOSH
        LOSD = LOSDH
        GOTO  50
    ENDIF
        .........................................................................
999 CONTINUE
        Z(I) = Y
        Z1 = Z(I) + Z1
        Ymean = Z1/I
        Y1 = ABS(Ymean)
20  CONTINUE
        SIGMA = 0.
        Z1 = 0.
    DO 50 I = 1,RUN
        Z1 = (Z(I)-Ymean)**2 +Z1
    IF (I == 1) THEN
        SIGMA = 0.
    ELSE
        SIGMA = SQRT(Z1/(I-1))
    ENDIF
50  CONTINUE
    WRITE(*,*) Tf, Y1, SIGMA
60  CONTINUE
    PAUSE
    END
```

Listing 10.12 presents a VISUAL FORTRAN simulation using the Kalman filtering technique. We consider the widespread near-constant acceleration tracking model discussed in Chapter 8 [see equations (8.58) and (8.61)]. The program contains the Riccati equations and expressions for the Kalman filter gains *K*1, *K*2, and *K*3. Assuming that a constant acceleration component *ATH* of a target equals 3-g and its *y*-coordinate trajectory is presented by *YT,* we consider the Kalman filter for the stochastic process with a measurement noise *SIGNOISE1* and a process noise *SIGNOISE2*; both of them are the zero-mean white noise processes with the standard deviation SIGN1 and SIGN2, respectively [see equation (8.47)–(8.52), (8.58), and (8.61)].

LISTING 10.12
FORTRAN Program. Target Parameters Estimation Using Kalman Filter

```
IMPLICIT NONE
INTEGER  RUN, idum
REAL gasdev
REAL*8  P11, P12, P13, P22, P23, P33, M11, M12, M13, M22, M23, M33, K1, K2, K3
REAL*8   YT, YTH, YTDH, ATH, RES, Tf, T, T1, S, H, TS2, TS3, TS4, TS5
REAL*8  ATNOISE, YTNOISE, SIGNOISE1, SIGNOISE2, SIGN1, SIGN2
        RUN = 50
        indum = 425001
        Tf = 10.
        TS = 0.1
        H = 0.01
        SIGNOISE1 = 10.
```

```
        SIGNOISE2 = 10.
        TS2 = TS*TS
        TS3 = TS2*TS
        TS4 = TS3*TS
        TS5 = TS4*TS
        SIGN1 = SIGNOISE1**2
        SIGN2 = SIGNOISE2**2
    DO 20  I = 1, RUN
        P11 = SIGN1
        P12 = 0.
        P13 = 0.
        P23 = 0.
        P22 = 5.**2
        P33 = SIGN2
        YTH = 2500.
        YTDH = 30.
        ATH = 3.*9.81
        T = 0.
        S = 0.
        YD = 0.
        Y = 0.
10  IF(T > Tf - 0.0001) GOTO 999
        T = T+H
        S = S+H
    IF(S < TS - 0.0001) GOTO 100
        S = 0.
        YTNOISE = gasdev(idum)*SIGNOISE1
11      YT = 2500. + 35.*T  +3.*9.81*T**2
        M11 = P11+ TS*P12 + 0.5*TS2*P13 + TS*(P12+TS*P22+0.5*TS2*P23)
        M11 = M11+0.5*TS2*(P13+TS*P23 + 0.5*TS2*P33) + TS5* SIGN2/20
        M12 = P12 +TS*P22 +0.5*TS2*P23 + TS*(P13 +TS*P23+0.5*TS2*P33) +TS4* SIGN2/8
        M13 = P13 + TS*P23 + 0.5* TS2*P33 + TS3* SIGN2/6
        M22 = P22 + TS*P23 + TS*(P23+TS*P33) + SIGN2*TS3/3
        M23 = P23 + TS*P33 +0.5*TS2* SIGN2
        M33 = P33 + SIGN2*TS
        K1 = M11/(M11+SIGN1)
        K2 = M12/(M11+SIGN1)
        K3 = M13/(M11+SIGN1)
        P11 = (1.-K1)*M11
        P12 = (1.-K1)*M12
        P13 = (1.-K1)*M13
        P22 = -K2*M12 + M22
        P23 = -K2*M13 + M23
        P11 = -K3*M13 + M33
        RES = YT + YTNOISE – YTH - TS*YDH - 0.5*TS*TS*ATH
75      YTH = YTH+TS*YTDH  + 0.5*TS*TS*ATH + K1*RES
76      YTDH = YTDH + TS*ATH + K2*RES
77      ATH = ATH + TS*ATH + K3*RES
100 CONTINUE
        T1 = T
999 WRITE(*,*) T1, YTH
20  CONTINUE
    PAUSE
    END
```

Instead of the Riccati equation in the form (8.48) and (8.49) here we use the equivalent form

$$M_n = A_n P_{n-1} A_n^T + B_n Q_n B_n^T, \; K_n = M_n H^T [H M_n H^T + R_n], \; P_n = (I - K_n H_n) M_n \qquad (10.2)$$

where $M_n = P(n,n\text{-}1)$, $P_n = P(n, n)$ [see equations (8.48) and (8.51)], A_n, H_n, and $B_n Q_n B_n^T$ are presented by equations (8.58) and (8.61), respectively, and $R_n = (SIGNOISE1)2$. The estimates of Y, its derivative YD, and the target acceleration AT are given by statement *labels* 75–77.

The programs considered above can be used only at the initial stage of analysis and design. The discussed planar models do not allow users to obtain reliable estimates of the miss distance for weave maneuvers. These models and the corresponding computational programs are effective for qualitative rather than quantitative analysis. They are efficient for testing some ideas, for comparing various guidance laws, and for analyzing the influence of various parameters on missile performance. To obtain more precise and reliable estimates, the 3-DOF and 6-DOF engagement models should be used. The components of the programs considered above can be used as parts of the computational programs corresponding to these more complicated models.

Listing 10.13 presents the most important components of the main part of the computational program of three-dimensional engagement simulation based on the 3-DOF missile model discussed in Chapter 8. We do not present here information about the target position, velocity and acceleration, the initial missile position, velocity and acceleration, flight time, the aerodynamic parameters of the missile, or thrust and drag data, that is, all information required to build the 3-DOF missile model. We assume that this information is contained in specially created modules (a module is a set of declarations that are grouped together under a global name and are made available to other program units by using the USE statement) and is available by using the appropriate *CALL* statements. For example, the missile position, velocity, and acceleration at the beginning of the controlled boost stage of flight are generated by the statement *CALL boost* (*Tin*, *T*, *RM*1, *RM*2, *RM*3, *VM*1, *VM*2, *VM*3, *AM*1*F*, *AM*2*F*, *AM*3*F*), where *Tin* is time of launch, the beginning of the controlled boost stage, *T* is time counted after launch, *RMi*, *VMi*, and *AMiF* (i = 1–3) are the missile position, velocity, and acceleration; indices 1, 2, and 3 correspond to north, east, and down coordinates of the NED coordinate system, respectively. If we simulate the midcourse or homing stages the analogous information should be input by the statement *CALL initial* (*T*, *RM*1, *RM*2, *RM*3, *VM*1, *VM*2, *VM*3, *AM*1*F*, *AM*2*F*, *AM*3*F*). Thrust and drag data should be entered by the statements *CALL thrust* and *CALL drag*, respectively. It is worthwhile to include in a separate module various parameters of the missile model (their values differ for different types of missiles), which are entered in the main program by *CALL var*.

We assume that readers who are interested in creating the three-dimensional engagement computational program based on Listing 10.13 are familiar with the basics of VISUAL FORTRAN, can declare the variables used in the program, and write the auxiliary programs that are called by the main program. Even if thrust and drag components of total missile acceleration are ignored (it can be justified for some scenarios during the homing stage), the three-dimensional engagement simulation program enables us to obtain more accurate results than the computational programs based on the missile guidance model in Figure 4.4. Readers can easily simplify the missile–target engagement simulation program to use it instead of the programs of Listings 10.9–10.11. The symbol "!," indicating that the statement of a certain line is ignored, will be used for comments that should be added in the program to make it workable.

The integration step size *H* is different for the midcourse and homing stages. For the midcourse stage the sampling interval *H*1 = 0.25 *s* and *H* = 0.02 *s*. For the homing stage (range RTM < 1000 *m*) the sampling interval *H*1 = 0.01 *s* and *H* = 0.001 *s*. During the sampling interval *H*1 the missile commanded acceleration, thrust, and drag are constant; the real missile acceleration *AMiF* (i = 1–3) changes depending on the missile dynamic characteristics. The subroutine *CALL KINEMAT* (*XX*, *XD*,

LISTING 10.13
FORTRAN Three-Dimensional Engagement Simulation

```
use mboost, only : boost
use track,   only : track_smooth
use minitial, only : initial
use mthrust, only: thrust
use mdrag, only: drag
use mvar, only: var

IMPLICIT NONE
! VARIABLE DECLARATIONS
    CALL thrust(THRUST)
    CALL drag(DRAG)
    CALL var(KVECTOR)
    CALL boost (Tin, RM1, RM2, RM3, VM1, VM2, VM3, AM1F, AM2F, AM3F)
!   CALL initial (Tk, RM1, RM2, RM3, VM1, VM2, VM3, AM1F, AM2F, AM3F)
        g = 9.81
        Tk = Tin +T
        T1 = Tk
    CALL track_smooth(Tk, RT1, RT2, RT3, VT1, VT2, VT3, AT1, AT2, AT3)
        S = 0.
        RTM1 = RT1-RM1
        RTM2 = RT2-RM2
        RTM3 = RT3-RM3
        RTM = SQRT(RTM1**2 + RTM2**2 + RTM3**2)
        LOS1 = RTM1/RTM
        LOS2 = RTM2/RTM
        LOS3 = RTM3/RTM
        VTM1  =  VT1-VM1
        VTM2  =  VT2-VM2
        VTM3  =  VT3-VM3
        VC  =  -(RTM1*VTM1  +  RTM2*VTM2  +  RTM3*VTM3)/RTM
        LOS1D = (VTM1 + LOS1* VC)/RTM
        LOS2D = (VTM2 + LOS2* VC)/RTM
        LOS3D = (VTM3 + LOS3* VC)/RTM
    GOTO 10
40  CONTINUE
    IF (T1 + H + epsilon(H) < Tk + H1) THEN
        T1 = T1+H
        T = T+H
    GOTO 23
    ELSE
        Tk = Tk + H1
        T = Tk – Tin
    ENDIF
23      RM1 = RM1OLD + 0.5*H*H*AM1F + VM1OLD*H
        RM2 = RM2OLD + 0.5*H*H*AM2F + VM2OLD*H
        RM3 = RM3OLD + 0.5*H*H*AM3F + VM3OLD*H
        VM1 = VM1OLD + H*AM1F
        VM2 = VM2OLD + H*AM2F
        VM3 = VM3OLD + H*AM3F
        VM = SQRT(VM1**2 + VM2**2 + VM3**2)
        UVM1 = VM1/VM
        UVM2 = VM2/VM
```

```
        UVM3 = VM3/VM
        S = S + H
75  IF (S<0.09999 ) GOTO 10
        S = 0.
76  WRITE(*,*)T, RTM1, RTM2, RTM3
10  IF (VC<0.) GOTO 999
        RM1OLD = RM1
        RM2OLD = RM2
        RM3OLD = RM3
        VM1OLD = VM1
        VM2OLD = VM2
        VM3OLD = VM3
    IF(T1 > Tk) GOTO 33
        T1 = Tk
78  IF(RTM<RG) THEN
        H = 0.001
        H1 = 0.01
    ELSE
        Thom = T
        H = 0.01
        H1 = 0.25
    ENDIF

CALL track_smooth(Tk, RT1,RT2, RT3, VT1, VT2, VT3, AT1, AT2, AT3)
        RTM1 = RT1-RM1
        RTM2 = RT2-RM2
        RTM3 = RT3-RM3
        RTM = SQRT(RTM1**2 + RTM2**2 + RTM3**2)
        LOS1 = RTM1/RTM
        LOS2 = RTM2/RTM
        LOS3 = RTM3/RTM
        VTM1 = VT1-VM1
        VTM2 = VT2-VM2
        VTM3 = VT3-VM3
        VC = -(RTM1*VTM1 + RTM2*VTM2 + RTM3*VTM3)/RTM
    IF (VC<0.) GOTO 999
        LOS1D = (VTM1 + LOS1* VC)/RTM
        LOS2D = (VTM2 + LOS2* VC)/RTM
        LOS3D = (VTM3 + LOS3* VC)/RTM
        AM1 = 4.*VC*LOS1D
        AM2 = 4.*VC*LOS2D
        AM3 = 4.*VC*LOS3D-g
        AL = (AM1*UVM1 + AM2*UVM2 + AM3*UVM3)
        AL1 = AL*UVM1
        AL2 = AL*UVM2
        AL3 = AL*UVM3
        NAC1 = AM1 — AL1
        NAC2 = AM2 — AL2
        NAC3 = AM3 — AL3
        NAC = SQRT(NAC1**2 + NAC2**2 + NAC3**2)
    IF  (NAC == 0.) THEN
        UNAC1 = 0.
        UNAC2 = 0.
        UNAC3 = 0.
    ELSE
        UNAC1 = NAC1/NAC
```

```
        UNAC2 = NAC2/NAC
        UNAC3 = NAC3/NAC
    ENDIF
        UB1 = UVM1*COS(AOA) + UNAC1*SIN(AOA)
        UB2 = UVM2*COS(AOA) + UNAC2*SIN(AOA)
        UB3 = UVM3*COS(AOA) + UNAC3*SIN(AOA)
        AB = AM1*UB1 + AM2*UB2 + AM3*UB3
        AB1 = AB*UB1
        AB2 = AB*UB2
        AB3 = AB*UB3
        AMN1 = AM1 —AB1
        AMN2 = AM2 —AB2
        AMN3 = AM3 —AB3
        AMN = SQRT(AMN1**2 + AMN2**2 + AMN3**2)
        G1 = MIN(K1-K3*(VM/340.)*Q, K5)
        G2 = MIN(K2-K4*(VM/340.)*Q, K5)
        BT1 = K6
        BT2 = K7
        NLIM = G1 + (G2-G1)*(T-BT1)/BT2
    IF (AMN>NLIM) THEN
        LIMFAC = NLIM/AMN
    ELSE
        LIMFAC = 1.
    ENDIF
        AMN1 = AMN1*LIMFAC
        AMN2 = AMN2*LIMFAC
        AMN3 = AMN3*LIMFAC
        AMN = SQRT(AMN1**2 + AMN2**2 + AMN3**2)
        CN = AMN /Q/Sref
77      AOA = K8+K9*CN+K10*(CN**2)
    CALL thrust(THRUST)
    CALL drag (DRAG)

        TAM1 = THRUST* UB1 - DRAG* UVM1 + AMN1
        TAM2 = THRUST* UB2 - DRAG* UVM2 + AMN2
        TAM3 = THRUST* UB3 - DRAG* UVM3 + AMN3
        TAM = SQRT(TAM1**2 + TAM2**2 + TAM3**2)

33      B2 = -1./wz**2
    CALL KINEMAT(XX, XD, TAM1, TAM2, TAM3)
    DO  M = 1,9
        K0(M) = XD(M)
        X(M) = XX(M) + 0.5*H*K0(M)
    END DO
    CALL KINEMAT(X, XD, TAM1, TAM2, TAM3)
    DO  M = 1,9
        K1(M) = XD(M)
        X(M) = XX(M) + 0.5*H*K1(M)
    END DO
    CALL KINEMAT(X, XD, TAM1, TAM2, TAM3)
    DO  M = 1,9
        K2(M) = XD(M)
        X(M) = XX(M) + H*K2(M)
    END DO
    CALL KINEMAT(X, XD, TAM1, TAM2, TAM3)
    DO  M = 1,9
```

```
        K3(M) = XD(M)
        XX(M) = XX(M)+ H*(K0(M) + 2.*(K1(M) + K2(M)) + K3(M))/6
    END DO
        AM1F = XX(1) + (B2*XX(3))
        AM2F = XX(4) + (B2*XX(6))
        AM3F = XX(7) + (B2*XX(9))
    GOTO 40
999 CONTINUE
    WRITE(*,*) T, RT1, RT2, RT3, RM1, RM2, RM3, RTM
    PAUSE
    END
```

TAM1, *TAM*2, *TAM*3) is similar to the subroutine described in Listings 10.8 and 10.10, only here we deal with the three-dimensional model, so that the expressions of Listing 10.8 for the acceleration component *TAM*1 should be repeated for two other components *TAM*2 and *TAM*3; the dimension of the system of differential equations $M = 9$ and the relationship between *AMiF* and *TAMi* ($i = 1$–3) is similar to the relationship between *AM*1*F* and *TAM*1 of Listing 10.8. Writing such a program does not present any difficulty. The *IF*(*T*1 > *Tk*) *GOTO* 33 statement, where *Tk* is the time counted with the step *H*1 and *T*1 is the time counted with the step *H*, enables the program to calculate the missile position *RMi*, velocity *VMi*, and acceleration *AMiF* ($i = 1$–3) between sampling instants (i.e., within *H*1 intervals). The target information [its position *RTi,* velocity *VTi*, and, if it is available, acceleration *ATi* ($i = 1$–3)] enters the main program each *H*1 seconds [see statement *CALL* track_smooth(*Tk*, *RT*1, *RT*2, *RT*3, *VT*1, *VT*2, *VT*3, *AT*1, *AT*2, *AT*3)]. It is assumed that the estimates of the target parameters indicated above are obtained by filtering the results of the measurements of these parameters. The computational program of Listing 10.12, generalized for the three-dimensional case, can be used to produce such estimates. It is possible to use the α,β filter considered in the computational program in Listing 10.10. The Kalman filters are now more popular than the α,β filters; however, the latter type of filter is still widely used in practice. As indicated in Chapter 8, to estimate the target acceleration the α,β,γ filter should be used. The computational program in Listing 10.10 can be easily enhanced for this cased based on equations (8.40)–(8.43).

Based on the missile and target data at moment T_k, range vector *RTM*, and closing velocity *VC*, the components of the line-of sight *LOSi* and its derivative *LOSDi* ($i = 1$–3) are determined [see equations (1.8), (1.11), and (1.12)]. The LOS rates are used in the guidance law, a commanded acceleration *AMi* ($i = 1$–3). For simplicity, here we considered only PN guidance with the effective navigation ratio equal to 4. The compensation of the gravity force is applied to its "down" component. More complicated guidance laws can be included in the program, similar to Listings 10.9 and 10.10 (some of them require the estimates of target acceleration components). As indicated in Chapter 8, for tail-controlled missiles based on the estimate of the angle of attack *AOA* [this part of the program should be created separately, as described in Chapter 8; see equations (8.65) and (8.66)], the components of the commanded missile acceleration orthogonal to the missile body should be calculated. First, the projection *AL* of the guidance law commanded acceleration *AMi* on the velocity vector and its components *ALi* ($i = 1$–3) are determined [*UVMi* are the components of the unit velocity vector; see equations (8.67) and (8.68)]. Then the acceleration normal to the velocity vector *NAC* = (*NAC*1, *NAC*2, *NAC*3) [see equation (8.69)] and the unit vector *UNAC* = (*UNAC1, UNAC*2, *UNAC*3) orthogonal to the velocity vector [see equation (8.70)] are calculated. Based on the unit vector along the body axis *UB* = (*UB*1, *UB*2, *UB*3) [see equation (8.71)], the components of the commanded acceleration normal to the missile body *AMN* = (*AMN*1, *AMN*2, *AMN*3) are determined according to equation (8.72); preliminarily, the projection *AB* of the guidance law commanded acceleration *AMi* on the body axis and its components *ABi* ($i = 1$–3) are determined.

As mentioned in Chapter 8, the autopilot acceleration limit *NLIM* (pitch, roll/yaw) can be presented by half-empirical expressions. They reflect the fact that during flight the missile is

subjected to varying pressure depending on the missile altitude and velocity. In the program this limit is presented in a general form, and the coefficients $K1$–$K7$ should be specified. The normal component of the guidance law is presented according to equation (8.73). The normal force coefficient *CN* is determined based on the expression analogous to equation (8.3). Its values can be used to determine approximately the angle of attack. Statement *label* 77 presents a simple regression expression to determine *AOA*; in reality, in this part of the program a more sophisticated algorithm, similar to the algorithms discussed in Chapter 8, should be introduced. The total acceleration *TAMi* ($i = 1$–3), consisting of the sum of the normal component of the guidance law, thrust, and drag, serves the input of the system of differential equations describing the flight-control system dynamics [see equation (8.75)]. Its output, a real missile acceleration *AMiF* ($i = 1$–3), is integrated twice using equation (8.64), so that the new missile position and velocity are determined. Based on the new information about the target, the new cycle of iterations begins. The status of the missile and target location is displayed every 0.1 *s* (see *labels* 75 and 76). In the program the homing time *Thom* is determined by $RTM = RG$. It can also be estimated in advance. In this case, the statement with *label* 78 should be written directly with respect to *Thom*. The simulation is terminated when the closing velocity changes sign, since it means that the distance between the missile and target reached a minimum.

To understand the above program (more precisely, the part of a workable program) the reader needs general programming knowledge. To make it workable, the reader does not need sophisticated programming techniques but does need understanding and insight. The indicated modules that should be created present relatively simple programs. The main difficulty is to get data upon which these programs can be created. As mentioned earlier, even if the thrust and drag information is not available, the simplified version of the three-dimensional engagement simulation program enables us to obtain more accurate results than the computational programs based on the missile guidance model in Figure 4.4. The described program can be enhanced and includes more efficient laws than PN guidance. It can be used as part of a more sophisticated program including the 6-DOF missile model. The author hopes that he did not insult talented artists by suggesting that a sophisticated program resembles real art. He also hopes that this book will arm the reader with knowledge that can be used to create sophisticated computational programs satisfying the requirements and taste of their creators.

REFERENCES

1. Chapman, S.J., *Introduction to Fortran* 90/95, McGraw-Hill, Boston, 1998.
2. Etzel, M. and Dickinson, K., *Digital Visual Fortran 90 Programmer's Guide*, Digital Press, Boston, 1999.
3. Higham, D.J. and Higham, N.J., *MATLAB Guide*, SIAM, Philadelphia, 2000.
4. Zarchan, P., Tactical and strategic missile guidance, *Progress in Aeronautics and Astroronautics*, 124, AIAA, Washington, DC, 1999.

Glossary

Active homing guidance A system of homing guidance wherein both the source for illuminating the target and the receiver for detecting the energy reflected from the target as the result of the illumination are carried within the missile.

Actuator A mechanism that furnishes the force required to displace a control surface or other control element.

Aegis A computerized combat system used on U.S. Navy ships capable of simultaneous operation against surface, underwater, and air threats.

Aerodynamic missile A missile that uses aerodynamic forces to maintain its flight path. See also ballistic missile; guided missile.

Airfoil A part or surface, such as a wing, canard, or tail, whose shape and orientation control stability, direction, and lift.

Air-based system An antimissile system weapon fired from an aircraft.

Air-launched ballistic missile A ballistic missile launched from an airborne vehicle.

Altitude The vertical distance of a level, a point, or an object considered as a point, measured from mean sea level.

Angle of attack The angle between the missile longitudinal **x**-axis and the projection of the missile velocity vector on the **xz** plane.

Aspect angle The angle between the longitudinal axis of the target (projected rearward) and the line-of-sight to the interceptor measured from the tail of the target.

Attitude The position of a body as determined by the orientation of its axes with respect to some frame of reference. If not otherwise specified, this frame of reference is fixed to the Earth.

Autopilot A mechanical, electrical, or hydraulic system used to guide a vehicle without assistance from a human being.

Azimuth In astronomy, the horizontal angular distance from a reference direction, usually the northern point of the horizon, to the point where a vertical circle, passing through a celestial body, intersects the horizon, usually measured clockwise.

Azimuth angle An angle measured clockwise in the horizontal plane between a reference direction and any other line.

Ballistic missile A missile that after an initial burst of power coasts toward its target without any significant lift from its surface to alter the course of flight. Part or most of the missile's trajectory is not subject to propulsion or control.

Ballistic trajectory The trajectory traced after the propulsive force is terminated and the body is acted upon only by gravity and aerodynamic drag.

Booster An auxiliary or initial propulsion system that travels with a missile and that may or may not separate from the parent craft when its impulse has been delivered. A booster system may contain, or consist of, one or more units.

Boost phase The first phase of a missile's trajectory as the missile flies with its booster still burning. In the case when part of the boost phase can be controlled, the terms *controlled* and *uncontrolled boost stages* are used. Often the boost phase is identified only with the uncontrolled boost stage, that is, it is a part of the missile flight between initial firing and the time when the missile reaches a velocity at which it can be controlled.

Canard A small surface forward on the body used as an aerodynamic control.

Closing velocity The negative derivative of the range.

Countermeasures Measures taken by an attacker to deceive a missile defense system (jammers, decoys, and chaff).

Drag Force of aerodynamic resistance most influenced by the viscosity of the medium in which the missile is traveling. Drag acts along the velocity vector and impedes the missile's motion.

Doppler effect The phenomenon evidenced by the change in the observed frequency of the reflected wave caused by a time rate of change in the effective length of the path of travel between the source and the point of observation.

Doppler radar A radar system that differentiates between fixed and moving targets by detecting the apparent change in frequency of the reflected wave due to motion of the target or the observer.

Early-warning radar A surveillance radar that provides detection and tracking of approaching missiles or aircraft.

Elevation The vertical distance of a point or level on or affixed to the surface of the Earth measured from mean sea level. See also altitude.

Elevation angle An angle measured clockwise in the vertical plane between a reference direction and any other line.

Endo-atmospheric Less than one hundred kilometers above the Earth's surface.

Engagement In air defense, an attack with guns or air-to-air missiles by an interceptor aircraft, or the launch of an air defense missile by air defense artillery and the missile's subsequent travel to intercept.

Exo-atmospheric One hundred or more kilometers above the Earth's surface.

Fin A fixed or movable airfoil used to stabilize and control a missile in flight.

Guidance A dynamic process of directing an object toward a given point, which may be stationary or moving.

Guided missile An unmanned vehicle moving above the surface of the Earth whose trajectory or flight path is capable of being altered by an external or internal mechanism. See also aerodynamic missile; ballistic missile.

Hit-to-Kill A missile defense approach in which an interceptor rams the target, destroying it by force of impact.

Homing guidance A system by which a missile steers itself toward a target by means of a self-contained mechanism controlled by a certain guidance law.

Homing phase A part of missile flight controlled by the missile-contained system.

ICBM Intercontinental ballistic missile, a land-based missile with a range of more than 5,500 kilometers.

Illuminate Direct radar energy at an object sufficient to obtain radar targeting information.

Inertial guidance A guidance system designed to project a missile over a predetermined path, wherein the path of the missile is adjusted after launching by devices wholly within the missile and independent of outside information. The system measures and converts accelerations experienced to distance traveled in a certain direction.

Inertial navigation system A self-contained navigation system using inertial detectors, which automatically provides vehicle position, heading, and velocity. Also called INS.

Inertial reference frame One which is not accelerating.

Infrared Waves with wavelengths slightly longer than those forming the color red. Every type of object radiates a unique infrared signature, which can be identified by measuring the received energy.

Infrared imagery That imagery produced as a result of sensing electromagnetic radiations emitted or reflected from a given target surface in the infrared position of the electromagnetic spectrum (approximately 0.72 to 1,000 microns).

Integrated fire control system A system that performs the functions of target acquisition, tracking, data computation, and engagement control, primarily using electronic means and assisted by electromechanical devices.

Intercept point The point to which a vehicle is guided to complete an interception.

Interceptor A kill vehicle joined with a booster that together are launched against an offensive missile.

Kill probability A measure of the probability of destroying a target.

Kill vehicle A self-contained package of sensors, thrusters, and navigation gear that, once separated from its booster, can identify a target and maneuver into a collision with it.

Land-based system An antimissile system that uses locations on land to shoot interceptors at an incoming missile.

Lift A component of the total aerodynamic force acting on a body perpendicular to the undisturbed airflow relative to the body. Lift is directed perpendicularly up with respect to drag and is the main force controlling the flight of an aerodynamic missile.

Line-of-sight The line that starts at the reference point (e.g., the missile) and passes through the objective of the guidance (the target).

Mach Speed of sound at sea level (331.46 m/s) that is measured in multiples (Mach 1, Mach 2, and so forth).

Mach number The ratio of the velocity of a body to that of sound in the surrounding medium.

Maneuver A movement to place a pursuer in a position of advantage over the enemy.

Midcourse guidance The guidance applied to a missile between termination of the boost phase and the start of the terminal phase of flight.

Midcourse phase Coming between the boost and terminal phases. A part of missile flight when the missile is guided by an external weapon control system. See also boost phase; terminal phase.

Miss distance The displacement between the missile and target.

Missile A weapon that is launched and guided toward a target.

Missile control system A system that serves to maintain attitude stability and to correct deflections. See also missile guidance system.

Missile guidance system A system that evaluates flight information, correlates it with target data, determines the desired flight path of a missile, and communicates the necessary commands to the missile flight control system. See also missile control system.

Navigation A dynamic process of directing an object toward a given stationary point.

Parallel navigation Guidance when the direction of the line-of-sight is kept constant (i.e., the line-of-sight rate equals zero).

Passive homing guidance A system of homing guidance wherein the receiver in the missile utilizes radiation from the target.

Pitch The movement of a missile or an aircraft about its lateral axis.

Propellant The ejected gas from a rocket.

Proportional navigation A method of homing guidance in which the missile acceleration commands are proportional to the line-of-sight rate.

Pursuit An offensive operation designed to catch or cut off a hostile force attempting to escape with the aim of destroying it.

Radar A radio detection device that provides information on range, azimuth, or elevation of objects.

Ramjet A jet-propulsion engine containing neither compressor nor turbine that depends for its operation on the air compression accomplished by the forward motion of the engine.

Range The distance between any given point and an object or target. In two-point guidance systems, the range means the distance between the missile and target.

Rocket A vehicle propelled by the recoil force produced when part of its mass is ejected at high velocity; it does not rely on interaction with its environment for propulsion.

Roll The rotary motion of a missile or an aircraft around its longitudinal axis.

Sea-based system An antimissile system that operates from floating platforms, whether Navy ships or specially outfitted barges.

Seeker A device used in a moving object, especially a missile, that locates a target by detecting light, heat, or other radiation.

Semiactive homing guidance A system of homing guidance wherein the receiver in the missile utilizes radiation from the target, which has been illuminated by an outside source.

Sideslip angle The angle between the missile longitudinal x-axis and the projection of the missile velocity vector on the **xy** plane.

Surface-to-air guided missile A surface-launched guided missile for use against air targets.

Surface-to-surface guided missile A surface-launched guided missile for use against surface targets.

Terminal guidance The guidance applied to a guided missile between midcourse guidance and arrival in the vicinity of the target.

Thrust The instantaneous recoil force produced by a rocket.

Time-of-flight Elapsed time from the instant a missile leaves a launcher.

Time-to-go Calculated time to go until the end of the flight assuming that it will correspond to intercept.

Trajectory The dynamic path followed by an object under the influence of gravity or other forces.

Warhead That part of a missile, rocket, or other munitions that contains either the nuclear or thermonuclear system, high-explosive system, chemical or biological agents, or inert materials intended to inflict damage.

Yaw The rotation of a missile or an aircraft about its vertical axis.

Appendix A

A.1 LYAPUNOV METHOD

Control theory, whether it is presented in a classical or modern form, leans on the only and solid foundation—the Lyapunov theory of stability of motion.

Although the Lyapunov theory is the most effective for analysis of stability of processes described by nonlinear differential equations, we will apply the Lyapunov method to analysis of stability of linear differential equations, which are widely used in the book. Intuitively, the stability of a motion means that under slightly altered initial conditions at t_0 the alteration in the motion will remain slight for all $t > t_0$.

More precisely, the solution $\boldsymbol{x}_0(t)$ of the differential equation

$$\dot{\boldsymbol{x}} = \boldsymbol{A}\boldsymbol{x}, \quad \boldsymbol{x}(t_0) = \boldsymbol{x}(0) \tag{A1}$$

is said to be stable (or the system described by the differential equation (A1) is stable about the equilibrium point $\boldsymbol{x}_0 = 0$), if for every $\varepsilon > 0$ there exists such $\delta(\varepsilon, t_0) > 0$ that for every solution $\boldsymbol{x}(t)$ and for all $t \geq 0$ we have $\|\boldsymbol{x}(t) - \boldsymbol{x}_0(t)\|^2 < \varepsilon$ provided $\|\boldsymbol{x}(0) - \boldsymbol{x}_0(0)\|^2 < \delta$, where

$$\|x\|^2 = \sum x_i^2.$$

(In the case of linear differential equations with constant coefficients δ does not depend on t_0.)

System (A1) is said to be asymptotically stable, if it is stable and $\lim_{t\to\infty} \boldsymbol{x}(t) \to 0$.

Stability and asymptotic stability are determined based on the Lyapunov method, which assumes the utilizations of the so-called positive definite and positive semidefinite functions $V(\boldsymbol{x}) \geq 0$. The positive definite $V(\boldsymbol{x})$is positive for all $\mathbf{x} \neq 0$. The negative definite function has the opposite sign.

Theorem: System (A1) is asymptotically stable, if there exists such positive definite function $V(\boldsymbol{x})$ ($V(0) = 0$) that its derivative along (A1) is negative definite.

The derivative of $V(\boldsymbol{x})$ along (A1) equals

$$\frac{dV}{dt} = \frac{\partial V^T}{\partial x} \boldsymbol{A}\boldsymbol{x} \tag{A2}$$

By choosing $V(\boldsymbol{x}) = \boldsymbol{x}^T W \boldsymbol{x}$, where W is a symmetric positive definite matrix, instead of (A2) we have $\boldsymbol{x}^T(\boldsymbol{W}\boldsymbol{A} + \boldsymbol{A}^T\boldsymbol{W})\boldsymbol{x}$, so that the asymptotic stability condition is

$$\boldsymbol{W}\boldsymbol{A} + \boldsymbol{A}^T\boldsymbol{W} = -R < 0 \tag{A3}$$

that is, the matrix (A3) must be negative definite [2].

The physical interpretation of the above theorem is the following. $V(\boldsymbol{x})$ is bowl shaped. The condition (A3) implies that $V(\boldsymbol{x}(t))$ decreases monotonically with time along any trajectory of (A1). Hence $V(\boldsymbol{x}(t))$ will eventually approach zero as $t \to \infty$. Since $V(\boldsymbol{x})$ is positive definite, we have

$V(0) = 0$ only at $\boldsymbol{x} = 0$. Hence, if we can find positive definite matrices W and R that are related by (A3), then every trajectory of (A1) will approach zero as $t \to \infty$. The function $V(\boldsymbol{x})$ is called a Lyapunov function of the system (A1).

There exist various modifications of the Lyapunov method, various definitions of stability for special types of dynamic systems [3,4]. Here we discuss the possible application of the Lyapunov method to the stability analysis of systems operation on a finite interval $[0, t_F]$. By introducing

$$\tau = \frac{1}{t_F - t} \tag{A4}$$

the interval $[0, t_F]$ with respect to t is transformed into the interval $[1/t_F, \infty]$ with respect to τ. Taking into account

$$\frac{d}{dt} = \tau^2 \frac{d}{d\tau} \, ,$$

the equation (A1) can be presented as

$$\frac{d\boldsymbol{x}}{d\tau} = \frac{1}{\tau^2} \boldsymbol{A}\boldsymbol{x} \tag{A5}$$

If $V(\boldsymbol{x})$ is the Lyapunov function with respect to equation (A5), the solution of equation (A5) is stable on τ-interval. Since the transformation (A4) does not change the sign of

$$\frac{dV}{d\tau} = \frac{1}{\tau^2} \frac{dV}{dt} \, ,$$

the solution of equation (A5) is stable also on t-interval (i.e., for each stable trajectory on τ-interval there exists a stable trajectory on the finite interval, in a sense that $V(\boldsymbol{x})$ will decrease, when $t \to t_F$). However, because for $\tau \to \infty$ $dV/d\tau$ is always zero, the decrease of $\boldsymbol{x}$ cannot be asymptotic.

A.2 BELLMAN–LYAPUNOV APPROACH

Let us consider a dynamic system described by the following equation

$$\dot{\boldsymbol{x}} = \boldsymbol{A}\boldsymbol{x} + \boldsymbol{B}\boldsymbol{u}, \quad \boldsymbol{x}(t_0) = \boldsymbol{x}(0) \tag{A6}$$

where $\boldsymbol{x}$ is an m-dimensional state vector, $\boldsymbol{u}$ is an n-dimensional control vector, and $\boldsymbol{A}$ and $\boldsymbol{B}$ are matrices of appropriate dimensions.

We will determine the control law $\boldsymbol{u}$ that minimizes the cost functional

$$I = \frac{1}{2}(\boldsymbol{x}^T(t_F)C_0\boldsymbol{x}(t_F)) + \int_{t_0}^{t_F} (\boldsymbol{x}^T(t)R\boldsymbol{x}(t) + \|\boldsymbol{u}(t)\|^2)dt) \tag{A7}$$

where C_0 and R are symmetric positive semidefinite matrices.

To find the optimal control we will use the dynamic programming approach [1]. The derivation of the Bellman functional equation is given according to the optimality principle: every tail of the optimal trajectory is the optimal trajectory.

Let the optimal functional value be

$$\varphi(\boldsymbol{x}(t_0), t_0) = \min_{u(t)} I \tag{A8}$$

Then in accordance with the optimality principle, it can be written

$$\varphi(\boldsymbol{x}(t_0), t_0) = \min_{u(t)} \frac{1}{2}\{\boldsymbol{x}^T(t_F) C_0 \boldsymbol{x}(t_F) + \int_{t_0}^{t_0+\delta} (\boldsymbol{x}^T(t) R\boldsymbol{x}(t) + \|\boldsymbol{u}(t)\|^2) dt$$

$$+ \int_{t+\delta}^{t_F} (\boldsymbol{x}^T(t) R\boldsymbol{x}(t) + \|\boldsymbol{u}(t)\|^2) dt\}$$

$$= \min_{u(t)} \{\frac{1}{2}[\boldsymbol{x}^T(t_F) C_0 \boldsymbol{x}(t_F) + \int_{t_0}^{t_0+\delta} (\boldsymbol{x}^T(t) R\boldsymbol{x}(t) + \|\boldsymbol{u}(t)\|^2) dt] + \varphi(\boldsymbol{x}(t_0+\delta), t_0+\delta)\} \tag{A9}$$

Suppose that δ is small enough and that there exist partial derivatives of $\varphi(\boldsymbol{x})$ for $\boldsymbol{x} \in [\boldsymbol{x}(t_0), \boldsymbol{x}(t_0+\delta)]$. Then expanding $\varphi(\boldsymbol{x}(t_0+\delta),(t_0+\delta))$ into the Taylor series in the vicinity of $\boldsymbol{x}(t_0)$, after appropriate transformations we obtain

$$\varphi(\boldsymbol{x}(t_0), t_0) = \min_{u(t)} \{\frac{1}{2}(\boldsymbol{x}^T(t_0) R\boldsymbol{x}(t_0) + \|\boldsymbol{u}(t_0)\|^2)\delta + \varphi(\boldsymbol{x}(t_0), t_0)$$

$$+ \frac{\partial\varphi}{\partial t}\delta + \frac{\partial\varphi^T}{\partial x}(\boldsymbol{A}\boldsymbol{x}(t) + \boldsymbol{B}\boldsymbol{u}(t))\Big|_{\substack{x=x_0\\u=u_0}} \delta + O(\delta)\} \tag{A10}$$

where

$$\frac{\partial\varphi^T}{\partial x} = (\frac{\partial\varphi}{\partial x_1}, \ldots, \frac{\partial\varphi}{\partial x_m})$$

is a row vector, and it is assumed that $\lim_{\delta\to 0} O(\delta)/\delta = 0$.

Tending δ to zero and taking into account that, in accordance with the optimality principle, the strategy must be optimal regardless of the state in which the system is at the actual instant, that is, $\boldsymbol{x}(t_0)$ and $\boldsymbol{u}(t_0)$ can be treated as the current values of the vectors $\boldsymbol{x}$(t) and $\boldsymbol{u}$(t), we obtain the required functional equation as follows

$$\min_{u(t)} \{\frac{1}{2}(\boldsymbol{x}^T(t) R\boldsymbol{x}(t) + \|\boldsymbol{u}(t)\|^2) + \frac{\partial\varphi}{\partial t} + \frac{\partial\varphi^T}{\partial x}(\boldsymbol{A}\boldsymbol{x}(t) + \boldsymbol{B}\boldsymbol{u}(t)) = 0 \tag{A11}$$

For the existence of the minimum of the expression in braces, its derivative with respect to $\boldsymbol{u}(t)(d/du\{\})$ must be equal to zero, i.e.,

$$\boldsymbol{u}(t) = -\boldsymbol{B}^T \frac{\partial \varphi}{\partial x} \tag{A12}$$

Subtituting equation (A12) in equation (A11), we obtain

$$\frac{1}{2}\boldsymbol{x}^T(t)R\boldsymbol{x}(t) + \frac{\partial \varphi}{\partial t} + \frac{\partial \varphi^T}{\partial x}\boldsymbol{A}\boldsymbol{x}(t) - \frac{1}{2}\frac{\partial \varphi^T}{\partial x}\boldsymbol{B}\boldsymbol{B}^T\frac{\partial \varphi}{\partial x}\boldsymbol{u}(t) = 0 \tag{A13}$$

The solution of the considered problem reduces to finding the function $\varphi(\boldsymbol{x})$ satisfying the Bellman functional equation (A13) [or the equivalent equation (A11)].

The solution will be sought in the form

$$\varphi(\boldsymbol{x}) = \frac{1}{2}\boldsymbol{x}^T(t)W(t)\boldsymbol{x}(t) \tag{A14}$$

Its substitution in equations (A12) and (A13) gives

$$\boldsymbol{u}(t) = -\boldsymbol{B}^T W(t)\boldsymbol{x}(t) \tag{A15}$$

$$\dot{W} + \boldsymbol{A}^T W + W\boldsymbol{A} - W\boldsymbol{B}\boldsymbol{B}^T W + R = 0 \tag{A16}$$

This is the so-called Riccati differential equation. Comparing equations (A7) and (A14) for $t = t_F$, we conclude that $W(t_F) = C_0$. For the quadratic integral criterion with the infinite upper limit [see equation (A7)] W is a constant matrix and instead of equation (A16) we have the so-called algebraic Riccati equation, which corresponds to the stationary solution of (A16) [5]

$$\boldsymbol{A}^T W + W\boldsymbol{A} - W\boldsymbol{B}\boldsymbol{B}^T W + R = 0 \tag{A17}$$

Comparing (A17) with (A3), we can see that equation (A17) is the Lyapunov equation (A3) for the closed-loop system with control (A15), and W is the Lyapunov function for this system.

The above analysis was focused on establishing the linkage between the Lyapunov method, which is used in this book to design new guidance laws, and the optimal approach, more precisely, a class of optimal system based on minimization of the integral quadratic cost functional. The discrete analog of Riccati equations, applied to the optimal filtering problem, is given in Chapter 8.

In conclusion, we will obtain the expression for the optimal PN guidance law (2.56) given in Chapter 2. For equations (2.54) and (2.55) the matrices in equations (A6) and (A7) are

$$\boldsymbol{A} = \begin{bmatrix} 0 & 1 \\ 0 & 0 \end{bmatrix} \quad \boldsymbol{B} = \begin{bmatrix} 0 \\ 1 \end{bmatrix}, \quad C_0 = \begin{bmatrix} C & 0 \\ 0 & 0 \end{bmatrix}, \quad R = 0 \tag{A18}$$

so that equation (A16) can be presented as

$$\begin{bmatrix} \dot{w}_{11} & \dot{w}_{12} \\ \dot{w}_{12} & \dot{w}_{22} \end{bmatrix} + \begin{bmatrix} 0 & w_{11} \\ 0 & w_{12} \end{bmatrix} + \begin{bmatrix} 0 & 0 \\ w_{11} & w_{12} \end{bmatrix} - \begin{bmatrix} w_{12}^2 & w_{12}w_{22} \\ w_{12}w_{22} & w_{22}^2 \end{bmatrix} = 0,$$

$$w_{12}(t_F) = w_{22}(t_F) = 0, \quad w_{11}(t_F) = C$$

The solution of the nonlinear matrix Riccati equation presents significant difficulties, even for this relatively simple problem. It is easy to check that

$$w_{11}(t) = \frac{3}{3/C + (t_F - t)^3}, \quad w_{12}(t) = \frac{3(t_F - t)}{3/C + (t_F - t)^3}, \quad w_{22}(t) = \frac{3(t_F - t)^2}{3/C + (t_F - t)^3}$$

satisfy the obtained Riccati equation, so that the expression of the optimal control $u(t) = -a_M(t) = -w_{12}x_1 - w_{22}x_2$ coincides with equation (2.56).

REFERENCES

1. Bellman, R., *Dynamic Programming,* Princeton University Press, Princeton, NJ, 1957.
2. Bellman, R., *Introduction to Matrix Analysis,* McGraw-Hill, New York, 1960.
3. Martynyuk, A. (ed.), *Advances in Stability at the End of the 20th Century* (Stability, Control, Theory, Methods and Applications), CRC Press, Boca Raton, FL, 2002.
4. Rumyantsev, V.V., On asymptotic stability and instability of motion with respect to a part of the variables, *Journal of Applied Mathematics and Mechanics,* 35, 1, 19–30, 1971.
5. Yanushevsky, R., *Theory of Optimal Linear Multivariable Control Systems*, Nauka, Moscow, 1973.

Appendix B

B.1 LAPLACE TRANSFORM

For a function $f(t)$ defined on $0 \le t < \infty$, its Laplace transform, denoted as $F(s)$, is obtained by the following integral

$$L\{f(t)\} \equiv F(s) = \int_0^{\infty} f(t)e^{-st}\,dt$$

where s is the Laplace variable and L is called the Laplace transform operator.

The Laplace transform exists and is defined for $s > \sigma$ if $f(t)$ is a function piecewise continuous on $[0, K]$ (for every $K > 0$) and does not grow asymptotically faster than $Me^{\sigma t}$ (i.e., $|f(t)| \le Me^{\sigma t}$).

In actual physical systems the Laplace transform is often interpreted as a transformation from the time-domain point of view, in which inputs and outputs are understood as functions of time, to the frequency-domain point of view, where the same inputs and outputs are seen as functions of complex variables. There is a unique "mapping" between functions in the "t-domain" and the corresponding functions in the "s-domain."

The inverse Laplace transform is determined as

$$L^{-1}\{F(s)\} = f(t) = \frac{1}{2\pi i}\int_{\sigma-i\infty}^{\sigma+i\infty} F(s)e^{st}\,ds$$

Conditions for the existence of the inverse Laplace transform are:

(i) $\lim F(s) = 0, \quad s \to \infty$;
(ii) $\lim sF(s), \quad s \to \infty$, is finite.

Usually, the Laplace transform is used for the solution of linear differential equations with constant coefficients, and we deal with rational functions of the complex variable s with real-valued coefficients (i.e., with single-valued functions).

B.2 PROOF OF THEOREM

The integral (4.13) and the related expression (4.53) for $P(t_F, s)$ present multiple-valued functions. We will show that $P(t_F, s)$ is the Laplace transform of $P(t_F, t)$, which is bounded and is tending to 0, if condition (4.64) is satisfied.

The function $P(t_F, s)$ is a multiple-valued function that has infinitely many branches, which are obtained, if we fix a branch of each factor in equation (4.34). By denoting the last complex exponent factor as $x^p = e^{p\ln|x| + pi(\arg x + 2\pi k)}$, it can be presented as $x_0^p e^{p2k\pi i}$, $k = 0,1,2,...$, where x_0^p corresponds to $k = 0$ [see equations (4.38)–(4.41) given for $k = 0$ and $s = i\omega$]. It follows from (4.34) that for real s $\ln|x| = 0$, so that, since p is purely imaginary, $x^p = e^{p_1(\arg x + 2k\pi)}$, $k = 0,1,2,\ldots$, where

$$p_1 = \frac{N\omega_j(D_j - \zeta_j\omega_j C_j)}{2\sqrt{1-\zeta_j^2}},$$

that is, values of x^p are real for real s.

By fixing the branches of all other factors of equation (4.34) in such a way that they are real for real s and taking an arbitrary k branch of the last factor, we obtain infinitely many branches $P_k(t_F,s)$, $k = 0,1,2\ldots$, real for $s > 0$. Evidently, $P_k(t_F,s) = P(t_F,s)e^{2\pi p_1 k}$, so it suffices to consider only $P(t_F,s)$.

The function $P(t_F,s)$ defined by equation (4.34) is analytic in the region $C_v = \{s\text{: Re}s > -\sigma\}$ where $\sigma = \min(1/\tau_k, \zeta_j\omega_j)$, $k = 1,.., l$; $j = 1,\ldots, m$. It is analytic in the right-half plane (Re$s \geq 0$), real-valued for real s and

$$P(t_F,s) = O(\frac{1}{|s|^{\alpha}}),\ \ P'(t_F,s) = O(\frac{1}{|s|^{\alpha+1}}),\ \ s \to \infty,\ \ s \in C_v, \tag{B1}$$

for some $\alpha > 0$

Define for $t > 0$ and $0 < \gamma < \sigma$

$$y_0(t) = \frac{1}{2\pi i}\int_{\gamma-i\infty}^{\gamma+i\infty} P(t_F,s)e^{t_F s}ds = \lim_{\alpha\to\infty}\frac{1}{2\pi i}(\frac{1}{t}P(t_F,s)e^{ts}\Big|_{\gamma-ia}^{\gamma+ia} - \frac{1}{t}\int_{\gamma-ia}^{\gamma+ia} P'(t_F,s)e^{ts}ds) \tag{B2}$$

$y_0(t)$ can be rewritten in the form

$$y_0(t) = \frac{1}{2\pi}\int_{-\infty}^{\infty} P(t,\gamma+iz)e^{(1+iz)t}dz \tag{B3}$$

Since $P(t_F,s)e^{ts}$ is real for real s, then, by the symmetry principle, the numbers $P(t_F,\gamma + iz)e^{(1\pm iz)t}$ are complex-conjugates. Therefore, the imaginary part of the integrand of (B3) is an odd function of z. Hence, the integral does not change if one replaces the integrand with its real part, so that $y_0(t)$ is real-valued.

It follows from equations (B1) and (B2) that $y_0(t)$ tends to 0 as $t \to \infty$. Based on established relationships between the considered branches $P_k(t_F,s)$, we can conclude that each of these branches is the Laplace transform of a real-valued function $y_k(t)$ tending to 0 as $t \to \infty$ and $y_k(t) = y_0(t)e^{2\pi p_1 k}$, $k = 0,1,2\ldots.$, and $y_k(t)$ is absolutely integrable on $[0, \infty]$.

We used the principal branch, $k = 0$, because it satisfies the zero condition for the lower limit of integration of equation (4.13) [see equations (4.35)–(4.37), (4.39), and (4.40)].

The above consideration corresponds to the case when $N > 2$ is an integer. If N is not an integer, the factor s^{N-2} of equation (4.34) is a multiple-valued function. In this case, the exponent s^{N-2} is not well defined in the neighborhood of zero, so that instead of $C_v = \{s\text{: Re}s > -\sigma\}$ we have $C_v = \{s\text{: Re}s > -\sigma/\{s: -\sigma < s \leq 0\}\}$ and the contour of integration in (B2) should be replaced with the contour consisting of four intervals, i.e.,

$$y_0(t) = \frac{1}{2\pi i}(\int_{-\gamma-i\infty}^{-\gamma} + \int_{-\gamma}^{-0} + \int_{+0}^{-\gamma} + \int_{-\gamma}^{-\gamma+i\infty})P(s,t_F)e^{ts}ds \tag{B4}$$

It follows from equations (B1) and (B2) that $y_0(t)$ tends to 0 as $t \to \infty$ (see also References [1,2]).

REFERENCES

1. Yanushevsky, R., Analysis and design of missile guidance systems in frequency domain, 44th AIAA Space Sciences Meeting, paper AIAA 2006-825, Reno, Nevada, 2006.
2. Yanushevsky, R., Frequency domain approach to guidance system design, *IEEE Transactions on Aerospace and Electronic Systems*, 43, 2007.

Appendix C

C.1 AERODYNAMIC REGRESSION MODELS

For a chosen range of altitudes and Mach numbers Missile Datcom provides tabulated data about the lift, drag, and axial and normal force coefficients as a function of trim angles of attack, that is, for each pair *ij* of the Mach number and altitude values [*Mach*(*i*), *Alt*(*j*)] we have a table with lines containing coefficients C_{Lk}, C_{Dk}, C_{Nk}, and C_{ak} corresponding to a certain angle of attack α_{Tk} ($k = 1,2,...,m_{ij}$), where m_{ij} indicates that the trim angles of attack are bounded and depend upon *Mach*(*i*) and *Alt*(*j*).

To present, for example, the relationship between α_T and C_N by the second-order polynomial $\alpha_T = k_{10} + k_{11}C_N + k_{12}C_N^2$, we should substitute α_{Tk} and C_{Nk} in this equation. As a result, we obtain $m_{ij} > 3$ linear equations that should be solved with respect to unknown coefficients k_{10}, k_{11}, and k_{12}, that is, we should solve the system of linear equations

$$\boldsymbol{Ck} = \boldsymbol{\alpha} \tag{C1}$$

where $\boldsymbol{k} = (k_{10}, k_{11}, k_{12})$ is an unknown vector; $\boldsymbol{\alpha} = (\alpha_{T1},...,\alpha_{Tm_{ij}})$ is the vector of trim angles (in obvious cases, here and earlier in the book we do not specify whether it is a row or column vector); $\boldsymbol{C}$ is the m_{ij}x3 matrix of the following form [2]

$$\boldsymbol{C} = \begin{vmatrix} 1 & C_{N1} & C_{N1}^2 \\ 1 & C_{N2} & C_{N2}^2 \\ ... & .... & ... \\ 1 & C_{Nm_{ij}} & C_{Nm_{ij}}^2 \end{vmatrix} \tag{C2}$$

In various problems of finding the functional relationship based on experimental data we have overdetermined systems of linear equations, similar to equations (C1) and (C2).

The unknown coefficients k_{10}, k_{11}, and k_{12} are determined by minimizing the sum of squares of the deviations of the data from the regression model (i.e., $\min_k \|\boldsymbol{\alpha} - \boldsymbol{Ck}\|^2$). The optimal solution is presented as [1]

$$\boldsymbol{k} = \boldsymbol{C}^{+}\alpha, \quad \boldsymbol{C}^{+} = (\boldsymbol{C}^T\boldsymbol{C})^{-1}\boldsymbol{C}^T \tag{C3}$$

where the so-called pseudoinverse matrix $\boldsymbol{C}^{+}$ is written, assuming that the columns of $\boldsymbol{C}$ are linearly independent. The more general expression of $\boldsymbol{C}^{+}$ is given in Reference [1].

Using MATLAB, the least square solution can be found with the backslash operator (i.e., $\boldsymbol{k} = \alpha\backslash\boldsymbol{C}$).

REFERENCES

1. Albert, A., *Regression and the Moor-Penrose Pseudoinverse*, Academic Press, NewYork, 1972.
2. Phillips, G.M., *Interpolation and Approximation by Polynomials*, Springer-Verlag, New York, 2003.

Appendix D

D.1 RUNGE–KUTTA METHOD

Most of the differential equations in the book have no closed-form analytical solutions, so that numerical integration techniques should be used to solve or simulate these equations. We will describe the Runge–Kutta method, which is simple, accurate, and widely used in practice.

For a differential equation of the form

$$\dot{y} = f(y,t) \tag{D1}$$

we will describe the Runge–Kutta numerical integration procedure.

The fourth-order Runge–Kutta method is one of the standard algorithms for solving differential equations. Before we give the algorithm of the fourth-order Runge–Kutta method, we will derive the second-order Runge–Kutta method, which is also used in many applications.

We start with the original differential equation and integrate it formally:

$$y_{n+1} = \int_0^{t_n} f(t,y)dt + \int_{t_n}^{t_{n+1}} f(t,y)dt = y_n + \int_{t_n}^{t_{n+1}} f(t,y)dt \tag{D2}$$

where $y_n = y(t_n)$.

Various computational procedures depend on how the integral at the right side of equation (D2) is calculated. By changing this integral for $h\dot{y}(t)$, we obtain the Euler formula, which has accuracy $O(h^2)$

$$y_{n+1} = y_n + h\dot{y}_n + O(h^2) = y_n + hf(t_n, y_n) + O(h^2) \tag{D3}$$

where $h = t_{n+1} - t_n$ is the integration interval.

Integrating equation (D2) using the trapezoid formula we obtain

$$y_{n+1} = y_n + 0.5h(f(t_n,y_n) + f(t_{n+1},y_{n+1})) + O(h^3) \tag{D4}$$

so that, based on equation (D3), we have

$$y_{n+1} = y_n + 0.5h(f(t_n,y_n) + f(t_{n+1},y_{n+1})) + O(h^3), \quad y_{n+1} = y_n + hf(t_n,y_n) \tag{D5}$$

Integrating equation (D2) using the rectangle formula we obtain

$$y_{n+1} = y_n + hf(t_n + 0.5h, \quad y(t_n + 0.5h)) + O(h^3) \tag{D6}$$

where

$$y(t_n + 0.5h) = y_n + 0.5hf(t_n,y_n)$$

Instead of two components presented in the second-order Runge–Kutta method, the fourth-order formula requires knowledge of four terms

$$\begin{aligned} k_1 &= f(t_n, y_n) \\ k_2 &= f(t_n + 0.5h, y_n + 0.5k_1) \\ k_3 &= f(t_n + 0.5h, y_n + 0.5k_2) \\ k_4 &= f(t_n + h, y_n + hk_3) \end{aligned} \tag{D7}$$

and

$$y_{n+1} = y_n + \frac{h}{6}(k_1 + 2k_2 + 2k_3 + k_4) + O(h^5) \tag{D8}$$

We demonstrate the fourth-order Runge–Kutta method by considering the system of differential equations (8.75). According to equations (D7) and (D8) we have

$$k_{1i}^1 = x_{2in}, \qquad k_{2i}^1 = x_{3in},$$

$$k_{3i}^1 = -\frac{\omega_M^2}{\tau} x_{1in} - \frac{\omega_M^2 + 2\zeta\omega_M}{\tau} x_{2in} - \frac{2\zeta\omega_M\tau + 1}{\tau} x_{3in} + \frac{\omega_M^2}{\tau} a_{MTin}$$

$$\boldsymbol{k}_1 = (k_{1i}^1, k_{2i}^1, k_{3i}^1)^T \quad , \qquad \boldsymbol{y}_n = (x_{1in}, x_{2in}, x_{3in})^T$$

$$x_{jin}^1 = x_{jin} + 0.5hk_{ji}^1 \,,$$

$$k_{1i}^2 = x_{2in}^1, \qquad k_{2i}^2 = x_{3in}^1,$$

$$k_{3i}^2 = -\frac{\omega_M^2}{\tau} x_{1in}^1 - \frac{\omega_M^2 + 2\zeta\omega_M}{\tau} x_{2in}^1 - \frac{2\zeta\omega_M\tau + 1}{\tau} x_{3in}^1 + \frac{\omega_M^2}{\tau} a_{MTin}$$

$$\boldsymbol{k}_2 = (k_{1i}^2, k_{2i}^2, k_{3i}^2)^T \,,$$

$$x_{jin}^2 = x_{jin} + 0.5hk_{ji}^2 \,,$$

$$k_{1i}^3 = x_{2in}^2, \qquad k_{2i}^3 = x_{3in}^2,$$

$$k_{3i}^3 = -\frac{\omega_M^2}{\tau} x_{1in}^2 - \frac{\omega_M^2 + 2\zeta\omega_M}{\tau} x_{2in}^2 - \frac{2\zeta\omega_M\tau + 1}{\tau} x_{3in}^2 + \frac{\omega_M^2}{\tau} a_{MTin}$$

$$\boldsymbol{k}_3 = (k_{1i}^3, k_{2i}^3, k_{3i}^3)^T$$

$$x_{jin}^3 = x_{jin} + hk_{ji}^2, \;\; \boldsymbol{y}_n^3 = (x_{1in}^3, x_{2in}^3, x_{3ni}^3)^T$$

$$k_{1i}^4 = x_{2in}^3, \qquad k_{2i}^4 = x_{3in}^3,$$

$$k_{3i}^4 = -\frac{\omega_M^2}{\tau} x_{1in}^3 - \frac{\omega_M^2 + 2\zeta\omega_M}{\tau} x_{2in}^3 - \frac{2\zeta\omega_M \tau + 1}{\tau} x_{3in}^3 + \frac{\omega_M^2}{\tau} a_{MTin}$$

$$\boldsymbol{k}_4 = (k_{1i}^4, k_{2i}^4, k_{3i}^4)^T \qquad (i = 1,2,3)$$

$$\boldsymbol{y}_{n+1} = \boldsymbol{y}_n + \frac{h}{6}(\boldsymbol{k}_1 + 2\boldsymbol{k}_2 + 2\boldsymbol{k}_3 + \boldsymbol{k}_4) \tag{D9}$$

Index

D

E

H

I

J

K

L

N

O

P

Q

R

S

T

U

V

W

Y

Z

Mechanical Engineering

MODERN MISSILE GUIDANCE

Written by an expert with more than 30 years of experience, **Modern Missile Guidance** contains new analytical results, obtained by the author, that can be used for analysis and design of missile guidance and control systems. This book covers not just new methods nor is it merely a compilation of older methods, although it includes both. The book discusses, in a logical progression, with its clear elucidation of the guidance laws, the entire field from missile dynamics to modeling and testing missile guidance and control systems.

In contrast to existing books that discuss very simple and often unrealistic guidance system models, this book presents missile guidance models that describe more precisely the dynamics of the missile flight control system, making analytical results more effective in practice. The analysis of missile guidance system models in the time-domain and in the frequency-domain allows the generation of different guidance laws that supplement each other.

Taking a modern, rigorous approach that leads to improved performance in missile guidance applications, the book examines new guidance laws, and corresponding algorithms for generating and testing these laws, and includes effective new software programs developed by the author. The author provides an innovative presentation of the theoretical aspects of modern missile guidance that quite possibly cannot be found in any other book. It delineates new ideas that, once crystallized, will significantly improve missile systems performance.

62263



6000 Broken Sound Parkway, NW
Suite 300, Boca Raton, FL 33487
270 Madison Avenue
New York, NY 10016
2 Park Square, Milton Park
Abingdon, Oxon OX14 4RN, UK



www.crcpress.com